Investigation into Shrinkage of High-Performance Concrete Used for Iowa Bridge Decks and Overlays

Final Report
September 2013

IOWA STATE UNIVERSITY
Institute for Transportation

Sponsored by
Iowa Highway Research Board
(IHRB Project TR-633)
Iowa Department of Transportation
(InTrans Project 11-419)

About the Institute for Transportation

The mission of the Institute for Transportation (InTrans) at Iowa State University is to develop and implement innovative methods, materials, and technologies for improving transportation efficiency, safety, reliability, and sustainability while improving the learning environment of students, faculty, and staff in transportation-related fields.

Disclaimer Notice

The contents of this report reflect the views of the authors, who are responsible for the facts and the accuracy of the information presented herein. The opinions, findings and conclusions expressed in this publication are those of the authors and not necessarily those of the sponsors.

The sponsors assume no liability for the contents or use of the information contained in this document. This report does not constitute a standard, specification, or regulation.

The sponsors do not endorse products or manufacturers. Trademarks or manufacturers' names appear in this report only because they are considered essential to the objective of the document.

Non-Discrimination Statement

Iowa State University does not discriminate on the basis of race, color, age, religion, national origin, sexual orientation, gender identity, genetic information, sex, marital status, disability, or status as a U.S. veteran. Inquiries can be directed to the Director of Equal Opportunity and Compliance, 3280 Beardshear Hall, (515) 294-7612.

Iowa Department of Transportation Statements

Federal and state laws prohibit employment and/or public accommodation discrimination on the basis of age, color, creed, disability, gender identity, national origin, pregnancy, race, religion, sex, sexual orientation or veteran's status. If you believe you have been discriminated against, please contact the Iowa Civil Rights Commission at 800-457-4416 or the Iowa Department of Transportation affirmative action officer. If you need accommodations because of a disability to access the Iowa Department of Transportation's services, contact the agency's affirmative action officer at 800-262-0003.

The preparation of this report was financed in part through funds provided by the Iowa Department of Transportation through its "Second Revised Agreement for the Management of Research Conducted by Iowa State University for the Iowa Department of Transportation" and its amendments.

The opinions, findings, and conclusions expressed in this publication are those of the authors and not necessarily those of the Iowa Department of Transportation.

Technical Report Documentation Page

1. Report No. IHRB Project TR-633	**2. Government Accession No.**	**3. Recipient's Catalog No.**	
4. Title and Subtitle Investigation into Shrinkage of High-Performance Concrete Used for Iowa Bridge Decks and Overlays		**5. Report Date** September 2013 **6. Performing Organization Code**	
7. Author(s) Kejin Wang, Scott M. Schlorholtz, Sri Sritharan, Hasitha Seneviratne, Xin Wang, Qizhe Hou		**8. Performing Organization Report No.** InTrans Project 11-403	
9. Performing Organization Name and Address Institute for Transportation Iowa State University 2711 South Loop Drive, Suite 4700 Ames, IA 50010-8664		**10. Work Unit No. (TRAIS)** **11. Contract or Grant No.**	
12. Sponsoring Organization Name and Address Iowa Highway Research Board Iowa Department of Transportation 800 Lincoln Way Ames, IA 50010		**13. Type of Report and Period Covered** Final Report **14. Sponsoring Agency Code** IHRB Project TR-633	
15. Supplementary Notes Visit www.intrans.iastate.edu for color pdfs of this and other research reports.			
16. Abstract High-performance concrete (HPC) overlays have been used increasingly as an effective and economical method for bridge decks in Iowa and other states. However, due to its high cementitious material content, HPC often displays high shrinkage cracking potential. This study investigated the shrinkage behavior and cracking potential of the HPC overlay mixes commonly used in Iowa. In the study, 11 HPC overlay mixes were studied. These mixes consisted of three types of cements (Type I, I/II, and IP) and various supplementary cementitious materials (Class C fly ash, slag and metakaolin). Limestone with two different gradations was used as coarse aggregates in 10 mixes and quartzite was used in one mix. Chemical shrinkage of pastes, free drying shrinkage, autogenous shrinkage of mortar and concrete, and restrained ring shrinkage of concrete were monitored over time. Mechanical properties (such as elastic modulus and compressive and splitting tensile strength) of these concrete mixes were measured at different ages. Creep coefficients of these concrete mixes were estimated using the RILEM B3 and NCHRP Report 496 models. Cracking potential of the concrete mixes was assessed based on both ASTM C 1581 and simple stress-to-strength ratio methods. The results indicate that among the 11 mixes studied, three mixes (4, 5, and 6) cracked at the age of 15, 11, and 17 days, respectively. Autogenous shrinkage of the HPC mixes ranges from 150 to 250 microstrain and free dying shrinkage of the concrete ranges from 700 to 1,200 microstrain at 56 days. Different concrete materials (cementitious type and admixtures) and mix proportions (cementitious material content) affect concrete shrinkage in different ways. Not all mixes having a high shrinkage value cracked first. The stresses in the concrete are associated primarily with the concrete shrinkage, elastic modulus, tensile strength, and creep. However, a good relationship is found between cementitious material content and total (autogenous and free drying) shrinkage of concrete.			
17. Key Words bridge decks—cracking—high-performance concrete—mix evaluation—overlays—shrinkage		**18. Distribution Statement** No restrictions.	
19. Security Classification (of this report) Unclassified.	**20. Security Classification (of this page)** Unclassified.	**21. No. of Pages** 154	**22. Price** NA

INVESTIGATION INTO SHRINKAGE OF HIGH-PERFORMANCE CONCRETE USED FOR IOWA BRIDGE DECKS AND OVERLAYS

Final Report
September 2013

Principal Investigator
Kejin Wang, Professor
Department of Civil Construction and Environmental Engineering, Iowa State University

Co-Principal Investigators
Scott M. Schlorholtz, Scientist
Department of Biotechnology, Iowa State University

Sri Sritharan, Professor
Department of Civil Construction and Environmental Engineering, Iowa State University

Research Assistants
Hasitha Seneviratne, Xin Wang, Qizhe Hou

Sponsored by
the Iowa Highway Research Board and
the Iowa Department of Transportation
(IHRB Project TR-633)

Preparation of this report was financed in part through funds provided by the
Iowa Department of Transportation
through its Research Management Agreement with the
Institute for Transportation
(InTrans Project 11-403)

A report from
Institute for Transportation
Iowa State University
2711 South Loop Drive, Suite 4700
Ames, IA 50010-8664
Phone: 515-294-4015 Fax: 515-294-0467
www.intrans.iastate.edu

TABLE OF CONTENTS

LIST OF FIGURES

LIST OF TABLES

ACKNOWLEDGMENTS

The authors would like to acknowledge the Iowa Department of Transportation and Iowa Highway Research Board for providing financial and technical support as well as concrete materials for this project. Special thanks to the technical advisory committee members, Kevin Jones, Todd Hanson, Chengsheng Ouyang, James Nelson, Ahmad Abu-Hawash, and Wayne Sunday, for their comments and insights throughout the project and to Mark Dunn for supporting and managing the project. Assistance from Robert Steffes, Gilson Lomboy, Brian Zimmerman, and Jeremy McIntyre in performing experiments is also deeply appreciated. During her visit at Iowa State University, Chen Yu from the Changsha University of Science and Technology in China participated in the mortar shrinkage testing and the project report preparation and her contributions are greatly acknowledged.

EXECUTIVE SUMMARY

High-performance concrete (HPC) is used increasingly in buildings and bridge structures due to its high strength, superior workability, and excellent durability. However, with high cementitious material content, low water-to-cementitious material ratio, and various admixtures, HPC often possesses a high risk of shrinkage cracking. Many states have reported cracking on HPC bridge decks at early ages, and this problem is a great concern in Iowa.

This research project was aimed at evaluating various shrinkage components (such as chemical, autogenous, and drying shrinkage) in the HPC mixes used for bridge decks and overlays in Iowa, assessing the cracking potential of the HPC mixes, and providing recommendations for reducing the concrete shrinkage cracking potential.

In this project, 11 mixes were composed of three types of cement (Type I, I/II, and IP), various supplementary cementitious materials (SCMs) (Class C fly ash, slag, and metakaolin at the cement replacement levels of 20, 25, and 5.6 percent, respectively), and different chemical admixtures (normal water reducer, mid-range water reducer, retarder, and air-entraining agent). Limestone, with two different gradations, was used as coarse aggregate in 10 mixes and quartzite was used in one mix.

Chemical shrinkage tests were performed for pastes. Autogenous and free drying shrinkage tests were performed for mortar and concrete. In addition, restrained (ring) shrinkage tests were performed for concrete on all 11 mixes. Mechanical properties (such as elastic modulus and compressive and splitting tensile strength) of these concrete mixes were also evaluated at different ages. Creep coefficients of these concrete mixes were estimated using International Union of Laboratories and Experts in Construction Materials, Systems and Structures (RILEM) B3 and National Cooperative Highway Research Program (NCHRP) Report 496 models. Cracking potential of the concrete mixes was assessed based on the simple stress-to-strength ratio method as well as the ASTM C 1581 stress rate method.

The following observations and conclusions can be drawn from the experimental work:

- Among the 11 mixes studied, three of them (Mixes 4, 5, and 6) cracked during the restraint ring tests. Mix 4 had two of three specimens cracked at 13 and 18 days. Mix 5 had one of three specimens cracked at 11 days; and Mix 6 had its three ring specimens cracked at 16, 16.5, and 18 days.
- Autogenous shrinkage of the HPC mixes ranged from 150 to 250 microstrain and free dying shrinkage of the HPC mixes ranged from 700 to 1200 microstrain at 56 days.
- Predictions based on the simple peak shrinkage stress-to-splitting tensile strength ratio with the consideration of concrete creep indicates the following:
  - Mixes 4, 5, and 6 have high cracking potential, which is consistent with the results of ring tests and only the concrete rings made with these three mixes cracked.
  - Mixes 1, 7, 8, 9, and 10 have medium cracking potential.
  - Mixes 2, 3, and 11 have low cracking potential.
  - This method seems to provide a better prediction for concrete cracking potential than the

ASTM C 1581 average stress rate method.

- Not all mixes having high shrinkage cracked. Cracking is associated mainly with restrained shrinkage strain, modulus of elasticity, and creep coefficient. This behavior can be observed in Mixes 7 and 10, which had comparable shrinkage to Mixes 4 and 6 but did not display cracking.
- 20% Class C fly ash replacement for cement reduced all types of shrinkage in paste, mortar, and concrete.
- 25% ground granulated blast-furnace slag (GGBFS) replacement for cement reduced chemical shrinkage of paste and autogenous shrinkage of mortar noticeably, but it increased free drying shrinkage and restrained shrinkage of concrete significantly.
- Replacing cement by 20% fly ash and 5.6% metakaolin increased chemical shrinkage of paste and autogenous shrinkage of concrete. However, it had little effect on restrained shrinkage of concrete.
- Mixes with cement content greater than 700 lb/yd^3 (Mixes 4 and 6) showed high potential for cracking.
- Mixes made with Type I cement yielded greater shrinkage than those made with Type I/II cement, which in turn yielded greater shrinkage than those made with Type IP cement.
- Mixes with high cementitious material content generally displayed high total (autogenous + free drying) shrinkage.
- Mass loss shows a strong linear relation with free drying shrinkage for a given mix.
- The trend of free drying shrinkage of mortar is similar to that of concrete.
- The stress resulting from restrained drying shrinkage has an acceptable linear relationship with the stress from free drying shrinkage of concrete.

The following recommendations are proposed based on the above observations and conclusions:

- Use of GGBFS and metakaolin alone generally increases free and restraint drying shrinkage of concrete. They should be used together with fly ash in the concrete for bridge deck and overlays.
- The order of preference for cement selection may be Type IP, Type I/II, and then Type I in consideration of shrinkage cracking resistance.
- Drying shrinkage increases with the cementitious content and paste volume of concrete. Cautions should be taken when total cementitious material content in concrete is over 700 lb/yd^3.
- Results from mortar shrinkage measurements can be used as a good indicator for concrete shrinkage.
- The simple calculation of shrinkage stress-to-splitting tensile strength ratio with consideration of creep can be used to estimate concrete cracking potential.
- Creep behavior of these concrete mixes were estimated based on the existing models used for this project and should be measured in the future.
- Some shrinkage control methods, such as internal curing (IC) and use of shrinkage-reducing agents (SRAs), may be considered for use in mixes 4, 5, and 6 to control concrete cracking.
- The research implementation may include modifying high and moderate shrinkage cracking potential mixes by using IC/SRA and/or by balancing the water-to-binder ratio, cementitious content, and tensile strength. It is proposed to conduct a field study and to monitor and compare the performance of the high and low shrinkage cracking mixes side-by-side.

1. INTRODUCTION

1.1 Problem Statement

High-performance concrete (HPC) is used increasingly in building and bridge structures due to its high strength, superior low-permeability, and excellent durability. However, because of the high cementitious material content, low water-to-cementitious material ratio (w/cm) or water-to-binder ratio (w/b), and various admixtures in the concrete, HPC used in bridge decks and overlays often possesses a high risk of shrinkage cracking. Over the past decade, many states in the US have reported shrinkage-induced cracking in bridge concrete at early ages (Wan et al. 2010, Whiting et al. 2000) and this problem is a great concern in Iowa.

Cracks weaken concrete and permit water and harmful chemical ingress into the structures, thereby accelerating the deterioration and corrosion of reinforcement in concrete (Shah et al. 1997). Shrinkage causes concrete slabs to curl and warp, which affects the girder-to-deck composite action, ultimately decreasing the load-carrying capacity of the bridge (Tarr and Farny 2008). In addition, shrinkage may bring about stress loss in prestressed concrete structures and affect camber and deflection of bridge girders.

To assess the crack risk of HPC, it is important to understand its shrinkage behavior (such as shrinkage components, amount, and occurring time). To control the cracking, it is necessary to compensate for the effects of material constituents (i.e., cementitious materials, aggregate, and admixtures) on the concrete shrinkage behavior (Krauss and Rogalla 1996, Miyazawa and Monteiro 1996, Cusson and Hoogeveen 2007).

A great deal of research has been conducted in the US on fiber reinforcement and internal curing of concrete in an attempt to reduce shrinkage-induced cracking. However, little study has been performed in Iowa. This study is aimed at filling the research gap and investigating the shrinkage behavior of HPC used in Iowa bridge decks and overlays.

In this study, the major shrinkage components (chemical, autogenous, and drying shrinkages) of 11 typical batches of HPC mixtures used commonly in Iowa are examined. The magnitude of the shrinkages and effects of material constituents on these shrinkages are evaluated. It is expected that the research results will provide Iowa engineers with the insight needed to improve both concrete mix proportion and construction practices to reduce the shrinkage-induced cracking of HPC bridge decks and overlays.

1.2 Background

Concrete shrinkage is composed of plastic shrinkage, chemical shrinkage, autogenous shrinkage, drying shrinkage, and carbonation shrinkage. Mechanisms for these shrinkages have been studied extensively.

Plastic shrinkage occurs in wet concrete, when the rate of water evaporation on a concrete surface is higher than the rate of water bleeding inside the concrete. An effective way to control plastic shrinkage is to control the rate of water evaporation on the concrete surface.

Chemical shrinkage results from cement hydration and produces a product with a decreased volume. This shrinkage is related directly to the chemistry and degree of hydration of cementitious materials, and it is an internal reduction of volume.

Autogenous shrinkage is defined as a volume change when concrete has no moisture transfer to the surrounding environment. It occurs in different stages, even during the very early stage while the concrete is still liquid. As cement hydrates, more water is consumed and concrete starts stiffening. During this stiffening stage, water menisci develop in fine pores, and they generate stress on the pore walls, causing the concrete to shrink. As cement hydration continues consuming more water from the concrete, especially in the concrete with a low w/b (<0.4) or with silica fume, some pores in the paste become empty, and the concrete is subjected to self-desiccation. As concrete reaches a hardened stage, self-desiccation results in shrinkage. Different from chemical shrinkage, autogenous shrinkage is an external volume reduction.

Drying shrinkage results from the water loss in hardened concrete. In concrete, the mixing water, which is designed for cement hydration and workability, is often not completely consumed by cement hydration. It will evaporate when the concrete is exposed to a drying condition. As the water leaves, the concrete shrinks due to the development of capillary tension, surface tension, and disjoining pressure (Rougelot et al. 2009). When the ambient relative humidity (RH) is sufficiently low, the interlayer water in the calcium-silicate-hydrate (C-S-H) gel in concrete may also be removed and cause the concrete to shrink.

Drying shrinkage is closely related to the amount of water, the structure (size and distribution) of the pores, and the chemistry of the pore solutions in concrete. Typical concrete drying shrinkage has been measured at 520 to 780 millionths, but it can potentially exceed 1100 millionths (Tarr and Farny 2008). Although having a low w/b, HPC may have comparable or higher water content to/than normal-strength concrete (NSC) and, therefore, also display significant drying shrinkage.

Carbonation shrinkage occurs when the concrete is exposed to air containing carbon dioxide (CO_2), which reacts with cement constituents as well as cement hydration products. The carbonation process proceeds slowly and usually produces a small shrinkage at relative humidity below 25%, or near saturation.

Most shrinkage results from the paste, while aggregate in concrete generally resists shrinkage. Besides environmental conditions (relative humidity and temperature) and configuration of structures (size and shape of a concrete member), concrete shrinkage is affected significantly by its mix characteristics, such as type of cementitious materials, w/b, water or paste content, type of aggregate, and fine-to-coarse aggregate ratio.

HPC is known as a type of concrete with adequate workability, high strength, high elastic modulus, low permeability, and enhanced durability. Because of its high strength or low w/b, HPC risk of autogenous shrinkage is greater than NSC. Because of its high paste content or reduced aggregate content, HPC risk of drying shrinkage may also be greater than NSC. In addition, water reducers (WRs) are commonly used in HPC, and they change concrete pore structures (pore size and distributions) and pore chemistry and may contribute to overall shrinkage. With high shrinkage potential, the use of HPC in bridge decks and overlays has not solved all of the durability problems in concrete practice.

In recent years, a great deal of work has been done on autogenous shrinkage of HPC. Lee et al. (2006) found that at the same w/b, granulated blast furnace slag (GBFS) concrete exhibited higher autogenous shrinkage than that of their control concrete. The researchers suggested that the GBFS replacement level and particle shape contributed greatly to the high level of shrinkage. Persson (1998) observed that shrinkage of HPC was dependent on the type and content of silica fume. The autogenous shrinkage results mainly from the pore refinement and decline of the internal humidity in HPC.

Note that, although various studies have been conducted on HPC shrinkage, not all of the results may be applicable to concrete made with local constituents (e.g., aggregates) due to the complex effects of concrete materials on shrinkage. This research focused on the HPC mixes used for Iowa bridge decks and overlays.

1.3 Objectives

The overall objective of this study was to investigate the shrinkage behavior of HPC used for Iowa bridge decks and overlays. The specific objectives of this investigation include the following:

- Identify major components of shrinkages (chemical, autogenous, and drying shrinkages) in Iowa bridge concretes
- Evaluate the influence of various constituent materials, such as types and contents of cementitious material and aggregate, and admixtures, on these shrinkages
- Provide recommendations for improving Iowa HPC mix design and construction practice to reduce the shrinkage-induced cracking

1.4 Scope

In this study, 11 HPC mixes recommended by the Iowa Department of Transportation (Iowa DOT) were evaluated. The chemical shrinkage of paste samples, autogenous shrinkage and free drying shrinkage of mortar and concrete specimens, and restrained ring shrinkages and cracking of concrete specimens were all measured in accordance with the related ASTM specifications. Compressive strength, splitting tensile strength, and elastic modulus of concrete specimens were also tested.

2. LITERATURE REVIEW

This chapter introduces primary research on concrete shrinkage, including the mechanisms and models, test methods, factors that influence chemical, autogenous, drying and restrained shrinkage, and shrinkage cracking behaviors.

2.1 Chemical Shrinkage

When cement reacts with water, there is a diminution in the sum of their volumes, called chemical shrinkage (Tazawa et al. 1995). Hydration of the primary cement clinker minerals and also the secondary reactions, including ettringite formation, result in chemical shrinkage (Jensen and Hansen 1999). Chemical shrinkage amounts to typically 6 to 7 ml/100g of cement reacted (Tazawa and Miyazawa 1995). Related to the hydration process, it is the driving force of autogenous shrinkage. Research has indicated that the early-age shrinkage also contributes significantly to the ultimate shrinkage of the concrete, thus increasing risk of the concrete cracking at the later age (Holt 2001).

2.1.1 Mechanism and Models

Cement hydration is a complex set of exothermic chemical reactions. Each chemical compound may react with water in different ways, each reaction has its own volume stoichiometry, and the reaction (or hydration) products may undergo transition to different forms. There are several mechanisms by which a cement paste changes its volume (shrinks or swells) during a hydration process under a sealed condition, or without moisture transfer from the paste to the environment.

The major mechanisms include hydration shrinkage, self-desiccation shrinkage, thermal contraction or expansion, crystallization swelling, and shrinkage due to phase transition or dehydration. These volume changes in a cement paste or concrete may occur simultaneously. It is the overall shrinkage, which is often measured from samples under a sealed condition, that controls concrete performance.

Given that chemical shrinkage of concrete is induced by cement hydration, the magnitude of chemical shrinkage is related directly to cement chemistry and degree of cement hydration. All chemical constitutes in cement that have fast hydration rates (such as tricalcium silicate/C_3S compared to dicalcium silicate/C_2S) can result in a high chemical shrinkage at early age. Although small percentages, tricalcium aluminate/C_3A, tetracalcium aluminoferrite/C_4AF and potassium oxide/K_2O cement constituents are found to influence autogenous shrinkage 10 times as large as C_2S and C_3S (Persson 2000).

Previous research has shown that the chemical shrinkage of a cement paste can be determined by its chemical composition. The basic reactions of cement phase composition are generally defined by four reactions of C_3S, C_2S, C_3A, and C_4AF. Holt (2001) and Tazawa et al. (1995) reported that the magnitude of chemical shrinkage can be estimated using the molecular weight and densities of the compound as they change from the basic to reaction products. The basic

reactions of cement phases are well understood and defined generally by the following equations, which can be also found in the studies of Mounanga et al. (2004) and Tazawa et al. (1995).

C_3S: $C_3S + 5.3\ H \rightarrow C_{1.7}SH_4 + 1.3\ CH$ (**2-1**)

C_2S: $C_2S + 4.3\ H \rightarrow C_{1.7}SH_4 + 0.3\ CH$ (**2-2**)

C_3A: $C_3A + 6\ H \rightarrow C_3AH_6$ (**2-3**)

$C_3A + 3\ C\bar{S}H_2 + 26\ H \rightarrow C_6A\ \bar{S}_3H_{32}$ (**2-4**)

$C_6A\ \bar{S}_3H_{32} + 2\ C_3A + 4\ H \rightarrow 3\ C_4A\ \bar{S}H_{12}$ (**2-5**)

C_4AF: $C_4AF + 3\ C\bar{S}H_2 + 30\ H \rightarrow C_6A\ \bar{S}_3H_{32} + CH + FH_3$ (**2-6**)

$C_6A\ \bar{S}_3H_{32} + 2\ C_4AF + 12\ H \rightarrow 3\ C_4A\ \bar{S}H_{12} + 2\ CH + 2\ FH_3$ (**2-7**)

$C_4AF + 10\ H \rightarrow C_3AH_6 + CH + FH_3$ (**2-8**)

Using the densities and molar volume of cementitious materials (Bentz 1997), it is possible to calculate the chemical shrinkage (V_{CS}) based on the differences in volumes between initial or basic reactants (V_b) and final hydration/reaction products (V_r).

2.1.2 Test Methods

Justnes et al. (2000a) listed three principal measurement methods of chemical shrinkage: dilatometry, gravimetry, and pycnometry. The principles of the three methods are shown in Figure 2.1.

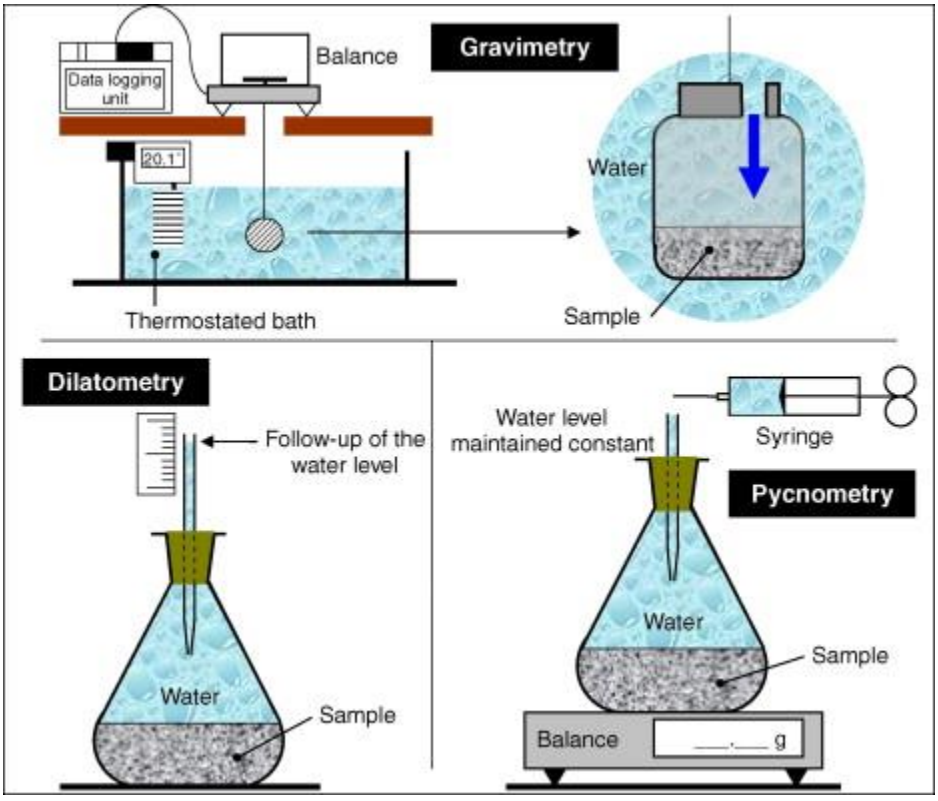

Figure 2.1. Chemical shrinkage measurement methods (Bouasker et al. 2008)

ASTM C 1608, Test Method for Chemical Shrinkage of Hydraulic Cement Pastes, measures the internal (absolute) volume change of hydraulic cement paste that results from hydration using dilatometry. The chemical shrinkage is expressed as the measured grams of absorbed water per gram of cement in the tested paste specimen. Although time-consuming, this method is relatively precise and economical and is therefore widely used.

Gravimetry is an indirect measurement of volume change by recording reduced buoyancy under water by weighing. If the weight change of a container filled with paste and excess water having at least one flexible wall was recorded, the chemical shrinkage was measured). The setup is shown in Figure 2.2.

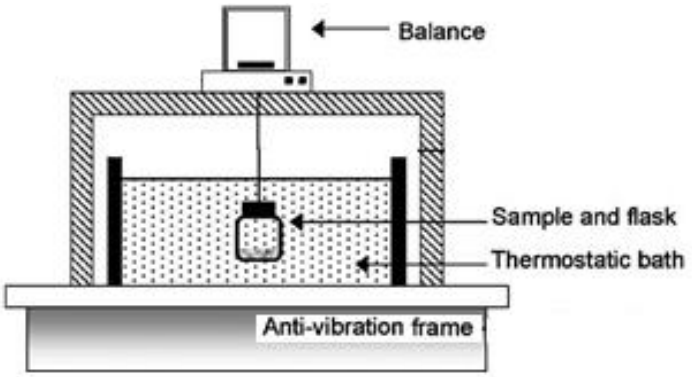

Figure 2.2. Schematic diagram of the test device used for chemical shrinkage measurements using the gravimetry method (after Lura and Jensen 2007)

As shown in Figure 2.3, the comparison of punctual measures by dilatometry and continuous measures by the weighing method indicated a very good correlation of the two types of results (Boivin et al. 1998).

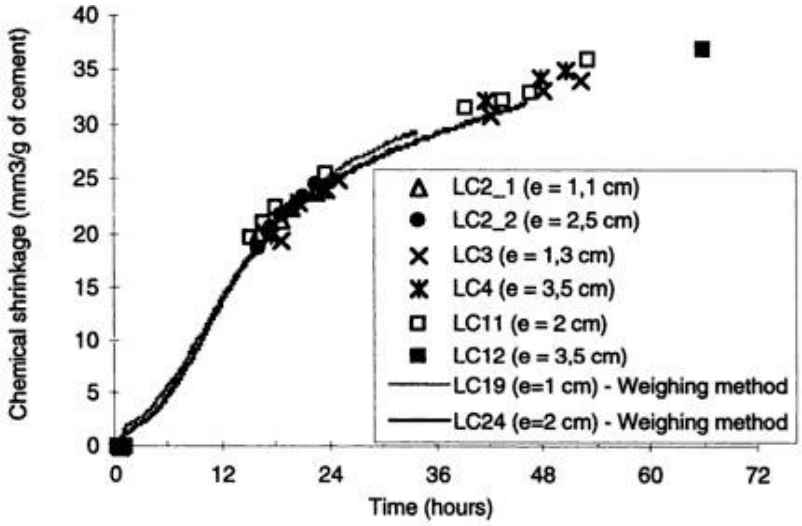

Figure 2.3. Comparison between measures by dilatometry and gravimetry (Boivin et al. 1998)

The third method, pycnometry, is carried out by filling a pycnometer with paste and topping it with water. Water is added to refill the pycnometer at different ages, and the weight increase relates to the total volume change.

2.1.3 Factors Influencing the Measurements

The four main minerals in cement, tricalcium silicate (C_3S), dicalcium silicate (C_2S), tricalcium aluminate (C_3A), and tetracalcium aluminoferrite (C_4AF), have different hydration rates and induce different volume changes. Justnes et al. (1999) confirmed C_3A contributes significantly to chemical shrinkage because C_3S is the most abundant mineral in cement clinker, which induces larger volume reductions than C_2S. The results shown in Figure 2.4 indicated the enhanced reactivity of the finer cement relative to the coarser one led to the desired higher chemical shrinkage (Bentz et al. 2008).

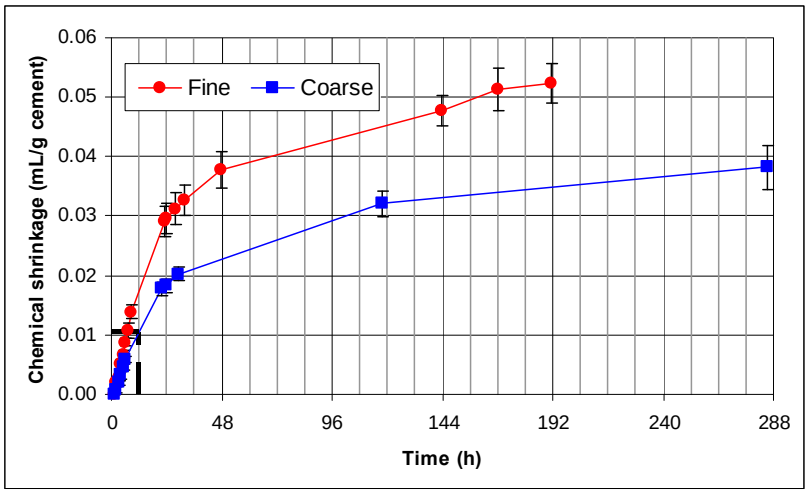

Figure 2.4. Chemical shrinkage at 25°C for w/c = 0.35 cement pastes (Bentz et al. 2008)

Greater shrinkage was found in the reaction of silica fume with calcium hydroxide: about 20 ml/100g of silica fume reacted (Jensen and Hansen 2001). Wild et al. (1998) observed an increase in chemical shrinkage of cement pastes containing between 0 and 15% metakaolin (MK), but at MK content greater than 15%, the researchers observed a reduction in chemical shrinkage. Cement with fly ash showed less chemical shrinkage than pure cement in the first 16 hours with a water-to-cement ratio (w/c) of 0.375. It could be explained by the fact that the pozzolanic reaction of fly ash is much slower. When ground to an ultrafine state, the ground granulated blast-furnace slag (GGBFS) could be very active and apparently promoted hydration of cement (Sarkar 1994) and, thus, increased the amount of cement hydration and chemical shrinkage.

Test results showed that the super-plasticized mixture has chemical shrinkage greater than the reference mixture in the first 72 hours. It may be a result of the improved cement dispersion and faster rate of hydration reactions generating shrinkage (Tazawa and Miyazawa 1995).

Several references can be found to investigate the influence of the sample size (thickness) of the tested cement paste on the final value of the chemical shrinkage (Tazawa et al. 1995, Boivin et al. 1998). It was found for low w/c, the chemical shrinkage decreased with increasing sample thickness (Sant et al. 2006). This effect was not observed for ratios equal to or greater than 0.4.

2.2 Autogenous Shrinkage

Different from chemical shrinkage, which is an internal volume change, autogenous shrinkage of cement paste and concrete is defined as the external macroscopic volume change occurring with no moisture transferred to the exterior surrounding environment (Aitcin 1998). The relationship between chemical and autogenous shrinkages is shown in Figure 2.5.

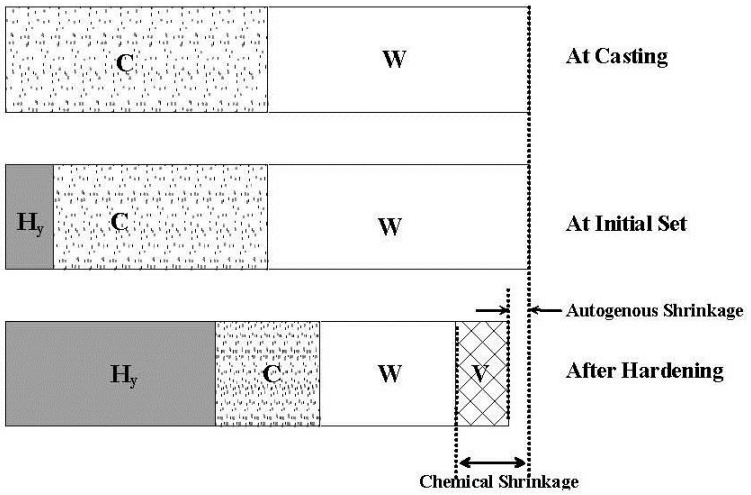

Figure 2.5. Relationship between chemical shrinkage and autogenous (Japan Concrete Institute 1999)

Sant et al. (2006) compared the results of chemical and autogenous shrinkage for a paste with a w/c of 0.30. After setting, the shrinkage that was measured in a hardening sealed specimen (i.e., the autogenous shrinkage) was much less than the chemical shrinkage, given that the newly-formed structure of the cement paste resists the volume change. Although there was agreement that the chemical and autogenous shrinkage diverge around the time of set, there was a lack of a consistent standard to measure the response of these materials at early ages (Aitcin 1998, Justnes et al. 2000b).

2.2.1 Mechanism and Models

Barcelo et al. (2005) thought it was clear that autogenous shrinkage could not be explained only by the physical mechanism of self-desiccation induced by the volume balance of hydration. It seemed that the creation of the early hydrated products resulted in an autogenous swelling phenomenon that decreases with time. The researchers summarized the mechanism of autogenous shrinkage of cement paste as shown in Figure 2.6.

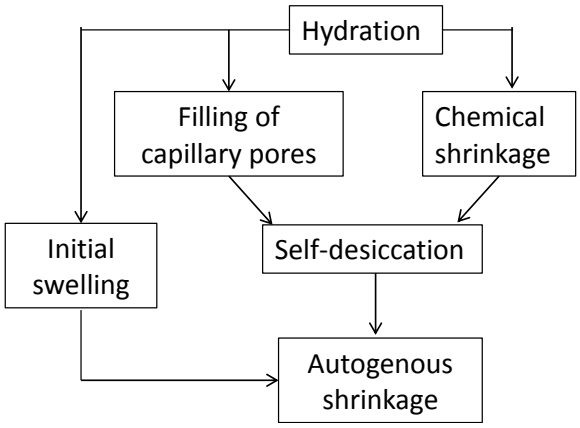

Figure 2.6. Proposed mechanism of autogenous shrinkage at early age (after Barcelo et al. 2005)

Various mechanisms suggested to cause autogenous shrinkage were evaluated from the point of view of their soundness and applicability to quantitative modeling of autogenous shrinkage by Lura et al. (2003). The researchers thought the capillary tension approach is advantageous, because it has a sound mechanical and thermodynamical basis. Hua et al. (1997) studied the autogenous shrinkage on a macroscopic scale and also on the scale of the hydrating grains, without going into the colloidal details of the hydrates. They thought self-desiccation is a consequence of hydration, and that hydration takes place only at high relative humidity.

2.2.2 Test Methods

Measurements of the autogenous strain of cement paste have been carried out in two different ways: measurement of volumetric strain and measurement of linear strain. Volumetric measurement is performed by placing the fresh cement paste in a rubber membrane submerged in water. The change in volume of the cement paste is measured by the amount of water displaced. Linear measurement is performed by placing the cement paste in a rigid mold with low friction. The length change of the cement paste may be recorded at the end of the specimen.

The volumetric method indicates three to about five times higher strain than the linear technique. One reason for the inconsistency between the strain measurements after setting is transport of water through the rubber membrane, occurring when the buoyancy liquid used is water. After setting, penetrated water may partially fill the internal voids produced by chemical shrinkage, causing an increase of the submerged weight or a decrease in the water level that is interpreted as volumetric shrinkage.

According to ASTM C 1698, which was adopted in this study, a sealed, flexible, corrugated mold system combines the advantages of linear and volumetric measurement of autogenous strain, while avoiding most of the disadvantages. A specimen of freshly-mixed paste or mortar is prepared using a corrugated mold that offers little resistance to length change of the specimen.

2.2.3 Factors Influencing the Measurements

It was found by Tazawa and Miyazawa (1995) that alumina cement and high-early-strength cement exhibit large early autogenous shrinkage and lead to large ultimate shrinkage. Moderate-heat cement and belite-type low-heat cement show small autogenous shrinkage. Blast-furnace slag cement shows large autogenous shrinkage over a long period. Autogenous shrinkage depends greatly on the contents and degree of hydration of C_3A and C_4AF. Finer grain cement leads to greater shrinkage starting at an earlier age. A cement with a fineness of 5570 cm^2/g or higher undergoes an autogenous shrinkage of 1000 to 1200 $\times 10^{-6}$ at an age of 24 hours.

Results showed that autogenous shrinkage increased corresponding to the increase in the degree of hydration of fly ash (Termkhajornkit et al. 2005). The autogenous shrinkage and the pore structure of the hardened cement paste with the combination of fly ash and silica fume, or fly ash and blast furnace slag, were tested (Li et al. 2010). The results indicated fly ash can reduce the autogenous shrinkage, silica fume can increase the autogenous shrinkage, and the effect of blast furnace slag is between those two.

Jiang et al. (2005) investigated the effects of w/b, silica fume (SF), and GBFS on autogenous RH change and autogenous shrinkage (AS) of HPC pastes. The results indicated that w/b is a chief factor that affects autogenous RH change and AS of cement pastes. The lower the w/b, the higher the autogenous RH reduction and the AS increment. SF increases the autogenous RH reduction and AS increment of cement paste at early ages, and GBFS increases the autogenous RH reduction and AS increment at later ages.

The autogenous shrinkage of concrete made with w/b ranging from 0.27 to 0.42 and blast-furnace slag (BFS) replacement level of 0, 30, and 50% was evaluated by Lee et al. (2006). The concrete made with BFS exhibited higher autogenous shrinkage than ordinary concrete without any BFS, and the higher the BFS replacement level, the greater the autogenous shrinkage at the same w/b.

Gleize et al. (2007) reported the effects of partial replacements (5, 10, 15, and 20%) of portland cement by high-purity MK on the autogenous shrinkage of pastes (w/b of 0.3 and 0.5). It is shown at early ages that the increase of autogenous shrinkage of the cement-MK pastes was due to heterogeneous nucleation, and that the long-term autogenous shrinkage of cement-MK pastes, for both w/b ratios, decreased as the cement replacement level with MK increased.

Meddah et al. (2011) found that the addition of a combination of shrinkage-reducing agents (SRAs) and expansive additives (EXAs) resulted in a significant reduction and a gradual development of both autogenous shrinkage and self-tensile stress.

Baroghel-Bouny et al. (2006) found that w/c does not influence the rate and magnitude of chemical shrinkage in a significant manner within the w/c range of 0.30 to 0.60 and the curing temperature range of 10° to 50°C. However, w/c has a kinetic effect within the w/c range of 0.25 to 0.30. At a given age, the magnitude of one-dimensional autogenous shrinkage increases

linearly as w/c decreases from 0.60 to 0.25 as a result of the self-desiccation process and the structural swelling. Conversely, the magnitude of "pure" drying shrinkage decreases as w/c decreases from 0.60 to 0.25.

2.3 Drying Shrinkage and Restrained Ring Shrinkage

2.3.1 Mechanism and Models of Drying Shrinkage

Drying shrinkage is caused by the loss of internal water. As shown in Figure 2.7, there are two cement particles at the surface of a paste subjected to drying (Radocea 1992). When the evaporating water (W) exceeds the internal water, which moves from the inside of the concrete to the surface, a stress generates and it causes the meniscus to be lowered with the increasing capillary pressure. As the diameter of the capillary decreases, the capillary pressure (and therefore the shrinkage) increases accordingly.

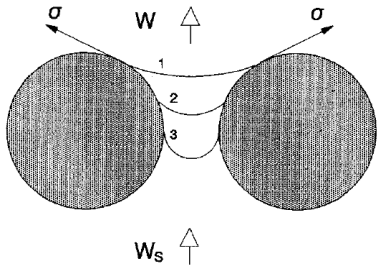

Figure 2.7. Stresses pulling the water meniscus lower between two cement particles due to moisture transfer and capillary pressure development (Radocea 1992)

Mehta and Monteiro (1993) described the various pore sizes along with the solid particles of the hydrated cement paste (Figure 2.8). Holt (2001) and Koenders (1997) studied the pore size distribution in concrete. The interaction of the pore spaces and internal water is influenced by the surrounding environment. As the pore size decreases, the internal relative humidity quickly drops, which in turn induces stress and shrinkage.

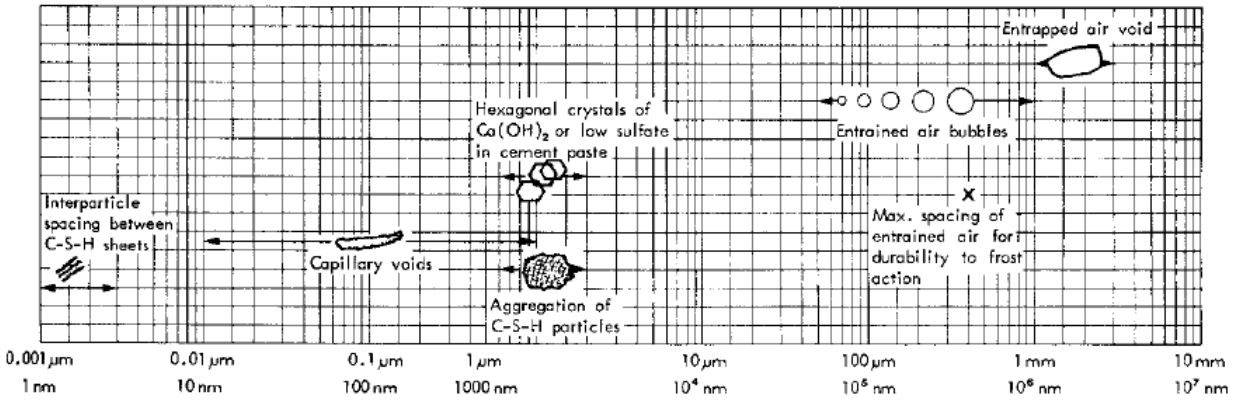

Figure 2.8. Distribution of solids and pores in hydrated cement paste (Mehta and Monteiro 1993)

2.3.2 Test Methods

ASTM C 157/C 157M-08 specifies the measurement of length change of mortar prisms due to drying shrinkage. ASTM C 1581 describes evaluation of concrete cracking potential of restrained ring samples under drying conditions. Figure 2.9 and Figure 2.10 show sample configuration and test results.

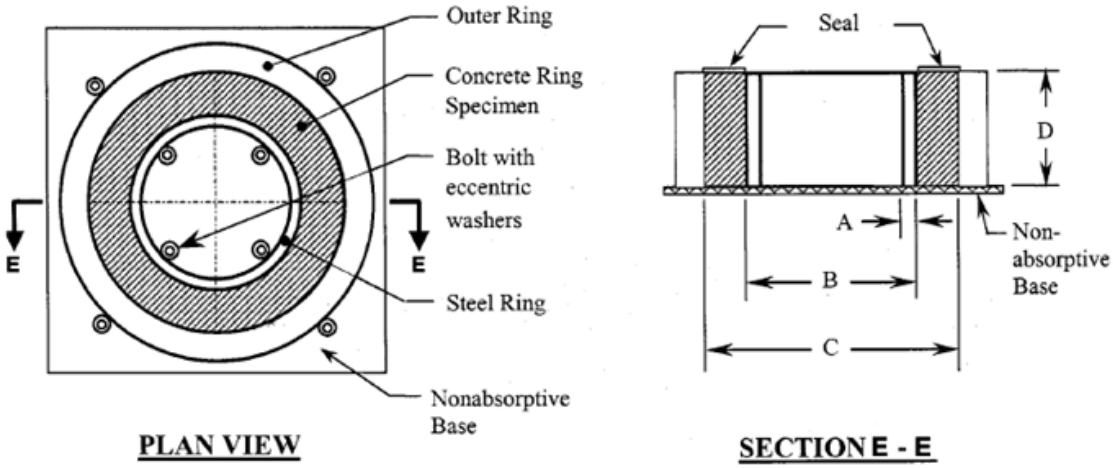

Figure 2.9. Setup for ring tests

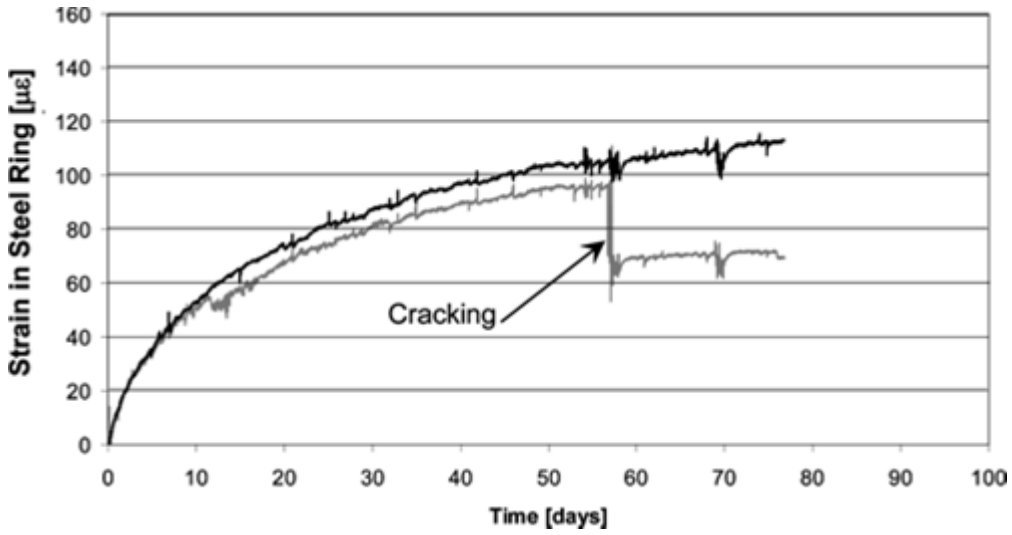

Figure 2.10. Sample results from restraint ring tests (Brown et al. 2007)

Based on the modified ASTM C 157, Mokarem et al. (2008) studied the measurement of early-age shrinkage of Virginia concrete mixtures (Figure 2.11). The early-age specimens were tested for the first 24 hours after casting in the modified molds. The specimens were covered with wet burlap and plastic during the duration of testing. The length change measurements were performed using linear variable differential transformers (LVDTs) and the data were acquired using a data acquisition machine. After testing, the data were downloaded and compiled.

Figure 2.11. Bolt/washer assembly and test setup with LVDTs (Mokarem et al. 2008)

Given that drying shrinkage is greatest at the surface exposed to the environment, it caused nonlinear shrinkage profiles to develop through the thickness. The resulting differential strain causes axial and bending stresses. The restrained ring is used to evaluate cracking sensitivity or time to cracking due to restrained drying shrinkage. A concrete annulus was cast around a stiff steel ring that restrains the shrinkage, resulting in the development of tensile stresses (Hansen 2011).

2.3.3 Factors Influencing Drying Shrinkage and Restrained Cracking

Al-Attar (2008) found that using saturated coarse aggregate always yields higher shrinkage strain than dry aggregate. The percentage increase seemed to be affected by the aggregate water absorption. Almudaiheem and Hansen (1987) found that shrinkage decreases with increasing aggregate content and that aggregate content had a more profound influence on shrinkage than did the specimen size.

Hooton et al. (2008) studied the effect of slag cement on drying shrinkage and observed that the paste fraction of concrete is normally the only part that undergoes drying shrinkage. Therefore, minimizing and maximizing the paste volume is the most important consideration. In an investigation on expansive cement by Saito et al. (1991), it was determined that expansive cement as a mortar showed a large amount of shrinkage reduction. Expansive cement used in concrete had a more negligible effect on shrinkage.

Gupta et al. (2009) presented the results of an experimental investigation carried out to evaluate the shrinkage of high-strength concrete, which was made by partial replacement of cement with fly ash and silica fume. The conclusion could be drawn that the shrinkage strain of concrete with replacement of cement by 10% fly ash and silica fume, respectively, at various ages were more (6 to 10%) than the shrinkage strain of concrete without fly ash and silica fume.

Quangphu et al. (2008) studied the influence of shrinkage-reducing admixtures (SRAs) on drying shrinkage of HPC. Conclusions could be drawn (Figure 2.12) that the SRA effectively reduces some mechanical properties of HPC. The shrinkage strains of HPC with SRA were only as high as 41% of the average free shrinkage of concrete without SRA after 120 days of drying.

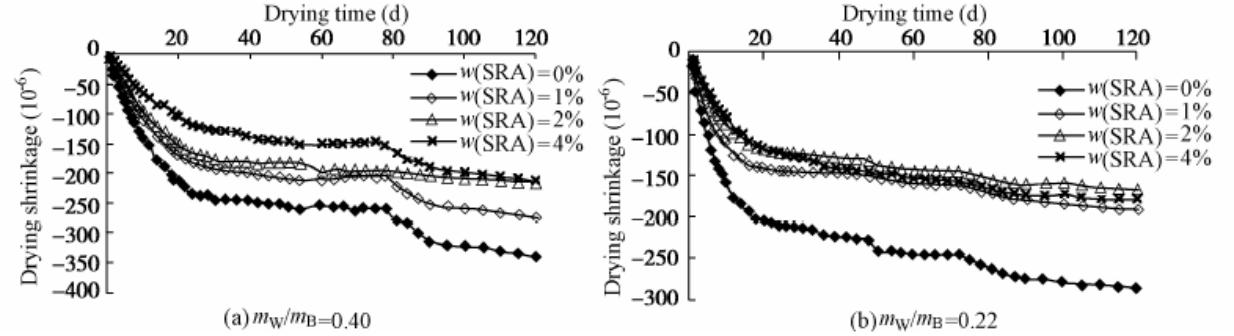

Figure 2.12. Drying shrinkage of HPC with and without SRA (Quangphu et al. 2008)

Specimens were exposed to different temperature, humidity, and wind conditions to monitor the moisture loss and cracking of specimens (Almusallam et al. 1999). It was shown that the relative humidity had a direct effect on the rate of water evaporation when no wind was present. However, as the wind became a factor, the relative humidity had less or no impact on the rate of evaporation and, as expected, temperature had a direct influence on the rate of water evaporation.

2.4 Research on Shrinkage-Induced Cracking

Igarashi et al. (2000) investigated the development of internal stresses induced by restrained autogenous shrinkage in high-strength concrete at early ages. The restrained autogenous shrinkage resulted in a relatively high stress that sometimes caused premature cracking in the high-strength concrete. This occurred mainly when the ratio between the restraining stress and the tensile strength approached 50%.

Yang et al. (2005) experimentally investigated autogenous shrinkage of high-strength concrete containing silica fume under drying at early ages. The results showed that the percentage of autogenous shrinkage was macroscopically 50 to 20% based on the present method, while it was 70 to 30% based on the conventional superposition principle (SP). The latter resulted in overestimating autogenous shrinkage strain under drying conditions.

Darquennes et al. (2011) designed a test rig to monitor autogenous deformation for concretes with different slag content. Restrained shrinkage was studied by means of a temperature stress testing machine. Following these experiments, the slag cement concretes cracked later than the portland cement concrete despite the fact that they are characterized by larger autogenous shrinkage. This behavior is mainly due to the expansion of their cement matrix at early age and their largest capacity to relax internal stresses.

The effect of reinforcement on early-age cracking in high-strength concrete was investigated by Sule and van Breugel (2004). To separate thermal effects, autogenous shrinkage specimens were cured isothermally and semi-adiabatically. Further test variables were the reinforcement percentage (0, 0.75, 1.34, and 3.02%) and configuration (one reinforcement bar and four reinforcement bars). The researchers showed that reinforcement could induce the formation of

smaller cracks. These smaller cracks can postpone the moment at which major cracks are formed.

Kawashima and Surendra (2011) studied the early-age drying shrinkage behavior of fiber-reinforced concrete. The cellulose fibers used in this study were 100% virgin specialty cellulose fibers with an alkaline-resistant coating. They had an average length of 2.1 mm, an average diameter of 16 μm, and a density of 1.1 g/cc. It was found with the w/c = 0.5 mortar (M50), the addition of cellulose fibers did not lead to any reduction in drying shrinkage and that the situation is similar in concrete. Conclusions could be drawn that fiber does not contribute to the unrestrained drying shrinkage in either mortar or concrete. Shah and Weiss (2006) investigated the shrinkage cracking of fiber-reinforced concrete and found that the addition of reinforcing fibers in the mix reduced the crack widths of the concrete significantly.

2.5 Research on Shrinkage and Cracking by Other States

2.5.1 Minnesota (2011)

The Minnesota DOT (2011) collected data during construction of bridges between 2005 and 2011. The data included construction practices and environmental conditions during construction and bridge inspection results. Based on their review of the referenced documents, a series of recommendations, including raw materials, mix proportion design, and construction practice, was proposed, as follows:

- Use Type II Cement and limit cement content to 470 lb/y^3
- Water-to-binder ratio (w/b) should range between 0.40 and 0.45 (preferably 0.40) and the water content should be kept below 300 lb/y^3
- Specify air content of 6 percent or higher by volume
- Coarse aggregate content of 1,800 to 1,850 lb/y^3 and use aggregate size up to 1.5 in.
- Replace 20% of the cement by weight with fly ash and limit silica fume to 6% by weight of cement, and add between 1 and 2% SRA by weight of cement
- Place the deck when the temperatures are between 45°F and 80°F and when the daily temperature fluctuation is less than 50°F; maintain the girder/deck differential temperature under 22°F for at least 24 hours after the concrete is placed, avoid placement when the evaporation rate is 0.20 $lb/ft^2/hr$ for normal concrete and 0.10 $lb/ft^2/hr$ for concrete with w/c of 0.40 or lower, and avoid placements during high winds
- Apply mist water or an evaporation retarder film immediately after screeding; apply a white-pigmented curing compound uniformly in two directions when bleed water diminishes but before the surface dries, protect concrete with a protective barrier, such as wet burlap, curing membranes, vinyl covers, etc., or use the AASHTO "Water Method" for a minimum of 7 days

2.5.2 Illinois (2011)

A study was performed by the Illinois Center for Transportation regarding concrete roadway construction in hot weather (Popovics 2011). The main objective was to develop improved specifications and procedures with respect to monitoring and maintaining plastic concrete temperatures to assure near- and long-term concrete quality in the state of Illinois. Based on their recommendations, the revised specification would read as follows:

"The temperature of mixed concrete immediately before placing shall not be less than 10°C (50°F) nor more than 32°C (90°F). Aggregates and water may be heated or cooled as necessary to produce concrete within these temperature limits. When the temperature of the plastic concrete reaches 30°C (85°F) an approved retarding admixture shall be used. Plastic concrete temperatures of up to 35°C (96°F) immediately before placing may be permitted if the specific mixture has been demonstrated to satisfy the FDOT high temperature mixing procedure test. Mineral admixtures may be used up to 50% cement replacement for these high temperature situations. If the mixture does not pass the FDOT high temperature mixing procedure test, then it is not approved for hot weather use, and work on the project must cease if the concrete temperatures before placement exceed 90°F (32.2°C)." (Popovics 2011)

2.5.3 Wisconsin (2006)

The Wisconsin DOT attempted to control cracking in HPC using high-range, water-reducing admixtures and steel fibers (Naik et al. 2006), but these measures had limited success in reducing deck cracking. Using SRAs in concrete mixes was advocated as one of the most effective ways to reduce shrinkage cracking. SRAs worked by reducing capillary tension in concrete pores, decreasing volume changes as the concrete dries. The objective of this research was to investigate the effectiveness of SRAs for reducing autogenous shrinkage (shrinkage produced independently of external influence) and drying shrinkage in concrete mixtures made with and without fly ash.

The three SRAs showed similar performance in reducing the drying shrinkage and autogenous shrinkage of concrete, eliminating much of the initial drying shrinkage. The admixtures reduced the four-day drying shrinkage for Grade A and A-FA concrete mixtures by up to 67 to 83%, and reduced the 28 day drying shrinkage by up to 48 to 66%. Specific findings included the following:

- In most cases, two of the SRAs worked like water-reducing admixtures and often increased the concrete's strength and its resistance to chloride ion penetration. The third SRA sometimes decreased the concrete's strength, and did not considerably affect chloride ion penetrability.
- None of the SRAs caused changes in air content or slump of fresh concrete mixtures during the first hour.
- Using crushed dolomitic limestone in the concrete mixture led to the lowest early-period drying shrinkage, followed by semi-crushed river gravel and crushed quartzite stone. Over

time, however, the level of drying shrinkage became similar among the three aggregate types, with river gravel often leading to the highest late-period drying shrinkage. Use of 30% more cement and fly ash resulted in either similar or higher autogenous shrinkage and either similar or lower drying shrinkage.

2.5.4 Michigan (2007)

Michigan had a focus on corner cracking in concrete decks of skew highway bridges (Fu et al. 2007). Cracking intensity in the decks was viewed as an effect of several possible causal factors, which were collected from 40 bridge decks, including 20 straight and 20 skewed structures. Analysis of the inspection results indicated no clearly-agreeable causal relations. Two skew decks were instrumented using temperature and strain sensors for the concrete and the ambient environment. Concrete deck temperature and strain response were correlated to thermal, shrinkage, and truck-wheel loads. Test results and thereby-calibrated finite element analysis results showed that the main cause of skew deck corner cracking was cement concrete's thermal and shrinkage load.

Based on current Michigan practice of skew deck design and construction, the following approaches are listed and recommended:

- Reduction or relaxation of constraint. Changing the composite deck configuration to a noncomposite or less composite one can be an option. At the end of a span, reducing the rigidity of the end diaphragm or backwall can reduce the constraint as well. For concrete bridges, smaller end diaphragms should be considered to reduce the stiffness of the constraint to the deck. In the case of backwall encasing the beam ends, the stiffness of the backwall should be minimized if possible.
- Optimization of the ingredients in the concrete mix to reduce the potential of cracking, by reducing the heat to be generated in a short period of time and the tendency of shrinkage. One option is to change the type of cement used.
- Increase the amount of steel reinforcement in the acute angle corner areas and the end areas of skewed decks, to reduce the stress in the concrete deck. These areas will benefit from such reinforcement in the direction along the skew for potential cracking perpendicular to it. Specifically, additional reinforcement along the deck edge (i.e., along the beam support line) is recommended over one beam spacing in the longitudinal direction, with a spacing of 4 in. in both top and bottom layers. To minimize possible complexity in construction, the top and bottom additional rebar sizes can be respectively the same as those regularly designed.

2.5.5 Virginia (2008)

Using a modified ASTM C 157 test method, Mokarem et al. (2008) studied early-age shrinkage of various Virginia concrete mixtures. Through this study, the researchers found that early-age shrinkage of typical (A4) concrete mixtures with and without slag cement, fly ash, or silica fume is less than the early-age shrinkage of A4 ternary concrete (PC, slag, and fly ash), rapid-hardening cement overlays, and lightweight self-consolidating concrete mixtures. Early-age

shrinkage of mixtures with rapid hardening cements is greater than that of mixtures using portland cement, slag cement, fly ash, or silica fume. Mixtures with lower early-age shrinkage tended to have greater shrinkage at later ages and greater total shrinkage than mixtures with higher early-age shrinkage.

2.5.6 Florida (2005)

Tia et al. (2005) evaluated shrinkage cracking potential of concrete used in bridge decks in Florida. The result of the testing program indicated that use of SRAs was effective in reducing the free shrinkage strains and shrinkage-induced stresses of all of the concrete mixtures tested, while the compressive strength, splitting-tensile strength, and elastic modulus of the concrete were not significantly affected. The addition of fly ash as a mineral admixture was found to be effective in reducing the free shrinkage strain and shrinkage-induced stresses of the concrete.

2.5.7 Texas (2003)

The mechanisms of drying and autogenous and carbonation shrinkage were presented and discussed along with related creep issues (Folliard et al. 2003). Thermal stresses also played a role in bridge deck cracking. These stresses resulted from the heat of hydration, diurnal temperature changes, and solar radiation. Current and proposed test methods were introduced and evaluated. Both conventional and innovative methods of controlling drying shrinkage were presented. Some innovative materials were discussed, including fibers, shrinkage-compensating concrete, SRAs, and extensible concrete. The use of innovative materials combined with improved design and construction practices could eliminate restrained shrinkage cracking.

Folliard et al. (2003) investigated use of fibers, SRAs, calcium-sulfoaluminate admixtures (CSAs), and high-volume fly ash to control drying shrinkage cracking in Texas concrete bridge decks. The investigators reported that the SRA mixture has a smaller overall shrinkage amount compared to the other mixtures, but only for the specimens kept in the moisture- and temperature-controlled shrinkage room. SRA failed to provide a lower shrinkage value when subjected to the field conditions.

The CSA mixture shrinks just as much as the other mixtures do. A fibers mixture will still allow shrinkage to occur but the resultant cracking is spread out, and reduces the manifesting of cracking by limiting crack size. Finally, the HVFA mixture imparts the properties of concrete that help to limit stress buildup, such as high creep, low early strength, and low modulus of elasticity, to the mixture so that stress concentrations around flaws are avoided and crack sizes are minimized.

In this study, free shrinkage of concrete (AASHTO T160), restrained shrinkage (AASHTO PP34-99), and early-age strength properties, specifically compression (AASHTO T22), tension (AASHTO T198), and modulus of elasticity (ASTM C469) testing are highly recommended for determining the propensity for drying shrinkage cracking of concrete. The investigators pointed out that “an individual test by itself will not provide sufficient information as to whether a certain

concrete mixture will have a high or low propensity for drying shrinkage cracking. However, the combination of results from all of these laboratory tests will enable one to determine the relative susceptibility to drying shrinkage cracking."

2.5.8 Transportation Pooled Fund Study (2007)

Deshpande et al. (2007) evaluated the effects of paste volume, w/c, aggregate type, cement type, curing period, and the use of mineral admixtures and superplasticizers on the free shrinkage of concrete with the goal of establishing guidelines to reduce cracking in reinforced concrete bridge decks. The results indicate that concrete shrinkage decreases with an increase in the aggregate content (and a decrease in the paste content) of the mix. For a given aggregate content, no clear effect of w/c ratio on the shrinkage is observed.

In general, granite coarse aggregates result in lower shrinkage than limestone coarse aggregates. A similar conclusion cannot be made with quartzite coarse aggregate, although in some cases shrinkage of concrete containing quartzite coarse aggregate was lower than that of concrete containing limestone.

The use of partial volume replacement of portland cement by Class C fly ash without changing the water or aggregate content generally leads to increased shrinkage. The use of partial volume replacement of portland cement by blast furnace slag without changing the water or aggregate content can lead to increased early-age shrinkage, although the ultimate shrinkage is not affected significantly. An increase in the curing period helps to reduce shrinkage.

The use of Type II coarse ground cement results in significantly less shrinkage compared to Type I/II cement. The use of superplasticizers in concrete appears to increase shrinkage to a certain degree. The results, however, do not present a clear picture of the effect of superplasticizer dosage on shrinkage.

2.6 Summary

As the use of HPC has increased, problems with early-age cracking have become prominent. The reduction in w/b, incorporation of silica fume, and increase in binder content for HPCs all contribute to this problem. The literature review on both chemical shrinkage and autogenous shrinkage found the following general trends:

- Shrinkage increases with paste content (the shrinkage value is generally the highest in paste, followed by mortar, and then concrete)
- Shrinkage is generally higher in the concrete containing fine powders and/or super-plasticizer, probably due to the pore refinement
- Shrinkage potential may be higher for concrete made with cements containing a high C_3A content
- Shrinkage reduces when fly ash is used as a cement replacement

- Autogenous shrinkage increases with decreasing w/b, while drying shrinkage increases with increasing w/b
- Shrinkage is lower if bleed water is present on the material surface, and shrinkage may be higher if the set time is delayed (by chemicals, temperature, etc.)

The cracking due to the drying shrinkage can be minimized or controlled by observing the following preventive steps:

- Minimize the mix water content by maximizing the size and amount of coarse aggregate and using low-shrinkage aggregate
- Use the lowest amount of mix water required for workability and do not permit overly-wet consistencies
- Consider using internal curing and SRA, which can reduce drying shrinkage and shrinkage-induced cracking
- Consider using cellulose fibers, which have less effect on drying shrinkage but are very effective in mitigating drying shrinkage-induced cracking when good dispersion is achieved
- Provide isolation joints to release the restraint from adjoining elements of a structure

3. EXPERIMENTAL WORK

In this study, experiments are designed to characterize the chemical, autogenous, and drying shrinkage properties of 11 HPC mixes used for Iowa bridge decks and overlays. The materials and procedures used for these experiments are discussed in this chapter.

3.1 Materials

The materials used in this research and their sources are listed in Table 3.1.

Table 3.1. Materials used and their sources

Materials	Source
Cement	Type IP Cement (Ash Grove)
	Type I/II Cement (Lafarge)
	Type I Cement (Lehigh)
Coarse aggregates	Limestone (Ft. Dodge Mine)
	Quartzite (Dell Rapids, SD)
Sand	Ames
Fly ash	Headwaters Resources
GGBFS	Holcim
Metakaolin	Davison Catalysts
Standard WR/WRDA 82	WR Grace
Mid-range WR/Mira 62	WR Grace
Retarder/Daratard 17	WR Grace
AEA/Daravair 1000	WR Grace

The three types of cement, Type I, Type I/II, and Type IP, together with the three types of SCMs, fly ash (FA), GGBFS, and MK, are listed in Table 3.2 with their chemical and physical properties.

Table 3.2. Chemical and physical properties of cementitious materials

Type	Chemical composition (%)									Mineral composition (%)				Fineness (m^2/kg)
	CaO	Al_2O_3	SiO_2	Fe_2O_3	SO_3	MgO	Na_2O	K_2O	LOI	C_3S	C_2S	C_3A	C_4AF	
I	63.0	5.2	20.0	2.6	3.0	3.0	0.07	0.54	2.5	60	14	6	9	398
I/II	63.1	4.6	20.2	3.2	3.4	2.4	0.09	0.67	1.2	57	15	7	10	397
IP	48.3	8.9	29.3	4.1	3.1	3.1	0.30	0.70	1.7	-	-	-	-	490
FA	23.7	22.0	37.3	6.3	1.6	5.3	1.16 (Na_2O)eq		0.25	-	-	-	-	15.8% (+325 Mesh)
GGBFS	37.1	9.2	36.8	0.76	-	9.5	0.34	0.41	-	-	-	-	-	534

Limestone and quartzite coarse aggregates were used. Original coarse aggregates were sieved and combined to the designated gradations (Table 3.3).

Table 3.3. Gradations of coarse aggregates used

Sieve Size	Mix Type (% passing)	
	O Mix	S Mix
1"	-	100.0
3/4"	100.0	99.0
1/2"	100.0	60.0
3/8"	80.0	29.0
#4	13.5	4.5
#8	1.0	1.0

Coarse aggregates were used in a saturated surface dry (SSD) condition and fine aggregates were used in an oven-dried condition. The gradation curves of aggregates are shown in Figure 3.1. The calculated fineness modulus of sand is 3.13.

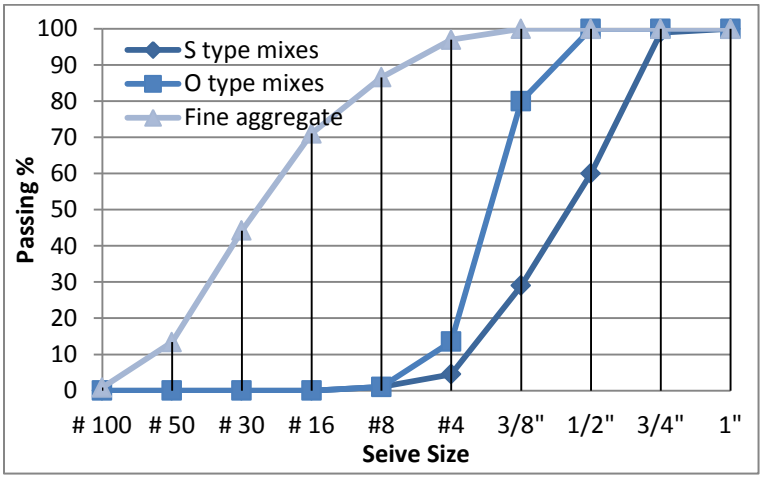

Figure 3.1. Gradation curves of coarse aggregates

The chemical admixtures include a polyacrylate-based, mid-range water reducer (MRWR), a lignosulfonate-based, normal-range water reducer (NRWR), a retarder, and an air-entraining agent (AEA). The dosage of AEA was determined based on the trial mix and the target air content is 6 to about 8%; while the dosages of WR and retarder were determined based on the suggestions from the Iowa DOT and the recommendations provided by the manufacturers. Table 3.4 gives the final dosages of chemical admixtures used in this project.

Table 3.4. Dosage of chemical admixtures

Type	Name	Dosage (fl. oz/100 lb)
Standard WR	WRDA-82	3.5
Mid-range WR	Mira-62	6.0
Retarder	Daratard 17	2.0
AEA	Daravair 1000	1.8

3.2 Mix Proportions

As shown in Table 3.5, 11 HPC mixes, selected by the Iowa DOT, were investigated. The differences in HPC-O and HPC-S mixes are mainly aggregate gradation and chemical admixture. HPC-O mixes have the mid-range water reducer (MRWR) while HPC-S has the normal-range water reducer (NRWR). The coarse aggregate gradation of HPC-O mixes is finer than that of HPC-S mixes.

Table 3.5. HPC mixes used for this study

No.	Mix	Cement	Fly Ash	GGBFS	Metakaolin
1	HPC-O	Ash Grove IP	0	-	-
2	HPC-O	Ash Grove IP	20%	-	-
3	HPC-S	Ash Grove IP	20%	-	-
4	HPC-O (control)	Lafarge I/II	0	-	-
5	HPC-S (control)	Lafarge I/II	0	-	-
6	O-4WR	Lafarge I/II	0	-	-
7	HPC-O	Lafarge I/II	0	25%	-
8	HPC-O (quartzite coarse aggregate)	Lafarge I/II	20%	25%	-
9	HPC-S	Lafarge I/II	20%	25%	-
10	HPC-O	Lafarge I/II	20%	-	5.6%
11	HPC-S	Lehigh I	20%	25%	-

These 11 mixes were divided into four groups as follows:

- **Group 1:** Mixes 1, 2, and 3 were all made with Ash Grove IP cement and w/b of 0.40. Comparison of Mixes 1 and 2 (both are O mixes) can show the effects of 20% fly ash replacement on measured properties. Comparison of Mixes 2 and 3 (both have 20% fly ash replacement for cement) can show the effects of different mixes. However, it shall be noted that Mix 3 has 77.7 lb/yd^3 less cementitious materials than Mix 2.
- **Group 2:** Mixes 4, 6, 7, and 10 for HPC-O mixtures were all made with Lafarge I/II cement but differ by FA, GGBFS, and MK replacements for cement. Shrinkage test results from this group may show the effects of different SCMs.
- **Group 3:** Mixes 8 and 9 were both made with Lafarge I/II cement and the same FA and GGBFS replacement percentages but different HPC type mixes. Shrinkage test results for this group may show the effects of different coarse aggregates and chemical admixtures.
- **Group 4:** Mixes 5 and 11 were both HPC-S mixes with w/b of 0.42. However, Mix 5 is made with 100% Lafarge I/II cement, while mix 11 is made with 25% FA and 25% GGBFS for Lehigh I cement. Shrinkage test results for this group may show the effects of ternary cementitious materials. Since Mix 11 is similar to Mix 9 expect for the type of cement used, the test results of these two mixes are also compared in the later discussions. Group 4 mixes also have a lower cementitious content than other mixes (expect for Mix 3) studied.

The shrinkage behavior of cement paste, mortar, and concrete of the four groups of HPC mixes were studied. The mix proportion used for paste was different from those for mortar and

concrete. For paste, w/cm was kept constant as 0.40 and no air-entraining agent was used. The mix proportions of mortar were basically the same as those of the concrete. That is, the mortar mixes were designed by removing coarse aggregates from the corresponding concrete.

All of the mix proportions used for paste, mortar, and concrete are presented in Table 3.6, Table 3.7, and Table 3.8. In the tables, FA is fly ash, GGBFS is ground granulated blast-furnace slag, MK is metakaolin, w/b is water-to-binder ratio, s/b is sand-to-binder ratio, AEA is air-entraining agent, MRWR is mid-range water reducer, and NRWR is normal-range water reducer.

Table 3.6. Mix proportions for cement paste

No.	Cement lb/yd^3	Fly ash lb/yd^3	GGBFS (MK) lb/yd^3	Cementitious Content lb/yd^3	AEA ml/yd^3	NRWR ml/yd^3	MRWR ml/yd^3	Retarder ml/yd^3	w/b
1	666.3	0	0	666.3	0	1182.3	394.1	354.7	0.40
2	521.2	130.3	0	651.5	0	1156.1	385.4	346.8	0.40
3	459.0	114.8	0	573.8	593.9	0	339.4	305.4	0.40
4	709.2	0	0	709.2	0	1258.4	419.5	377.5	0.40
5	624.5	0	0	624.5	646.4	0	369.4	332.5	0.40
6	825.7	0	0	825.7	854.6	0	0	439.5	0.40
7	519.7	0	173.2	692.9	0	1229.5	409.8	368.9	0.40
8	367.8	133.8	167.2	668.8	0	1186.6	395.5	356.0	0.40
9	323.9	117.8	147.2	588.9	609.6	0	348.3	313.5	0.40
10	502.2	135.0	(37.8)	675.0	0	1197.6	399.2	359.3	0.40
11	323.9	117.8	147.2	588.9	609.6	0	348.3	313.5	0.40

Table 3.7. Mix proportions for mortar

No.	Cement lb/yd^3	FA lb/yd^3	GGBFS (MK) lb/yd^3	Sand lb/yd^3	Water lb/yd^3	AEA ml/yd^3	NRWR (MRWR) ml/yd^3	Retarder ml/yd^3	w/b	s/b
1	666.3	0	0	1405.9	266.5	353.7	(1182.3)	394.1	0.40	2.11
2	521.2	130.3	0	1413.7	260.6	348.3	(1156.1)	385.4	0.40	2.17
3	459.0	114.8	0	1486.3	241.0	305.1	593.9	339.4	0.42	2.59
4	709.2	0	0	1403.9	283.7	378	(1258.4)	419.5	0.40	1.98
5	624.5	0	0	1457.3	262.3	332.1	646.4	369.4	0.42	2.33
6	825.7	0	0	1366.1	270.0	440.1	854.6	-	0.40*	1.65
7	519.7	0	173.2	1391.8	277.2	369.9	(1229.5)	409.8	0.40	2.01
8	367.8	133.8	167.2	1404.6	267.5	356.4	(1186.6)	395.5	0.40	2.10
9	323.9	117.8	147.2	1477.9	247.3	313.2	609.6	348.3	0.42	2.51
10	502.2	135.0	(37.8)	1401.3	270.0	359.1	(1197.6)	399.2	0.40	2.08
11	323.9	117.8	147.2	1477.9	247.3	313.2	609.6	348.3	0.42	2.51

*For Mix 6, the actual w/b is 0.33. It is increased to 0.40 for autogenous shrinkage test sample preparation because of the workability requirement.

Table 3.8. Mix proportions for concrete

No.	Cement lb/yd^3	FA lb/yd^3	GGBFS (MK) lb/yd^3	Limestone (Quartzite) lb/yd^3	Sand lb/yd^3	Water lb/yd^3	AEA ml/yd^3	NRWR (MRWR) ml/yd^3	Retarder ml/yd^3	w/b
1	666.3	0	0	1431.7	1405.9	266.5	354.7	(1182.3)	394.1	0.40
2	521.2	130.3	0	1439.6	1413.7	260.6	346.8	(1156.1)	385.4	0.40
3	459.0	114.8	0	1513.4	1486.3	241.0	305.4	593.9	339.4	0.40
4	709.2	0	0	1429.7	1403.9	283.7	377.5	(1258.4)	419.5	0.42
5	624.5	0	0	1483.9	1457.3	262.3	332.5	646.4	369.4	0.40
6	825.7	0	0	1386.8	1366.1	270.0	439.5	854.6	0	0.42
7	519.7	0	173.2	1417.4	1391.8	277.2	368.9	(1229.5)	409.8	0.33
8	367.8	133.8	167.2	(1430.4)	1404.6	267.5	356	(1186.6)	395.5	0.40
9	323.9	117.8	147.2	1504.8	1477.9	247.3	313.5	609.6	348.3	0.40
10	502.2	135.0	(37.8)	1427.1	1401.3	270.0	359.3	(1197.6)	399.2	0.42
11	323.9	117.8	147.2	1504.8	1477.9	247.3	313.5	609.6	348.3	0.40

3.3 Test Methods

3.3.1 Chemical Shrinkage Tests of Pastes

The chemical shrinkage test was performed on paste mixes according to ASTM C 1608 (the standard test method for chemical shrinkage of hydraulic cement paste).

3.3.1.1 Mixing Procedure for Paste

Two types of mixing methods were employed: hand mixing and ultrasonic mixing. Ultrasonic disruption is one widely-used method to disrupt cells and it's known for its strong ability to guarantee homogenizing. The ultrasonic device generates intense sonic pressure waves in a liquid media. The pressure waves cause streaming in the liquid and, under the right conditions, rapid formation of micro-bubbles, which grow and coalesce until they reach their resonant size, vibrate violently, and eventually collapse. This phenomenon is called cavitation. The implosion of the vapor phase bubbles generates a shock wave with sufficient energy to break covalent bonds. Shear from the imploding cavitation bubbles as well as from eddying induced by the vibrating sonic transducer disrupts cells.

The Sonicator XL-2020 ultrasonic processor was used in this study (Figure 3.2). The device has 11 ultrasonic disruption speeds, with speed 1 representing the least mixing and speed 11 the strongest mixing capacity. A tested paste sample is placed into a glass beaker and the mixing rod of the ultrasonic device is inserted into the sample to mix the sample. In this study, speed 7 was adopted based on experimental experience and previous research data.

Figure 3.2. Sonicator XL-2020 ultrasonic processor used in mixing process

When a paste was mixed with the ultrasonic disperser, the following procedure was used: 1) Add chemical admixture into distilled water, 2) Add cementitious materials into water and mix with ultrasonic disperser at speed 7 for 340 seconds, and 3) Hand-mix for 60 seconds.

When a paste was mixed by hand, the mixing procedure was as follows: 1) Add chemical admixture into DI water, and 2) Add cementitious materials into water and hand-mix in a beaker with a spatula for 5 minutes.

After mixing, the beaker with paste was put on a vibrating table to remove most of the entrained air.

3.3.1.2 Chemical Shrinkage Test Setup

Figure 3.3 includes a schematic representation of the test setup. Cement paste was put into three glass tubes for parallel experiments. Samples were 27 mm in diameter and 8 to 10 mm in height. The weights of the empty tube and filled tube were measured to determine the mass of the cement paste. The glass tubes were then filled to the top with DI water and plugged with a rubber stopper. Care was taken not to entrap any air bubbles (otherwise, the test results would be highly abnormal).

A drop of paraffin oil was placed in the top of each graduated capillary tube to minimize water evaporation from the tube during the testing period. The prepared specimens were placed in the constant temperature water bath at 23±1°C such that the tops of the glass vials were just above the water level in the bath.

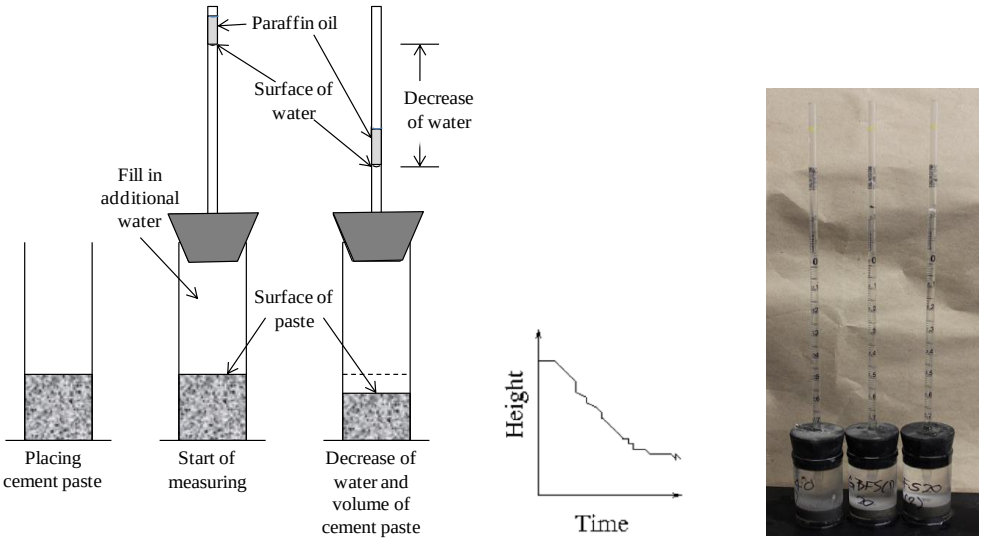

Figure 3.3. Schematic representation of chemical shrinkage test and image showing one group of samples

3.3.1.2 Chemical Shrinkage Measurements

The starting time of the experiments was when the cement contacted with water (time = 0) and the first measurement started at 1 hour (1h). The researchers recorded, periodically, the time to the nearest minute and the water level in the capillary tubes to the nearest 0.0025 mL for a total period of at least 24h. After the first 8h, the recording intervals were lengthened to 24h for the next 4 days and every 7 days for the remainder. The testing stopped at 91 days.

3.3.2 Autogenous Shrinkage Tests of Mortar

Autogenous shrinkage tests of mortar were performed according to ASTM C 1698 (the standard test method for autogenous strain of cement paste and mortar) using the Auto-Shrink device. For each mix, three cylindered samples (Ø 30 mm × L 300 mm) were prepared using polyethylene tubes. The following procedures were used for the sample preparation:

1. The mortar materials were mixed according to ASTM C 305, and the time of adding cementitious materials into water were recorded.
2. Sealed one end of three sample molds/three polyethylene tubes with plugs, and filled the tubes with the mortar mixture as shown in Figure 3.4.
3. Placed the sample tubes on the tube supporter of the Auto-Shrink device and consolidated them using a standard vibrating table.
4. Kept filling the sample tubes with mortar until the mortar reached 1.5 cm below the top of the tubes and then sealed the top opening of the tubes with another plug. (The tubes were sealed properly to avoid any evaporation.)
5. Placed the sample tubes horizontally on a smooth surface to avoid any unexpected bending or length change.

6. Placed the samples into the environmental chamber with a temperature of 23.0±1.0°C to minimize the influence of temperature variations.
7. Kept the Auto-Shrink device, including the reference bar, in the same environmental condition as the mortar samples to minimize temperature-related test errors.

Figure 3.4. Specimen preparations for autogenous shrinkage of mortar

According to ASTM C 1698, the first measurement for the autogenous shrinkage of a mortar sample should be performed at the final set time of the mortar. Therefore, the final set times of all 11 mixes of mortar were determined prior to the autogenous shrinkage sample preparation. The mortar set time tests were conducted according to ASTM C 403/C 403M, standard test method for time of setting of concrete mixtures by penetration resistance, as shown in Figure 3.5.

Figure 3.5. Test photos for final set time of mortar

In this study, the autogenous shrinkage measurements of mortar were taken at 0, 15, 30, and 45 minutes (min), 1 hr and 3 hrs, and 1 day (1d), 3d, 7d, 14d, and so forth until 56d from the final set time of the test mortar. The weight of specimens was recorded to check for obvious moisture loss.

The following procedure was used for each autogenous shrinkage measurement:

1. Recorded the length of the reference bar as shown in Figure 3.6(a).

2. Reset the measuring gauge to zero and removed the reference bar.
3. Placed the tested sample in the dilatometer bench and recorded the gauge reading.
4. At the early age, soft samples were handled carefully, using both hands to carry them, to avoid any damage. To obtain accurate results, it was important to place the reference bar and all samples in the same orientation. A line mark, shown in Figure 3.6(b), helped to keep all samples at the same position after each measurement.

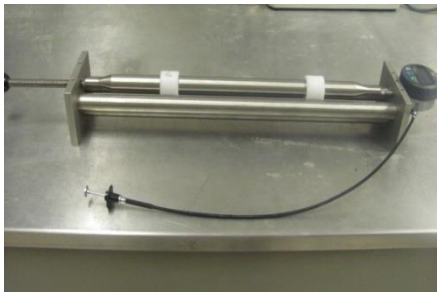

(a) dilatometer for measurement

(b) line mark on the corrugated tubes

Figure 3.6. Device and samples for mortar autogenous shrinkage measurement

3.3.3 Autogenous Shrinkage Tests of Concrete

All mixes were cast in accordance with ASTM C 192 (standard practice for making and curing concrete test specimens in the laboratory). During the mixing, oven-dried sand was used while course aggregates were used in the SSD condition.

Three specimens for each mixture were cast in prism molds (3 by 3 by 11.25 in.), oiled in advance, and had studs inserted into the ends of them. Freshly-mixed concrete was loaded in one layer and then compacted on a vibrating table. Excess was removed and leveled off. Concrete specimens were covered by a polythene sheet and wet towels to avoid moisture loss during the first 24 hours, demolded at the age of 1d, and then immediately double-wrapped with a self-sealing polythene film and an aluminum foil sealed with tape to avoid any moisture loss. After being sealed, the specimens were stored in an environment chamber at a constant 73^{o}F after measuring the initial length and weight.

As shown in Figure 3.7, length was measured using a length comparator, which was kept in the same temperature chamber to avoid any variations due to temperature change according to ASTM C 157 (the standard test method for length change of hardened hydraulic-cement mortar and concrete). The lengths of concrete specimens at 4, 7, 14, 21, 28, 35, 42, 49, and 56 days were measured relative to the standard bar, and their weights were also tested to monitor the moisture loss.

Figure 3.7. Samples, molds, and comparator for concrete autogenous shrinkage measurement

3.3.4 Free Drying Shrinkage Test of Mortar

The free drying shrinkage test of mortar was performed according to ASTM C 596 (the standard test method for splitting tensile strength of cylindrical concrete specimens). For each mix, four specimens (25×25 ×285 mm) were made. Based on ASTM C 305 (standard practice for mechanical mixing of hydraulic cement pastes and mortars of plastic consistency), the researchers used a mechanical mixer to mix mortar.

The filled the mixed mortar in two equal layers and then compacted each layer with the tamper. After molding, they moist cured the specimens in the mold in the curing room with 100% relative humidity for 24 hrs. Then, they unmolded the specimens and placed them into lime-saturated water storage for 48 hrs.

At the age of 72±0.5h, the specimens were removed from water and placed them in the environment room with 73^{o}F and 50% relative humidity for drying storage. The initial length measurements were taken immediately after the specimens were removed from water.

For each measurement, the reference bar was measured and recorded first. To achieve a reliable result, it was important to place the reference bar and the specimens in the same orientation. Marks were made on the reference bar and specimens to indicate the top and bottom. Measurements for both length change and mass loss of the specimens were taken at 1, 3, 7, 14, 21, 28, 35, 42, 49, and 56 days after they were stored in the dry air condition. The test device and specimens of free drying shrinkage of mortar are shown in Figure 3.8.

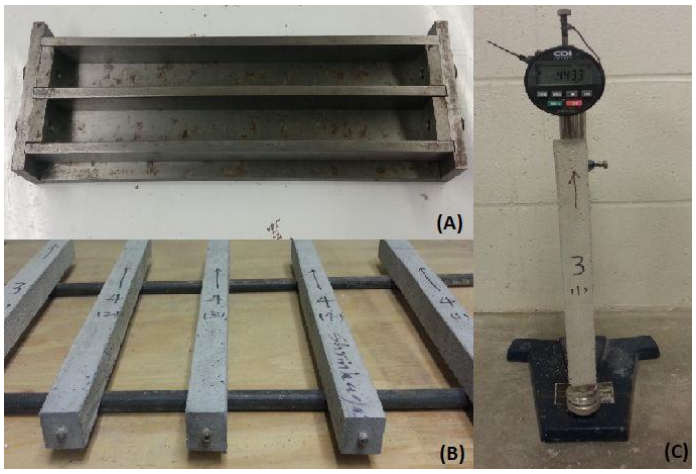

Figure 3.8. Test device of free drying shrinkage of mortar and specimens storage

3.3.5 Free Drying Shrinkage Test of Concrete

The specimen preparation for free drying shrinkage is the same as that for autogenous shrinkage, with all fresh mixtures cast in the same batch of concrete. The specimens were cured for 7 days in a 100% relative humidity room and were measured for the initial length, then stored in the environment room at 73^{o}F and 50% relative humidity. Length and weight measurements were taken at the ages of 3, 7, 14, 21, 28, 35, 42, 49, and 56 days, as seen in Figure 3.9, following the same procedures as those for autogenous shrinkage test of concrete.

Figure 3.9. Length measurements of concrete specimens

3.3.6 Restrained Ring Shrinkage Test of Concrete

Restrained ring tests were performed for concrete specimens according to ASTM C 1581 (the standard test method for determining age at cracking and induced tensile stress characteristics of mortar and concrete under restrained shrinkage). The ring molds were oiled and held in place using four 3 in. C-clamps (Figure 3.10(a)). The fresh mixtures were poured and compacted in two layers on a vibrating table. Leads of the strain gage were attached to the module to collect data every minute.

(a) (b)

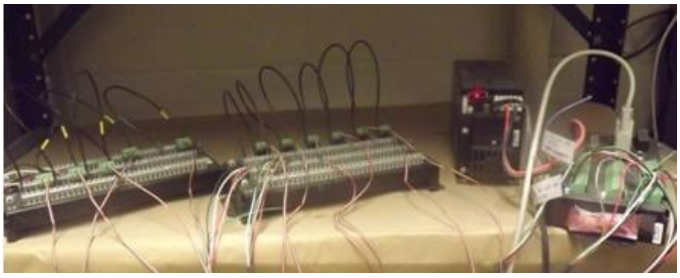

(c)

Figure 3.10. Mold, specimen, and data logger for concrete ring tests

The clamps were released immediately after the modules were connected. The specimens were then covered with polythene and stored at 73.5±3.5^{o}F. At the age of 1 day, the outer steel ring was removed as shown in Figure 3.10(b). The ring specimens were then placed in a 50% relative humidity and 735±3.5^{o}F environment room. The top surface was coated with a thin layer of wax.

As seen in Figure 3.10(c), two strain gages on the interior surface of the interior steel ring were mounted at mid-height locations diametrically opposite to each other. The gauges were placed to measure strain along the circumferential direction. The manufacturer's specifications were used for mounting and waterproofing the gauges on the steel ring and connecting lead wires to the strain gauge modules.

Test strain gauge response data were recorded automatically by the data logger. The data recorded were transferred into a Microsoft Excel spreadsheet and then converted to the shrinkage of concrete specimens with time. The record included the time and ambient temperature of the testing environment every day. The data logger program monitored the strains in the steel rings at intervals of 1 minute, recording the output of each strain gauge separately with the data acquisition system. A sudden decrease in compressive strain in one or both strain gauges indicated cracking of the ring. The specimens were checked every 3 days for cracks. The strain in the steel rings was recorded for 28 days after initiation of drying, unless cracking occurred prior to 28 days.

3.3.7 Strength and Elastic Modulus Test

Compressive strength was performed for all mixes according to ASTM C 39 (the standard test method for compressive strength of cylindrical concrete specimens). Specimens of 100 mm (4 in.)

diameter and 200 mm (8 in.) height were molded in two equal layers, applying 25 strokes of a 10 mm (3/8 in.) rod for each cast. Specimens were demolded at the age of 24 hrs and cured in a 100% humidity curing room. The same batches of fresh mixture were also used to cast the specimens for the elastic modulus test, which followed ASTM C 469 (the standard test method for static modulus of elasticity and Poisson's ratio of concrete in compression).

The tensile strength of concrete specimens was tested according to ASTM C 496 (the standard test method for splitting tensile strength of cylindrical concrete specimens). Specimens of 150 mm diameter and 300 mm height were cast in three equal layers and compacted with 25 strokes. The specimens were demolded at 24 hrs after cast and stored in a 100% humidity curing room for 28 days.

Specimens were tested for their strength and elastic modulus at the age of 1, 3, 7, 14, 28, and 56 days. Tensile strength of specimens was measured after 28 days curing.

4. TEST RESULTS AND DISCUSSION

This chapter covers the experimental results obtained from the chemical shrinkage, autogenous shrinkage, drying shrinkage, strength, and elastic modulus tests.

4.1 Chemical Shrinkage

Based on water level measurements, the chemical shrinkage of tested samples was computed as the volume (mL, per gram of cement) of water penetrated in the paste samples. The average value obtained from three samples in each mix was used as the final chemical shrinkage result of the mix.

4.1.1 Effect of Sample Size

Several researchers have investigated the influence of the sample size (thickness) on chemical shrinkage of cement pastes (Tazawa et al. 1999, Boivin et al. 1999, Sant et al. 2006). These researchers found that for pastes made with a low w/c ratio (<0.3), chemical shrinkage decreases with increasing samples size/thickness. This effect is due mainly to the permeability of the paste, which prevents water from permeating into the sample to fill the pores created by chemical shrinkage.

Although a water to cement ratio of 0.4 was used in this study, the presence of SCMs and chemical admixtures may have provided additional effects on paste permeability. Therefore, pre-tests were performed to investigate the effects of sample height on chemical shrinkage measurement to help select optimal sample size/height for further tests.

Two heights/thicknesses of paste samples were selected and they were 10 mm and 5 mm. For each sample size/height, pastes made with 80% portland cement and 20% fly ash, with and without water reducers, were tested. The results are shown in Figure 4.1.

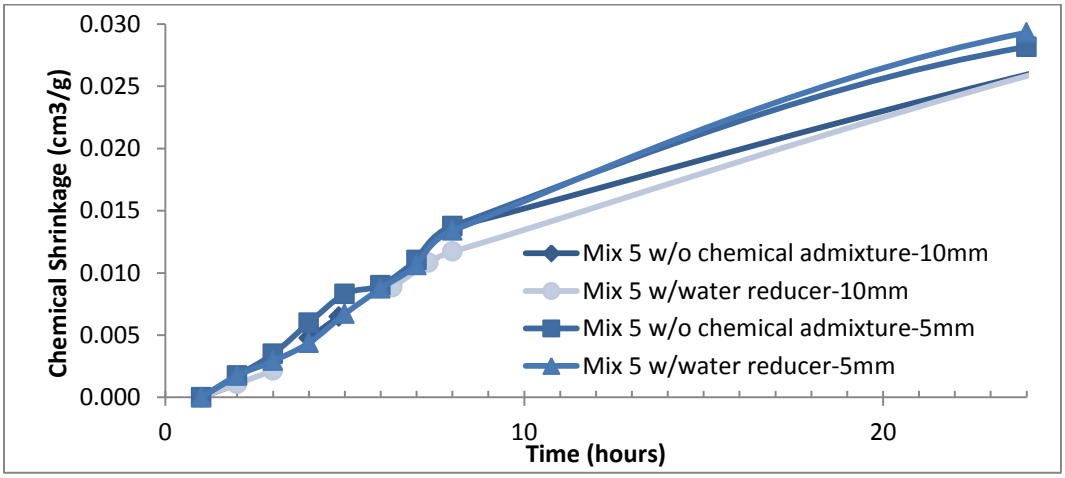

Figure 4.1. Influence of sample height on measured chemical shrinkage

The figure illustrates that the larger samples (10 mm height), with and without water reducers, all display smaller chemical shrinkage values than the small samples (5 mm height), and the difference is slightly enlarged when water reducers were used. This is consistent with previous research findings and confirms that chemical shrinkage measurements are noticeably affected by the permeability of the tested samples.

According to ASTM C 1608, the sample thickness for chemical shrinkage measurement should be 5 mm to 10 mm, which is approximately 5 to 10 g paste in the vial used in this testing. Therefore, a sample size of 7.5 g was selected for this study.

4.1.2 Effect of Mixing Method

Figure 4.2 shows the effect of mixing methods on chemical shrinkage measurement. The results show that hand-mixing produced higher chemical shrinkage values with larger variation than ultrasonic mixing.

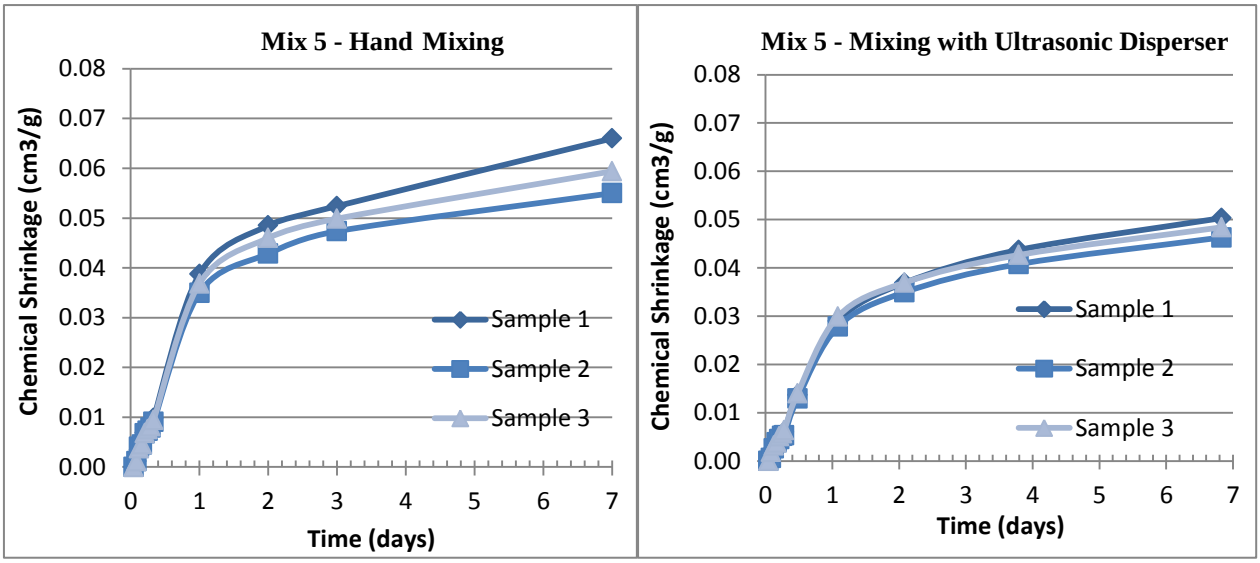

Figure 4.2. Effect of mixing methods on chemical shrinkage measurements

Chemical shrinkage measurements were taken an hour after the mixing due to the time needed for the samples to reach the temperature in the water bath. Ultrasonic-mixed samples showing smaller total chemical shrinkage than those mixed by hand may be due to a greater amount of chemical shrinkage involved in the first hour right after mixing (caused by the more-vigorous method of mixing). The smaller variations in the test results of the ultrasonic-mixed samples result primarily from the better homogeneity of the samples provided by the ultrasonic mixing.

4.1.3 Effect of SCMs

According to Justnes et al. (1999), the typical chemical shrinkage value for silica fume is 0.20 to 0.22 ml/g and 0.10 to 0.16 ml/g for Type F fly ash for complete hydration. Compared to OPC, those values are much higher in magnitude. However, these data are only partially based on experimental results combined with a set of hypothesized reactions (Feng et al. 2004). Several other researchers showed that the reaction degree of SCMs is usually quite low in blended cement and it is almost impossible to reach the 100% reaction rate (Termkhajornkit et al. 2005, Kocaba et al. 2012, Yajun and Cahyadi 2004). In other words, the SCMs works as fillers at the early age in blended cement mixtures to quite a high degree because the reaction degree is low. Figure 4.3 shows the influence of fly ash on the chemical shrinkage of cement pastes.

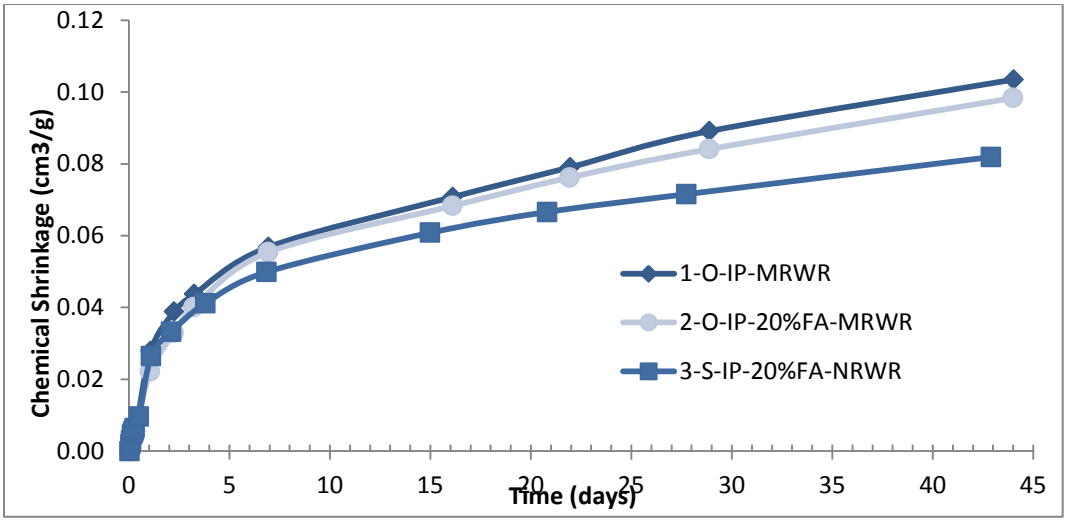

Figure 4.3. Effects of fly ash on chemical shrinkage (Group 1)

It can be seen from Figure 4.3 that 20% fly ash replacement decreases chemical shrinkage at nearly all ages compared to pure cement pastes. One possible explanation is that the glass content (silicate) in fly ash cement paste did not react in the early age due to lack of calcium hydroxide (CH) from cement hydration. Sakai and coworkers found that, regardless of glass content and composition, the fly ash in fly ash cement paste cured at 20ºC did not react until 7 days (Sakai et al. 2005).

Figure 4.4 shows the effect of metakaolin and slag on chemical shrinkage. Metakaolin replacement greatly increased chemical shrinkage after one day. In fact, Mix 10 with metakaolin displayed the highest chemical shrinkage of all the 11 mixes studied. This is probably due to its high pozzolanic properties (owing to its fineness and chemical composition) and its ability to enhance cement hydration. MK is reported to have a value of 20.10^{-4} of its pozzolanic reaction rate, a little lower than silica fume (27.10^{-4}), but much higher than fly ash (7.10^{-4}).

In the literature, a few researchers report about the role of MK in modifying the pore size distribution. In this respect, Wild et al. (1998) reported a refineness of the pore structure and a total intruded pore volume increase between 14 and 28 days for pastes with 5, 10, and 15% MK.

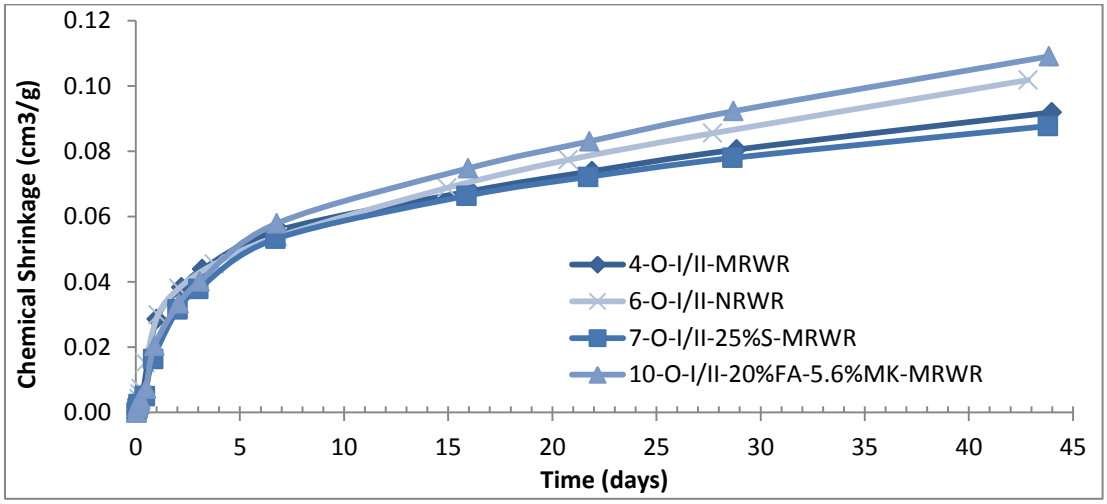

Figure 4.4. Effects of metakaolin and slag on chemical shrinkage (Group 2)

As to the effect of slag on chemical shrinkage, a definite conclusion couldn't be obtained. Total chemical shrinkage for pure pastes and pastes with slag replacement were very close at all ages. As to the rate of chemical shrinkage, pastes with slag addition showed a higher rate of chemical shrinkage between 3 days and 22 days. After that, pure pastes displayed a higher rate of chemical shrinkage.

As shown in Figure 4.5, combined replacement of fly ash and slag reduces chemical shrinkage at early stages and increases chemical shrinkage at later ages compared to pure cement paste. This is probably because cement hydration is enhanced and the resultant hydration product has a denser structure.

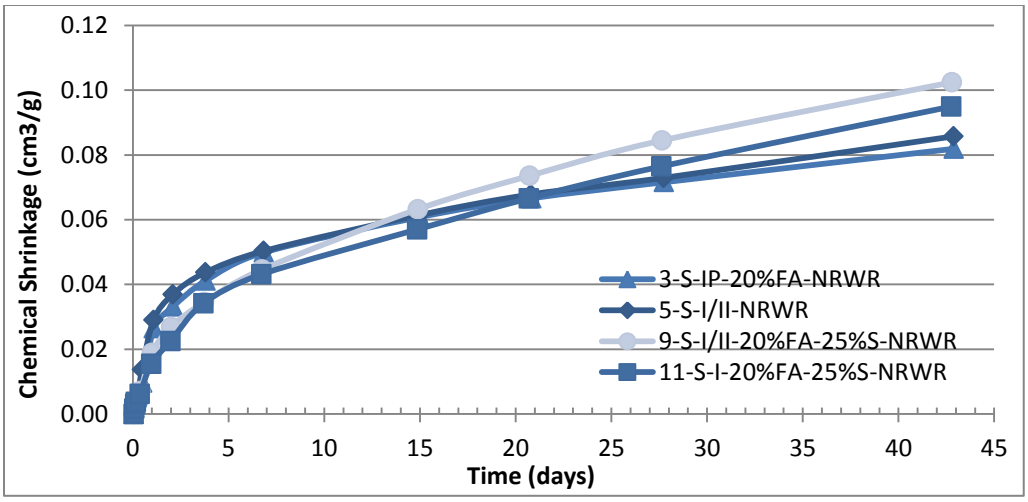

Figure 4.5. Co-effects of fly ash and slag on chemical shrinkage (Group 3)

4.1.4 Effect of Water Reducers

Two types of water reducers were used in this study, normal-range water reducers (NRWRs) and mid-range water reducer (MRWRs). Mix 8 and Mix 9 use 55% Type I/II cement, 20% fly ash, and 25% slag as cementitious materials. They differ in the type and amount of water reducers used.

Test results showed that Mix 9 with NRWRs exhibited a higher chemical shrinkage. In another case, Mix 2 and Mix 3 use 80% Type IP cement and 20% fly ash as cementitious materials. While Mix 2 used MRWRs and Mix 3 used NRWRs, test results showed that Mix 2 with MRWRs exhibited higher chemical shrinkage.

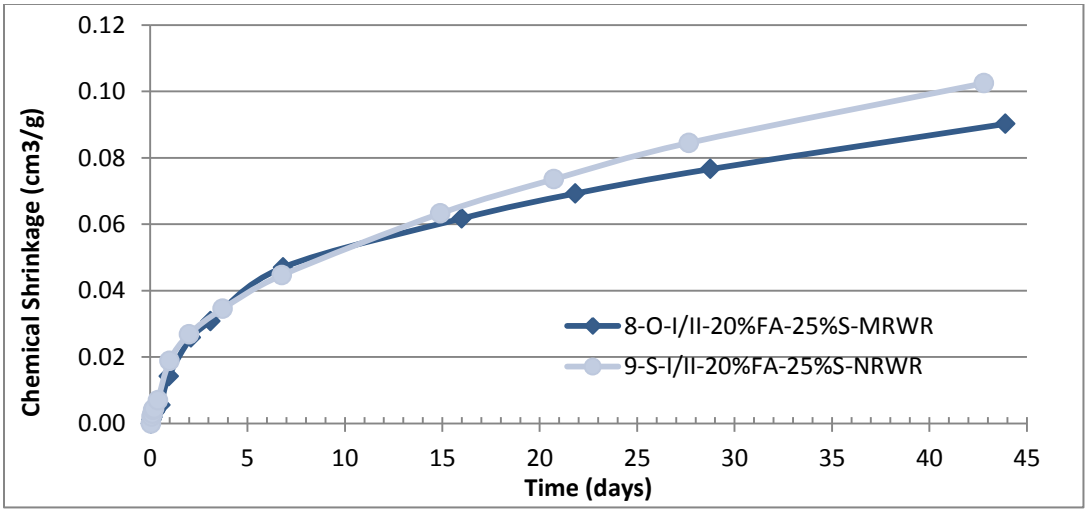

Figure 4.6. Effect of water reducer types (Group 4)

4.1.5 Effect of Cement Type

Three types of cement were used in this study: Type I from Leigh, Type I/II from Lafarge, and Type IP from Ash Grove. The three types differ in chemical composition and fineness (Type IP is finer than Type I/II, which has the same fineness as Type I cement), which has significant effects on resulting chemical shrinkage according to the literature.

As shown in Figure 4.7, Mix 1 with Type IP (blended Fly Ash) cement resulted in a higher total chemical shrinkage, in contrast to previous observations that fly ash replacement reduces chemical shrinkage. This is mostly due to the much higher fineness of Type IP cement (490 m^2/kg) in contrast to Type I/II Cement (390 m^2/kg).

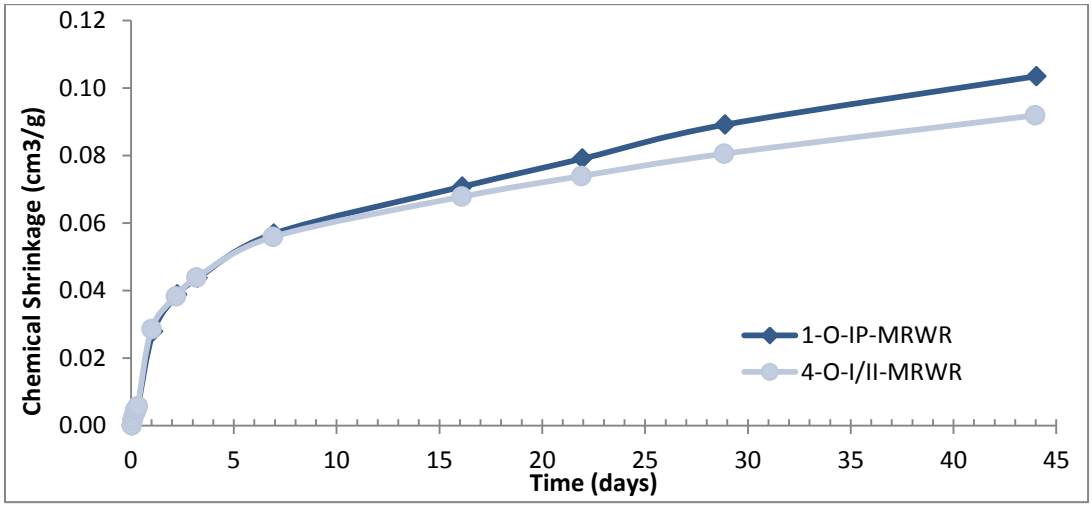

Figure 4.7. Effects of cement fineness on chemical shrinkage

4.1.6 Comparison of Chemical Shrinkage Measured among All Mixes

Table 4.1 summarizes the measured chemical shrinkage at 42 days for all 11 mixes.

Mix 10 with Lafarge I/II cement, 20% fly ash, and 5.6% metakaolin shows the greatest chemical shrinkage at 42 days, while Mix 3 with Type IP cement and 20% fly ash shows the smallest chemical shrinkage at 42 days. Cement paste with both fly ash and slag is recommended, given they reduce chemical shrinkage at early stages (which indicates that early-age autogenous shrinkage is not significant) and increase chemical shrinkage at later ages.

Table 4.1. Chemical shrinkage of paste at 42 days

Mix No.	Group	Cement	SCM	Water Reducer	Chemical Shrinkage at 42 day (cm^3/g)
1	1	Ash Grove IP	0	MRWR	0.1011
2	1	Ash Grove IP	20% FA	MRWR	0.0984
3	1	Ash Grove IP	20% FA	NRWR	0.0819
4	2	Lafarge I/II	0	MRWR	0.0919
5	4	Lafarge I/II	0	NRWR	0.0857
6	2	Lafarge I/II	0	NRWR	0.1018
7	2	Lafarge I/II	25% Slag	MRWR	0.0877
8	3	Lafarge I/II	20% FA 25%Slag	MRWR	0.0902
9	3	Lafarge I/II	20% FA 25%Slag	NRWR	0.1024
10	2	Lafarge I/II	20% FA 5.6% MK	MRWR	0.1091
11	4	Lehigh I	20% FA 25%Slag	NRWR	0.0950

4.2 Autogenous Shrinkage

This section presents the test results of autogenous shrinkage of both mortar and concrete. Autogenous shrinkage of mortar is determined based on ASTM C 1698 (the standard test method for autogenous strain of cement paste and mortar) and ASTM C 403/C 403M (the standard test method for time of setting of concrete mixtures by penetration resistance). Autogenous shrinkage of concrete is measured according to ASTM C 157 (the standard test method for length change of hardened hydraulic-cement mortar and concrete).

4.2.1 Autogenous Shrinkage of Mortar

Based on ASTM C 1698, the first autogenous shrinkage measurement was performed at the final set time of the tested mortar. This was because the external volume change can be measured only when the cement-based materials are set. Therefore, the initial and final set times of mortar were measured first for all 11 mixes being studied.

As shown in Figure 4.8, there exist quite a few differences from the set times among these 11 mixes of mortar, depending upon the w/b, chemical admixtures, SCMs, and cement type used. Mix 11 shows the longest for both initial and final set times, while Mix 6 shows the shortest set time. This may be because Mix 11 has a large amount of SCMs (20% FA and 25% GGBFS replacement) and retarder as well as a relatively high w/b (0.42), while Mix 6 is the only one without any retarder and has the lowest w/b (0.33). In general, most mixes have the final set time within the range of 8 to 12 hrs. (The detailed diagrams of the penetration resistance versus elapsed time for all mixes are included in the appendix.)

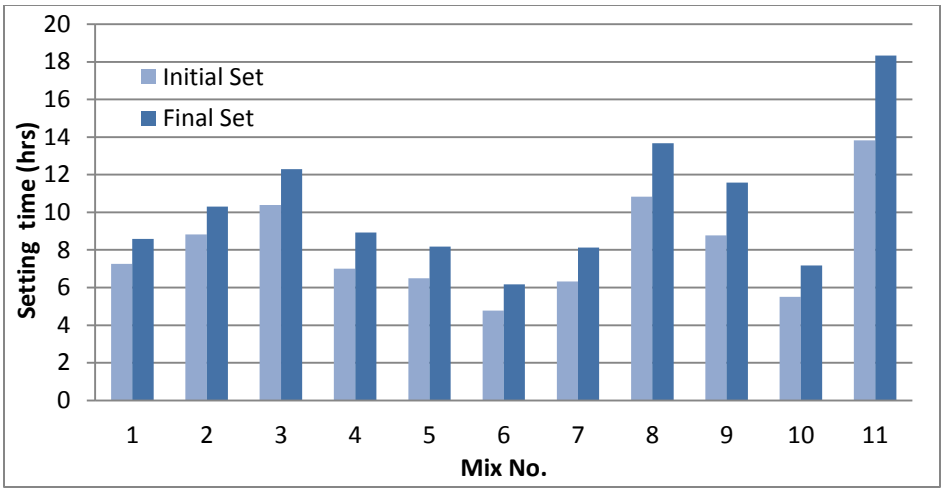

Figure 4.8. Set time of mortar for 11 mixes

The autogenous shrinkage results of mortar are illustrated in Figure 4.9 through Figure 4.12. The 56 day autogenous shrinkage values of these mixes are compared in Table 4.2 and Figure 4.13. Because autogenous shrinkage is very sensitive to the surrounding environmental temperature, the mixes in the same group were cast the same day to minimize this variable.

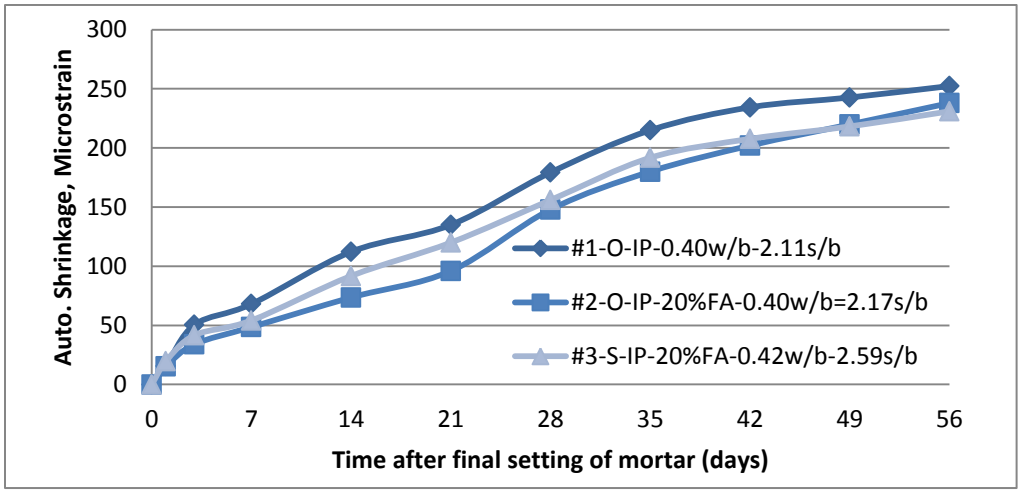

Figure 4.9. Autogenous shrinkage of mortar (Group 1)

Figure 4.9 shows the test results of autogenous shrinkage of mortar for Group 1, where Mixes 1, 2, and 3 are compared. The 20% fly ash replacement for cement (Mix 2) noticeably reduced the autogenous shrinkage of the mortar at all ages. Having slightly higher w/b and noticeably higher s/b, Mix 3 shows slightly higher autogenous shrinkage than Mix 2 before 28 days. After 28 days, autogenous shrinkage values of these two mixes were very close to each other

Figure 4.10 illustrates the results of autogenous shrinkage of mortar for Group 2, which includes Mixes 4, 6, 7, and 10.

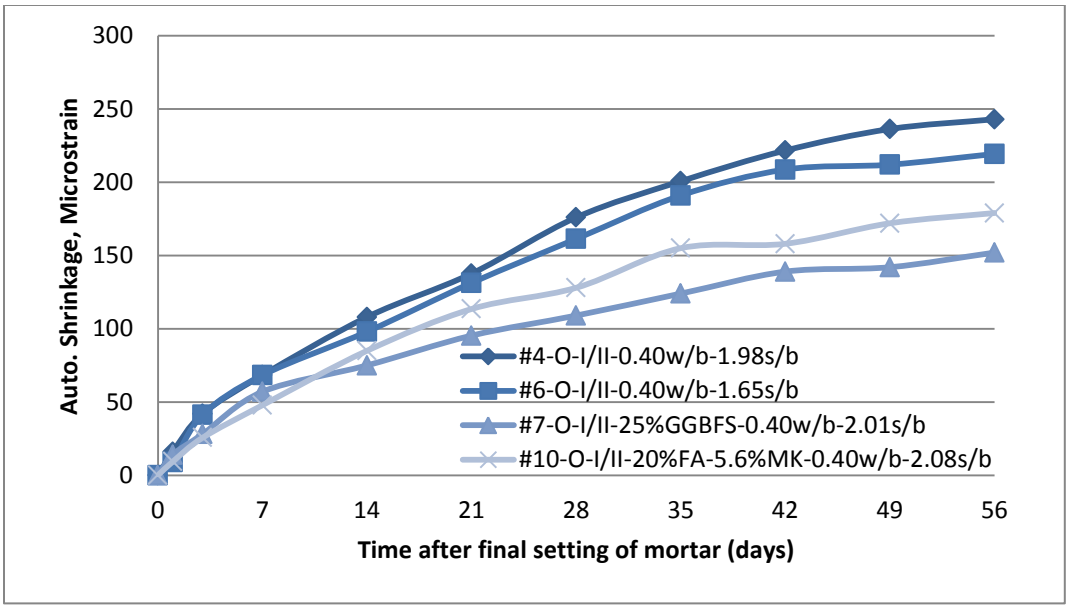

Figure 4.10. Autogenous shrinkage of mortar (Group 2)

These are all HPC-O mixes, having the same Lafarge I/II cement and the same w/b of 0.40 (including Mix 6 for this test), but different amounts of fly ash, GGBFS, and/or MK replacements. The order, from high to low, of the autogenous shrinkage values of these mixes is Mix 4 (the same as Mix 6), Mix 7, followed by Mix 10 before 7 days. After 14 days, the order becomes Mix 4, Mix 6, Mix 10, and then Mix 7. The order, from low to high, of s/b for these mixes is 6, 4, 7, and 10, showing the higher the s/b, the lower the paste content of the mortar.

The figure illustrates that, although having higher paste content, Mix 6 has slightly lower autogenous shrinkage than Mix 4 and, although having similar w/b and s/b, Mix 7 has noticeably lower autogenous shrinkage than Mix 10. These results imply that, not only the paste content but also the paste pore structure, which is altered by the SCMs and chemical admixtures used, play important roles in the autogenous shrinkage of the mortars.

Compared with Mix 7, Mix 10 showed increased autogenous shrinkage after 14 days. Given that fly ash replacement generally reduces autogenous shrinkage, it can be inferred that MK replacement for cement might have increased the autogenous shrinkage.

Figure 4.11 presents the results of autogenous shrinkage of mortar for Group 3, where Mixes 8 and 9 contain the same Lafarge I/II types of cement used and the same FA and GGBFS replacement percentages, but different admixtures and proportions.

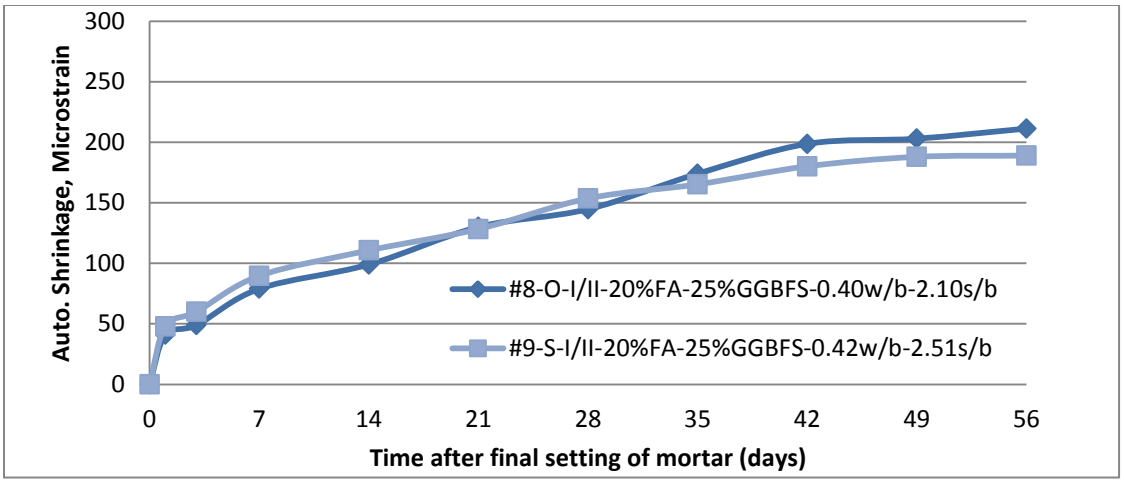

Figure 4.11. Autogenous shrinkage of mortar (Group 3)

There is little difference in autogenous shrinkage between these two mixes. (The same observation is also obtained from the free drying shrinkage of mortar.) The autogenous shrinkage values of Mix 8 are slightly high after 35 days, which may be related to the lower s/b of the mix, when compared with Mix 9.

Figure 4.12 shows the autogenous shrinkage test results for mortar in Group 4, including Mixes 5 and 11, both for HPC-S mixtures with the same w/b (0.42) and different types of cement and SCMs used. Given that 25% GGBFS or 20% FA replacement for cement reduces autogenous shrinkage (Figure 4.10), Mix 11 was expected to have lower autogenous shrinkage than Mix 5. However, as Figure 4.12 shows, the 20% FA replacement and 25% GGBFS replacement with Lehigh I cement increased autogenous shrinkage of mortar noticeably. This infers that Lehigh I cement might provide mortar with high autogenous shrinkage.

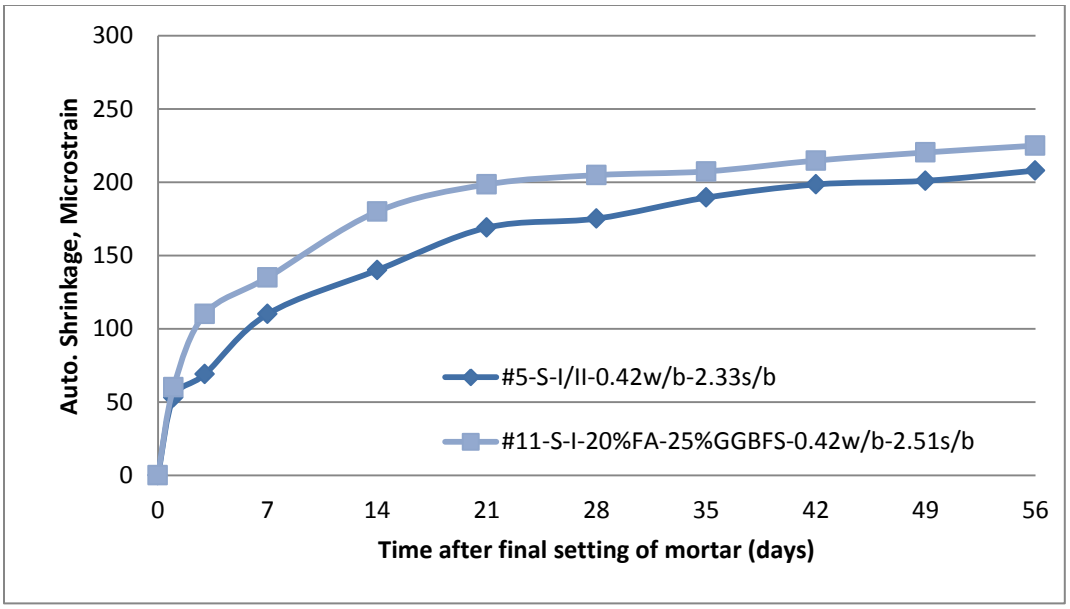

Figure 4.12. Autogenous shrinkage of mortar (Group 4)

Comparing Mix 11 to Mix 9, where the only difference in these two mixes is the type of cement, Mix 11 also has a higher autogenous shrinkage value than Mix 9. This further suggests that Lehigh Type I cement may contribute to the slightly high autogenous shrinkage of the mortar.

The autogenous shrinkage values of all mixes at 28 days are summarized in Table 4.2. The difference between the highest and the lowest autogenous shrinkage is almost 100 microstrains. Figure 4.13 illustrates that there is no clear correlationship between autogenous shrinkage and cementitious material content at different ages.

Table 4.2. Autogenous shrinkage of mortar at 28 days

Mix No.	Cement	SCM	w/b	Cementitious material content (lb/yd^3)	28 day auto-shrink (microstrain)
1	Ash Grove IP	0	0.40	666.3	176
2	Ash Grove IP	20% FA	0.40	651.5	148
3	Ash Grove IP	20% FA	0.40	573.8	152
4	Lafarge I/II	0	0.40	709.2	178
5	Lafarge I/II	0	0.42	624.5	175
6	Lafarge I/II	0	0.40	825.7	158
7	Lafarge I/II	25% Slag	0.40	692.9	109
8	Lafarge I/II	20% FA 25%Slag	0.40	668.8	145
9	Lafarge I/II	20% FA 25%Slag	0.42	588.9	151
10	Lafarge I/II	20% FA 5.6% MK	0.40	637.2	128
11	Lehigh I	20% FA 25%Slag	0.42	588.9	204

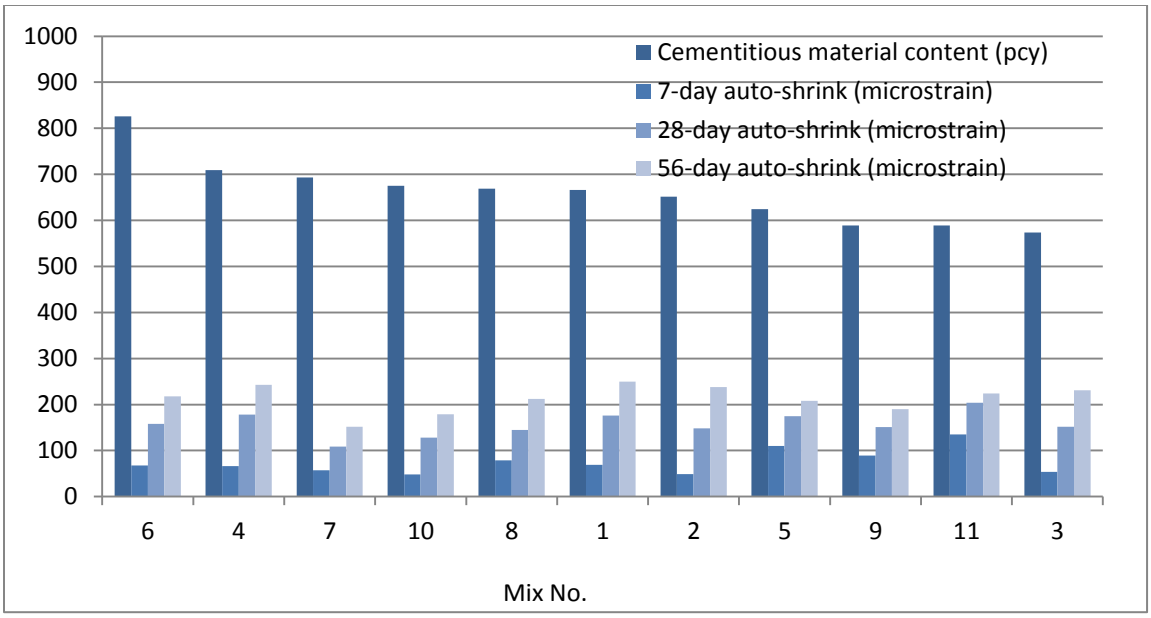

Figure 4.13. Autogenous shrinkage for mortar at 56d

4.2.2 Autogenous Shrinkage of Concrete

Autogenous shrinkage test results of the 11 concrete mixes studied are summarized in Figure 4.14 through Figure 4.18.

Figure 4.14 shows the test results for Group 1, which includes Mixes 1, 2, and 3.

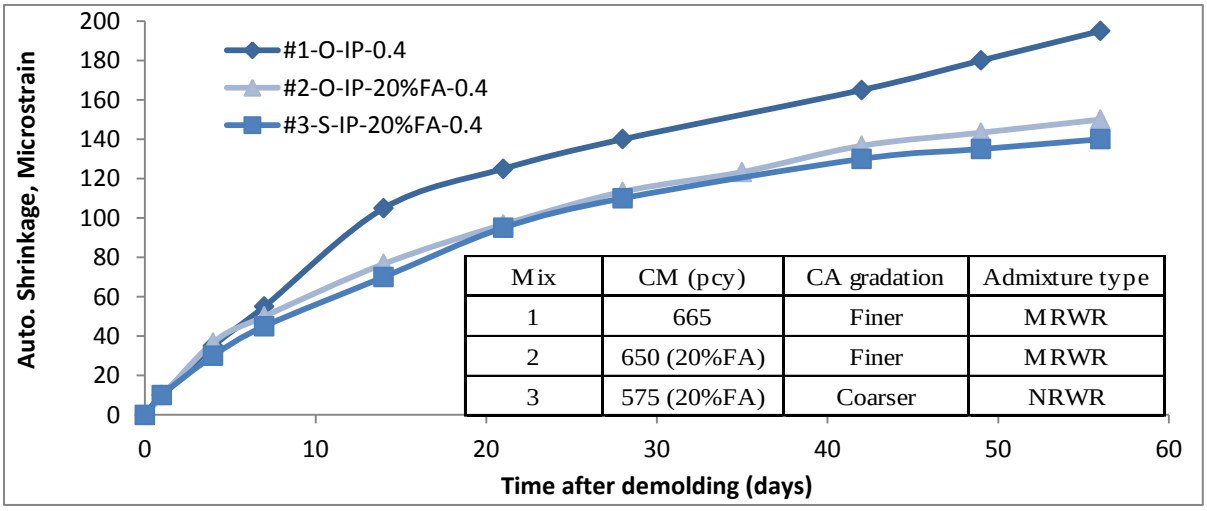

Figure 4.14. Autogenous shrinkage of concrete (Group1)

The same cement source was used in all three mixes. However, Mix 1 has no fly ash while Mixes 2 and 3 consist of 20% fly ash replacement for cement. The binder content for Mix 1 is 665 lb/yd^3 while it is 650 and 573 lb/yd^3 for Mixes 2 and 3, respectively.

Comparing the test results from Mixes 1 and 2, the inference is that fly ash replacement in the concrete reduces the autogenous shrinkage of concrete, which is consistent with what is observed from the autogenous shrinkage of mortar.

Mixes 2 and 3 differ in having two types of water reducers and also having different coarse aggregate gradation. Mix 2, being an O-type mix, has a mid-range water reducer while Mix 3, being an S-type mix, has a standard water reducer. The aggregate gradation of Mix 3 is coarser than that of Mix 2. The cement content of Mix 3 (575 lb/yd^3) is significantly less than that of Mix 2. Regardless the differences in their mix proportions, Mixes 2 and 3 have similar autogenous shrinkage values, all significantly less than that of Mix 1. This suggests that 20% fly ash replacement plays a significant role in reducing autogenous shrinkage of concrete.

The autogenous shrinkage test results of concrete Group 2 are shown in Figure 4.15.

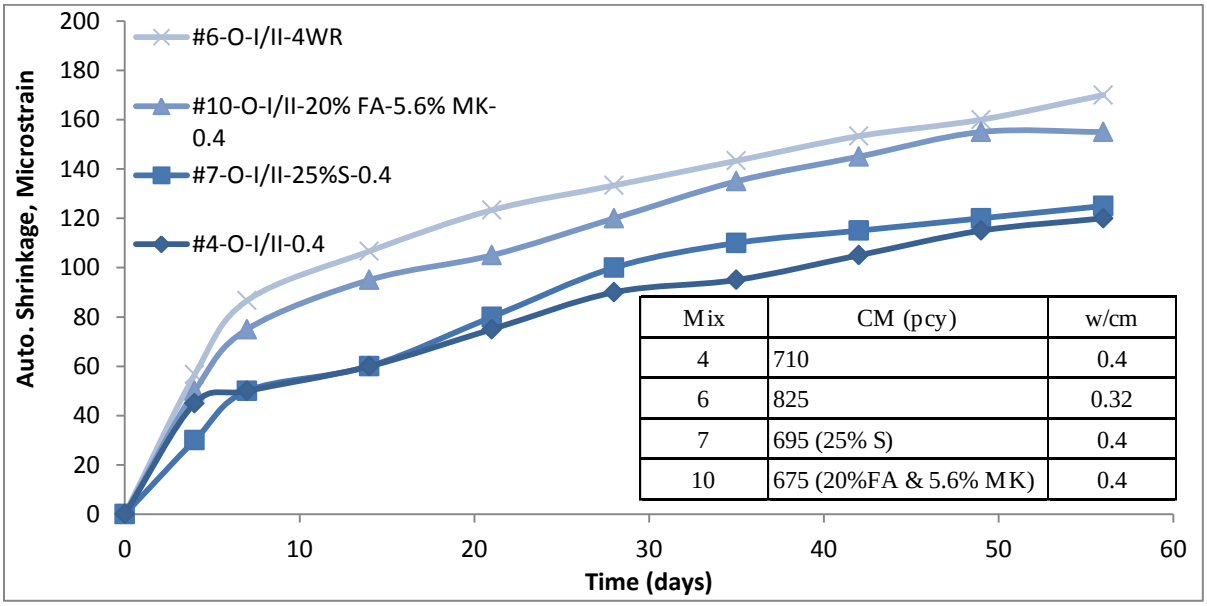

Mix	CM (pcy)	w/cm
4	710	0.4
6	825	0.32
7	695 (25% S)	0.4
10	675 (20%FA & 5.6% MK)	0.4

Figure 4.15. Autogenous shrinkage of concrete (Group 2)

The mixes in Group 2 are all O-type mixes and have the same cement (Lafarge I/II), water reducer, and aggregate gradations. The differences are that Mixes 4 and 6 don't have SCMs, while Mixes 7 and 10 do. Mix 6 has much lower w/b (0.32) than all other mixes (0.40). The order of the cementitious material content, from high to low, is Mix 6, 4, 7, and 10. Figure 4.15 shows that Mix 6 (w/b=0.32, cementitious material content of 825 lb/yd^3) has the highest autogenous shrinkage value at all ages, which confirms the general concern for the autogenous shrinkage of low w/b and high cementitious material content concrete. The comparison of Mixes 7 and 10 suggests that MK significantly increases the autogenous shrinkage given that fly ash replacement reduces the autogenous shrinkage (as Figure 4.14 shows). This inference is similar to that gained from the autogenous shrinkage of mortar.

Figure 4.16 illustrates the autogenous shrinkage of concrete of Group 3, which consists of Mixes 8 and 9.

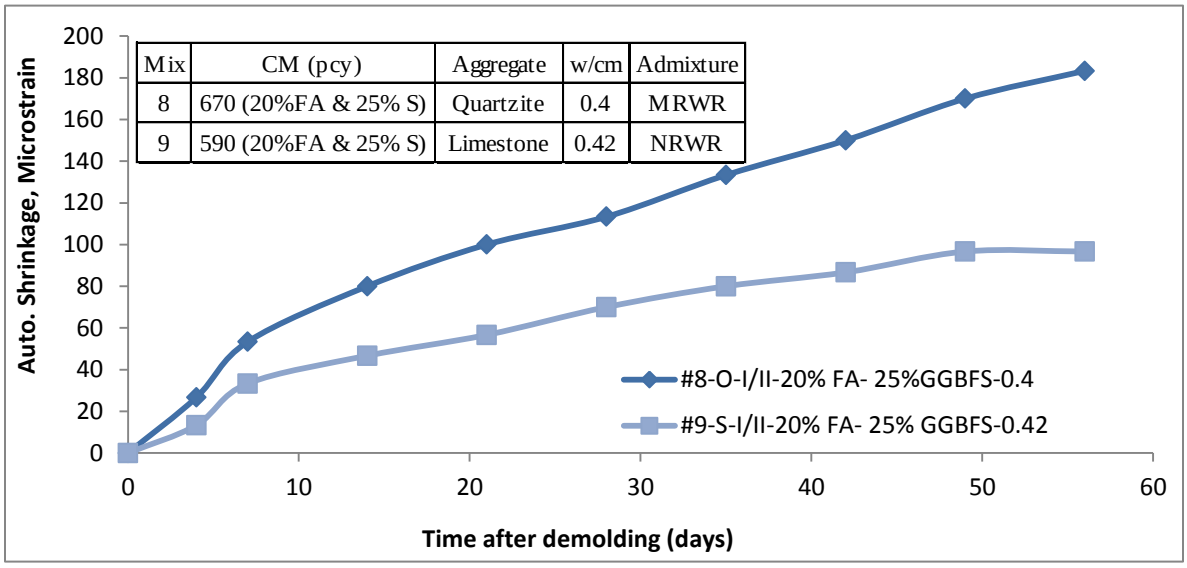

Figure 4.16. Autogenous shrinkage of concrete (Group 3)

Both mixes contain 20% fly ash and 25% GGBFS replacement but different w/b, cementitious content, water reducer type, coarse aggregate type and coarse aggregate gradation. Mix 8 contains 670lb/yd^3 while Mix 9 contains 590 lb/yd^3. This may result in the autogenous shrinkage of Mix 8 being significantly larger than Mix 9. Mix 8 contains high shrinkage-resistant aggregate quartzite while Mix 9 has limestone as the coarse aggregate.

Autogenous shrinkage test results of Group 4 are shown in Figure 4.17.

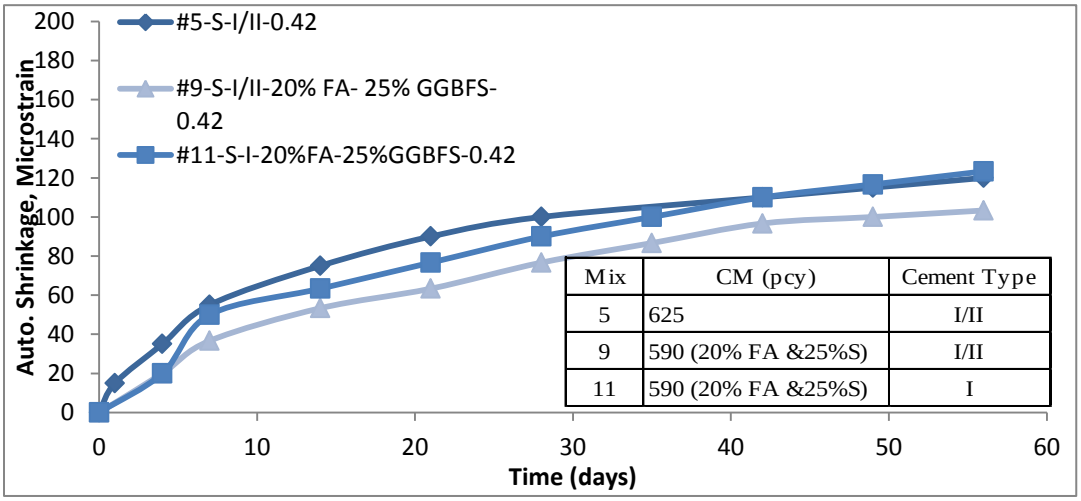

Figure 4.17. Autogenous shrinkage of concrete (Group 4)

All mixes in this group have the same water cementitious material ratio, water reducer, and coarse aggregate gradation. Comparison of Mixes 5 and 9 implies that combined 20% fly ash and 25% GGBFS replacement for cement has provided significant reduction in autogenous shrinkage of the concrete.

Mix 9 and Mix 11 are identical mixes in all aspects other than the cement type used. Mix 9 is composed of Type I/II cement while Mix 11 has Type I cement. Higher shrinkage in Type I cement is typical. Figure 4.17 shows Mix 11 displays consistently higher shrinkage than Mix 9. Again, these observations are similar to those obtained from the mortar autogenous shrinkage test results.

The slopes of the curves in Figure 4.14 through Figure 4.17 also illustrate the rates of shrinkage with time. Generally, greater amounts of shrinkage were observed in the first 28 days, but it decreased significantly thereafter. Use of 20% fly ash replacement alone showed a reduction of shrinkage from those of 100% cement mixtures. Use of GGBFS at 25% replacement alone increased autogenous shrinkage. The combination of 20% fly ash and 25% GGBFS showed little effect on concrete autogenous shrinkage.

Figure 4.18 illustrates the correlation of autogenous shrinkage and cementitious material content at different ages. Similar to mortar, no clear relationship was found.

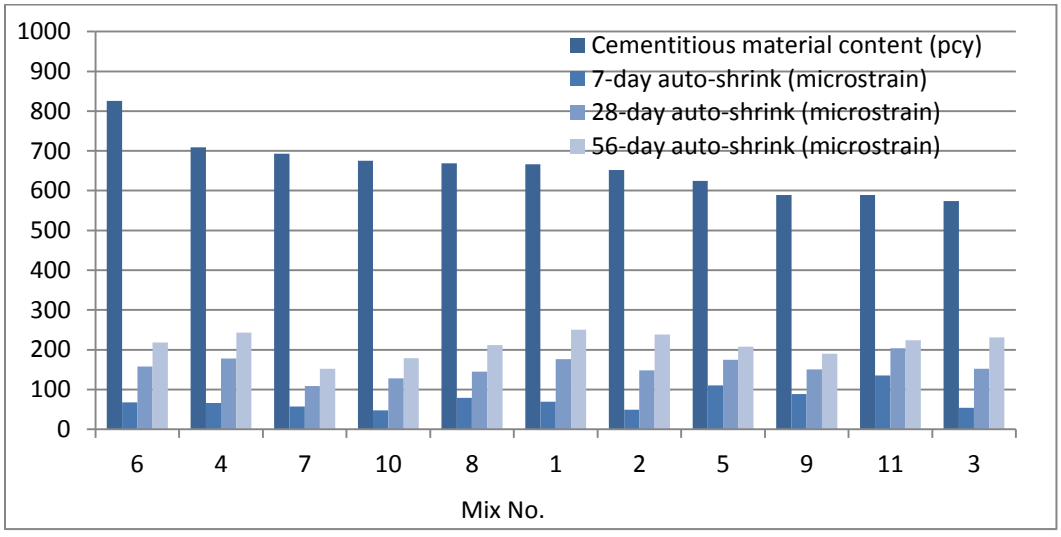

Figure 4.18. Correlation of autogenous shrinkage and cementitious content of concrete

4.3 Free Drying Shrinkage

Free drying shrinkage tests were performed for both mortar and concrete. The free drying shrinkage of mortar is determined based on ASTM C 596 (the standard test method for drying shrinkage of mortar containing hydraulic cement). Free drying shrinkage of concrete is determined according to ASTM C 157 (the standard test method for length change of hardened

hydraulic-cement mortar and concrete). In addition to shrinkage, water loss in mortar and concrete specimens were also monitored with time.

4.3.1 Mortar

4.3.1.1 Mass loss

The results of mass loss of mortar specimens for all 11 mixes are shown in Figure 4.19 through Figure 4.23. Figure 4.19 shows the mass loss test result of mortars in Group 1.

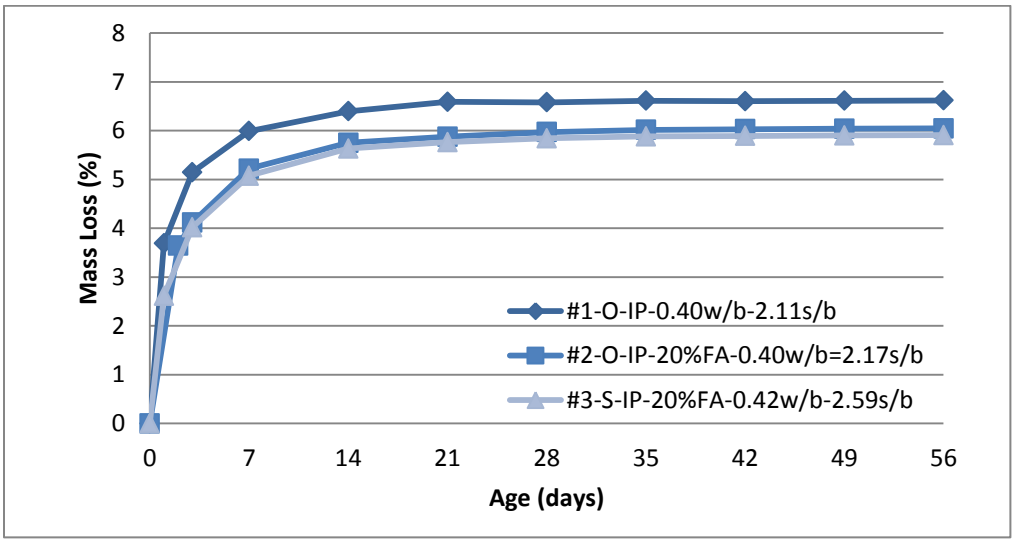

Figure 4.19. Mass loss of mortar (Group 1)

The figure shows that the major mass loss occurs during the first 7 days and that, after 21 days of drying, the mass loss becomes negligible. Mix 1 has relatively higher mass loss than Mix 2 and Mix 3, which have no significant difference. The trend of water loss of these specimens is consistent with the free drying shrinkage measured from the corresponding mortar specimens (Figure 4.25).

Figure 4.20 illustrates the mass loss of mortar specimens in Group 2. All four mixes in this group shows similar mass loss values at the first 7 days. After 14 days, their mass losses are differentiated. Mix 10 has the lowest mass loss value while Mix 6 has the highest mass loss, which is related to the high drying shrinkage value as discussed later.

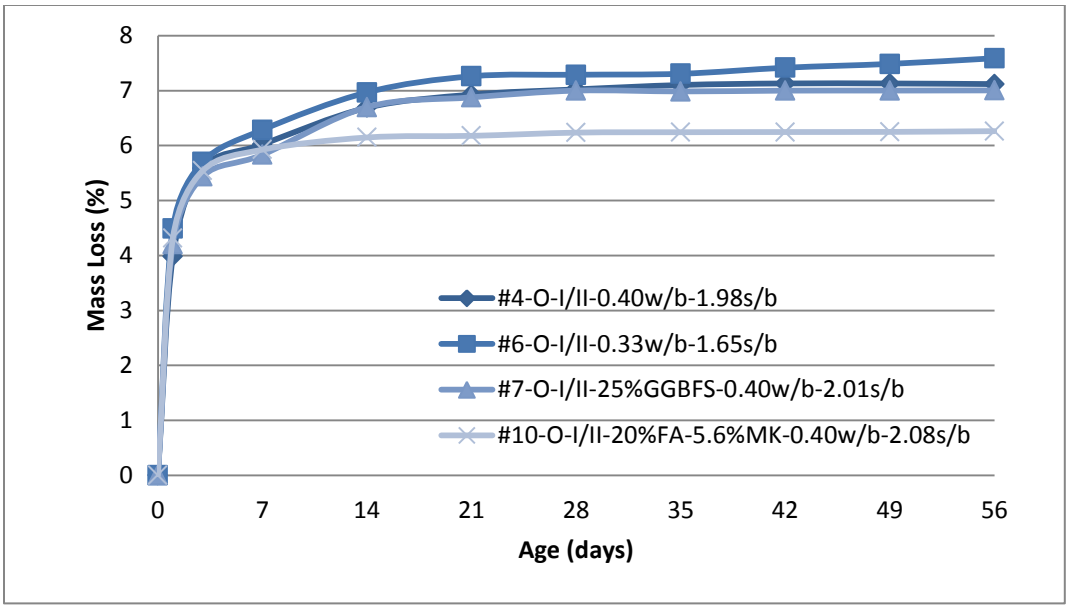

Figure 4.20. Mass loss of mortar (Group 2)

Figure 4.21 presents the results of mass loss of mortar specimens in Group 3. Mix 8 and 9 have very similar trends at all ages. Mass loss increases rapidly during the first 7 days and becomes stable thereafter. Mix 9 has relatively higher mass loss than Mix 8.

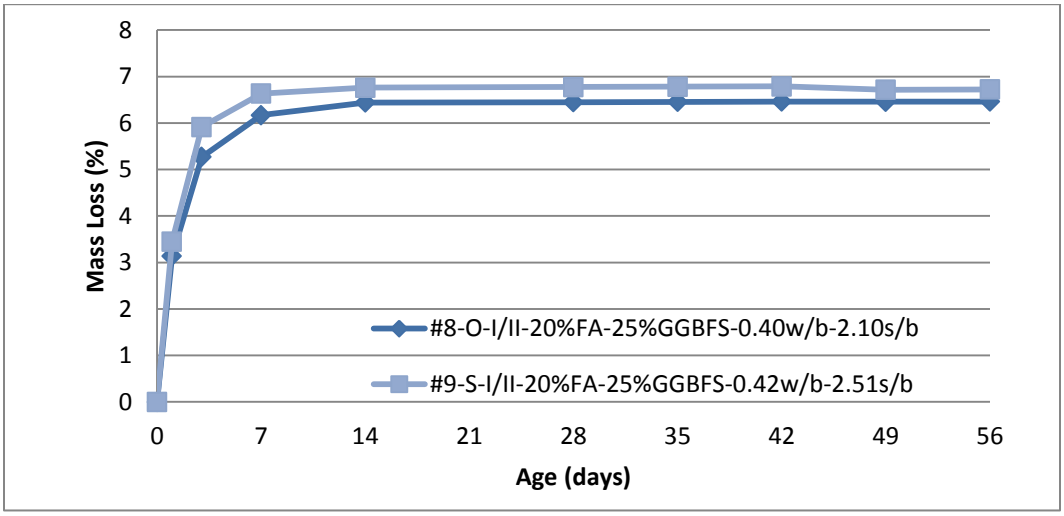

Figure 4.21. Mass loss of mortar (Group 3)

The results of mass loss of mortar specimens in Group 4 are illustrated in Figure 4.22. Mix 5 and 11 show very similar mass losses at the beginning and then differentiate significantly after 3 days. The mass loss of Mix 5 is obviously higher than that of Mix 11, which is also consistent with the results of free drying shrinkage shown later in Figure 4.28.

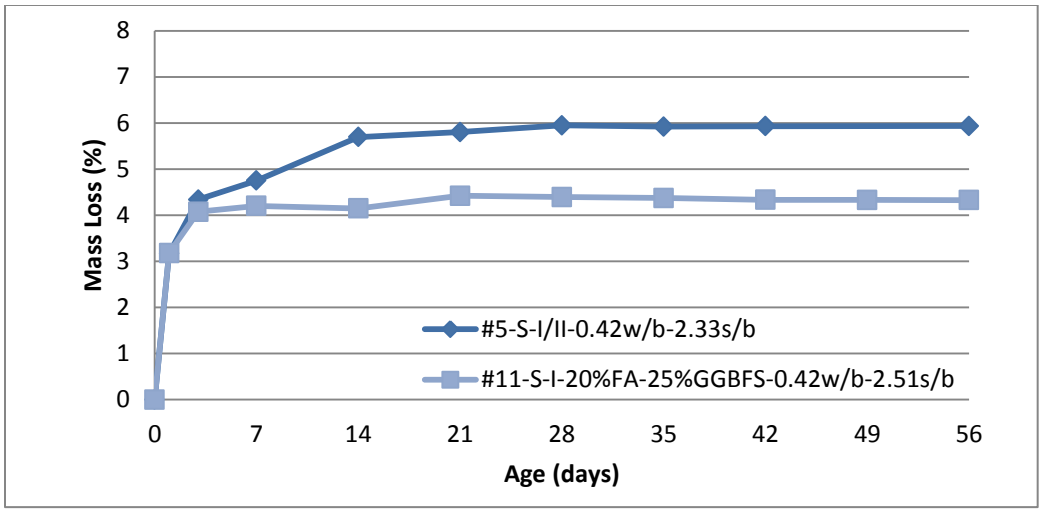

Figure 4.22. Mass loss of mortar (Group 4)

4.3.1.2 Free Drying Shrinkage

Figure 4.23 and Figure 4.24 indicate typical measurements of free drying shrinkage of a set of four mortar specimens. Both figures show that the variation in the measurements of the four samples is quite small and, therefore, the average of the four samples can be taken to obtain consistent and reliable results.

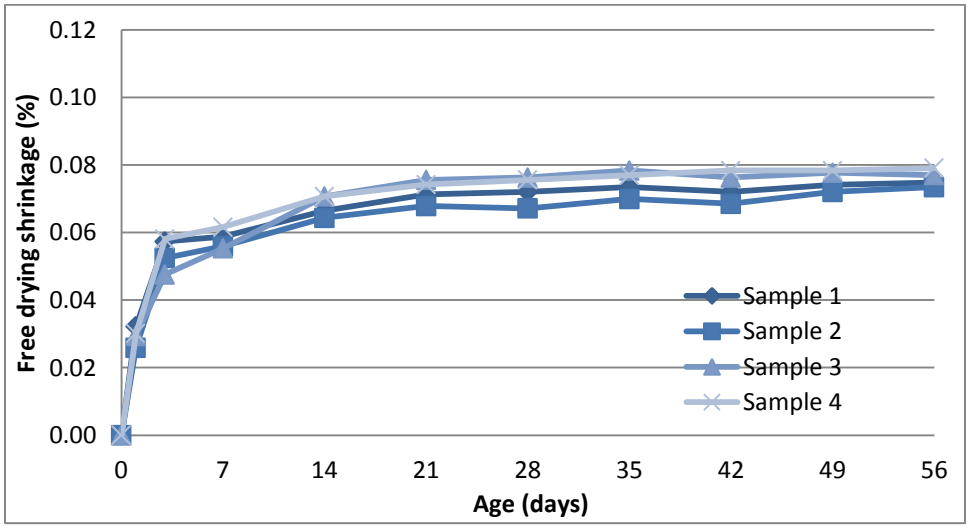

Figure 4.23. Typical free drying shrinkage measurements of Mix 1

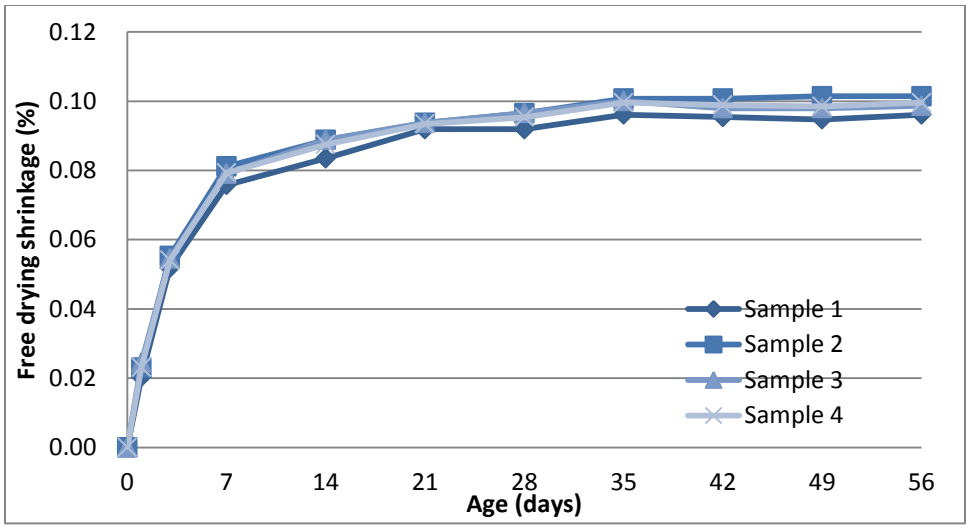

Figure 4.24. Typical free drying shrinkage measurements of Mix 11

The free drying shrinkage test results of mortar for all 11 mixes are presented in Figure 4.25 through Figure 4.28.

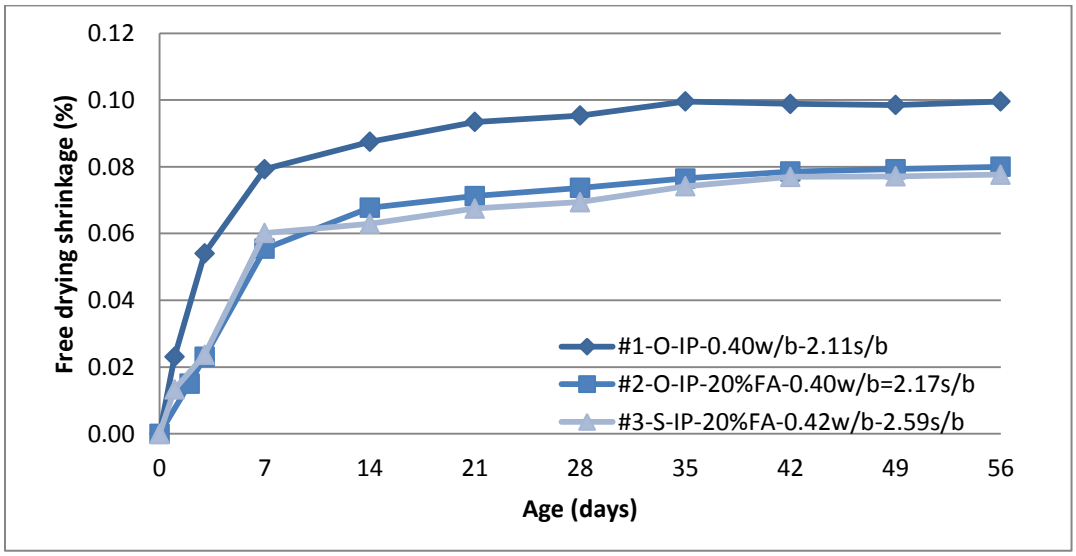

Figure 4.25. Free drying shrinkage of mortar (Group 1)

Figure 4.25 presents the results of free drying shrinkage of mortar in Group 1. In this group, all three mixes show significant increasing free drying shrinkage at the first 7 days, particularly for Mix 1, which has the largest shrinkage values at all ages. The shrinkages of all three mixes increase until the age of 35 days. After that, drying shrinkage of the samples has little change.

The trends and values of free drying shrinkage for Mix 2 and Mix 3 are very similar. As seen in Figure 4.25, 20% fly ash replacement decreases the free drying shrinkage of mortar. Both Mix 2 and Mix 3 have 20% FA replacement and their drying shrinkage is quite similar.

Figure 4.26 illustrates the results of free drying shrinkage of mortar specimens in Group 2. This group shows obvious increases in drying shrinkage the first 14 days and then becomes stable after 21 days.

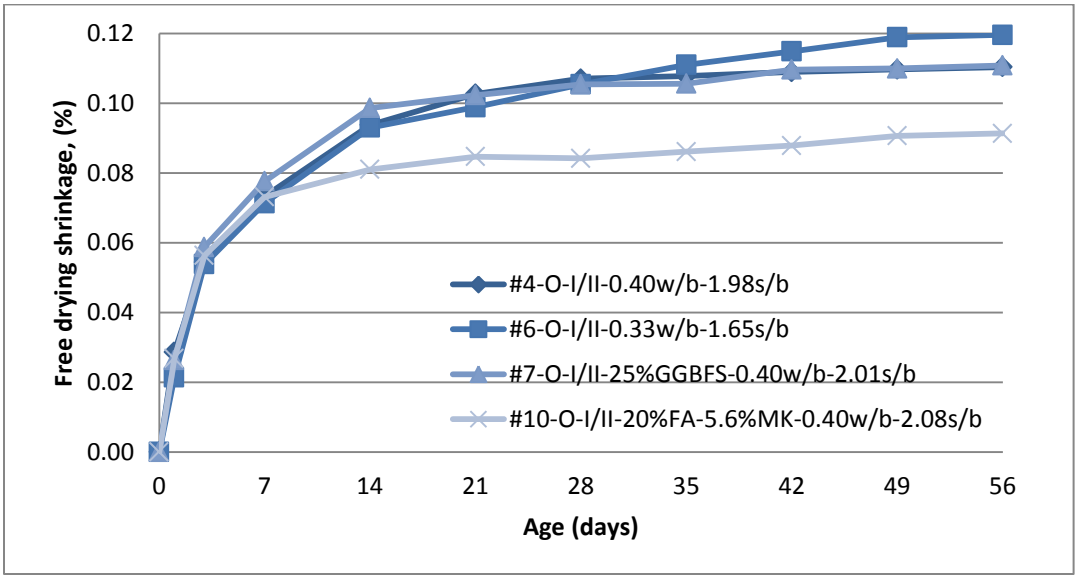

Figure 4.26. Free drying shrinkage of mortar (Group 2)

Mix 6 still shows a continued increase in shrinkage after 35 days, which may be attributed to its low s/b (1.65). Mix 10 displays the lowest shrinkage values among all the mixes in this group after 7 days, which is due mainly to the FA and MK replacements. Compared to Mix 4, 25% GGBFS replacement in Mix 7 appears to have little effect on the drying shrinkage of mortar.

Figure 4.27 shows the results of free drying shrinkage of mortars in Group 3, including Mix 8 and Mix 9.

Again, the shrinkage of all samples increase rapidly at the first 7 days and become stable thereafter. The shrinkage behavior for both Mix 8 and Mix 9 seems very similar, even though their w/b and s/b are different. The similar observation is also obtained from the autogenous shrinkage of their mortar mixes (Figure 4.26).

Table 4.5 shows that Mixes 8, 9, and 11 has the lowest free drying shrinkage among all 11 mixes studied. 20% FA and 25% GGBFS replacements lower the free drying shrinkage significantly.

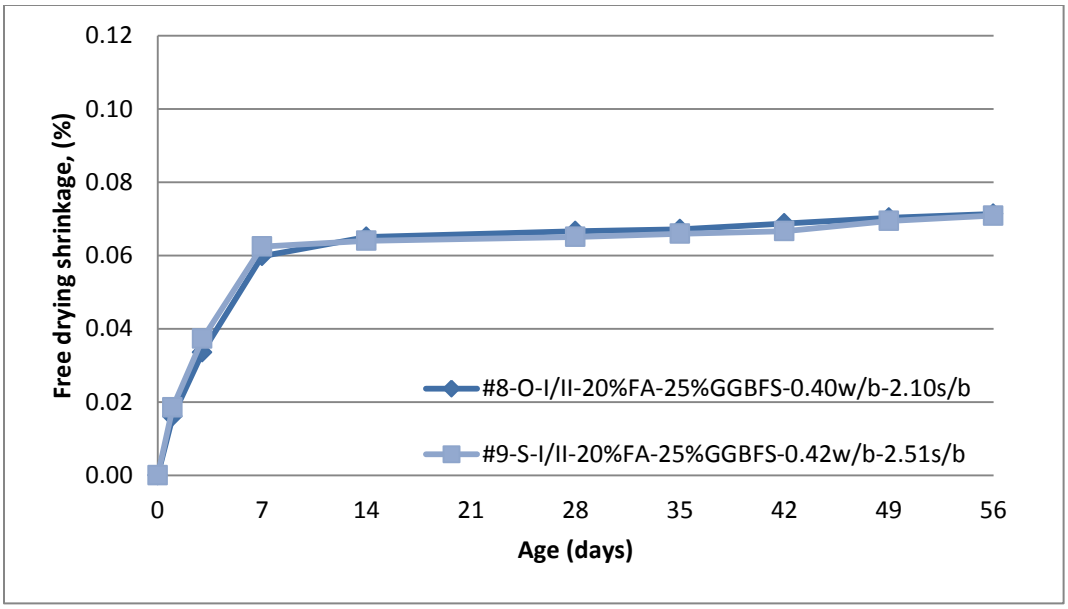

Figure 4.27. Free drying shrinkage of mortar (Group 3)

Figure 4.28 presents the results of free drying shrinkage of mortar for Group 4. For Group 4 mixes, there is a rapid increase at the first 14 days in drying shrinkage and the mixes become stable after 21 days. Mix 11 has almost the same shrinkage values as Mix 5 at the first two data points, however, that becomes lower after 7 days. It is shown again that replacement with both 20% FA and 25% GGBFS decreases the drying shrinkage of mortar remarkably, which is very good for shrinkage-induced cracking control.

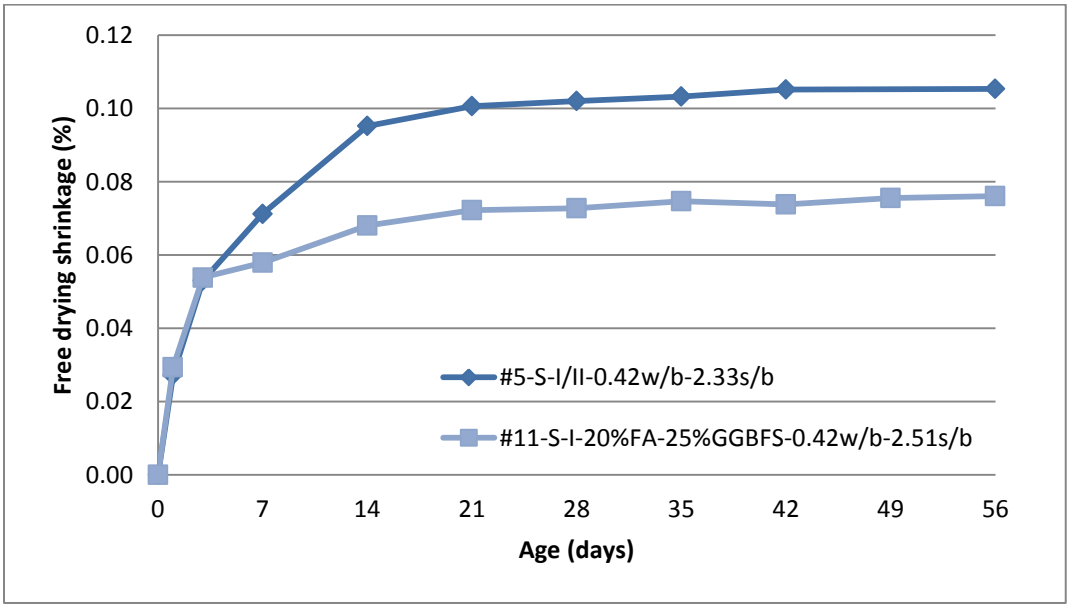

Figure 4.28. Free drying shrinkage of mortar (Group 4)

Table 4.3 summarizes all of the free drying shrinkage values of mortar at 56 days. There are five mixes that have greater than or equal to 0.1% of free drying shrinkage and the other mixes have less than 0.1%. Mixes 6, 4, and 7 show significantly higher shrinkage values, while Mixes 11, 8, and 9 have the lowest shrinkage values.

Table 4.3. Free drying shrinkage of mortar at 56 days

Mix No.	Cement	SCM	W/B	Water Reducer	Shrinkage at 56 day (microstrain)
1	Ash Grove IP	-	0.40	MRWR	1003
2	Ash Grove IP	20% FA	0.40	MRWR	805
3	Ash Grove IP	20% FA	0.40	NRWR	771
4	Lafarge I/II	-	0.40	MRWR	1110
5	Lafarge I/II	-	0.42	NRWR	1050
6	Lafarge I/II	-	0.40	NRWR	1198
7	Lafarge I/II	25% Slag	0.40	MRWR	1101
8	Lafarge I/II	20% FA and 25%Slag	0.40	MRWR	714
9	Lafarge I/II	20% FA and 25%Slag	0.42	NRWR	709
10	Lafarge I/II	20% FA and 5.6% MK	0.40	MRWR	913
11	Lehigh I	20% FA and 25%Slag	0.42	NRWR	761

Figure 4.29 illustrates the results of free drying shrinkage for all mixes at 56 days. As seen, Mixes 8 and 9 have the lowest free drying shrinkage values and Mix 6 has the highest free drying shrinkage value. It can again be seen that 20% FA and 25% GGBFS replacements clearly decrease free drying shrinkage of mortar.

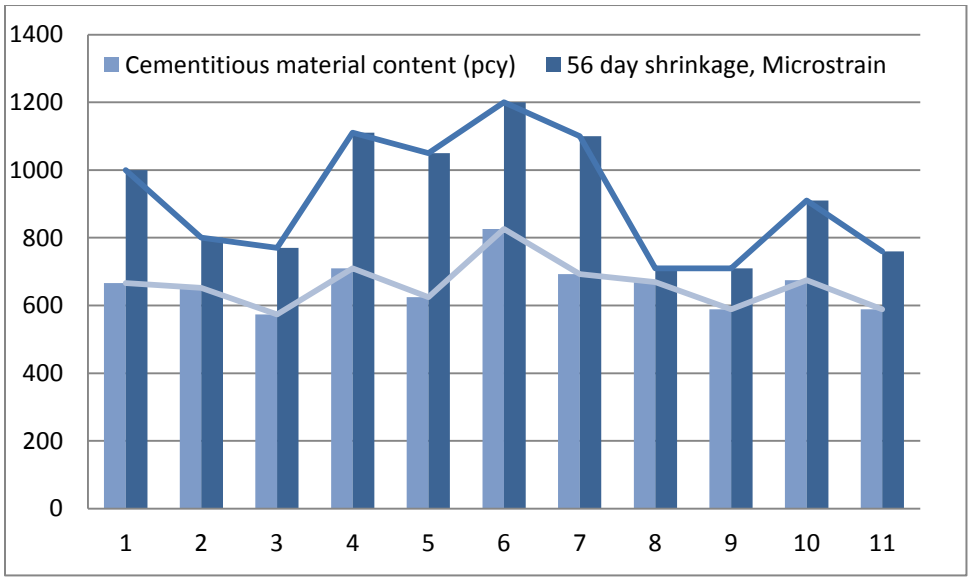

Figure 4.29. Free drying shrinkage of mortar for all mixes at 56 days

The trends for free drying shrinkage curves of mortars are very similar to those for mass loss of the corresponding mortars. A relationship may exist between mass loss and free drying shrinkage

of mortar, given drying shrinkage results from moisture loss in hardened mortar or concrete from the surrounding environment.

4.3.1.3 Summary

In summary, based on the experimental research for autogenous shrinkage and free drying shrinkage of mortar, the following conclusions can be drawn:

1. Ternary mixes with both GGBFS and FA replacements reduce autogenous shrinkage of mortar, but MK replacement seems to increase the autogenous shrinkage.
2. High s/b is beneficial for reducing both autogenous and drying shrinkage of mortar.
3. Type I cement provides mortar samples with higher autogenous shrinkage than Type IP cement.
4. The effects of SCMs on autogenous shrinkage are not always the same as on free drying shrinkage. FA replacement at 20% decreased free drying shrinkage of mortar but GGBFS replacement at 25% increased it.
5. The combination of 20% FA and 5.6% MK replacement and the combination of 20% FA and 25% GGBFS replacement decrease the drying shrinkage of mortar.
6. According to the measurements of autogenous shrinkage and free drying shrinkage of mortar, Mixes 8,9,10, and 11 are considered low-shrinkage concrete among all mixes studied.

4.3.2 Concrete

4.3.2.1 Mass Loss of the Specimens for Free Drying Shrinkage Test

Mass loss of concrete specimen results for all 11 mixes are presented in Figure 4.30 through Figure 4.33. Figure 4.30 shows the mass loss test results of concretes for Group 1. As shown, the major portion of mass loss occurs during the first 14 days. Mix 1 displays the least amount of mass loss and Mix 3 shows the greatest amount of mass loss. This behavior is not consistent with the mass loss of mortar. The trend for mass loss is consistent with the free shrinkage development as the majority of shrinkage occurs in the first 14 days.

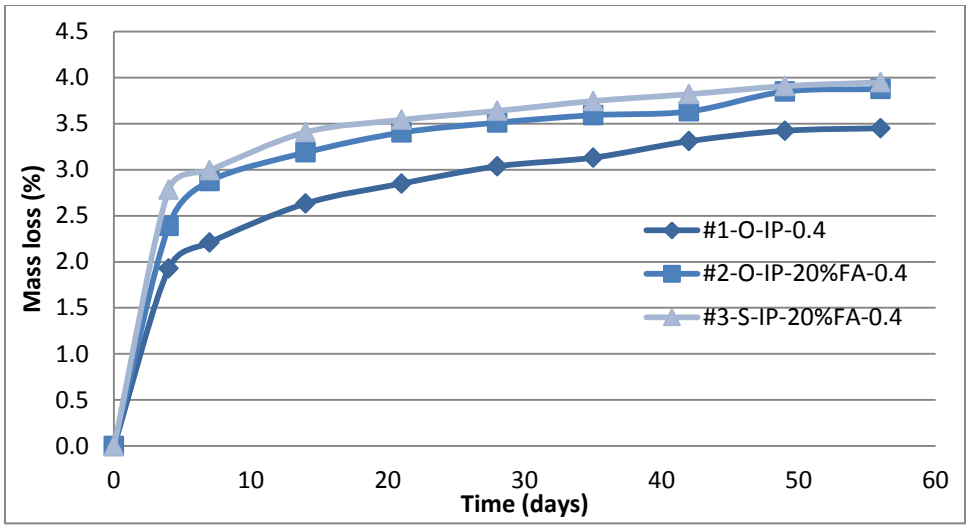

Figure 4.30. Mass loss of concrete (Group 1)

Figure 4.31 illustrates the results for mass loss of mortar specimens in Group 2. The mass loss is similar to that of Group 1 but smaller in magnitude. Mix 6 displays the least amount of mass loss while Mix 10 shows the greatest amount of mass loss. This is opposite from what was observed in mass loss in mortar bars.

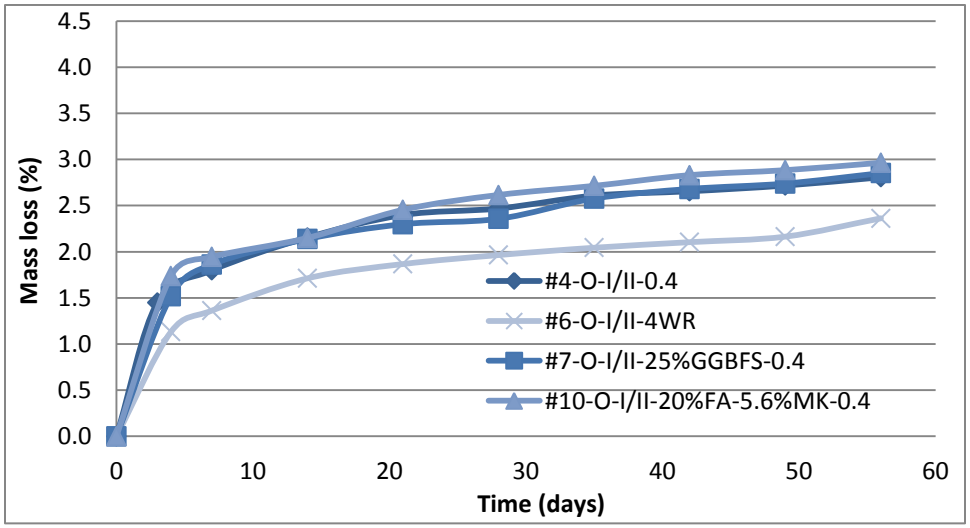

Figure 4.31. Mass loss of concrete (Group 2)

Figure 4.32 illustrates the results for mass loss of mortar specimens in Group 3. Mixes 8 and 9 have no significant differences in mass loss. The results obtained are consistent with the observations made for mortar. Mass loss is rapid in the first 7 days and slows rapidly at the age of 14 days for both Mix 8 and Mix 9.

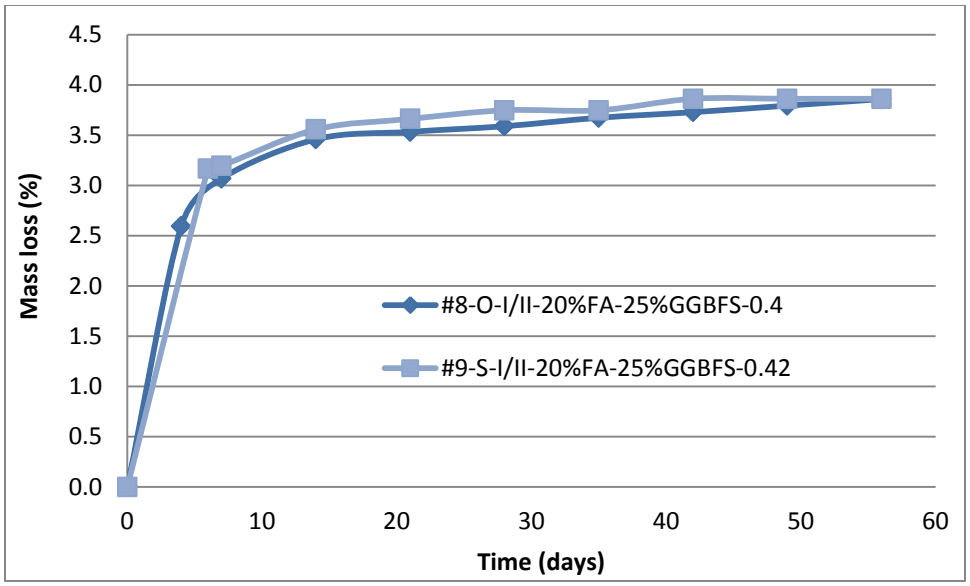

Figure 4.32. Mass loss of concrete (Group 3)

Figure 4.33 presents the results for mass loss of concrete in Group 4. Mix 5, which is the control mix, displays the least amount of mass loss while Mixes 9 and 11 show significantly large amounts of mass loss. The behavior of Mix 11 does not agree with the mortar mass loss. However, Mix 9 agrees with the behavior for mortar.

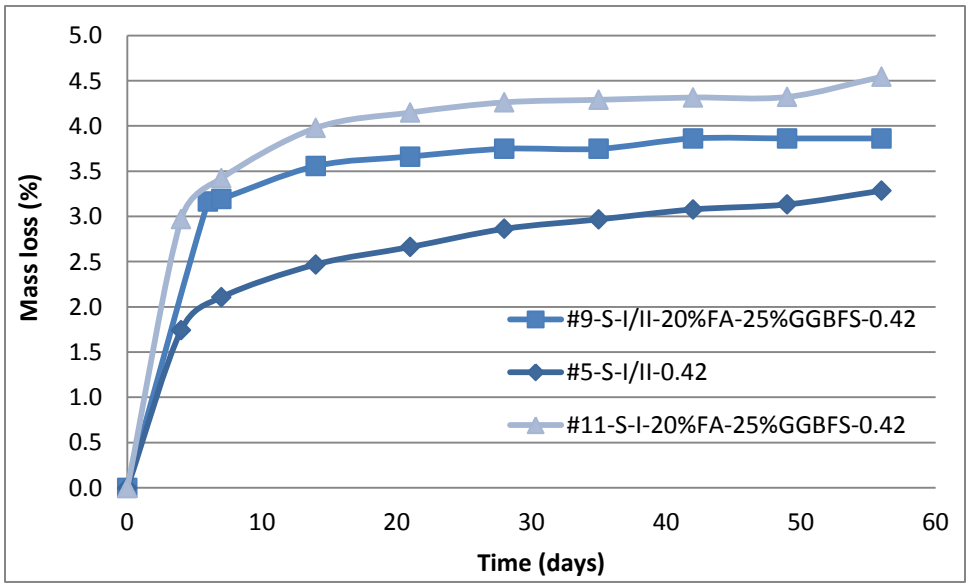

Figure 4.33. Mass loss of concrete (Group 4)

4.3.2.2 Free Drying Shrinkage

Typical Measurements

Typical free drying shrinkage measurements are shown in Figure 4.34 and Figure 4.35. Both plots indicate a very small variation among the three samples tested for each mix. Therefore, the average of the three samples have been taken as representative for each mix.

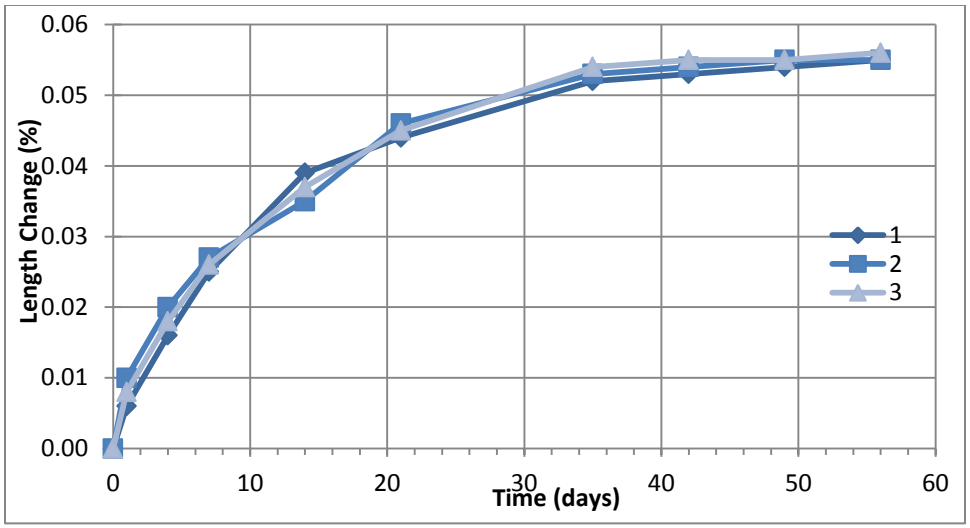

Figure 4.34. Typical free drying shrinkage measurement of mix 5

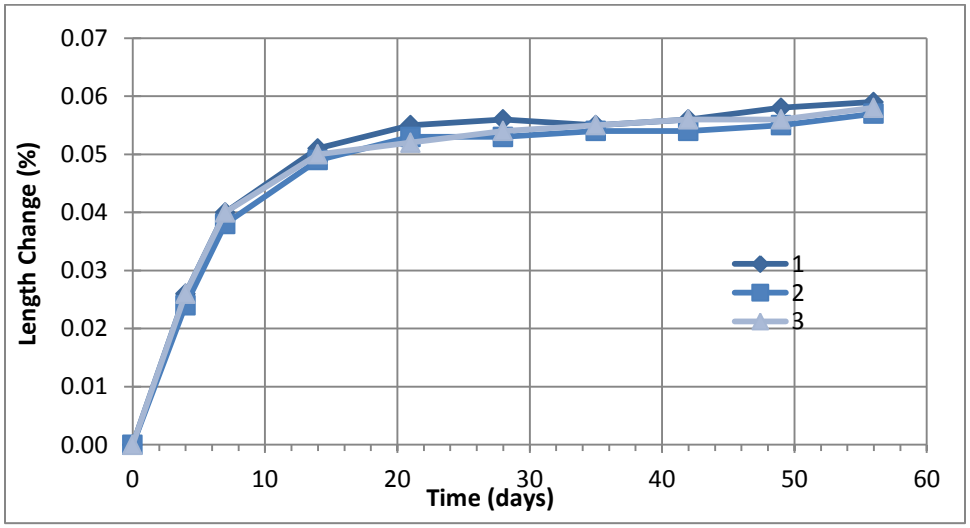

Figure 4.35. Typical free drying shrinkage measurement of mix 11

Free drying shrinkage of the 11 mixes is discussed in the following section. The behavior of the 11 test mixes are illustrated in Figure 4.36 through Figure 4.40.

Figure 4.36 illustrates the free drying shrinkage test results for concrete in Group 1. The shrinkage development of the three mixes is similar in the first 7 days of drying. The performance of Mixes 1 and 2 do not show a significant difference. The addition of FA in a mix generally reduces free drying shrinkage. It is not clear why the reduction observed for mortar has not occurred. Pore structure of mortar needs to be investigated to help explain this behavior.

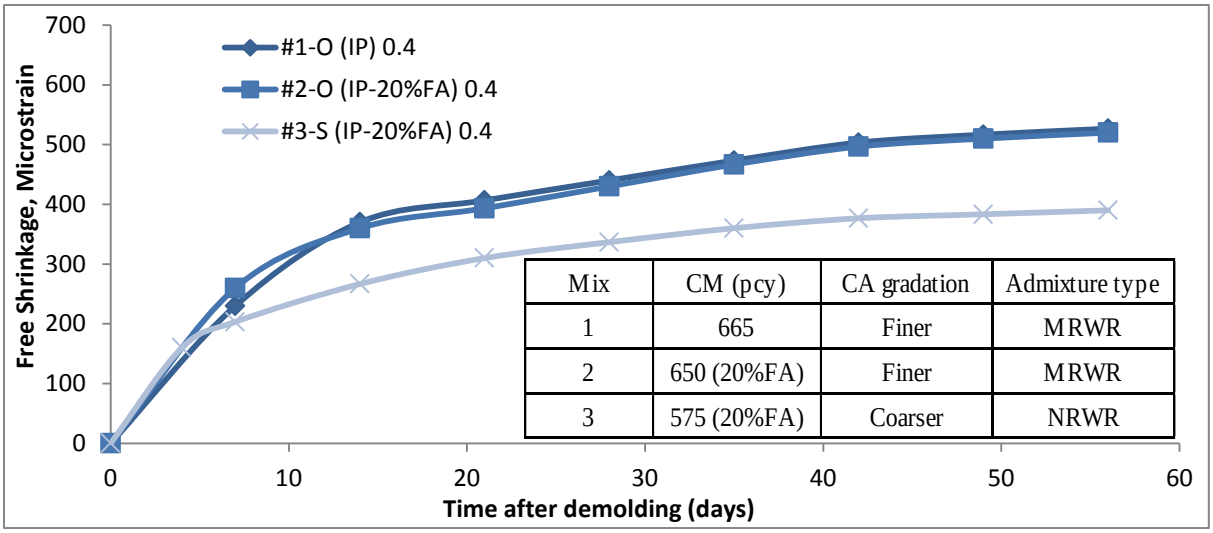

Figure 4.36. Free drying shrinkage of concrete (Group 1)

Mix 3 displays less free shrinkage than Mix 1 and Mix 2. Mix 3 is composed of a coarser coarse aggregate portion and has lesser cementitious material content compared to that of Mix 1 and 2.

Comparing the mass loss (Figure 4.30) and shrinkage (Figure 4.36), the mass loss of Mixes 2 and 3 are greater than that of Mix 1. This forms a partial explanation as to why Mix 2 displays greater shrinkage than Mix 1 with only Type IP cement.

Figure 4.37 shows the results for free drying shrinkage of concrete in Group 2. Mix 4 and Mix 6 have no SCMs in them. Mix 7, with the addition of 25% GGBFS, shows the greatest free drying shrinkage. Mix 6 shows higher shrinkage than Mix 4 due to the high cement factor. In Mix 10, the addition of 20% FA and 5.6% MK has reduced the free drying shrinkage of concrete compared to Mix 4. But the reduction is not a large one and the behavior is almost similar in the first 28 days. This may be a result of the MK having a shrinkage-increasing effect while the shrinkage-reducing effect of FA is countering this effect. Therefore, the combined effect of 20% FA and 5.6% MK reduces the free drying by a small amount.

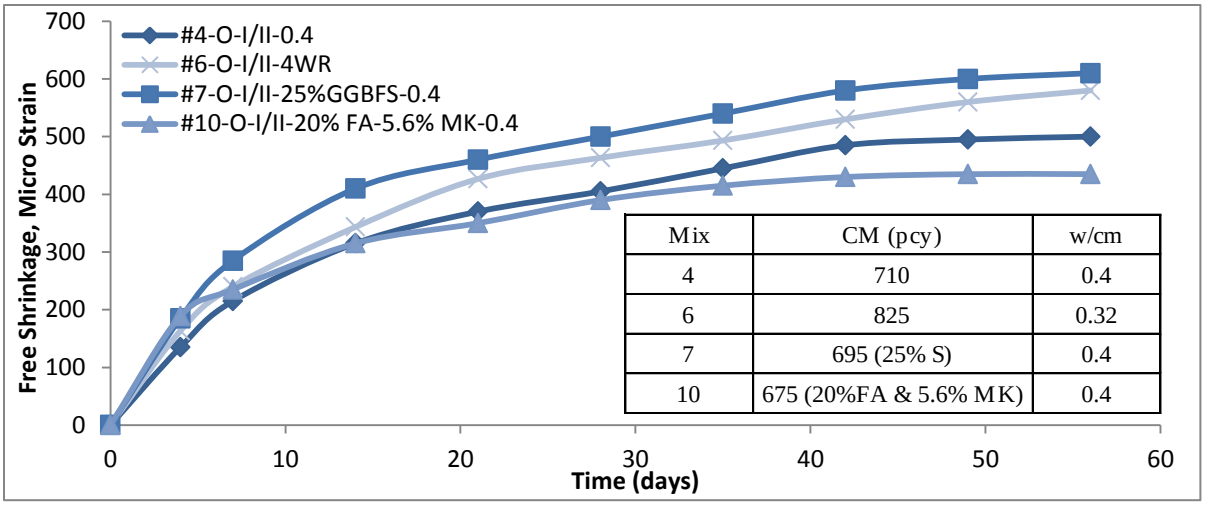

Mix	CM (pcy)	w/cm
4	710	0.4
6	825	0.32
7	695 (25% S)	0.4
10	675 (20%FA & 5.6% MK)	0.4

Figure 4.37. Free drying shrinkage of concrete (Group 2)

The results related to free drying shrinkage for concrete in Group 3 are shown in Figure 4.38. Mix 8 and Mix 9 differ by many factors. Among these factors are the two mixes employing two coarse aggregate types and two gradations. Mix 8 contains a coarser graded quartzite while Mix 9 employs a finer graded limestone. In addition to that, Mix 8 has higher paste content (0.302) than Mix 9 (0.274) leading to a greater amount of anticipated drying shrinkage in Mix 8 than Mix 9. Moreover, Mix 8 has a mid-range water reducer while Mix 9 has a standard water reducer. Although there are so many factors that differ, there is no significant difference in performance of the two mixes. The behavior of concrete is similar to that observed in mortar.

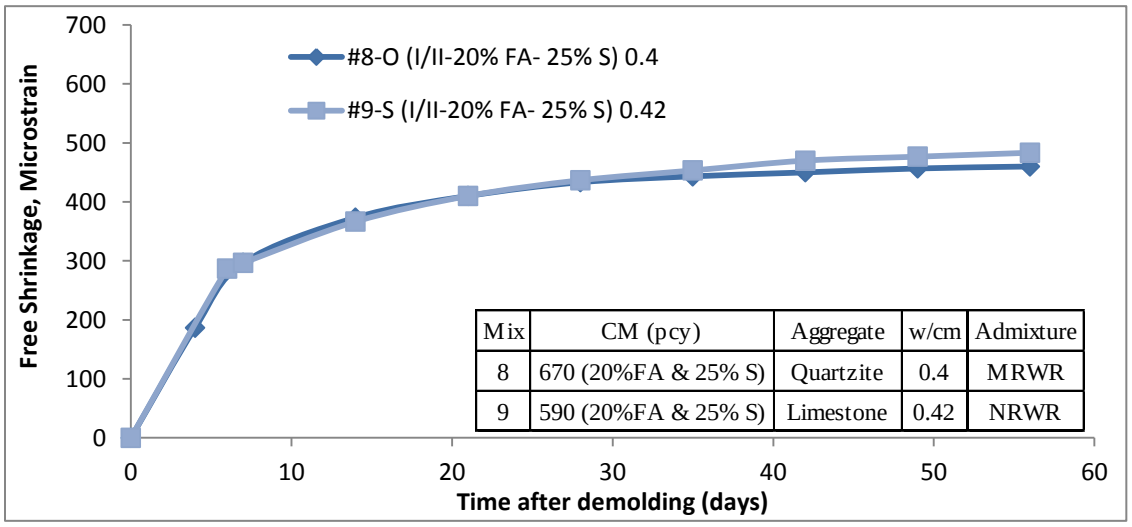

Mix	CM (pcy)	Aggregate	w/cm	Admixture
8	670 (20%FA & 25% S)	Quartzite	0.4	MRWR
9	590 (20%FA & 25% S)	Limestone	0.42	NRWR

Figure 4.38. Free drying shrinkage of concrete (Group 3)

Figure 4.39 illustrates the results of Group 4. Here, the results indicate that the addition of 20% FA and 25% GGBFS has had a positive effect on the mix and reduced the free drying shrinkage. Initially, Mix 5 and Mix 9 have similar shrinkage behavior, but due to the high levels of cement replacement, the rate of shrinkage reduces. It is also important to note that Mix 11 employs Type

I cement and Mix 9 employs Type I/II. With everything else being the same, Mix 11 displays higher shrinkage than Mix 9. The behavior is typical for Type 1 cements.

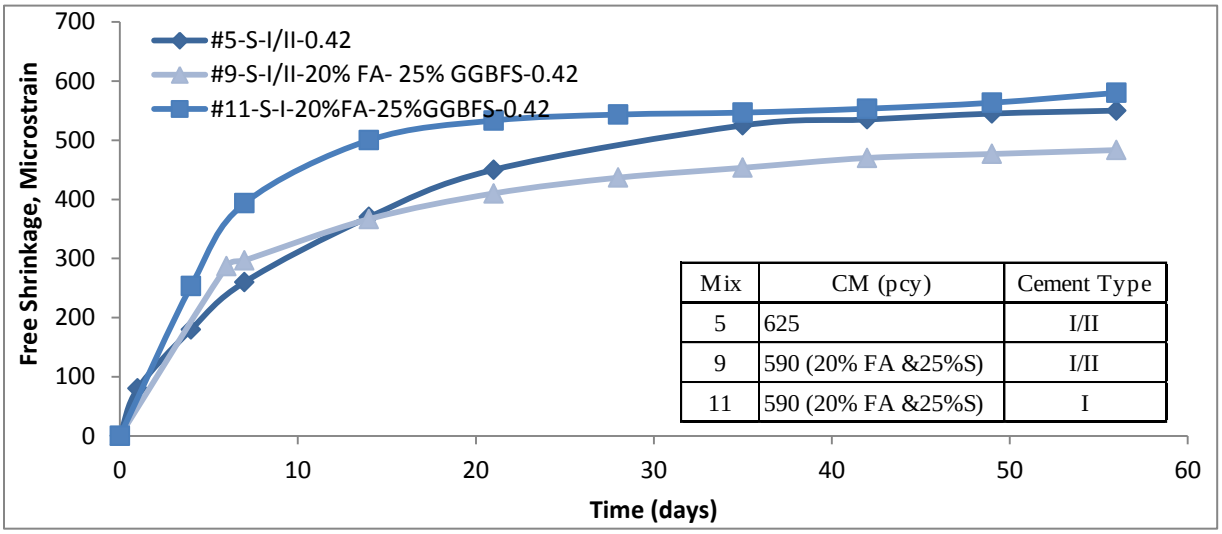

Mix	CM (pcy)	Cement Type
5	625	I/II
9	590 (20% FA &25%S)	I/II
11	590 (20% FA &25%S)	I

Figure 4.39. Free drying shrinkage of concrete (Group 4)

Shrinkage of these mixes slowed significantly after 28 days. Measurements were taken for 56 days and, upon approaching 56 days, the rate of shrinkage slowed significantly. The cementitious material content has a direct influence on the amount of free drying shrinkage for concrete (Figure 4.40).

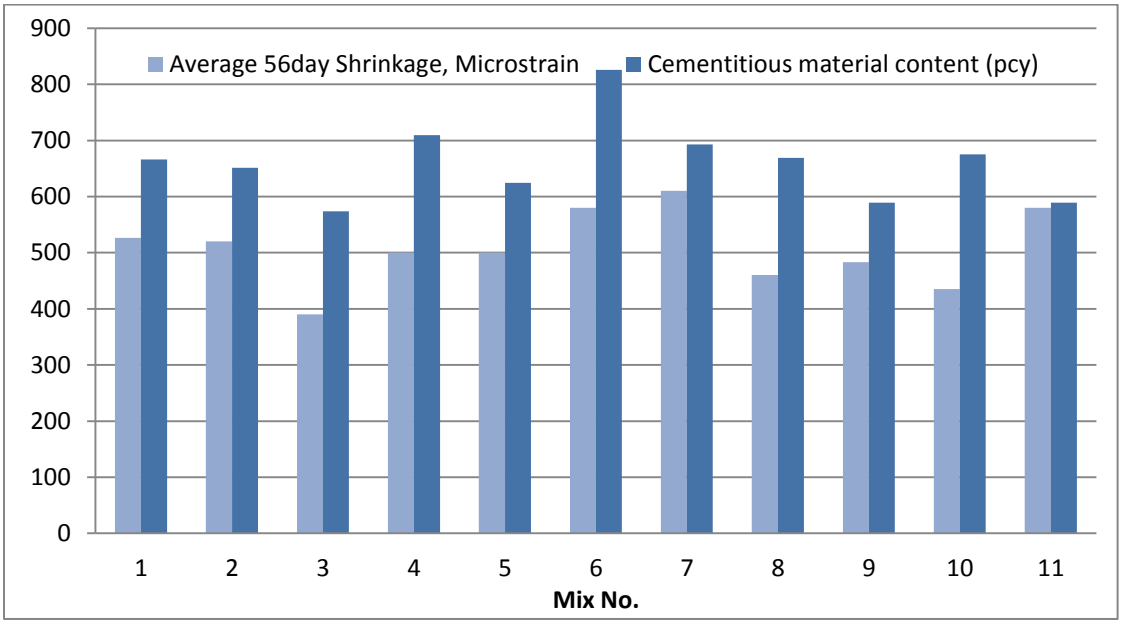

Figure 4.40. Free drying shrinkage of concrete at 56 days

Figure 4.41 illustrates the comparison of individual mixes, where the shrinkage of each mix is correlated individually to its moisture loss. The R^2 values range from 0.82 to 0.99, indicating that comparing free drying shrinkage of each mix with the moisture loss is a good measure of quality control for measurements.

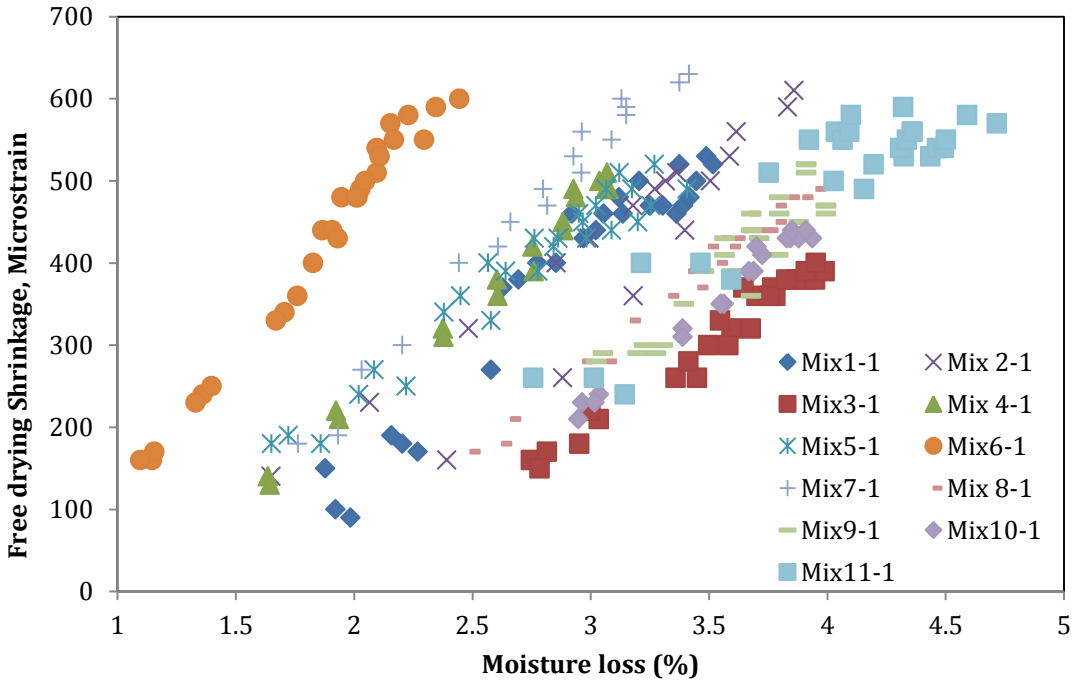

Figure 4.41. Free drying shrinkage versus mass loss (%)

4.3.2.3 Summary

1. The results for mass loss were consistent with free shrinkage observed in the mixes, i.e., more mass loss results in more free drying shrinkage and vice versa.
2. The variation observed in three shrinkage specimens made out of a batch is relatively small.
3. 25% GGBFS replacement for cement results in increased shrinkage. When used with 20% FA, both the rate of drying shrinkage development and the drying shrinkage observed is less than the mix without SCMs.
4. Use of FA reduces free drying shrinkage observed in a mix.
5. Using 5.6% MK with 20% FA increases autogenous shrinkage but reduces free drying shrinkage. This behavior is similar to that observed in mortar.

4.4 Restrained Ring Shrinkage

The restrained ring shrinkage test evaluates the cracking tendency of a concrete mix in addition to restrained shrinkage behavior. Typical results if three rings are made from one batch are close (Figure 4.42) and average shrinkage can be used as a representative result.

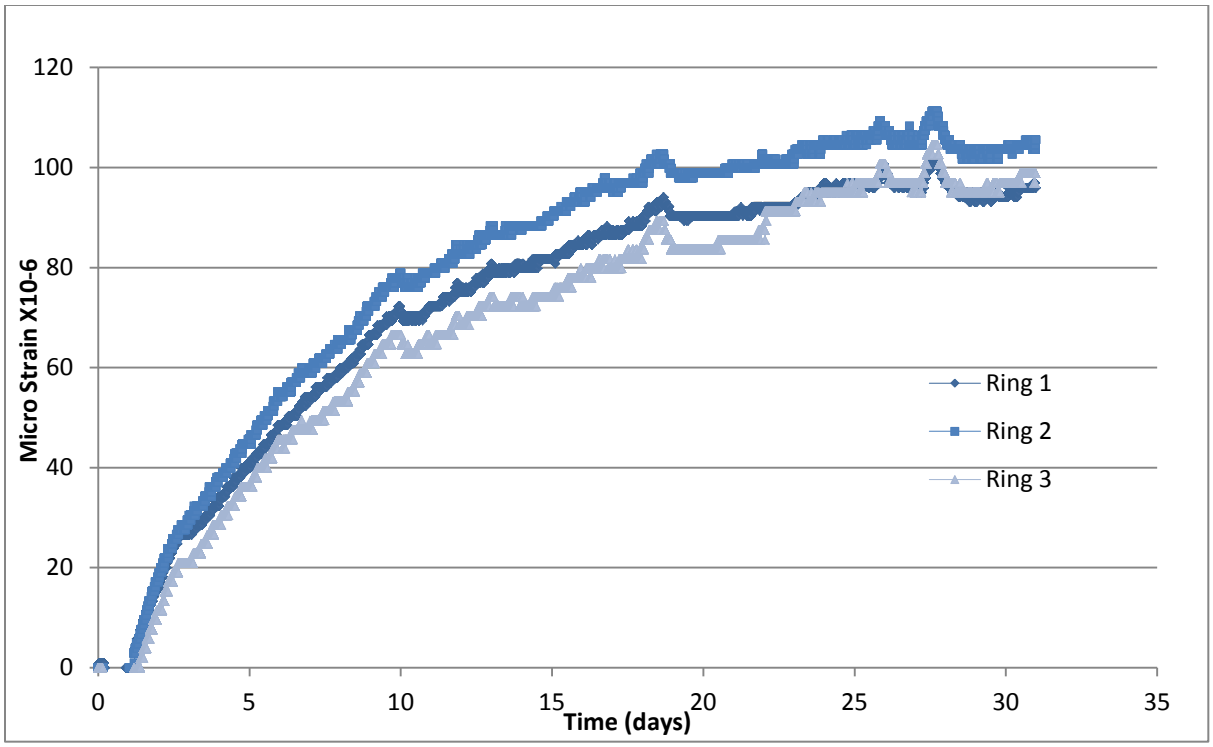

Figure 4.42. Typical result of restrained shrinkage Mix 10

Figure 4.43 illustrates the restrained ring shrinkage results for Group 1.

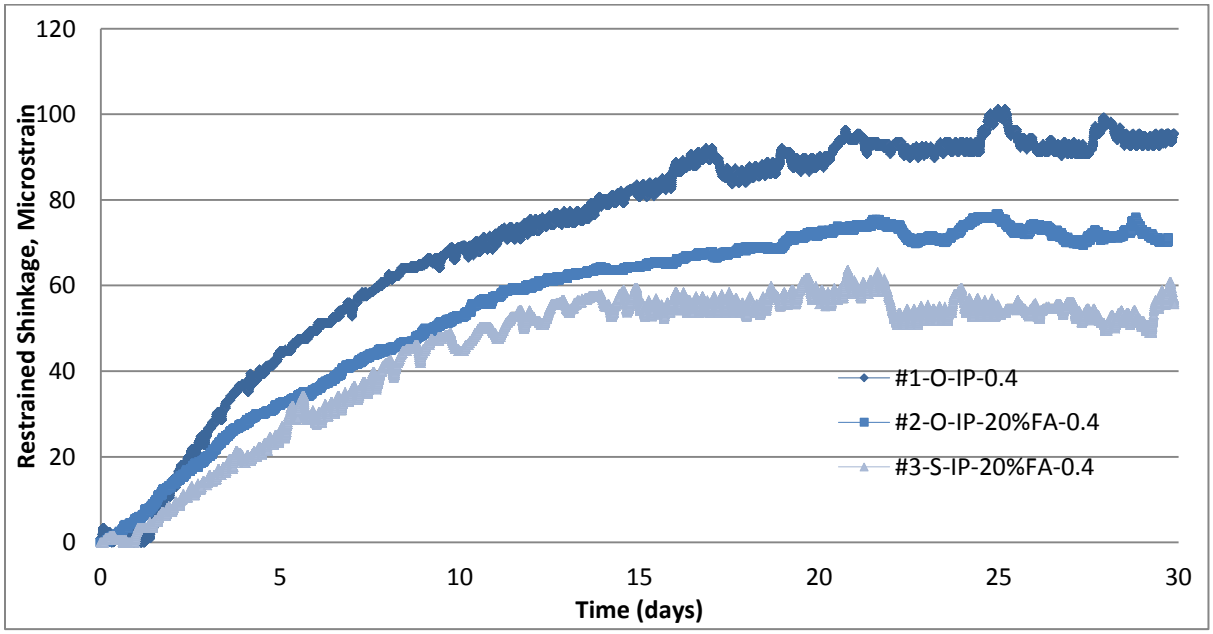

Figure 4.43. Restrained shrinkage of Group 1

Mix 1 displays the greatest amount of shrinkage having only Type IP cement in the mixture. Both Mix 2 and Mix 3 with 20% FA display lesser shrinkage than Mix 1. Mix 2 and Mix 3

display similar early-age behavior but Mix 3 shows less later-age shrinkage. The difference is small compared to that of Mix 1. The trend of restrained shrinkage is similar to that for corresponding free drying shrinkage of mortar specimens.

Restrained ring shrinkage of concrete in Group 2 is illustrated in Figure 4.44.

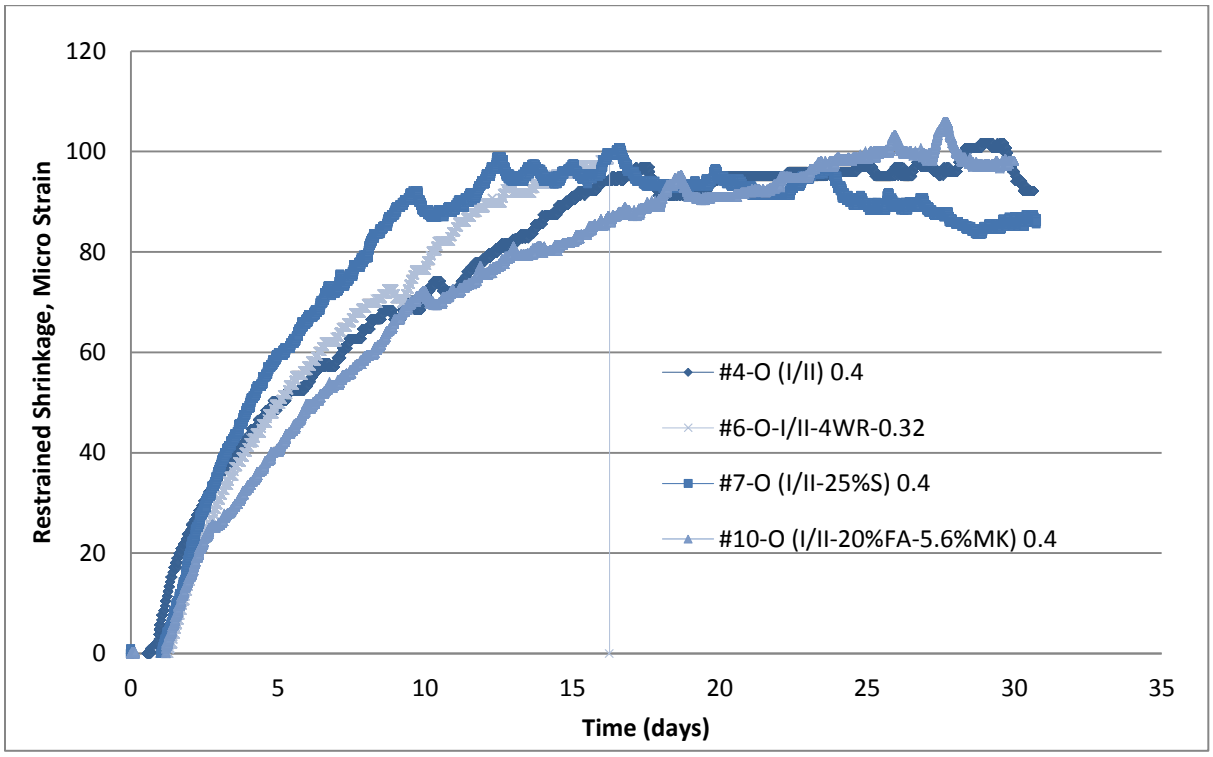

Figure 4.44. Restrained Shrinkage of Group 2

In this group of mixes, Mix 7 shows the greatest rate of early-age strain development, while Mix 10 shows the slowest. No rings made with these two mixes (Mixes 7 and 10) cracked. Although showing lower ring shrinkage values than Mix 7, all three ring specimens of Mix 6 cracked, at 16, 16.5, and 18 days, and two of three rings for Mix 4 cracked at 13 and 18 days.

Mix 4 and Mix 6 are composed of only Type I/II cement and Mix 6 has greater Type I/II cement content (w/c= 0.32). The replacement of cement by 25% slag had an influence toward increasing the rate at which the strain developed initially. However, the strain development slowed significantly after 7 days. The replacement of cement by 20% FA and 5.6% MK had an influence toward reducing the initial rate of shrinkage but the steady growth of shrinkage resulted in similar shrinkage at 28 days as that observed for Mix 4, which had no cement replacement.

The early-age shrinkage in Group 2 is similar to that observed in free drying shrinkage for both concrete and mortar. Mix 4 and Mix 6 cracked although the mixes were not the ones with the highest restrained shrinkage. This result indicates that these mixes had lower cracking resistance.

Figure 4.45 illustrates the restrained ring shrinkage for Group 3. The early-age performances of the mixes are identical. The inclusion of quartzite in Mix 8 is the most significant difference between the two mixes. The trend for early-age shrinkage is similar to that for free drying shrinkage of mortar and concrete.

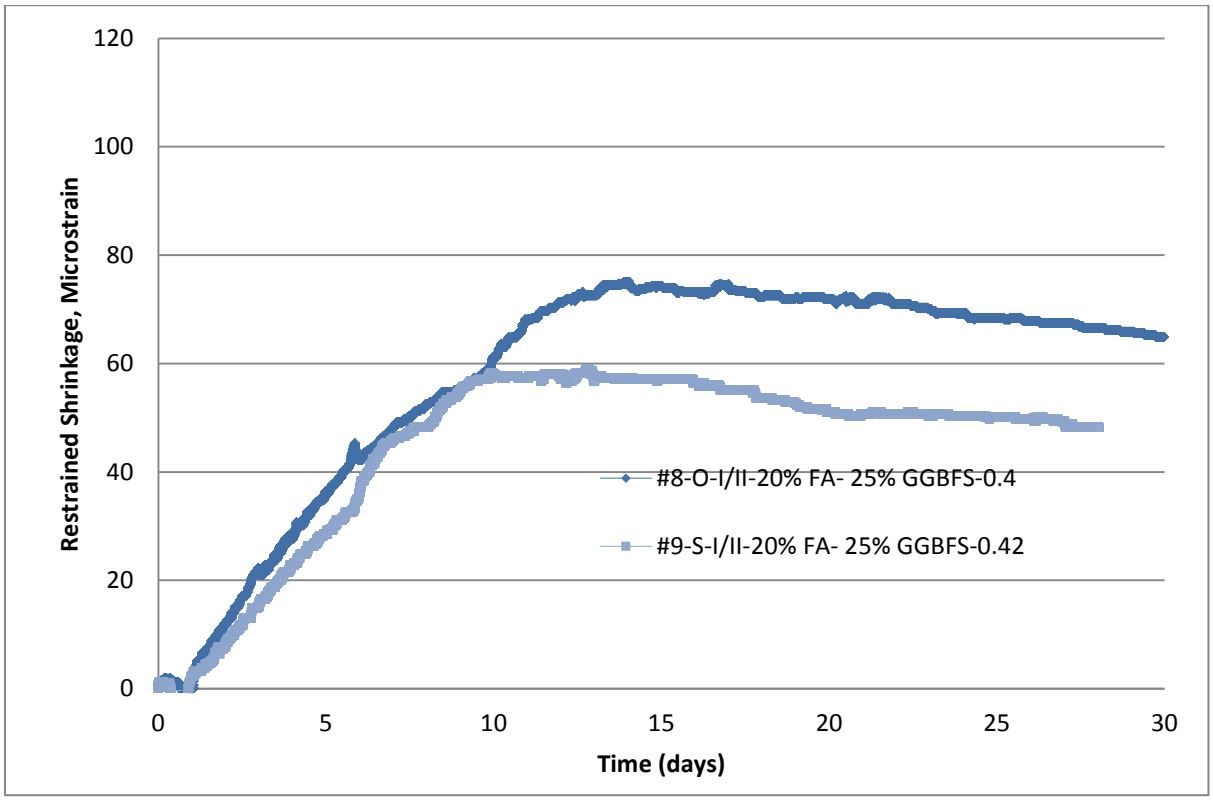

Figure 4.45. Restrained shrinkage of Group 3

Figure 4.46 illustrates the restrained shrinkage for Group 4, where the mixes have the same w/b, water reducer, and coarse aggregate gradation. Mix 5 is a control mix with no SCMs, while Mix 9 has 20% FA and 25% slag. Different from Mix 9, which has Type I/II cement, Mix 11 has Type I cement. Mix 5 has much higher restrained shrinkage than Mixes 9 and 11 and only Mix 5 has one ring cracked at the age of 11 days. This suggests that cement replacement with both 20% FA and 25% slag reduced both the rate and the shrinkage.

Figure 4.46 also illustrates that Mixes 9 and 11 had similar behavior at the early age. However, Mix 11, made with Type I cement, showed greater shrinkage than Mix 9, made with Type I/II cement, at the later age.

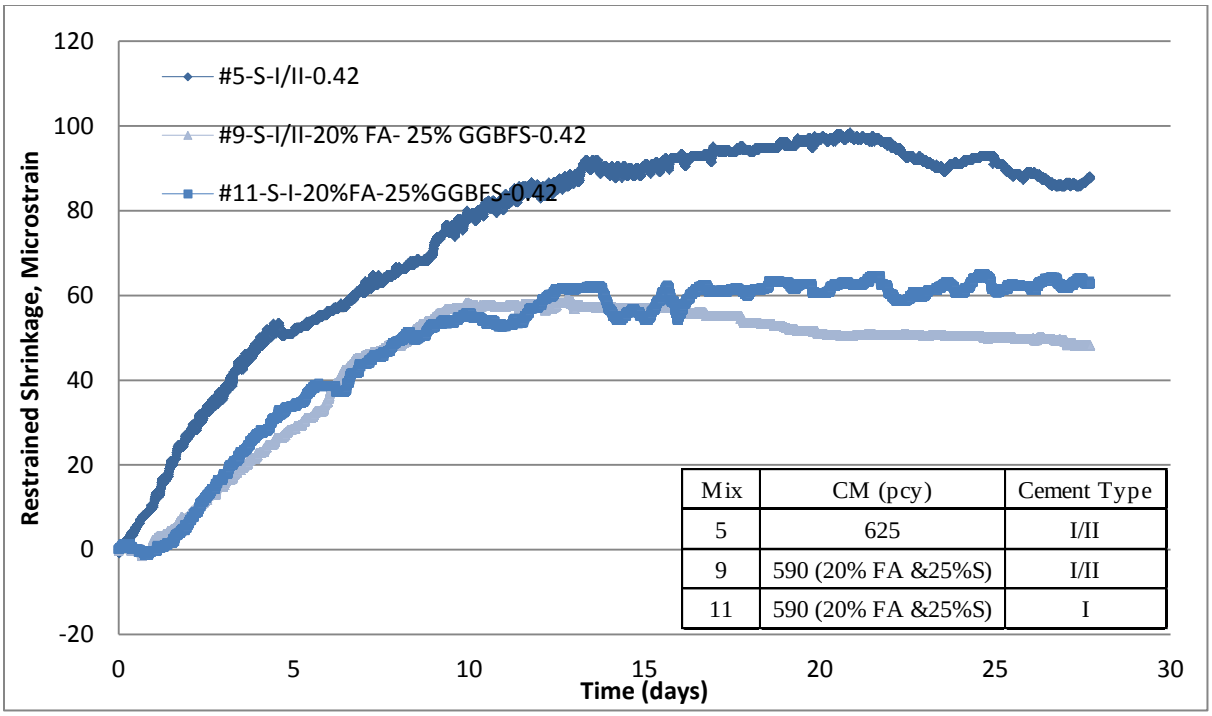

Figure 4.46. Restrained shrinkage of Group 4

ASTM C 1581 provides a method for ranking cracking potential of tested specimens. With ASTM C 1581, the strain rate factor for each tested specimen can first be found according to Equation 4-1:

$$\varepsilon_{net} = \alpha\sqrt{t} + k \qquad \textbf{(4-1)}$$

where:
ε_{net} is net strain, in./in., α is the strain rate factor for each strain gauge on the test specimen, (in./in.)/day$^{1/2}$, t is elapsed time, days, and k is the regression constant.

The strain rate factor of each tested specimen can then be found according to Equation 4-2:

$$q = \frac{G\,|\alpha_{avg}|}{2\sqrt{t_r}} \qquad \textbf{(4-2)}$$

where:
q is the stress rate in each test specimen, psi/day, G is a constant based on the ring dimension 10.5 by 10^6 psi (72.2GPa), $|\alpha_{avg}|$ is the absolute value of the average strain rate factor for each test specimen, (in./in.)/day$^{1/2}$, and t_r is the elapsed time at cracking or elapsed time when the test is terminated for each test specimen, days In this study, t_r was taken as 28 days for the mixes that no ring specimens displayed cracking.

Finally, the average stress rate, S, psi/day, is determined based on the stress rates of three tested specimens (Table 4.4). Figure 4.47* illustrates the order of the average stress rates for the concrete ring tested.

Table 4.4. Results of restrained concrete shrinkage

Mix	Total cementitous material content/pcy	Strain Rate α, (μstrain/day)			Cracking time t_r, (days)			Stress Rate q, (psi/day)			Average Stress Rate, S (psi/day)	ASTM C 1581 Cracing Porential Rating
		S1	S2	S3	S1	S2	S3	S1	S2	S3		
1	665	24.0	23.7	-	-	-	-	24	23	23.6	24	Moderate-Low
2	650	19.2	20.6	19.5	-	-	-	19.0	20.4	19.2	20	Moderate-Low
3	575	12.9	16.8	20.7	-	-	-	12.8	16.6	20.5	17	Moderate-Low
4	710	23.8	24.1	27.3	-	13	17	23.5	36.4	35.8	32	Moderate-High
5	625	26.8	24.7	22.6	11	-	-	26.6	24.5	35.7	25	Moderate-High
6	825	26.7	28.9	32.2	16	16	18	32.9	37.6	41.5	37	Moderate-High
7	695	34.2	36.6	37.2	-	-	-	33.8	36.2	36.8	36	Moderate-High
8	670	22.3	28.5	23.7	-	-	-	22.0	28.2	23.4	25	Moderate-High
9	590	19.7	29.6	33.0	-	-	-	19.5	29.3	32.7	27	Moderate-High
10	675	27.2	29.8	27.2	-	-	-	26.9	29.5	26.9	28	Moderate-High
11	590	24.1	27.8	21.5	-	-	-	23.9	27.5	21.3	24	Moderate-Low

- denotes uncracked concrete specimen at the age of 28 days, where t_r is taken as 28 days in the stress rate calculations

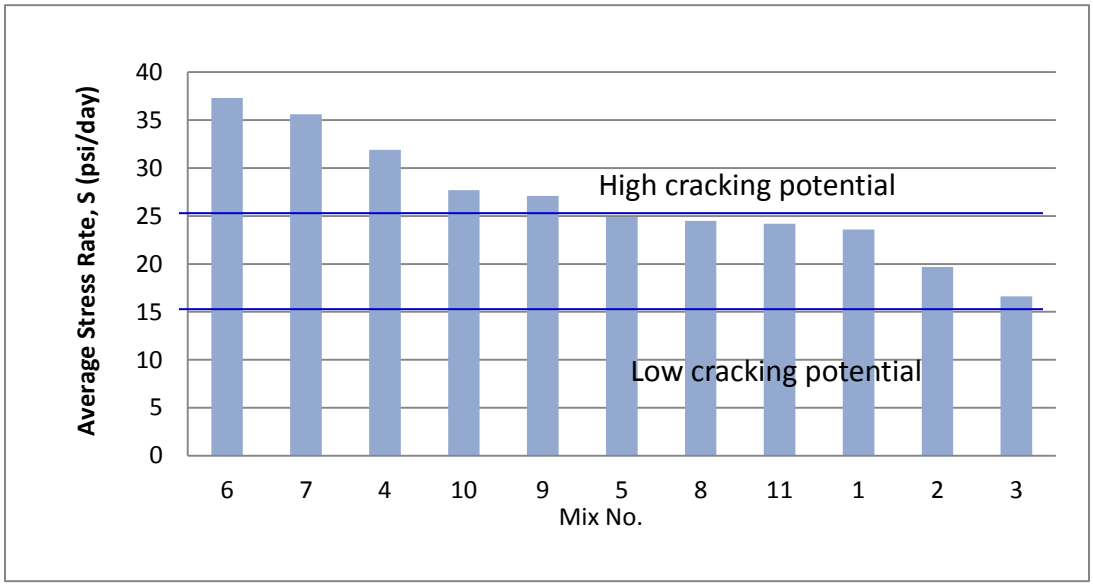

Figure 4.47. Cracking potential of ring concrete estimated from ASTM C 1581

Based on ASTM C 1581, the cracking potential for a mix is ranked as low if the average stress rate (S) calculated from the restrained ring specimens of the mix is ≤ 15 psi/day, moderate-low if S=15-25 psi/day, moderate-high if S=25-50 psi/day, and high if S≥50 psi/day. Table 4.4 presents the strain and stress as follows:

- Mixes 1, 2, 3, and 11 have moderate-low shrinkage cracking potential
- Mixes 4 through 10 have moderate-high shrinkage cracking potential

Based on Figure 4.47, Mix 7 has an average stress rate of 36, much higher than Mix 4 (average stress rate of 32), Mixes 10 and 9 have average stress rates of 28 and 27, respectively, which are higher than Mix 5 (average stress rate of 25). However, ring tests showed only Mixes 6, 4, and 5 cracked and Mixes 7, 10, and 9 did not. This suggests that the ASTM C 1581 estimation may not be accurate, particularly because the creep and strength of the concrete are not considered.

4.5 Mechanical Properties

The mechanical properties measured for the 11 mixes include compressive strength, elastic modulus, and splitting tensile strength. All measurements were performed using 4 by 8 in. cylinders.

4.5.1 Compressive Strength

The graphs in Figure 4.48 illustrate the compressive strength of the 11 mixes.

It is interesting to see in Group 1 that Mix 2, with 20% FA replacement, had increased concrete compressive strength, while Mix 3, also with 20% FA replacement, had reduced concrete compressive strength when compared with Mix 1, without FA. The lower strength of Mix 3 may be attributed to its lower cementitious material content and slightly higher w/b. However, it is not clear why Mix 2 had a higher strength than Mix 1.

For Group 2, Mix 6 with the greatest amount of cementitious materials (825.7 lb/yd^3) and lowest w/b (0.33) displays the greatest compressive strength. Mix 7, with 25% GGBFS replacement, and Mix 4, with no SCMs (710 lb/yd^3), have the same w/b and similar total cementitious material content (690 lb/yd^3). These two mixes display similar strength development, indicating that 25% GGBFS had little effect on concrete strength. Compared to Mix 7, Mix 10, with 20% FA and 5.6% MK displays higher strength, probably due to the high reactivity of MK.

For Group 3 mixes, although having the same cementitious materials, Mix 8 is a Type O-mix while Mix 9 is an S-mix. Compared to Mix 8, Mix 9 also has lower cementitious content (588.9 versus 668.8 lb/yd^3) and a slightly higher w/b, which may contribute to its lower strength.

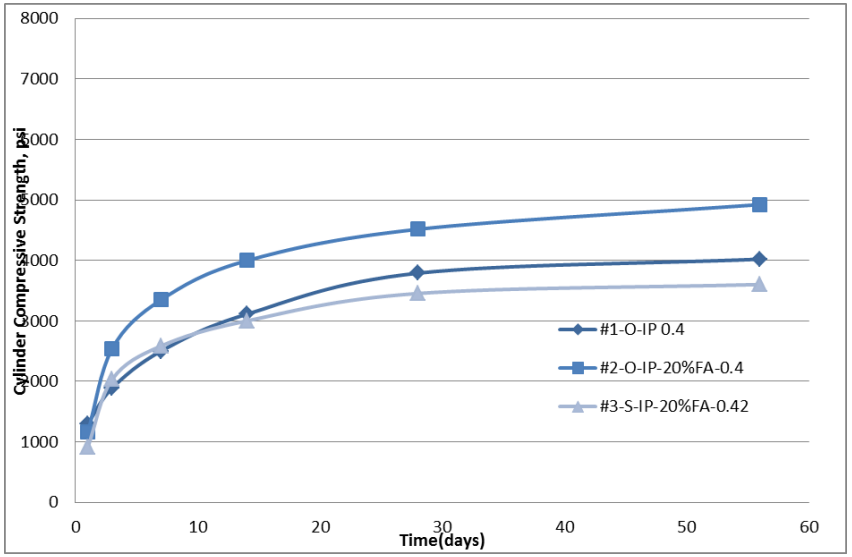

Group 1

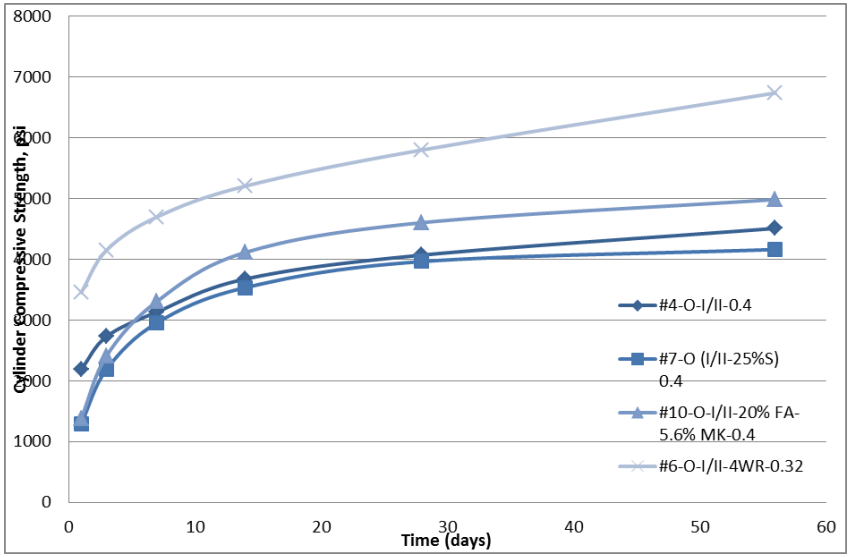

Group 2

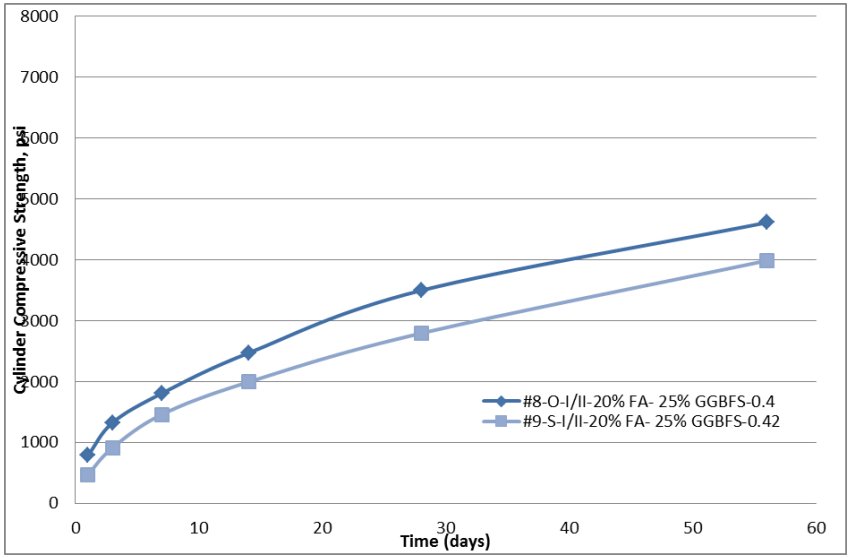

Group 3

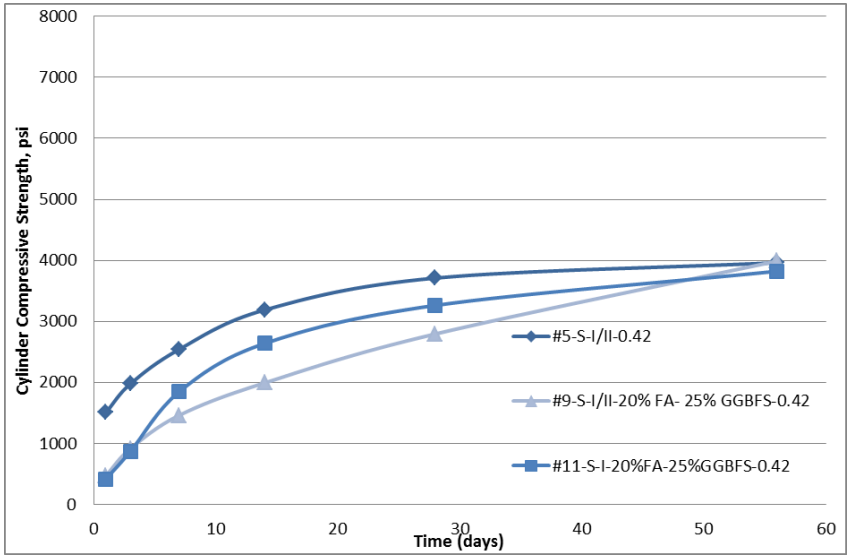

Group 4

Figure 4.48. Compressive strength (Groups 1 through 4)

For Group 4, where Mixes 8 and 9 are the same except for the cement type (Mix 9 with Type I/II and Mix 11 with Type I) and Mix 5 has no SCMs, it's clear that the Type I cement developed higher strength than the Type I/II cement prior to 56 days. Compared to Mix 5 (no SCMs), Mix 9 shows the slow strength development before 56 days, which is influenced by the high replacement level of cementitious materials (20% FA and 25% GGBFS). At 56 days, the compressive strength of all three mixes is very similar.

4.5.2 Elastic Modulus

The graphs in Figure 4.49 show the elastic modulus of the 11 mixes. Elastic modulus was calculated for the loading of 40% of the crushing load of the specimens.

Group 1 mixes show noticeable differences in the elastic modulus before 28 days. The SCM replacement and slightly high w/b reduced the elastic modulus of the concrete.

For Group 2, Mix 6 with the lowest w/b (0.33) had much greater elastic modulus. The replacement of cement by SCMs has decreased the elastic modulus for concrete Mixes 7 and 10.

For Group 3, the influence of quartzite and slightly lower w/b of Mix 8 provided the concrete with a greater elastic modulus compared to Mix 9.

When comparing Mix 5 to Mix 9, the replacement of cement by 20% FA and 25% GGBFS has influenced the concrete to show less elastic modulus. Compared to Mix 5 (without SCMs), Mix 9 (with 20% FA and 25% GGSBF) shows a lower elastic modulus value. Compared to Mix 9 (Type I/II cement), Mix 11 (Type I cement) displays a greater elastic modulus.

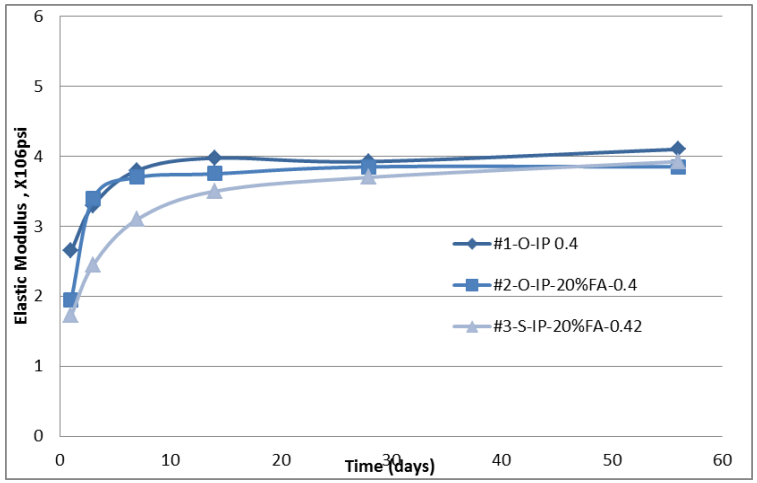

Group 1

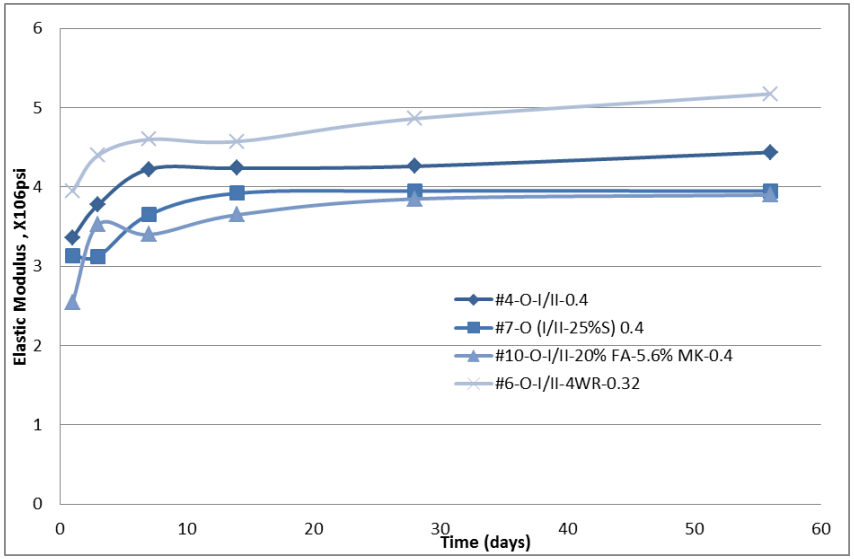

Group 2

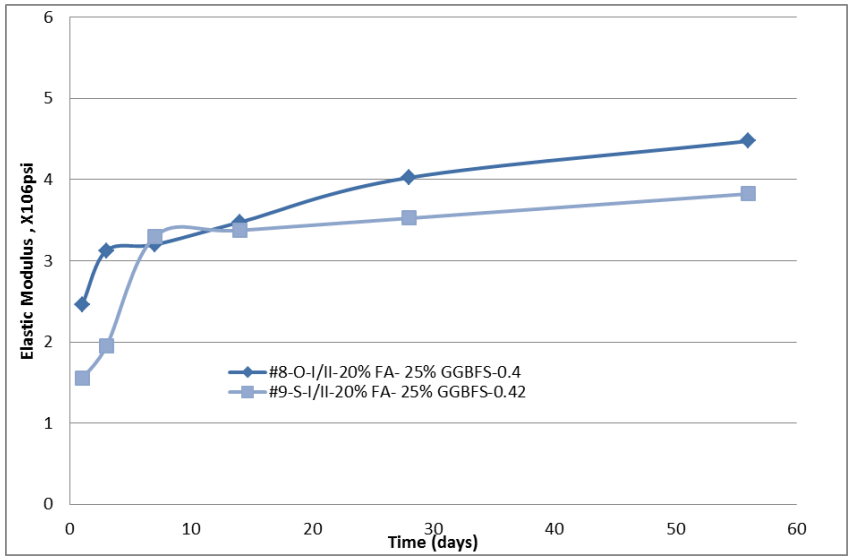

Group 3

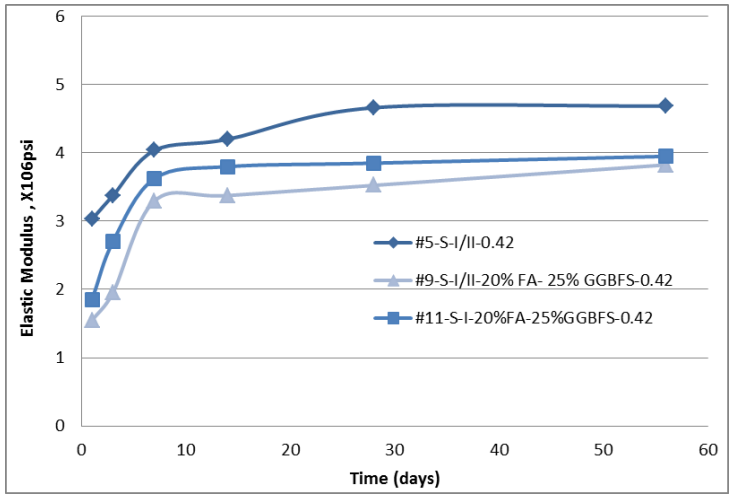

Group 4

Figure 4.49. Elastic modulus (Groups 1 through 4)

4.5.3 Split Tensile Strength

Splitting tensile test results are illustrated in Figure 4.50.

The three concrete mixes in Group 1 had insignificant differences in splitting tensile strength until 28 days. At 56 days, the order of the splitting tensile strength, from high to low, is Mix 2, 1, and then 3, similar to that for compressive strength.

For the four concrete mixes in Group 2, Mix 6 with a w/b of 0.33 had the highest splitting tensile strength as expected. Interestingly, both Mix 7, with 25% GGBFS, and Mix 10, with 20% FA and 5.6% MK, had higher splitting tensile strengths than Mix 4, without SCMs. After 28 days, Mix 10 (w/b=0.4) had splitting tensile strength higher than Mix 6 (w/b=0.33).

Before 14 days, the trend of the splitting tensile strength of Mixes 8 and 9 is similar to that for the compressive strength of the mixes. However, after 14 days, Mix 8, made with quartzite as coarse aggregate, displays significantly lower splitting tensile strength than Mix 9, made with limestone as coarse aggregate. This suggests that aggregate type has a more significant effect on concrete splitting tensile strength than on its compressive strength.

The figure shows that 20% FA and 25% GGBFS replacement for cement reduced splitting tensile strength of concrete at early ages (before 28 days) but not at later ages (after 28 days). Type I cement (Mix 11) also provides higher splitting tensile strength than Type I/II cement (Mix 9) at the early ages only.

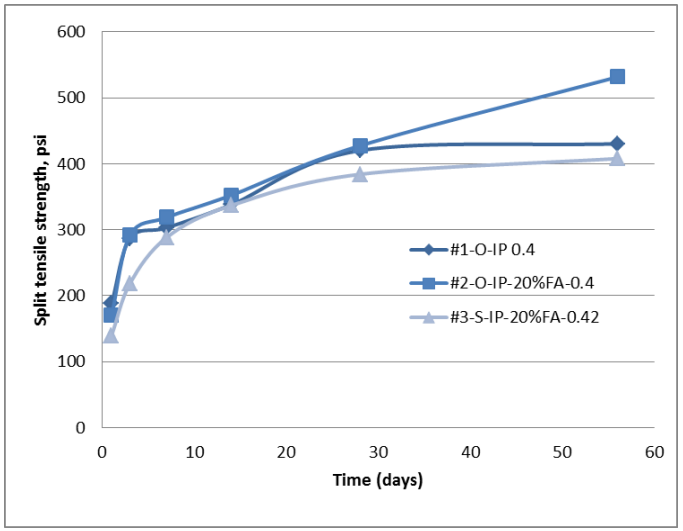

Group 1

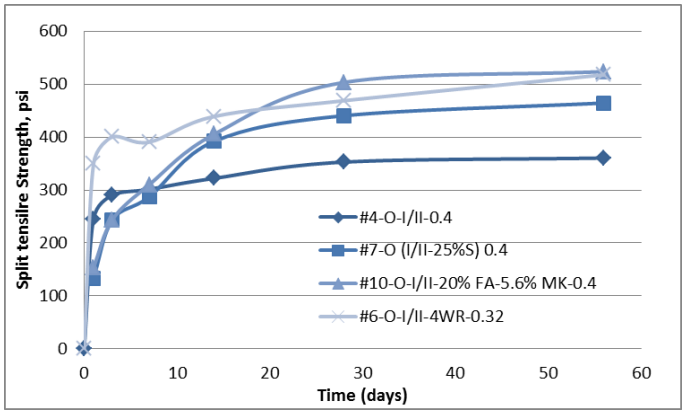

Group 2

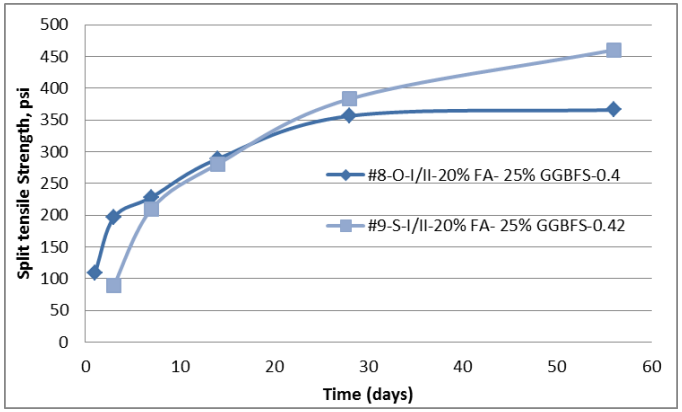

Group 3

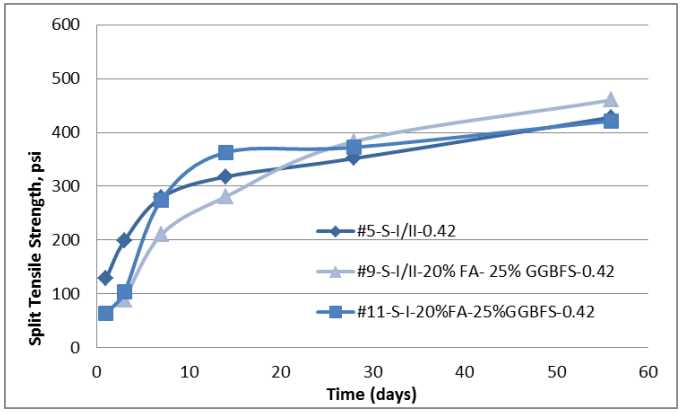

Group 4

Figure 4.50. Split tensile strength of concrete (Groups 1 through 4)

4.6 Relationships among Test Results

This section discusses the relationships that were observed among the test results. Relationships among results are useful tools to reassure the accuracy of data and can be used as an alternative tool to estimate performance of a mix in one test.

4.6.1 Chemical Shrinkage of Pastes and Autogenous Shrinkage of Mortar

As described previously, both chemical shrinkage (internal shrinkage) and autogenous shrinkage (external shrinkage) result from cement hydration. Figure 4.51 shows the relationship between chemical shrinkage of pastes and autogenous shrinkage of mortar at 7 days. The relationship is not very strong, partially because of the different w/b and s/b used in the mortars. However, the relationship is not found for the pastes at the later age (such as 28 days).

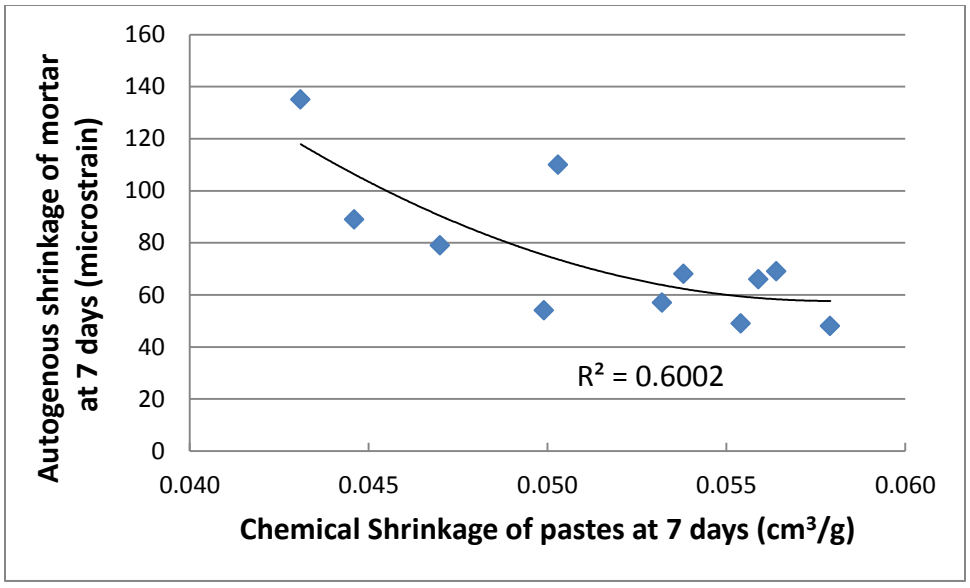

Figure 4.51. Relationship between chemical shrinkage of pastes and autogenous shrinkage of mortar at 7 days

4.6.2 Free Drying Shrinkage and Mass Loss of Concrete

The charts in Figure 4.52 show that moisture loss of the concrete prism is correlated linearly to the free drying shrinkage of concrete within the 56 day period of measurement. Therefore, measurement of mass loss can be a good indicator for the free drying shrinkage of concrete with R^2 values greater than 0.95 (Table 4.5).

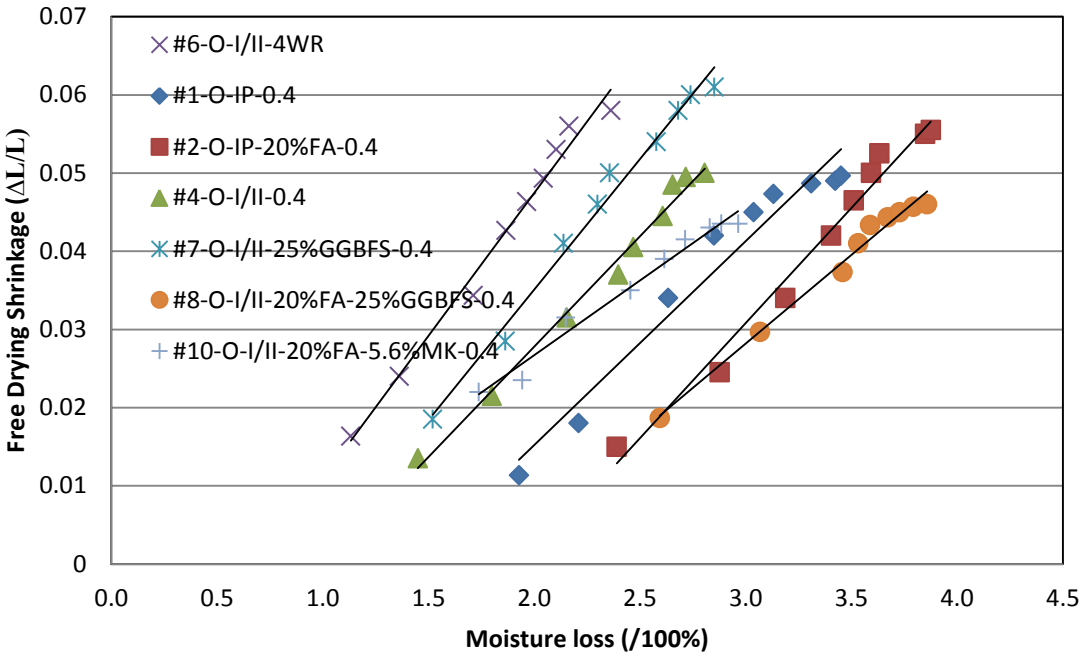

(a)

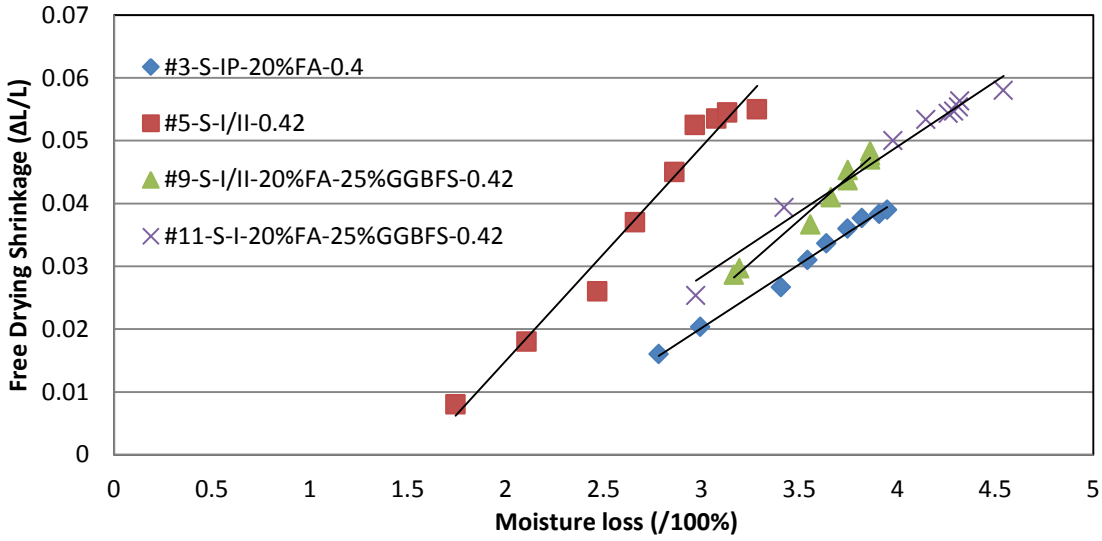

(b)

Figure 4.52. Free drying shrinkage versus mass loss of concrete

Table 4.5. Relationship between free drying shrinkage and moisture loss

Free Drying Shrinkage (y) versus Moisture Loss		
Mix No.	**Equation**	**R^2**
1	y = 0.0261 x -0.037	0.95
2	y = 0.0294 x -0.0575	0.98
3	y = 0.0203 x -0.0409	0.99
4	y = 0.0282 x -0.0287	0.99
5	y = 0.0341 x -0.0533	0.97
6	y = 0.0365 x-0.0256	0.99
7	y = 0.0333 x -0.0316	0.99
8	y = 0.0227 x -0.0399	0.99
9	y = 0.0274 x -0.0584	0.98
10	y = 0.0191 x -0.0114	0.98
11	y = 0.02808 x -0.034	0.98

4.6.3 Free Drying Shrinkage of Concrete and Mortar

Figure 4.53 and Figure 4.54 illustrate that there is a good linear relationship between the free drying shrinkage of concrete and mortar within 56 days for a given mix. O mixes (Figure 4.53) display a better correlation ($R^2 > 0.85$) than S mixes (Figure 4.54) ($R^2 > 0.7$). A summary of the relationship among the results is provided in Table 4.6.

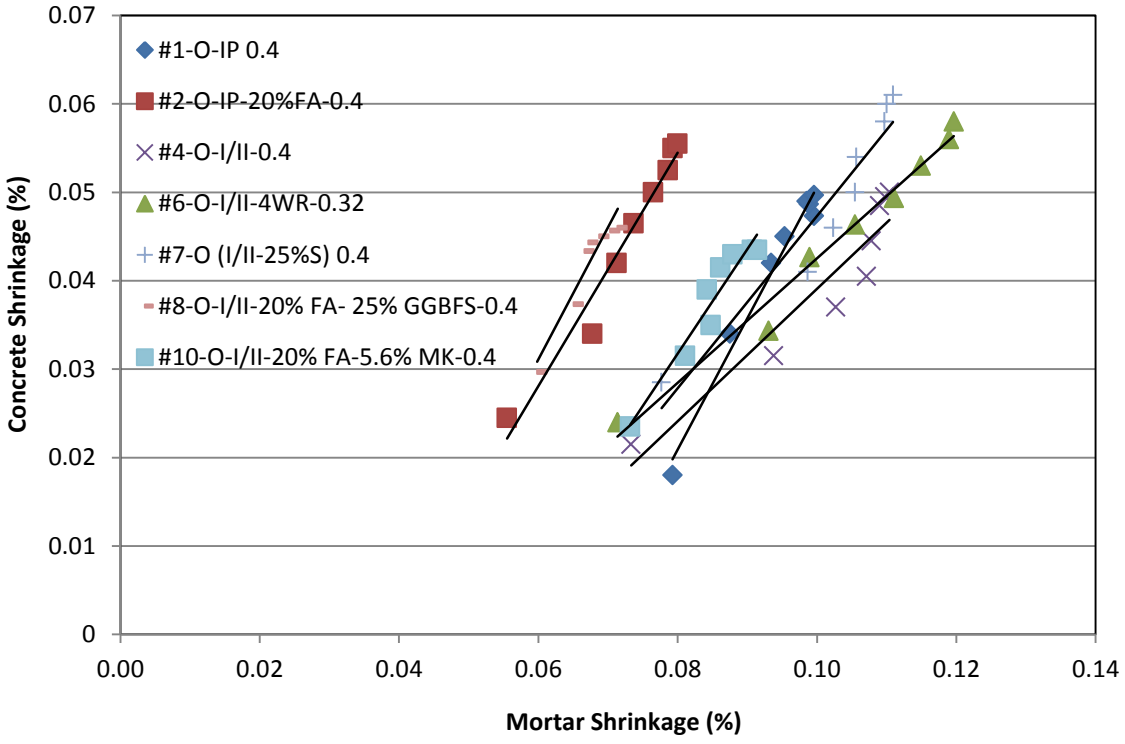

Figure 4.53. Free drying shrinkage of concrete versus mortar (Type O mixes)

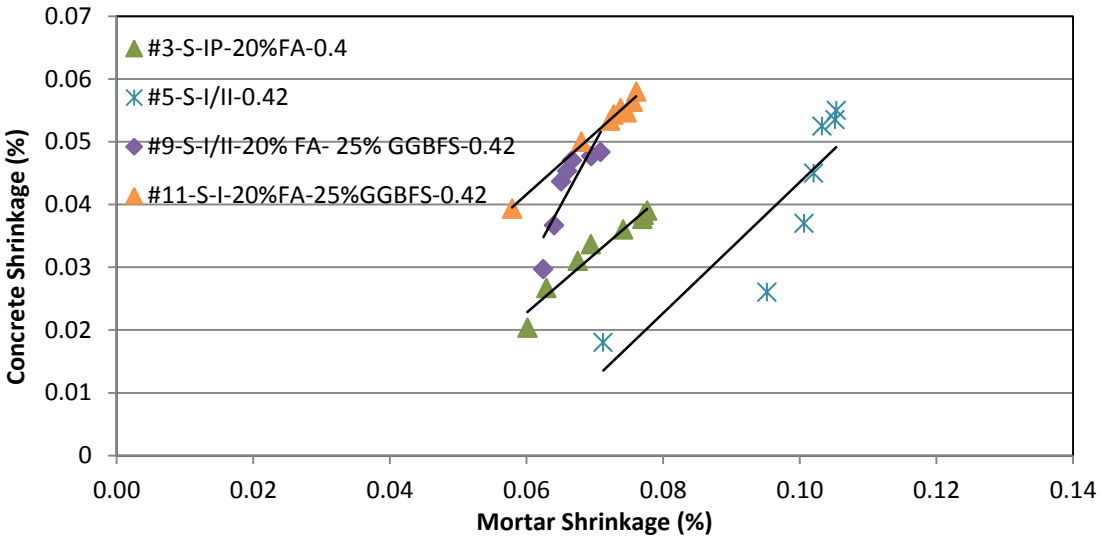

Figure 4.54. Free drying shrinkage of concrete versus mortar (Type S mixes)

Table 4.6. Relationship between free drying shrinkage of concrete and mortar

Concrete Shrinkage (y) versus Mortar Shrinkage (x)		
Mix No.	**Linear**	**R^2**
1	y = 1.4857 x -0.098	0.9789
2	y = 1.3180 x -0.051	0.9665
3	y = 0.9366 x -0.0334	0.9501
4	y = 0.7482 x -0.0357	0.8960
5	y = 1.0418 x -0.0606	0.7515
6	y = 0.7032 x -0.0278	0.9806
7	y = 0.9735 x -0.050	0.9132
8	y = 1.4951 x -0.0586	0.9058
9	y = 1.9985 x -0.090	0.7233
10	y = 1.1796 x -0.0626	0.9258
11	y = 0.9723 x -0.0167	0.9883

4.6.4 Restrained Drying and Free Drying Shrinkage of Concrete

Performing the ring shrinkage test poses several difficulties in casting and maintaining the environment for the proper evaluation of strain. During ring casting, compaction control is difficult because the clamps used in the test setup often tend to be too loose, affecting the size and shape of the ring specimen. Strain gauges attached to the surface of the ring are sensitive to environment (temperature and vibration), producing unreliable readings. The specimens are much larger, heavier, and more difficult to handle than other shrinkage test specimens are. If there is a good relationship between ring shrinkage test and other shrinkage test results, conducting ring shrinkage tests may be reduced or eliminated.

To relate results obtained from different shrinkage tests effectively, the shrinkage values resulting from different tests are rated according to the criteria in Table 4.7.

Table 4.7. Rating range for concrete shrinkage (microstrain)

Shrinkage Type	Low Rating	Medium Rating	High Rating
Autogenous	< 90	90 to 110	≥ 110
Free Drying	< 450	450 to 500	≥ 500
Ring	< 75	75 to 100	≥ 100

Based on the criteria listed in Table 4.7, the rating of different concrete shrinkage values is given in Table 4.8, which shows no relationship between the different concrete shrinkage measurements.

Table 4.8. Shrinkage rating

Mix No.	Concrete Shrinkage at 28 days (microstrain)					
	Autogenous Shrinkage		Free Drying Shrinkage		Ring Shrinkage	
	Shrinkage	Rating	Shrinkage	Rating	Shrinkage	Rating
1	140	high	440	med.	103	high
2	115	high	430	med.	75	med.
3	110	high	335	low	67	low
4	90	med.	405	low	107*	high
5	100	med.	450	med.	98	med.
6	115	high	465	med.	115*	high
7	100	med.	500	high	116	high
8	115	high	435	med.	80	med.
9	75	low	435	med.	76	med.
10	120	high	390	low	110	high
11	90	low	545	high	72	low

* Shrinkage at the time of cracking

4.6.5 Relationships between Shrinkage and Cementitious Material Content

In conventional concrete, only paste shrinks, while aggregate generally resists shrinkage. Figure 4.55 illustrates the relationship between cementitious material content used in this study and 56 day mortar and concrete shrinkage. The figure indicates that cementitious material content has a good relationship with concrete total shrinkage (autogenous and free drying shrinkage) (R^2=0.7394), but no relationship with concrete free drying shrinkage only. There is also a weak relationship with mortar free drying shrinkage (R^2=0.5376) as well as with mortar total shrinkage (R^2=0.5765).

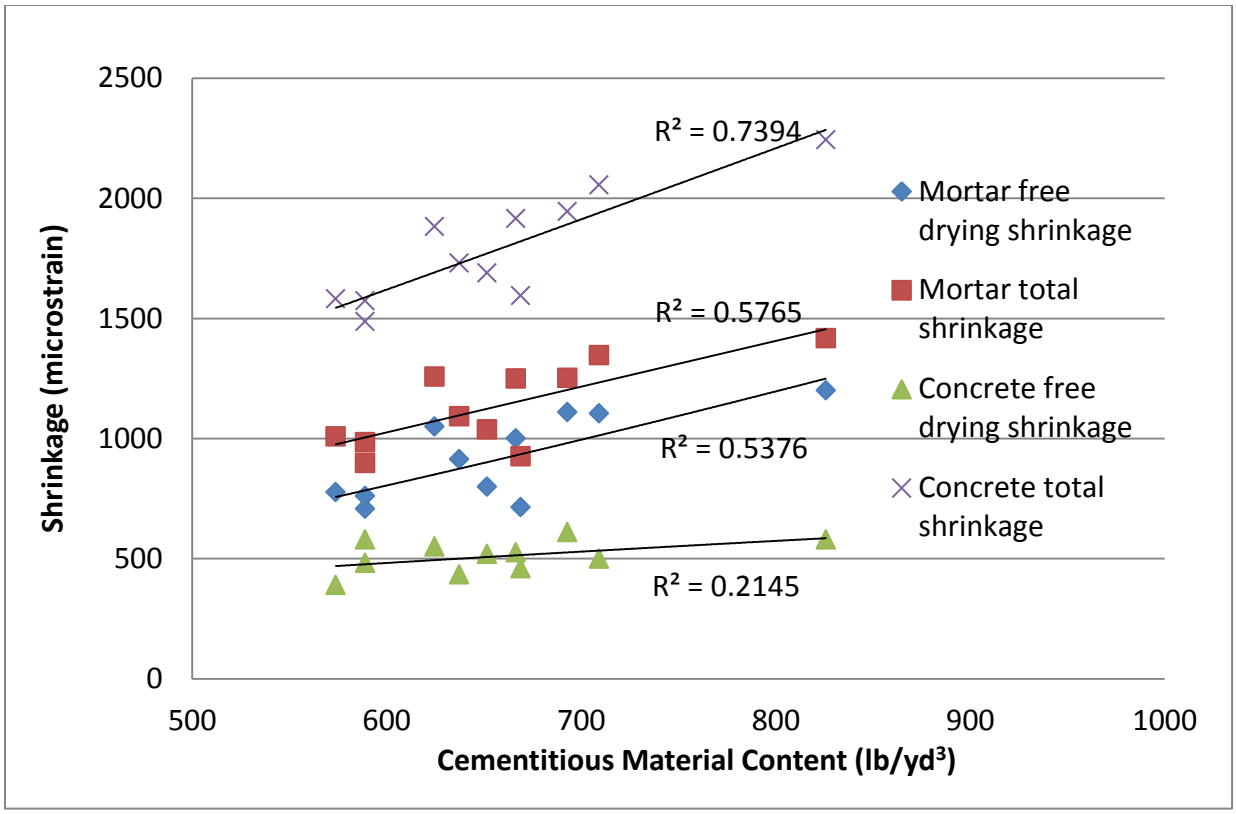

Figure 4.55. Effects of cementitious material content on 56 day shrinkage

4.6.6 Relationships among Strength Parameters

Figure 4.56 illustrates the relationship between restrained stress in the ring concrete and free drying stress of concrete prisms. The free drying stress of concrete is calculated from Equation 4-3:

$$\sigma_{free}(t) = E_c(t) \times \varepsilon_{free}(t) \quad \textbf{(4-3)}$$

where:
E_c is the elastic modulus of concrete.

Figure 4.57 illustrates the relationship between concrete compressive strength and elastic modulus and Figure 4.58 shows the relationship between compressive strength and splitting tensile strength.

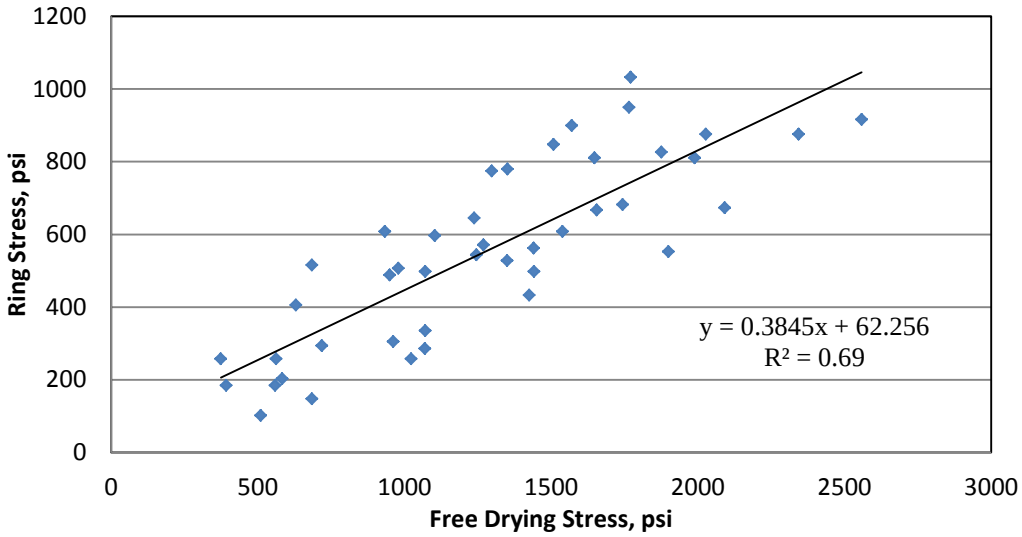

Figure 4.56. Relationship between ring stress and free drying shrinkage of concrete

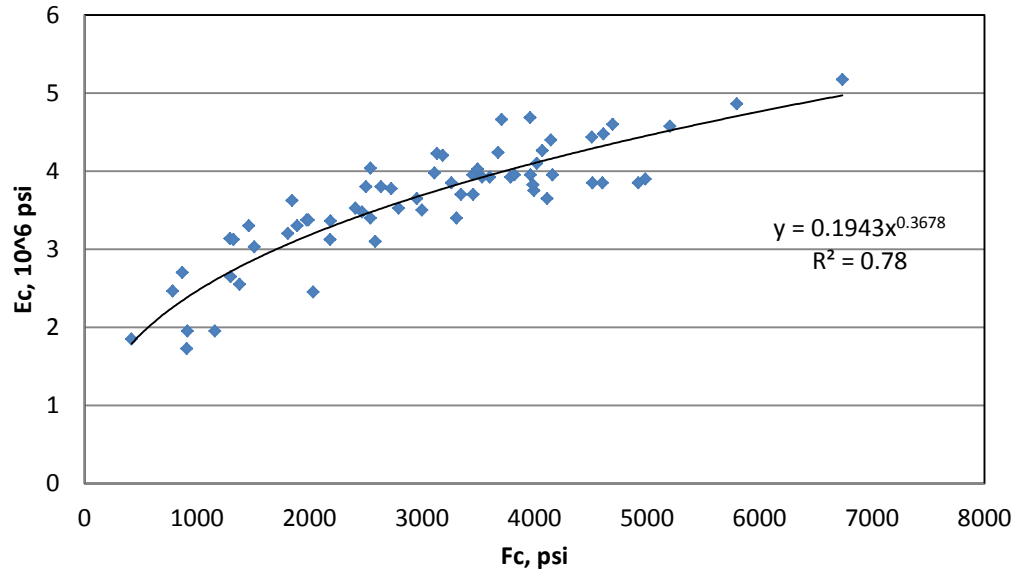

Figure 4.57. Relationship between elastic modulus and compressive strength of concrete

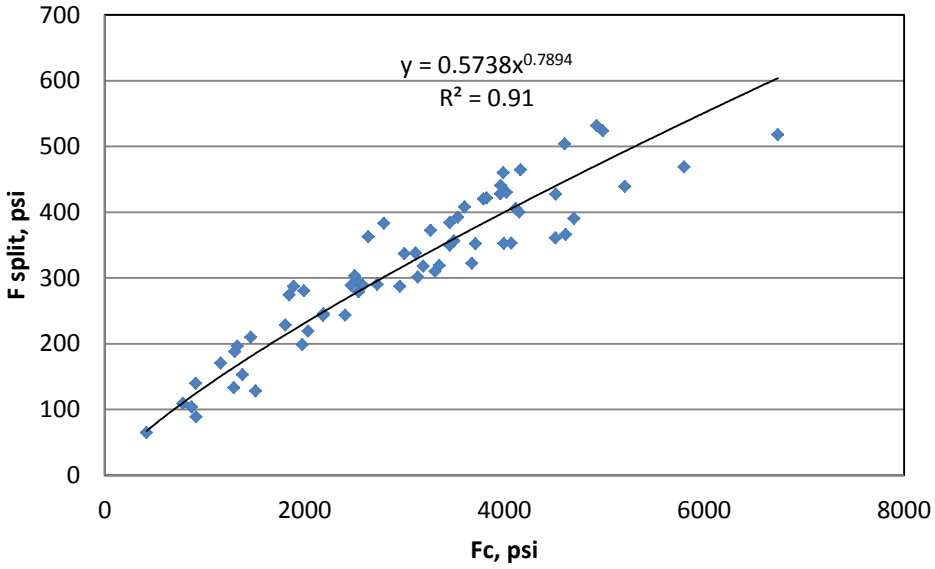

Figure 4.58. Relationship between splitting tensile and compressive strength of concrete

4.7 Concrete Cracking Potential

To assess concrete cracking potential, stresses developed in concrete specimens are computed. According to ASTM C 1581, the shrinkage-induced stress in restrained concrete can be calculated based on the steel ring strains and consideration of the equilibrium of the pressure between concrete and steel interfaces. The pressure (*p)* on the outer side of the ring is expressed as Equation. 4-4:

$$p = \varepsilon_{si} E_s \frac{R_{so}^2 - R_{si}^2}{2R_{so}^2} \quad \textbf{(4-4)}$$

where:
ε_{si} is the strain of steel ring measured at the interior side, E_s is the steel elastic modulus, R_{so} and R_{si} are the outer and inner radii, respectively. It is noted that because ε_{si} is the strain actually measured, it includes the effect of creep. From the calculated steel pressure, the shrinkage-induced stress (σ_c) on the inner wall of the concrete ring is determined using Equation 4-5:

$$\sigma_c = p\left[\frac{R_{co}^2 + R_{ci}^2}{R_{co}^2 - R_{ci}^2} + \nu\right] \quad \textbf{(4-5)}$$

where:
σ_c is the shrinkages stress, ν is the Poisson ratio (0.2) of concrete, and R_{co} and R_{ci} are the outer and inner radii, respectively.

Table 4.9 gives the ring stresses calculated according to Equation 4-2 as the ring stress-to-splitting strength ratio (σ_{ring}/F_{sp}) of the concrete at cracking time (otherwise 28 days). As reported in previous research (Lomboy et al. 2011), these simply-calculated ratios are much higher than the actual values in the concrete (all >1.0). Regardless of the high values, these σ_{ring}/F_{sp} ratios suggest the following among the HPC mixes studied (Figure 4.59):

- Mixes 5, 4, and 6 have the highest cracking potential (σ_{ring}/F_{sp}>2.75), which is consistent with the results from the ring tests
- Mixes 1, 8, 10, and 7 have medium cracking potential (σ_{ring}/F_{sp}=2.15-2.75)
- Mixes 2, 3, 9, and 11 have the lowest cracking potential (σ_{ring}/F_{sp}<2.15)

Table 4.9. Simple estimation of the cracking potential of concrete rings

Mix No.	Peak ε_{ring} (microstrain)	Peak $\sigma_{c\ ring}$ (psi)	F_{sp}, (psi)	$\sigma_{c\ ring}/F_{sp}$
1	103	949	357	2.658
2	75	667	363	1.837
3	68	608	326	1.865
4	107	916	300	3.053
5	98	949	298	3.185
6	115	1105	400	2.763
7	116	875	374	2.340
8	80	774	306	2.529
9	76	645	326	1.979
10	110	1032	428	2.411
11	72	673	316	2.130

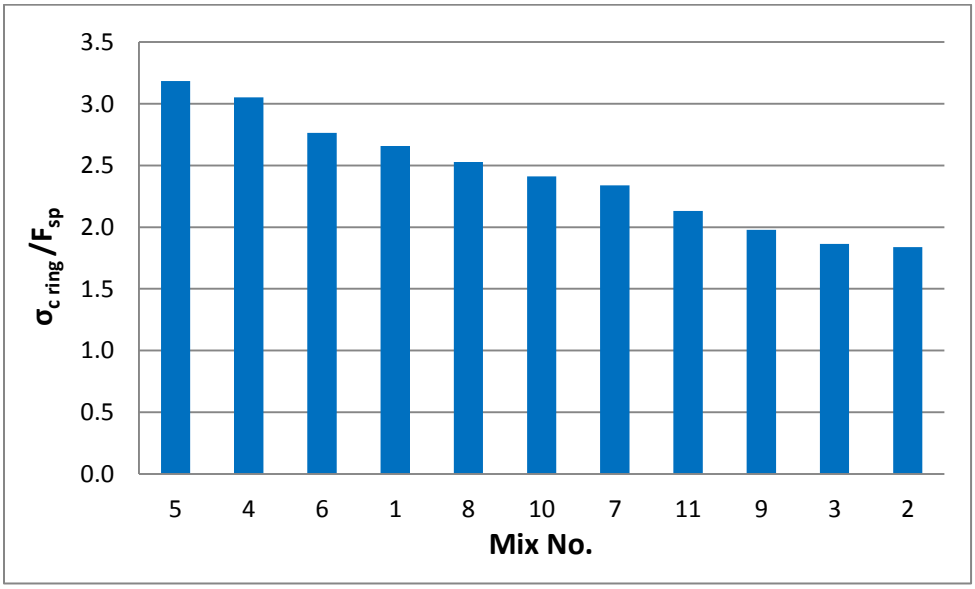

Figure 4.59. Cracking potential of concrete rings based on simple estimation

Table 4.10 provides another assessment of the cracking potential of the concrete mixes based on the ratio of the stress resulting from free shrinkage of concrete, with additional consideration of creep, to splitting tensile strength (F_{sp}).

Table 4.10. Concrete shrinkage potential estimated with creep

Mix No.	$\sigma_{free} = E^*\varepsilon_{free}$ (psi)		$\sigma_{free}/(1+\varphi)$, psi		$(\sigma_{free}/1+\varphi)/F_{sp}$	
	14 day	28 day	14 day	28 day	14 day	28 day
1	1351	1766	363	513	1.07	1.22
2	1350	1656	395	508	1.12	1.19
3	933	1246	243	343	0.71	0.89
4	1441	1876	414	560	1.37	1.74
5	1989	2344	542	678	1.71	1.93
6	1571	2253	516	766	1.32	1.74
7	1647	2028	466	600	1.19	1.36
8	1297	1744	315	490	1.09	1.37
9	1238	1539	277	396	0.99	1.03
10	1509	1771	457	558	1.13	1.11
11	1900	2092	479	575	1.29	1.36

The creep coefficient (φ) used is the average creep coefficient estimated from the International Union of Laboratories and Experts in Construction Materials, Systems and Structures (RILEM) B3 (Bazant and Baweja 1995, 2000) and National Cooperative Highway Research Program (NCHRP) Report 496 (Tadros et al. 2003, Al-Omaishi et al. 2009) models. The detailed calculations of the creep coefficient are included in the appendix.

Based on this stress-to-strength ratio, $\sigma_{free}/(1+\varphi)/F_{sp}$, the cracking potential for an HPC mix at 28 days is considered low if $\sigma_{free}/(1+\varphi)/F_{sp} \leq 1.0$, medium if $(\sigma_{ring}/1+\varphi)/F_{sp} = 1.0\text{-}1.5$, and high if $(\sigma_{ring}/1+\varphi)/F_{sp} > 1.5$. According to these criteria, cracking potential of the mixes are as follows:

- Mixes 3 and 9 have low cracking potential
- Mixes 1, 2, 7, 8, 9, 10, and 11 have medium cracking potential
- Mixes 4, 5, and 6 have high cracking potential

Figure 4.60 shows the order of the $\sigma_{free}/(1+\varphi)/F_{sp}$, ratios for the concrete mixes studied. This figure clearly shows that Mixes 6, 5, and 4 have noticeably high potential of cracking compared to the other mixes, which is consistent with the ring test results.

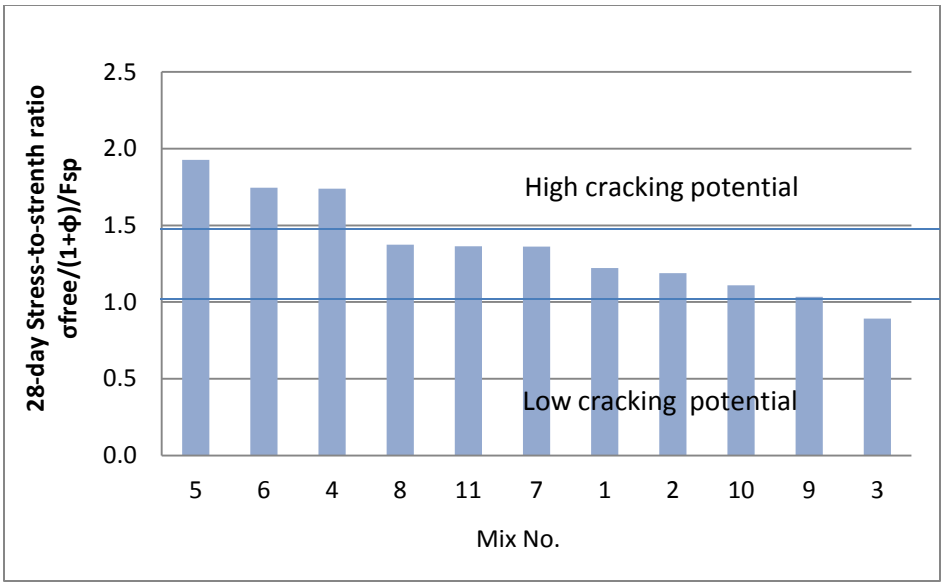

Figure 4.60. Cracking potential of concrete rings with creep consideration

5. SUMMARY, CONCLUSIONS, AND RECOMMENDATIONS

5.1 Summary

In this project, shrinkage behavior of 11 HPC mixes used commonly for Iowa bridges was studied. Chemical shrinkage of cement paste, autogenous shrinkage of mortar and concrete, free drying shrinkage of mortar and concrete, and restrained ring shrinkage of concrete were monitored. Compressive strength, elastic modulus, and splitting tensile strength were tested at different ages. Creep coefficients of these concrete mixes were estimated using the RILEM B3 (Bazant and Baweja 1995, 2000) and NCHRP Report 496 (Tadros et al. 2003, Al-Omaishi et al. 2009) models. This section summarizes all mix proportions and major test results discussed in the previous sections.

5.1.1 Mix Proportions Used

Table 5.1 and Table 5.2 provide the common and different mix design parameters used in the paste, mortar, and concrete samples in this research. All cementitious materials and admixtures used were the same for pastes, mortar, and concrete. The water-to-binder ratio (w/b) was the same for mortar and concrete except for Mix 6, while it was a constant (0.4) for all paste mixes. The mix proportions of mortars were the same as the mortars extracted from the corresponding concrete (i.e., concrete mixes without coarse aggregates).

Table 5.1. Common mix proportion parameters used in paste, mortar, and concrete

Mix No.	Cement Type	Cement	FA	GGBFS	Cementitious	AEA	NRWR	Retarder
		lb/yd^3	lb/yd^3	(MK) lb/yd^3	Materials lb/yd^3	ml/yd^3	(MRWR) ml/yd^3	ml/yd^3
1	Ash Grove IP	666.3	0	0	666.3	354.7	(1182.3)	394.1
2	Ash Grove IP	521.2	130.3	0	651.5	346.8	(1156.1)	385.4
3	Ash Grove IP	459.0	114.8	0	573.8	305.4	593.9	339.4
4	Lafarge I/II	709.2	0	0	709.2	377.5	(1258.4)	419.5
5	Lafarge I/II	624.5	0	0	624.5	332.5	646.4	369.4
6	Lafarge I/II	825.7	0	0	825.7	439.5	854.6	0
7	Lafarge I/II	519.7	0	173.2	692.9	368.9	(1229.5)	409.8
8	Lafarge I/II	367.8	133.8	167.2	668.8	356	(1186.6)	395.5
9	Lafarge I/II	323.9	117.8	147.2	588.9	313.5	609.6	348.3
10	Lafarge I/II	502.2	135.0	(37.8)	675.0	359.3	(1197.6)	399.2
11	Lehigh I	323.9	117.8	147.2	588.9	313.5	609.6	348.3

Table 5.2. Different mix proportion parameters used in paste, mortar, and concrete

Mix No.	Paste	Mortar		Concrete		
	w/b	w/b	s/b	Limestone (Quartzite) (lb/yd^3)	Sand (lb/yd^3)	w/b
1	0.40	0.40	2.11	1431.7	1405.9	0.40
2	0.40	0.40	2.17	1439.6	1413.7	0.40
3	0.40	0.42	2.59	1513.4	1486.3	0.42
4	0.40	0.40	1.98	1429.7	1403.9	0.40
5	0.40	0.42	2.33	1483.9	1457.3	0.42
6	0.40	0.40*	1.65	1386.8	1366.1	0.33
7	0.40	0.40	2.01	1417.4	1391.8	0.40
8	0.40	0.40	2.10	(1430.4)	1404.6	0.40
9	0.40	0.42	2.51	1504.8	1477.9	0.42
10	0.40	0.40	2.08	1427.1	1401.3	0.40
11	0.40	0.42	2.51	1504.8	1477.9	0.42

*For Mix 6 mortar, the actual w/b is 0.33. It is increased to 0.40 for the autogenous shrinkage test sample preparation because of the workability requirement.

5.1.2 Shrinkage of Pastes

Only chemical shrinkage was performed for paste mixes. Table 5.3 and Figure 5.1 display the chemical shrinkage of the pastes studied at different ages. A high chemical shrinkage value generally indicates fast hydration cementitious materials of the paste.

Table 5.3. Summary of chemical shrinkage test results

Mix No.	Paste		
	Chemical Shrinkage (cm^3/g)		
	7 day	28 days	42 days
1	0.0564	0.0881	0.1011
2	0.0554	0.0841	0.0984
3	0.0499	0.0720	0.0819
4	0.0559	0.0805	0.0919
5	0.0503	0.0733	0.0857
6	0.0538	0.0860	0.1018
7	0.0532	0.0780	0.0877
8	0.0470	0.0766	0.0902
9	0.0446	0.0854	0.1024
10	0.0579	0.0923	0.1091
11	0.0431	0.0769	0.0949

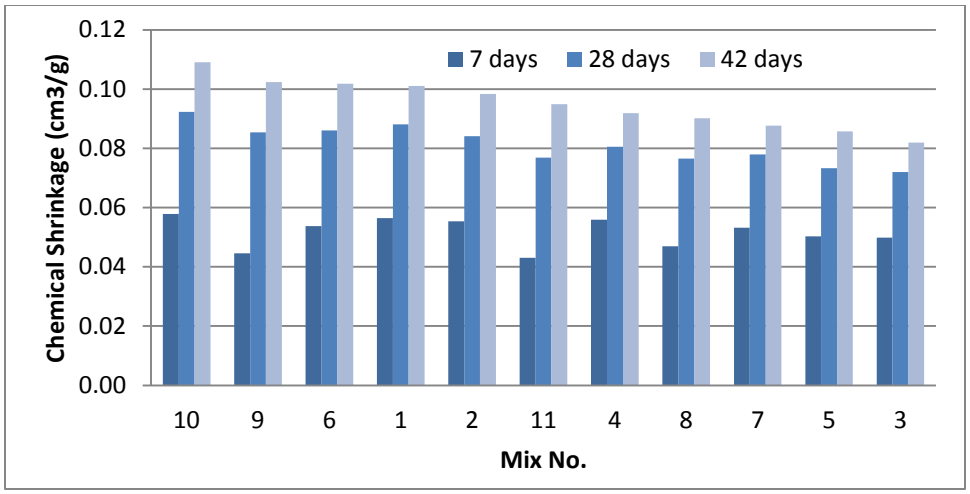

Figure 5.1. Summary of chemical shrinkage of pastes

The following observations can be made on the chemical shrinkage of the pastes studied:

- 20% fly ash replacement decreases chemical shrinkage at nearly all ages.
- 25% slag replacement does not affect chemical shrinkage of the paste significantly.
- Use of metakaolin increases chemical shrinkage of the paste greatly.
- Combined replacement of 20% fly ash and 25% slag reduces chemical shrinkage at early ages but increases chemical shrinkage at later ages when compared to the paste without SCMs.
- Using the recommended dosage of water reducer, Mix 2 with the mid-range water reducer exhibited higher chemical shrinkage when compared to Mix 3 with the normal-range water reducer.
- There is a relationship between chemical shrinkage of pastes and autogenous shrinkage of mortar at 7 days. The mixes having higher chemical shrinkage tend to show lower autogenous shrinkage at 7 days.

Figure 5.2 and Table 5.4 summarize all mortar shrinkage measurements at given ages.

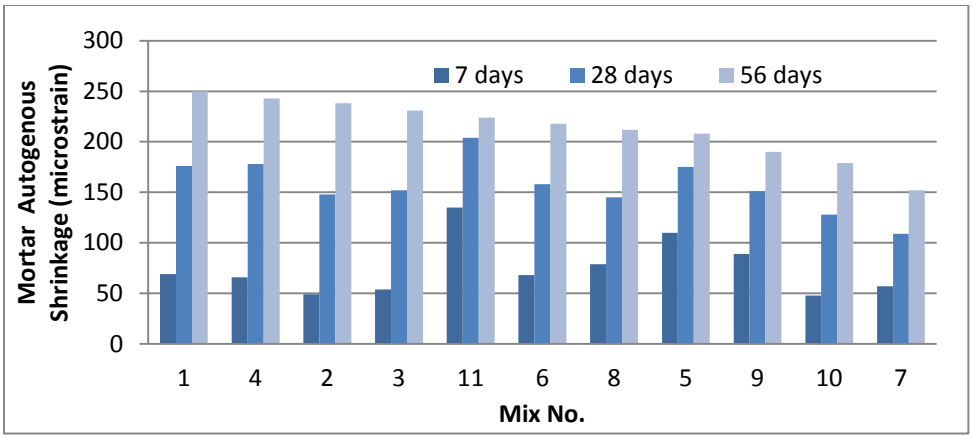

Autogenous shrinkage

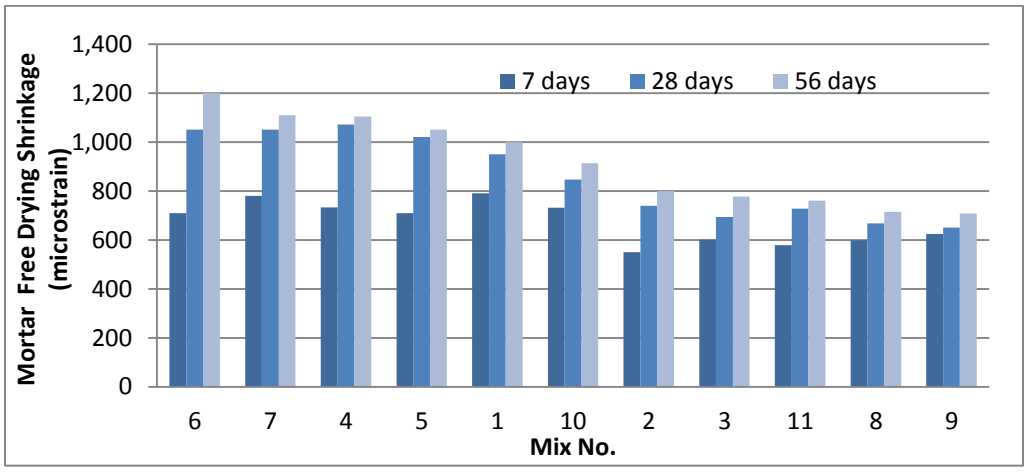

Free drying shrinkage

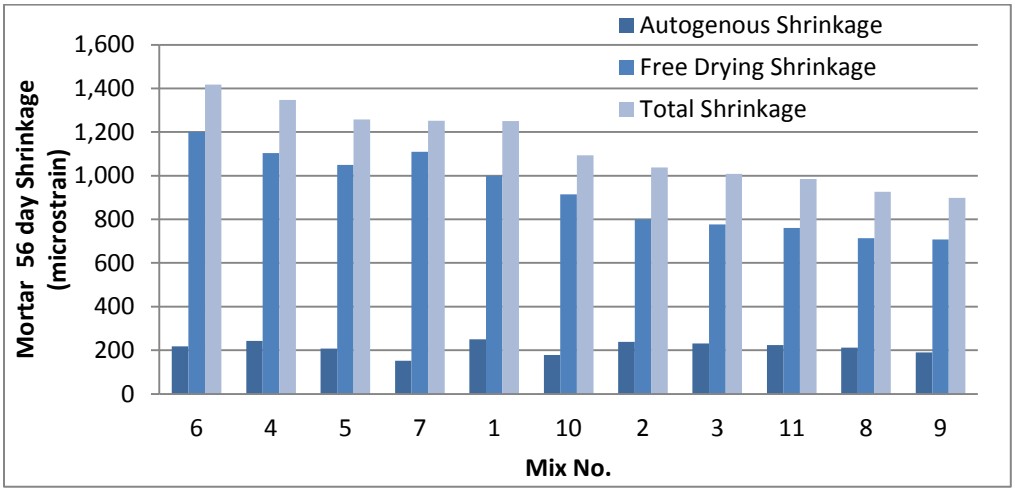

Different shrinkages at 56 days

Figure 5.2. Shrinkage of mortar at given ages

Table 5.4. Summary of mortar shrinkage

Mix No.	Mortar Shrinkage						
	Autogenous Shrinkage (microstrain)			Free Drying Shrinkage (microstrain)			Total (microstrain)
	7 day	28 day	56 day	7 day	28 day	56 day	56 day
1	69	176	250	790	950	1000	1250
2	49	148	238	550	740	800	1038
3	54	152	231	601	694	777	1008
4	66	178	243	733	1071	1104	1347
5	110	175	208	710	1020	1050	1258
6	68	158	218	710	1050	1200	1418
7	57	109	152	780	1050	1110	1252
8	79	145	212	598	667	714	926
9	89	151	190	624	650	708	898
10	48	128	179	731	847	914	1093
11	135	204	224	579	728	761	985

5.1.3 Shrinkage of Mortar

The following observations can be made on the shrinkage of the mortars studied:

- 20% fly ash replacement (Mixes 2 and 3) has noticeably-reduced autogenous and free drying shrinkage of the mortar (in comparison to Mix 1) at all ages.
- 25% GGBFS replacement reduces autogenous shrinkage significantly, while it increases free drying shrinkage of the mortar slightly (in a comparison of Mix 1 and Mix 7). As a result, the GGBFS replacement has little effect on the total (autogenous + free drying) shrinkage of the mortar at 56 days.
- The mix with 5.6% MK (Mix 10) also has relatively-low autogenous shrinkage but intermediate free drying shrinkage. Therefore, the total shrinkage of this mix is also intermediate.
- Although having higher paste content, Mix 6 shows slightly lower autogenous shrinkage than Mix 4. Although having similar w/b and s/b, Mix 7 has noticeably-lower autogenous shrinkage than Mix 10. These imply that not only the paste content but also the paste pore structure, which could be altered by the SCMs and chemical admixtures used, have played important roles in the autogenous shrinkage of the mortars. This observation is also confirmed by the comparison of Mixes 8 and 9.
- Different from autogenous shrinkage, drying shrinkage of Mixes 4 and 6 is similar and also for Mixes 8 and 9, while free drying shrinkage of Mix 10 is significantly lower than Mix 7.
- The only difference in Mixes 9 and 11 is the type of cement. Mix 11 (Type I cement) shows higher values in both autogenous and free drying shrinkage value than Mix 9 (Type I/II cement). This suggests that Lehigh Type I cement provides mortar with high shrinkage.
- Autogenous shrinkage ranges from about 150 to 250 microstrain and free dying shrinkage ranges from 700 to 1200 microstrain at the age of 56 days. Some mixes (Mix 11) show high

autogenous shrinkage but intermediate or low free drying shrinkage, and vice versa (Mix 7).

- Among 11 mortar mixes studied, Mixes 6, 5, and 4 have the highest total shrinkage, while Mixes 11, 2, 3, 8, and 9 have the lowest total shrinkage values. The trend is similar to that of cracking potential observed from ring shrinkage.

5.1.4 Shrinkage of Concrete

Table 5.5 and Figure 5.3 summarize all concrete shrinkage measurements at given ages.

Table 5.5. Summary of concrete shrinkage

Mix No	Autogenous Shrinkage (microstrain)			Free Drying Shrinkage (microstrain)			Ring Shrinkage (microstrain)	
	7 day	28 day	56 day	7 day	28 day	56 day	7 day	28 day
1	55	140	190	230	440	526	62	103
2	50	113	150	260	430	520	45	75
3	45	110	140	203	336	390	41	67
4	50	90	120	215	405	500	59	107 (15)
5	55	100	120	180	450	550	60	98
6	86	113	170	240	463	580	62	114 (17)
7	50	100	125	285	500	610	72	116
8	53	113	183	296	433	460	48	80
9	36	76	103	296	436	483	46	76
10	75	120	155	235	390	435	53	110
11	50	90	123	393	543	580	43	72

Note: The values indicated in parentheses are the age at which peak strains were recorded prior to 28 days.

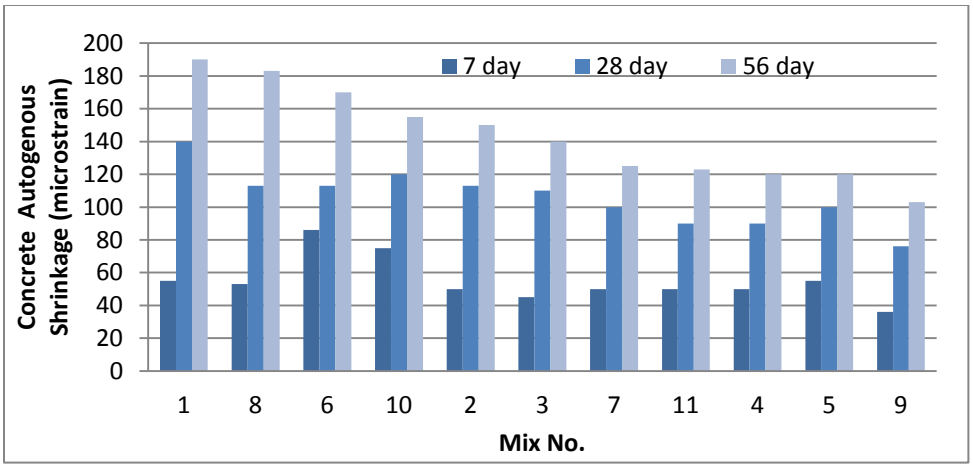

(a) Autogenous shrinkage

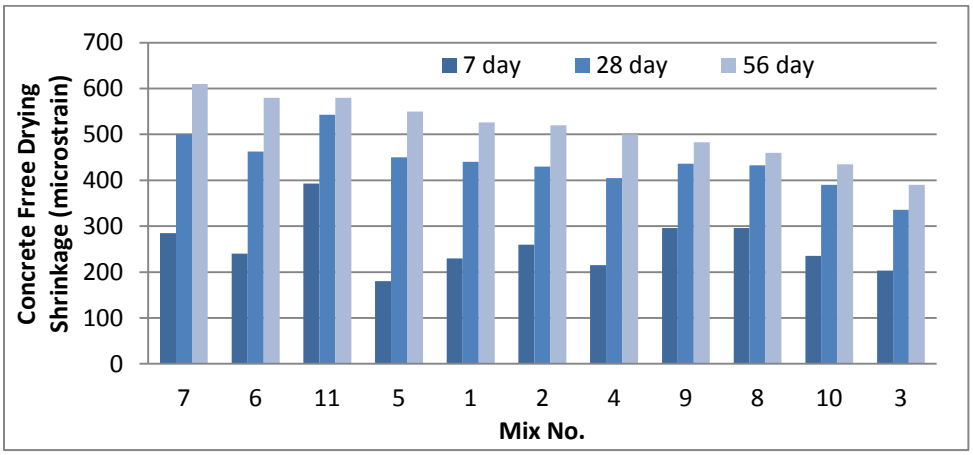

(b) Free drying shrinkage

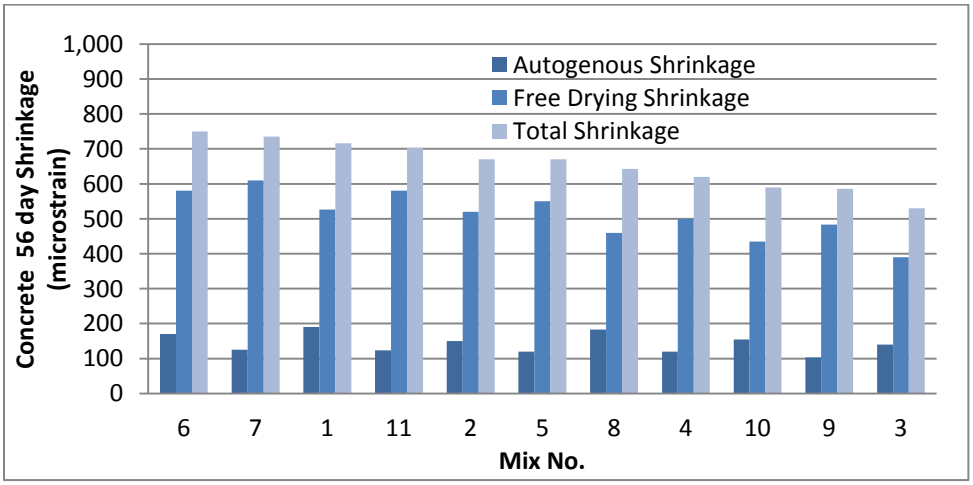

(c) Different shrinkages at 56 days

Figure 5.3. Shrinkage of concrete at given ages

The following observations can be made on the shrinkage of the concrete mixes studied:

- Similar to that observed from mortar, 20% fly ash replacement (Mixes 2 and 3) has noticeably reduced both autogenous and free drying shrinkage of the mortar (in comparison with Mix 1) at all ages.
- Similar to that observed from mortar, 25% GGBFS replacement reduces autogenous shrinkage significantly, while it increases free drying shrinkage of the concrete noticeably (in a comparison of Mix 1 and Mix 7). However, the total shrinkage of the mix having 25% GGBFS replacement (Mix 7) is still lower than that without GGBFS (Mix 1) at 56 days.
- Comparing to Mix 7 (with 25% GGBFS), the combination of 20% FA and 5.6% MK (Mix 10) shows low values in both autogenous shrinkage and free drying shrinkage. Therefore, the total shrinkage of Mix 10 is also low.
- Similar to that observed for mortar, Mix 11 (Type I cement) shows higher values in both autogenous and free drying shrinkage than Mix 9 (Type I/II cement). This, again, suggests that Lehigh Type I cement provides mortar with high shrinkage.
- Autogenous shrinkage ranges from about 150 to 250 microstrain and free drying shrinkage ranges from 700 to 1200 microstrain at 56 days. Some mixes (Mix 1) show high autogenous shrinkage but intermediate or low free drying shrinkage, and vice versa (Mix 7).
- Among 11 mortar mixes studied, Mixes 6, 7, 1, and 11 have the highest total shrinkage (≥700 microstrain), while mixes 10, 9, and 3 have the lowest total shrinkage values (<600 microstrain). Mixes 4 and 5, which cracked in ring tests, have low autogenous shrinkage, intermediate free drying shrinkage, and intermediate total shrinkage.
- Although the order of ring shrinkage is not consistent with that of free drying shrinkage or total shrinkage (Table 5.5), Figure 4.56 (see section 4.6.6) shows a relationship between ring stress and free drying shrinkage stress.
- In addition, as discussed in sections 4.6.2 and 4.6.3, for a given mix, there is a strong relationship between free drying shrinkage and mass loss of concrete and a strong relationship between free drying shrinkage of concrete and mortar.
- There is a good relationship between cementitious material content and total shrinkage (autogenous and free drying shrinkage) of concrete.

5.1.4 Mechanical Properties and Cracking Potential of Concrete

Table 5.6 shows the elastic modulus, compressive strength, splitting tensile strength, and creep coefficient (at 28 days) for concrete. Table 5.7 summarizes the cracking potential estimated from simple stress analysis (with and without creep consideration) as well as the stress rate (according to ASTM C 1581).

The normalized values in Table 5.7 (each value to the highest value in the corresponding data sets) are re-plotted in Figure 5.4.

Table 5.6. Summary of mechanical properties

Mix	Elastic Modulus X10^{6}psi			Compressive Strength, psi			Split Tensile Strength (psi)			Creep
No.	7 day	28 day	56 day	7 day	28 day	56 day	7 day	28 day	56 day	Coeff.
1	3.80	3.93	4.10	2500	3790	4020	300	420	430	2.663
2	3.70	3.85	3.85	3450	4515	4925	320	430	530	2.388
3	3.10	3.70	3.90	2590	3450	3600	290	385	410	2.788
4	4.20	4.25	4.45	3130	4070	4510	300	350	360	2.596
5	4.00	4.65	4.70	2540	3710	3960	280	350	430	2.684
6	4.60	4.85	5.20	4700	5800	6740	390	470	520	2.100
7	3.65	3.95	3.95	2950	3970	4160	290	440	465	2.598
8	3.20	4.00	4.45	1800	3500	4610	230	360	370	2.797
9	3.30	3.50	3.80	1460	2795	3990	210	380	460	3.160
10	3.40	3.85	3.90	3300	4600	4985	310	500	525	2.364
11	3.60	3.85	3.95	1850	3260	3820	275	370	420	2.890

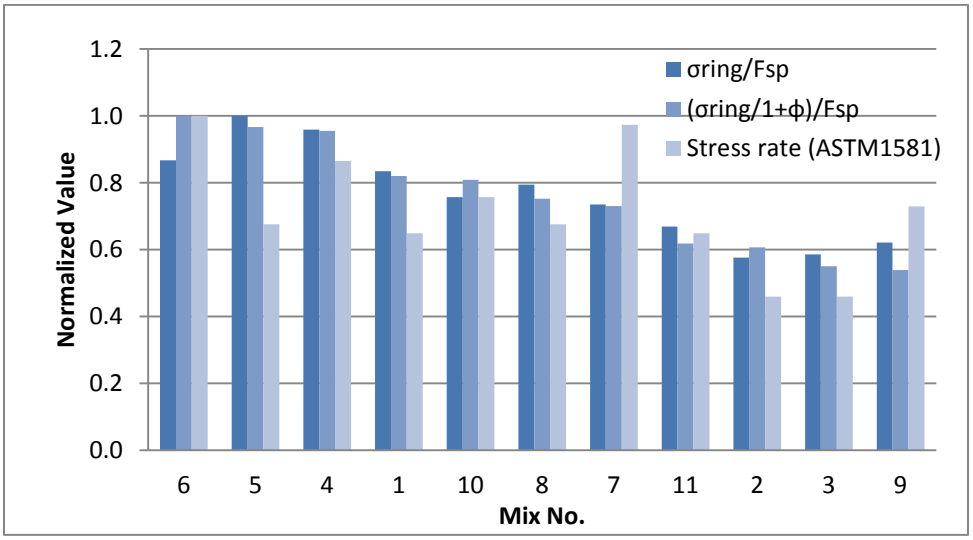

Figure 5.4. Normalized shrinkage stress-to-strength ratio of concrete

Table 5.7. Summary of cracking potential

Mix No.	Based on Free Shrinkage				Based on Ring Shrinkage		Stress Rate Method				
	$\sigma_{free} = E^*\varepsilon_{free}$ (psi)		$\sigma_{free}/(1+\varphi)$ (psi)		$(\sigma_{free}/1+\varphi)/F_{sp}$		Cracking Potential	Peak $\sigma_{ring}/F_{sp,}$ (psi/psi)	Cracking Potential	Average Stress Rate, S (psi/day)	ASTM Cracking Potential Rating
	14 day	28 day	14 day	28 day	14 day	28 day					
1	1351	1766	363	513	1.07	1.22	Medium	2.66	Medium	23.6	Moderate - Low
2	1350	1656	395	508	1.12	1.19	Low	1.84	Low	19.7	Moderate - Low
3	933	1246	243	343	0.71	0.89	Low	1.87	Low	16.6	Moderate - Low
4	1441	1876	414	560	1.37	1.74	High	3.05	High	31.9	Moderate - High
5	1989	2344	542	678	1.71	1.93	High	3.18	High	24.9	Moderate - High
6	1571	2253	516	766	1.32	1.74	High	2.76	High	37.3	Moderate - High
7	1647	2028	466	600	1.19	1.36	Medium	2.34	Medium	35.6	Moderate - High
8	1297	1744	315	490	1.09	1.37	Medium	2.53	Medium	24.5	Moderate - High
9	1238	1539	277	396	0.99	1.03	Low	1.98	Low	27.1	Moderate - High

10	1509	1771	457	558	1.13	1.11	Low	2.41	Medium	27.7	Moderate - High
11	1900	2092	479	575	1.29	1.36	Medium	2.13	Medium	24.2	Moderate - Low

The following observations can be made on the shrinkage of the concrete mixes studied:

- There is a good relationship between elastic modulus and compressive strength and an excellent relationship between compressive strength and splitting tensile strength.
- Concrete mixes with high shrinkage values may not always crack first and it is the combined effect of shrinkage and mechanical properties (elastic modulus, creep, and strength) that determine concrete cracking potential.
- Cracking potential assessed simply based on the stress/strength ratio correlates better with the cracking behavior observed from ring tests than that estimated from ASTM C 1581 based on concrete stress rates.
- Based on the stress/strength ratio calculated simply, Mixes 6, 5, and 4 have the highest cracking potential, while Mixes 11, 2, 3, and 9 have the lowest cracking potential of the 11 concrete mixes studied.

5.2 Conclusions

The following conclusions can be drawn from this study.

5.2.1 Concrete Shrinkage and Cracking Behavior

- Among the 11 mixes studied, cracking was observed in two of the three Mix 4 ring specimens at 13 and 18 days, in one of the three Mix 5 ring specimens at 11 days, and in the three Mix 6 ring specimens at 16, 16.5, and 18 days.
- Predictions based on the shrinkage stress-to-splitting tensile strength ratio with consideration of creep, Peak $(\sigma_{ring}/1+\varphi)/F_{sp}$, indicates the following:
  - Mixes 4, 5, and 6 have high cracking potential, which is consistent with the results of the ring tests.
  - Mixes 1, 7, 8, 9, and 10 have medium cracking potential.
  - Mixes 2, 3, and 11 have low cracking potential.
- Predictions based on ASTM C 1581 (the average stress rate in ring specimens) indicates the following:
  - Mixes 4 through 10 have moderate to high shrinkage cracking potential.
  - Mixes 1, 2, 3, and 11 have moderate to low shrinkage cracking potential.
  - The concrete cracking potential seems to be overestimated by ASTM C 1581 when compared with that estimated from the simple stress-to-strength ratio method.
- Not all mixes having high shrinkage cracked. Cracking is associated mainly with the restrained shrinkage strain ε_{sh}, modulus of elasticity E_c, and creep coefficient ϕ. This behavior can be observed in Mixes 7 and 10 where they have comparable shrinkage to Mixes 4 and 6 but do not display cracking.

5.2.2 Effect of Concrete Materials and Proportions

- 20% Class C fly ash replacement for cement reduced all types of shrinkage in paste, mortar, and concrete.
- 25% GGBFS replacement for cement didn't affect chemical shrinkage of the paste significantly. It reduced autogenous shrinkage noticeably and increased free drying shrinkage of mortar slightly. It increased free drying shrinkage and restrained shrinkage of concrete significantly.
- The combination of 20% Class C fly ash and 25% GGBFS reduced the shrinkage of mortar and concrete. The chemical shrinkage of the mixes was lower than the control mix (without fly ash and slag) initially, but, at the later age, the rate of the chemical shrinkage increased quickly and the mixes displayed a greater shrinkage than the control mix.
- The combination of 20% FA and 5.6% MK (Mix 10) provided increased chemical shrinkage of pastes and reduced autogenous shrinkage and free drying shrinkage of mortar. The restrained shrinkage of concrete was similar to that of the mixes without the fly ash and metakaolin.
- Mixes made with Type I cement yielded greater shrinkage than those with Type I/II cement.
- Mixes made with finer graded quartzite displayed similar shrinkage behavior to mixes made with coarse graded limestone as the coarse aggregate.
- Among three cracked concrete mixes, two of three Mix 6 samples cracked and had cementitious material content of 825.7 lb/yd^3, two of three Mix 4 samples cracked and had cementitious material content of 709.2 lb/yd^3, and the cementitious material content of the remainder of the mixes, including Mix 5, which had one of three samples crack, was under 700 lb/yd^3.
- Mix 8, made with finer-graded quartzite, displayed similar shrinkage behavior to Mix 9, made with coarse graded limestone as the coarse aggregate. Mix 8 also had lower splitting tensile strength than Mix 9 after 14 days. As a result, quartzite aggregate appeared not to reduce shrinkage cracking potential significantly. This also suggests that aggregate type has a more significant effect on concrete splitting tensile strength than on compressive strength.

5.2.3 Relationships

- Mass loss shows a strong linear relation with free drying shrinkage for a given mix.
- The trend of free drying shrinkage of mortar is similar to that of concrete.
- The stress resulting from restrained drying shrinkage has an acceptable linear relationship with the stress from free drying shrinkage of concrete.
- There is a good relationship between concrete compressive strength and elastic modulus and an excellent relationship between compressive strength and tensile strength.
- Cementitious material content has a good relationship with mortar free drying shrinkage, a weak relationship with mortar total shrinkage (autogenous and free drying shrinkage), and a weak relationship with concrete free drying shrinkage.

5.3 Recommendations

The following recommendations are proposed based on the above observations and conclusions:

1. Material selection and mix design
   - The present study has indicated that 20% fly ash reduces shrinkage, 5% metakaolin increases shrinkage, and 25% GGBFS has little effect on shrinkage. Therefore, use of fly ash in combination with metakaolin and/or GGBFS is recommended in the concrete used for Iowa bridge decks and overlays.
   - The order of preference for cement selection may be Type IP, Type I/II, and then Type I in consideration of their shrinkage cracking resistance.
   - Total shrinkage generally increases with the cementitious content or paste volume of concrete. Cautions should be taken when total cementitious material content in concrete is over 700 lb/ft^3.
2. Test methods
   - Given that free drying shrinkage has a good correlation with mass loss, mass loss can be used to assess free drying shrinkage of mortar/concrete.
   - Since the trend of total mortar shrinkage is similar to that of ring shrinkage of the corresponding concrete, mortar shrinkage can be used to approximately evaluate restrained concrete shrinkage.
   - Because the ring stress resulting from restrained drying shrinkage has an acceptable linear relationship with the stress from free drying shrinkage of concrete, the simple free drying shrinkage tests, using prism specimens, can be used to replace the complex restrained drying shrinkage tests, using ring specimens, thus providing an approximate assessment on the stresses developed in restrained concrete.
   - The simple calculation of shrinkage stress-to-splitting tensile strength ratio with consideration of creep can be used to estimate concrete cracking potential.
   - Elastic modulus and splitting tensile strength of the Iowa HPC mixes can be estimated easily based on compressive strength of the corresponding concrete using equations in this report.
3. Further research
   - Creep behavior of these concrete mixes was estimated based on the existing models used in this project and it should be investigated experimentally.
   - Pore structure of the concrete mixes may be studied and the results may be related to the concrete shrinkage behavior.
   - Internal curing and shrinkage-reducing agents may be considered to be used in Mixes 4, 5, and 6 to control concrete cracking.
   - Effects of aggregate characteristics (type, size, and bond with cement) on concrete shrinkage should be studied further.
4. Research implementation
   - It is recommended to continue the requirement for use of fly ash in combination with metakaolin and/or GGBFS in the concrete used for bridge decks and overlays in Iowa. Given that fly ash is not permitted in the current O-mix, it is suggested to use Type IP cement, instead of Type I or I/II cement, in future Iowa bridge deck and overlay projects.

- For the HPC mixes with high shrinkage cracking potential (such as Mixes 4, 5, and 6), further study shall be conducted to incorporate a shrinkage reducing agent (SRA) and internal current (IC) technique into the concrete to reduce the concrete shrinkage and cracking potential. The effects of SRA and IC on the mechanical property and durability of the concrete shall also be studied. For the HPC mixes with medium/moderate-high shrinkage cracking potential (such as Mixes 1, 7, 8, 10, and 11), further study can be conducted to modify the concrete mix proportions and balance water-to-cementitious ratio, cementitious content, shrinkage, and tensile strength of the concrete, thus further lowering the cracking potential of the concrete mixes.
- A field study shall be conducted to compare the performance of the high- and low-risk HPC mixes side-by-side. The high-risk mix may be the currently-used, high shrinkage cracking potential mix as identified in the present study (such as Mix 6), while the low-risk mix may be the one selected after mix proportion adjustment, with (or without) SRA or IC agents, and approved in the laboratory as a low shrinkage cracking potential mix. Quality control tests (including workability, air content, and compressive/tensile strength) of the field concrete may be conducted. Shrinkage and cracking behavior of the field concrete will be monitored over 3 to 5 years to verify the present and future research findings.

REFERENCES

Aitcin, P. C. (1998). "Autogenous Shrinkage Measurement," Autoshrink '98, Proceedings of the International Workshop on Autogenous Shrinkage of Concrete, Hiroshima, Japan, ed. E. Tazawa, 245-256.

Al-Attar, Tareq Salih. (2008). "Effect of Coarse Aggregate Characteristics on Drying Shrinkage of Concrete" *Journal of Engineering and Technology*. Vol. 26, No. 2.

Almudaiheem, Jamal A., and Hansen, Will. (1987). "Effect of Specimen Size and Shape on Drying Shrinkage of Concrete," *ACI Materials Journal*, Vol. 84, No.2, 130-135.

Almusallam A. A., M. Maslehuddin, M. Abdul-Waris, F. H. Dakhil, and O. S. B. Al-Amoudi. (1999). "Plastic shrinkage cracking of blended cement concretes in hot environments," *Magazine of Concrete Research*, Vol. 51, No. 4:241-6.

Al-Omaishi, N., M. K. Tadros, and S. J. Seguirant. (2009). "Elasticity modulus, shrinkage, and creep of high-strength concrete as adopted by AASHTO." *PCI Journal*. Summer 2009.

Barcelo, Laurent, Micheline Moranville, and Bernard Clavaud. (2005). "Autogenous shrinkage of concrete: a balance between autogenous swelling and self-desiccation," *Cement and Concrete Research*. Vol. 35:177-183.

Baroghel-Bouny, Ve´ronique, Pierre Mounanga, A. Khelidj. A. Loukili, and N. Rafai. (2006). "Autogenous deformations of cement pastes Part II. W/C effects, micro–macro correlations, and threshold value," *Cement and Concrete Research*, Vol. 36:123-136.

Bažant, Z. P., and Baweja, S. (1995). "Creep and shrinkage prediction model for analysis and design of concrete structures: Model B3." (RILEM Recommendation). *Materials and Structures*. 28, pp. 357-367 (Errata, Vol. 29, p. 126).

Bažant, Z. P., and Baweja, S. (2000). "Creep and shrinkage prediction model for analysis and design of concrete structures: Model B3." Adam Neville Symposium: Creep and Shrinkage-Structural Design Effects, ACI SP194, A. Al-Manaseer, ed., pp. 1-83 (update of 1995 RILEM Recommendation).

Bentz, D. P. (1997). "Three-Dimensional Computer Simulation of Portland Cement Hydration and Microstructure Development," *Journal of American Ceramic Society*, Vol. 80, No. 1:3-21.

Bentz, D. P., Sant, G., and Weiss, J. (2008). "Early-Age Properties of Cement-Based Materials I: Influence of Cement Fineness," *ASCE Journal of Materials in Civil Engineering*, Vol. 20, No. 7:502-508

Boivin S., Acker P., Rigaud S., Clavaud B. (1998). "Experimental assessment of chemical shrinkage of hydrating cement pastes," Proceedings of the International Workshop on Autogenous Shrinkage of Concrete. E. Tazawa (Ed.). AUTOSHRINK '98, Hiroshima, Japan, E & FN Spon, London, UK, 81-92.

Bouasker, M., Mounanga, P., Turcry, P., Loukili, A., and Khelidj, A. (2008). "Chemical Shrinkage of Cement Pastes and Mortars at Very Early Age: Effect of Limestone Filler and Granular Inclusions." *Cement and Concrete Composites*, 30(1). 13-22.

Brown, M. D., C. A. Smith, J. G. Sellers, K. J. Folliard, and J. E. Breen. (2007). "Use of Alternative Materials to Reduce Shrinkage Cracking in Bridge Decks," *ACI Materials Journal*, Vol. 104, pp. 629-637, November 1, 2007.

Burrows, R. W., Kepler, W. F., Hurcomb, D., Schaffer, J., and Sellers, G. (2004). "Three Simple Tests for Selecting Low-Crack Cement," *Cement and Concrete Composites*, Vol. 26, No. 5:509-519.

Cusson, D., and Hoogeveen, T. (2007). "An Experimental Approach for the Analysis of Early-Age Behaviour of High-performance Concrete Structures under Restrained Shrinkage," *Cement and Concrete Research*, Vol. 37:200-209.

Darquennes, Aveline, Stéphanie Staquet, M. Delplancke-Ogletree, and B. Espion. (2011). "Effect of autogenous deformation on the cracking risk of slag cement concretes," *Cement and Concrete Composites*, Vol. 33:368-379.

Deshpande, S., Darwin, D., and Browning, J. (2007). *Evaluating Free Shrinkage of Concrete for Control of Cracking in Bridge Decks*, Final Report for Transportation Pooled Fund Study TPF-5(051). University of Kansas Center for Research, Inc., Lawrence, KS.

Feng X., Garboczi, E. J., Bentz, D. P., and Stutzman, P. E. (2004). "Estimation of the degree of hydration of blended cement pastes by a scanning electron microscopy point-counting procedure," *Cement and Concrete Research*, Vol. 34, No. 10, 1787-1793.

Folliard, K., Smith, C., Sellers, G., Brown, M., and Breen, J. E. (2003). *Evaluation of Alternative Materials to Control Drying-Shrinkage Cracking in Concrete Bridge Decks*, FHWA and Texas Department of Transportation Report FHWA/TX-04/0-4098-4. Center for Transportation Research, University of Texas at Austin, TX.

Fu, G., Feng, J., Dimaria, J., and Zhuang, Y. (2007). *Bridge Deck Corner Cracking on Skewed Structures*, Final Research Report RC-1490 to the Michigan Department of Transportation. Wayne State University Center for Advanced Bridge Engineering, Detroit, MI.

Gleize, Philippe J. P., Martin Cyr, and Gilles Escadeillas. (2007). "Effects of metakaolin on autogenous shrinkage of cement pastes," *Cement and Concrete Composites*, Vol. 29:80-87.

Gupta, S. M., V. K. Sehgal, and S. K. Kaushik. (2009). "Shrinkage of High Strength Concrete," *World Academy of Science, Engineering and Technology* 50.

Hansen, W. (2011). "Report on early age cracking - A summary of the latest document from ACI Committee 231," *Concrete International*. 48-51.

Holt, Erika E. (2001). "Early age autogenous shrinkage of concrete," *VTT Building and Transport*. Technical editing Maini Manninen, Tummavuoren Kirjapaino Oy, Vantaa, 2001.

Hooton, D. R., Stanish, K., and Prusinski, J. (2008). "The Effect of Ground, Granulated Blast Furnace Slag (Slag Cement). on the Drying Shrinkage of Concrete – A Critical Review of the Literature," International Conference on Fly Ash, Silica Fume, Slag and Natural Pozzolans in Concrete.

Hua, C., A. Ehrlacher, and P. Acker. (1997). "Analyses and models of the autogenous shrinkage of hardening cement paste II. Modeling at scale of hydrating grains," *Cement and Concrete Research*, Vol. 27, No.2:245-258.

Igarashi, Shin-ichi, Arnon Bentur, and Konstantin Kovler. (2000). "Autogenous shrinkage and induced restraining stresses in high-strength concretes," *Cement and Concrete Research*, Vol. 30:1701-1707.

Japan Concrete Institute. (1999). *Autogenous Shrinkage of Concrete*, Technical Committee on Autogenous Shrinkage of Concrete Committee Report, edited by Ei-ichi Tazawa, E & FN Spon, London, pp. 1-62.

Jensen, O. M., and P. F. Hansen. (1999). "Influence of temperature on autogenous deformation and P humidity change in hardening cement paste," *Cement and Concrete Research*, Vol. 29:567-575.

Jensen, O. M., and P. F. Hansen. (2001). "Autogenous deformation and RH-change in perspective," *Cement and Concrete Research.* Vol. 3:1859 -1865.

Jiang, Zhengwu, Zhenping Sun, and Peiming Wang. (2005). "Autogenous relative humidity change and autogenous shrinkage of high-performance cement pastes," *Cement and Concrete Research*, Vol. 35:1539-1545.

Justnes, H., E. J. Sellevold, and B. Reyniers. (2000a). "Chemical shrinkage of cement pastes with plasticizing admixtures," *Nordic Concrete Research*, Vol. 24:39-54.

Justnes, H., F. Clemmens, P. Depuydt, D. Van Gemert, and E. J. Sellevold. (2000b). "Correlating the Deviation Point Between External and Total Chemical Shrinkage with Setting Time and Other Characteristics of Cement Pastes." Proceedings, Shrinkage 2000, International RILEM Workshop on Shrinkage of Concrete, 57-73.

Justnes, H., E. J. Sellevold, B. Reyniers, D. Van Loo, A. Van Gemert, F. Verboven, and D. Van Gemert. (1999). "The influence of cement characteristics on chemical shrinkage," Proceedings of the International Workshop on Autogenous Shrinkage of Concrete. E. Tazawa (Ed.). AUTOSHRINK '98, E & FN Spon, London, UK, 71- 80.

Kawashima, Shiho, and Surendra P. Shah. (2011). "Early-age autogenous and drying shrinkage behavior of cellulose fiber-reinforced cementitious materials," *Cement and Concrete Composites*, Vol. 33:201-208.

Kocaba, Vanessa, Gallucci, Emmanuel, and Scrivener, Karen L. (2012). "Methods for determination of degree of reaction of slag in blended cement pastes," *Cement and Concrete Research.* Vol. 42, Issue 3, pp. 511–525.

Koenders, E. A. B. (1997). "Simulation of Volume Changes in Hardened Cement-Based Materials," PhD dissertation, Delft University Press, 171.

Krauss, P. D., and Rogalla, E. A. (1996). *NCHRP Report 380: Transverse Cracking in Newly Constructed Bridge Decks*, National Cooperative Highway Research Program, Transportation Research Board, National Research Council, Washington, DC.

Lee, K. M., Lee, H. K., Lee, S. H. and Kim, G. Y. (2006). "Autogenous Shrinkage of Concrete Containing Granulated Blast-furnace Slag," *Cement and Concrete Research*, Vol. 36:1279-1285.

Li, Yue, Junling Bao, and Yilin Guo. (2010). "The relationship between autogenous shrinkage and pore structure of cement paste with mineral admixtures," *Construction and Building Materials*, Vol. 24:1855-1860.

Lin, F. (2005). "Modeling of hydration kinetics and shrinkage of Portland cement paste," PhD thesis, Columbia University.

Lomboy, G., K. Wang**,** and C. Ouyang. (2011). "Shrinkage and Fracture Properties of Semiflowable Self Consolidating Concrete," Special issue on Energy Efficient and Environmentally Friendly Paving Materials, *ASCE Journal of Materials in Civil Engineering*, Vol. 23, No. 11, pp. 1514-1524.

Lura, P., and Jensen, O. (2007). "Measuring Techniques for Autogenous Strain of Cement Paste." *Materials and Structures*, 40(4). 431-440.

Lura, Pietro, Ole Mejlhede Jensen, and Klaas van Breugel. (2003). "Autogenous shrinkage in high-performance cement paste: An evaluation of basic mechanisms," *Cement and Concrete Research*, Vol. 33, Issue 2, pp. 223-232.

Meddah, Mohammed Seddik, Masahiro Suzuki, and Ryoichi Sato. (2011). "Influence of a combination of expansive and shrinkage-reducing admixture on autogenous deformation and self-stress of silica fume high-performance concrete," *Construction and Building Materials*, Vol. 25:239-250.

Mehta, P. K., and P. J. M. Monteiro. (1993). *Concrete: Structure, Properties, and Materials*. Englewood Cliffs, NJ: Prentice Hall Canada.

Minnesota Department of Transportation. (2011). *Bridge Deck Cracking*, Transportation Research Synthesis. TRS 1105. November 2011.

Miyazawa, S., and Monteiro, P. J. M. (1996). "Volume Change of High-strength Concrete in Moist Conditions," *Cement and Concrete Research*, Vol. 26, Issue 4:567-572.

Mohr, B. J., and K. L. Hood. (2010). "Influence of bleed water reabsorption on cement paste autogenous deformation," *Cement and Concrete Research*, Vol. 40:220-225.

Mokarem, David W., D. Stephen Lane, H. Celik Ozyildirim, and Michael M. Sprinkel. (2008). *Measurement of early age shrinkage of Virginia concrete mixtures*, Virginia Transportation Research Council. Final Report, VTRC 08-R9, FHWA/VTRC 08-R9.

Mounanga P., A. Khelidj, A. Loukili, and V. Baroghel-Bouny. (2004). "Predicting $Ca(OH)_2$ content and chemical shrinkage of hydrating cement pastes using analytical approach". *Cement and Concrete Research*; Vol. 34:255-265.

Naik, Tarun R., Yoon-moon Chun, and Rudolph N. Kraus. (2006). *Reducing Shrinkage Cracking of Structural Concrete Through the Use of Admixtures*. Wisconsin Highway Research Program Project Report 0092-04-13. UWM Center for By-Products Utilization Department of Civil Engineering and Mechanics University of Wisconsin-Milwaukee. March 2006.

Persson, B. (1998). "Experimental Studies on Shrinkage of High-performance Concrete," *Cement and Concrete Research*, Vol. 28, No.7:1023-1036.

Persson, B. (2000). "Consequence of cement constituents, mix composition and curing conditions for self-desiccation in concrete." *Materials and Structures*, Vol.33:352-362.

Popovics, John, Jeffery Roesler, Carrie Peterson, Andres Salas, and Suyun Ham. (2011). *High Plastic Concrete Temperature Specifications for Paving Mixtures*. FHWA and Illinois Department of Transportation Report FHWA-ICT-11-087. Illinois Center for Transportation, University of Illinois at Urbana-Champaign, Urbana, IL.

Quangphu, Nguyen, Jiang Linhua, Liu Jiaping, Tian Qian, and Do Tienquan. (2008). "Influence of shrinkage-reducing admixture on drying shrinkage and mechanical properties of high-performance concrete," *Water Science and Engineering*, Vol.1, No. 4:67-74.

Radocea, A. (1992). "A Study on the Mechanism of Plastic Shrinkage of Cement-Based Materials," Doctoral dissertation, CTH Göteborg, Sweden, 125 pp.

Rougelot, T., Skoczylas, F., and Burlion, N. (2009). "Water desorption and shrinkage in mortars and cement pastes: experimental study and poromechanical model," *Cement and Concrete Research*, Vol. 39: 36-44.

Saito, Mitsuru, Kawamura, Mitsunori, and Arakawa, Seiichi. (1991). "Role of Aggregate in the Shrinkage of Ordinary Portland and Expansive Cement Concrete," *Cement and Concrete Composites*, Vol. 13, No.2, 115-121.

Sant, Gaurav, Pietro Lura, and Jason Weiss. (2006). "Measurement of Volume Change in Cementitious Materials at Early Ages: Review of Testing Protocols and Interpretation of Results," *The Transportation Research Record*.

Sarkar, S. L. (1994). "Roles of Silica Fume, Slag, and Fly Ash in the Development of High-Performance Concrete Microstructure," *American Concrete Institute Special Publication* 149-25:449-460.

Shah, H. R., and Weiss, W. J. (2006). "Quantifying Shrinkage Cracking in Fiber Reinforced Concrete Using the Ring Test," *Materials and Structures*, Vol. 39, No. 9, pp. 887-899.
Shah, S. P., Weiss, W. J., and Yang, W. (1997). "Shrinkage Cracking in High Performance Concrete," Proceedings of PCI/FHWA International Symposium on High Performance Concrete, New Orleans, LA, Oct. 20-22:148-158.
Sule, M., and K. van Breugel. (2004). "The effect of reinforcement on early-age cracking due to autogenous shrinkage and thermal effects," *Cement and Concrete Composites*, Vol. 26:581-587.
Tadros, M. K., N. Al-Omaishi, S. J. Seguirant, and J. G. Gallt. (2003). *NCHRP Report 496: Prestress Losses in Pretensioned High-Strength Concrete Bridge Girders*. National Cooperative Highway Research Program, Transportation Research Board, National Academy of Sciences, Washington, DC.
Tarr, Scott M., and Farny, James A. (2008). *Concrete Floors on Ground*, EB075, Fourth Edition, Portland Cement Association, Skokie, Illinois, USA.
Tazawa E., and S. Miyazawa. (1995). "Influence of cement and admixture on autogenous shrinkage of cement paste," *Cement and Concrete Research*, Vol. 25, No. 2:281-287.
Tazawa E., S. Miyazawa, and T. Kasai. (1995). "Chemical shrinkage and autogenous shrinkage of hydrating cement paste," *Cement and Concrete Research*. Vol. 25, No. 2:288 -292.
Termkhajornkit, Pipat, T. Nawa, M. Nakai, and T. Saito. (2005). "Effect of fly ash on autogenous shrinkage," *Cement and Concrete Research*, Vol. 35:473-482.
Tia, Mang, Rajarajan Subramanian, Danny Brown, and Chuck Broward. (2005). *Evaluation of Shrinkage Cracking Potential of Concrete Used in Bridge Decks in Florida*, Final Report for the Florida Department of Transportation. University of Florida, Department of Civil and Coastal Engineering, Gainesville, FL.
Wan, B., Foley, C. M., and Komp, J. (2010). *Concrete Cracking in New Bridge Decks and Overlays*, Wisconsin Highway Research Program Report, WHRP 10-05.
Whiting, D. A., Detwiler, R. J., and Lagergren, E. S. (2000). "Cracking Tendency and Drying Shrinkage of Silica Fume Concrete for Bridge Deck Applications," *ACI Materials Journal*, Vol. 97, No.1:71-78.
Wild, S., Khatib, J. M., and Roose, L. J. (1998). "Chemical shrinkage and autogenous shrinkage of portland cement-metakaolin pastes." *Advances in Cement Research*, Vol. 10, No. 3:109-119.
Yajun, J., and Cahyadi, J. H. (2004). "Simulation of silica fume blended cement hydration," *Materials and Structures*, Vol. 37, pp. 397-404.
Yang, Yang, Ryoichi Sato, and Kenji Kawai. (2005). "Autogenous shrinkage of high-strength concrete containing silica fume under drying at early ages," *Cement and Concrete Research*, Vol. 35:449-456.

APPENDIX A.

A.1 Chemical Shrinkage Test Results of Individual Specimens

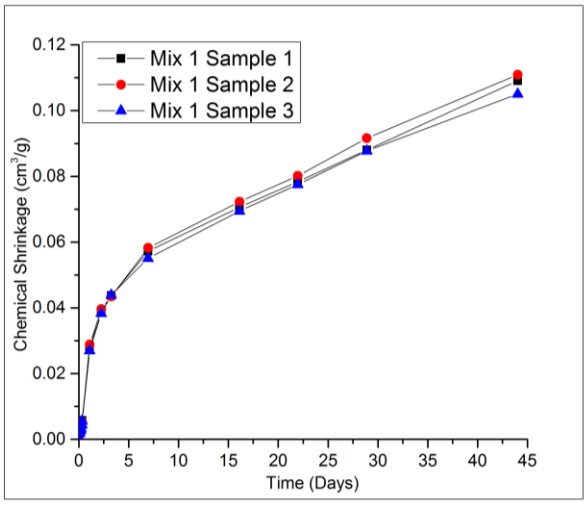

Figure A.1. Mix 1 chemical shrinkage results

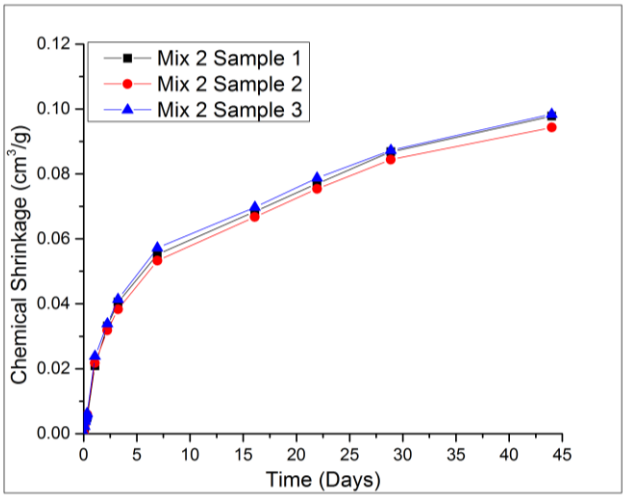

Figure A.2. Mix 2 chemical shrinkage results

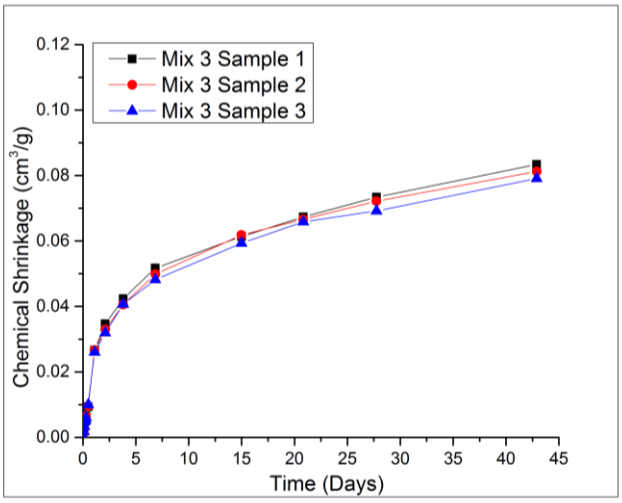

Figure A.3. Mix 3 chemical shrinkage results

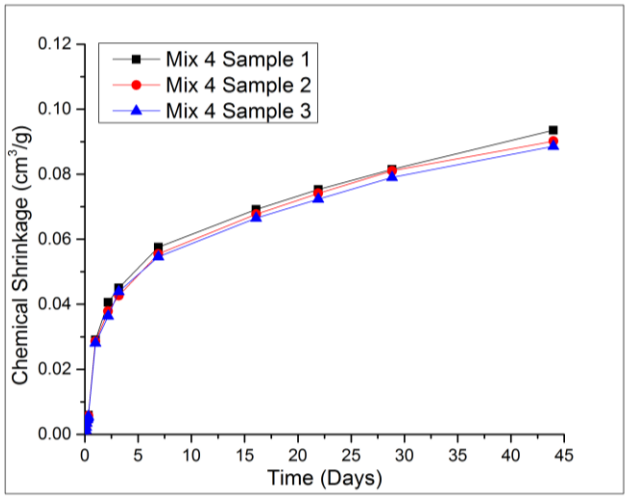

Figure A.4. Mix 4 chemical shrinkage results

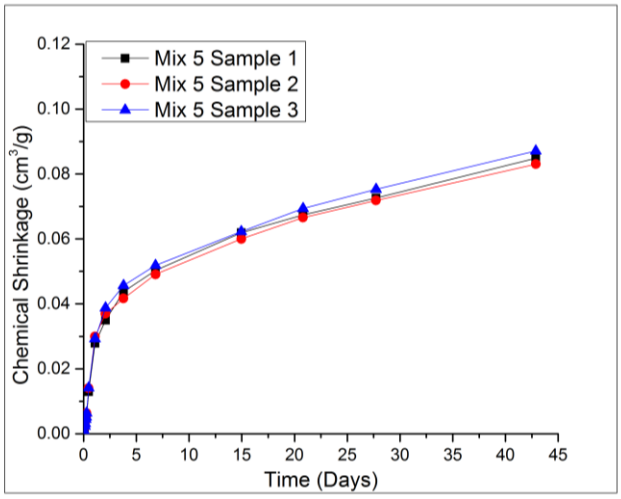

Figure A.5. Mix 5 chemical shrinkage results

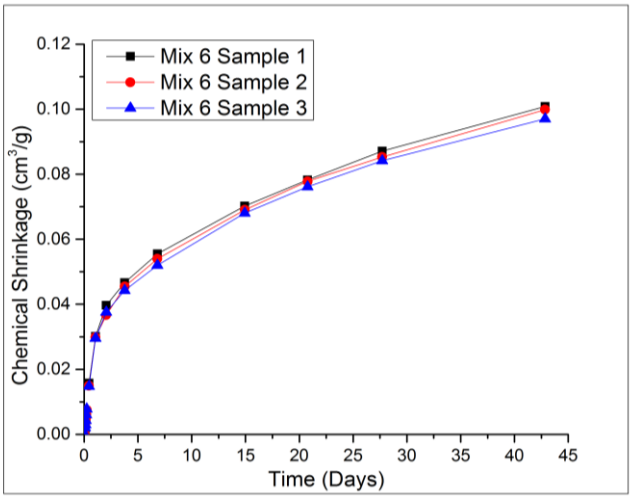

Figure A.6. Mix 6 chemical shrinkage results

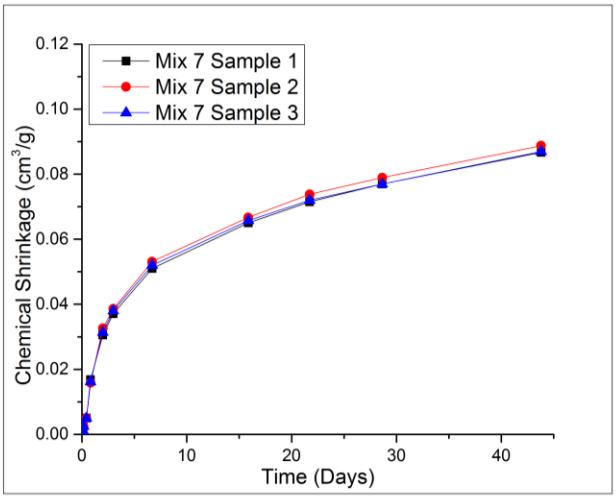

Figure A.7. Mix 7 chemical shrinkage results

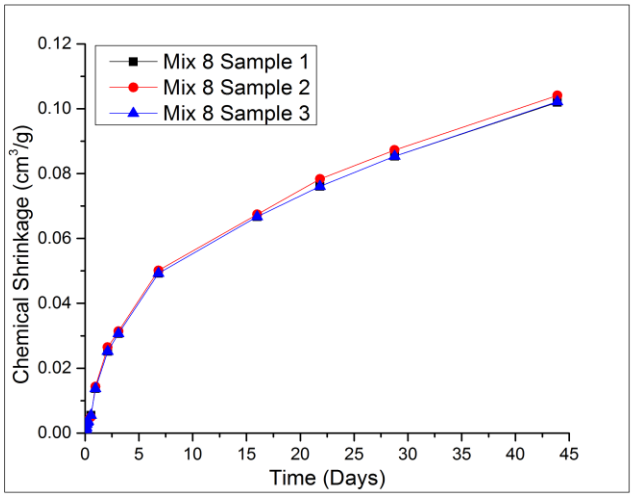

Figure A.8. Mix 8 chemical shrinkage results

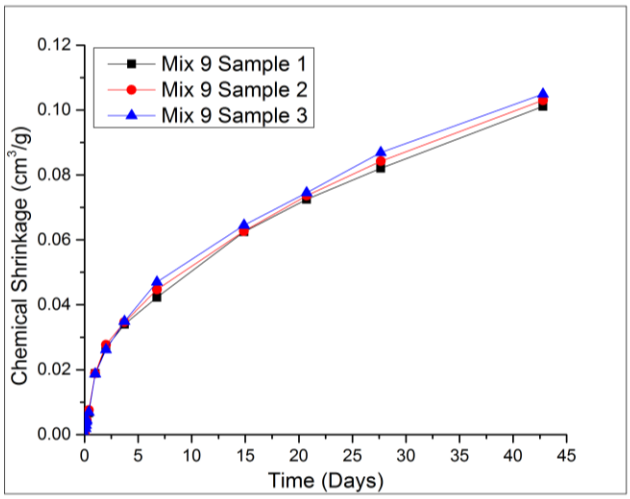

Figure A.9. Mix 9 chemical shrinkage results

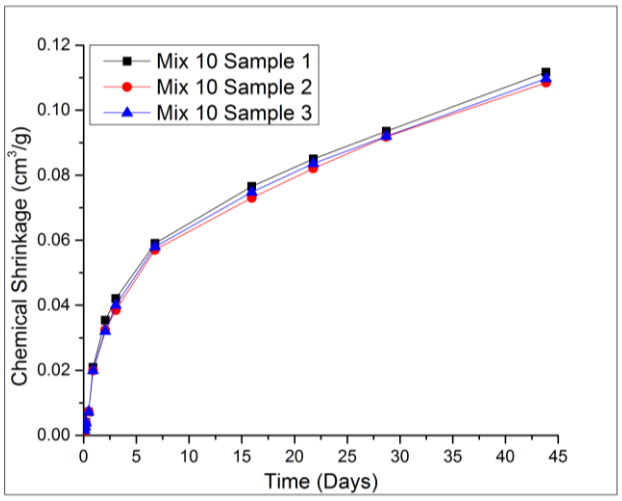

Figure A.10. Mix 10 chemical shrinkage results

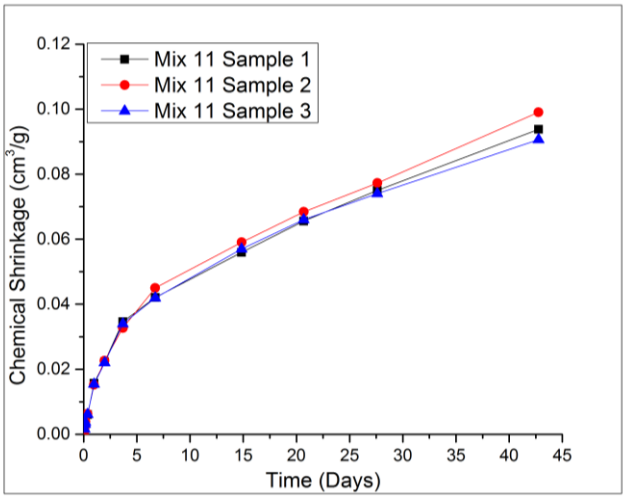

Figure A.11. Mix 11 chemical shrinkage results

A.2 Autogenous Shrinkage Test Results of Individual Specimens

A.2.1 Mortar

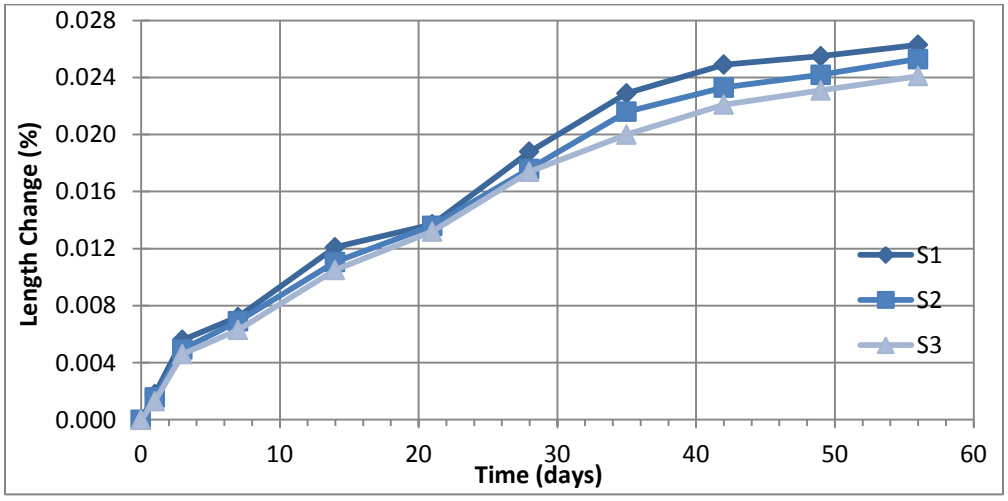

Figure A.12. Mix 1 autogenous shrinkage results

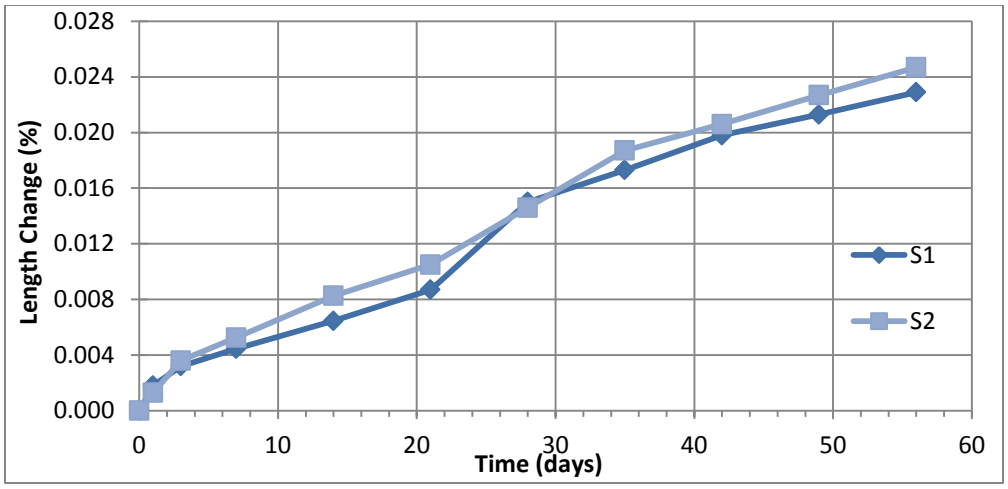

Figure A.13. Mix 2 autogenous shrinkage results

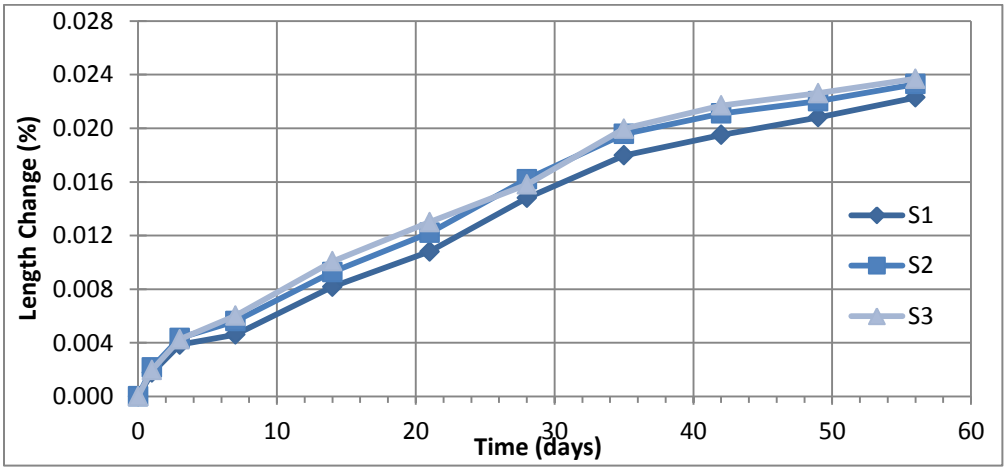

Figure A.14. Mix 3 autogenous shrinkage results

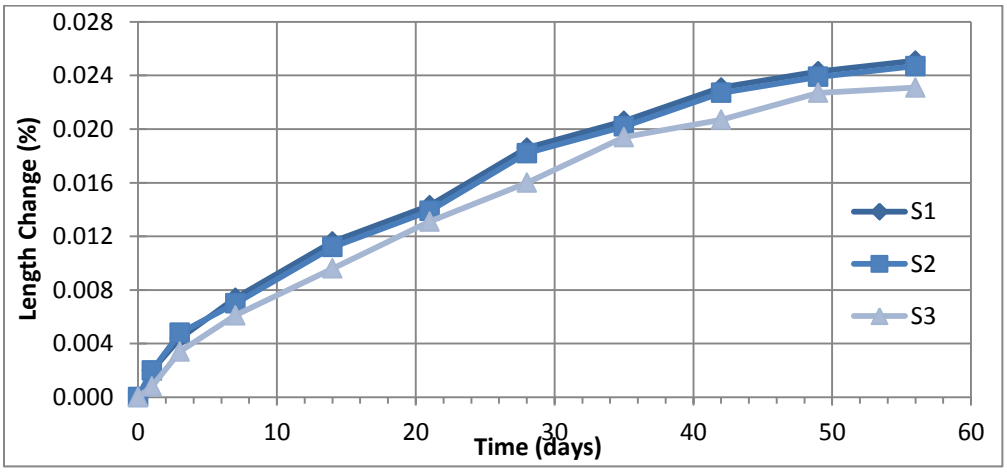

Figure A.15. Mix 4 autogenous shrinkage results

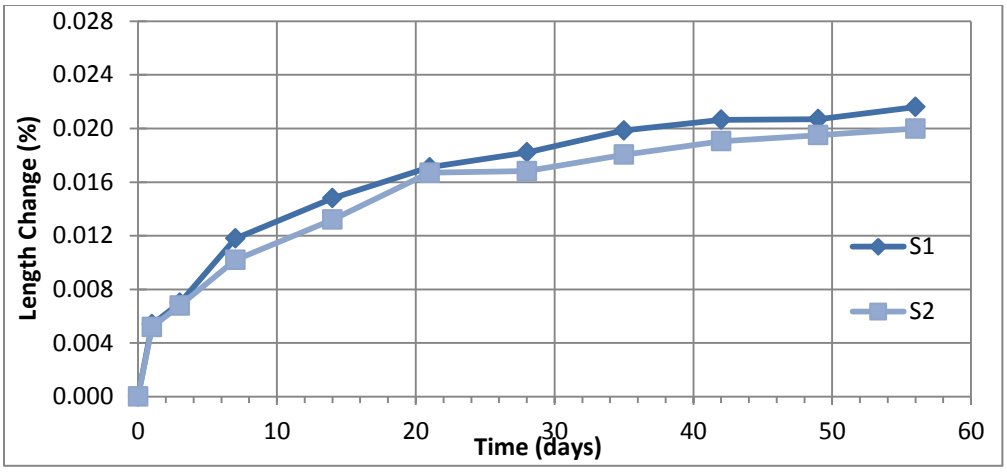

Figure A-16. Mix 5 autogenous shrinkage results

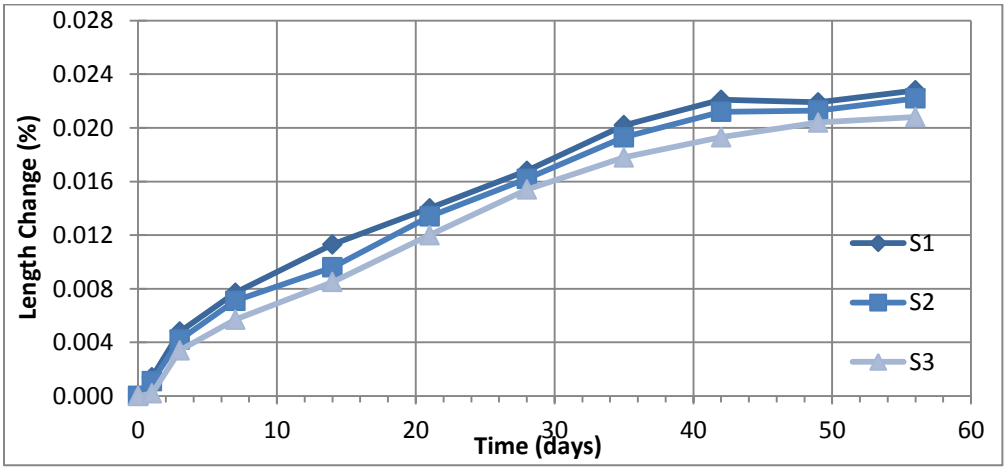

Figure A.17. Mix 6 autogenous shrinkage results

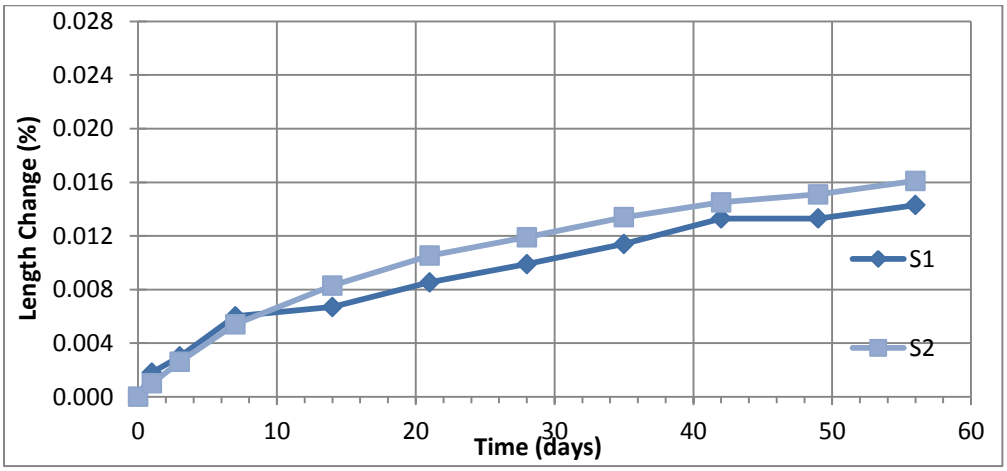

Figure A.18. Mix 7 autogenous shrinkage results

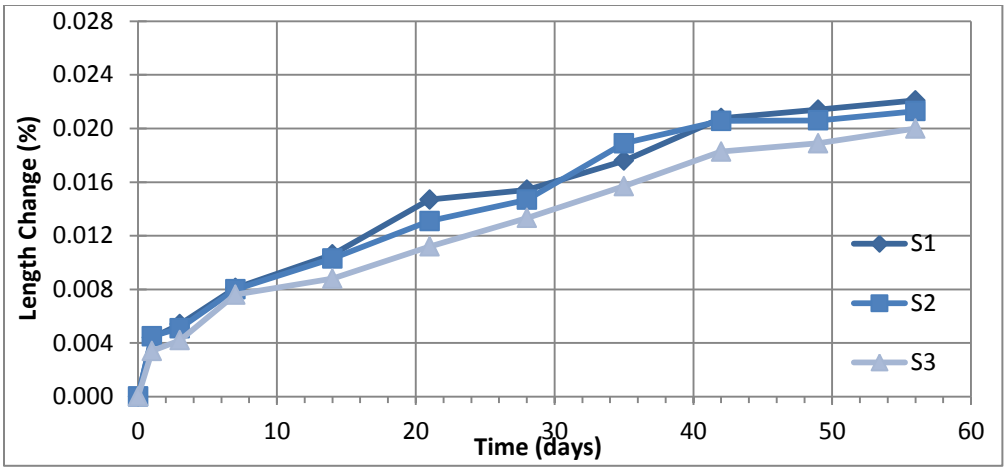

Figure A.19. Mix 8 autogenous shrinkage results

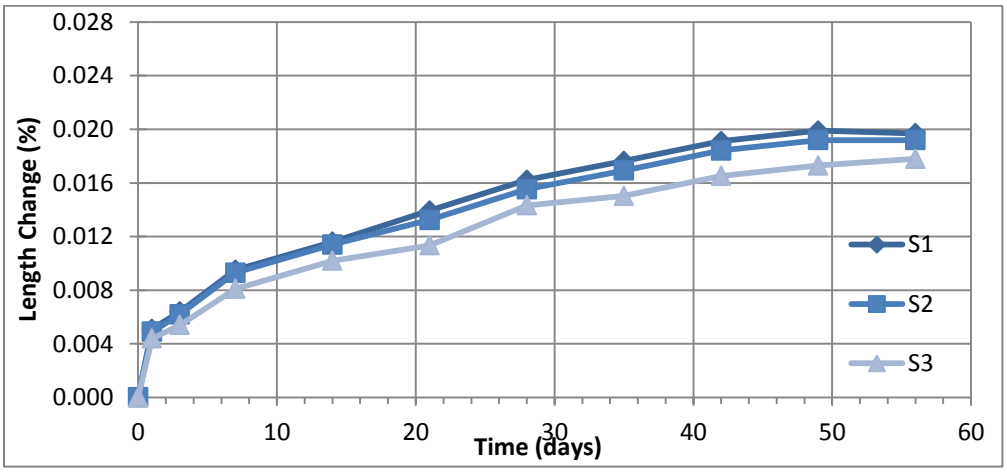

Figure A.20. Mix 9 autogenous shrinkage results

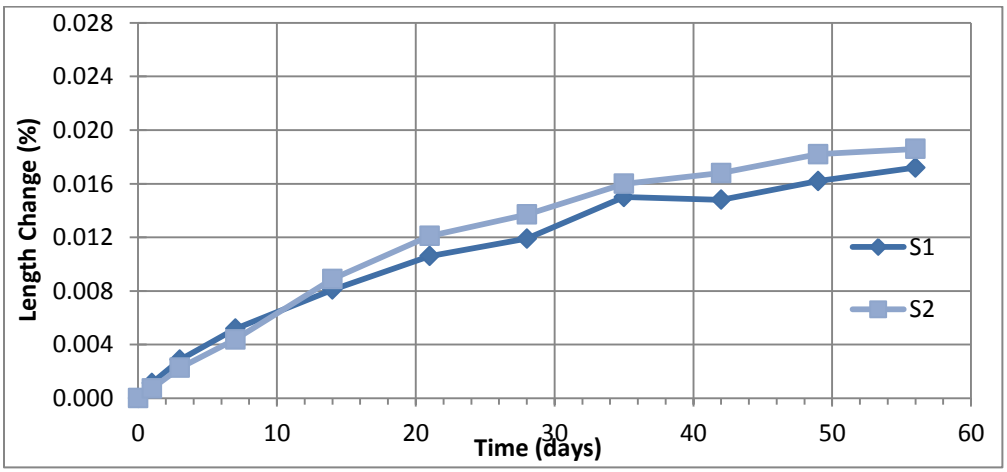

Figure A.21. Mix 10 autogenous shrinkage results

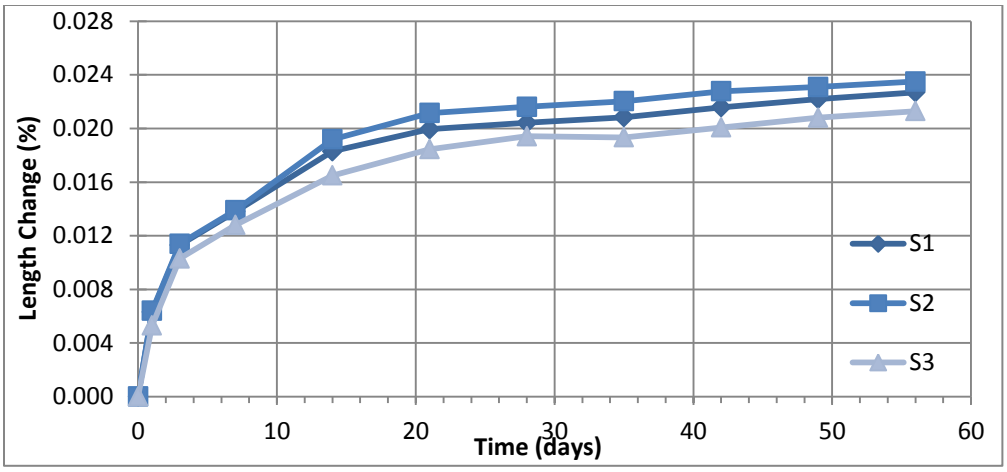

Figure A.22. Mix 11 autogenous shrinkage results

A.2.2 Concrete

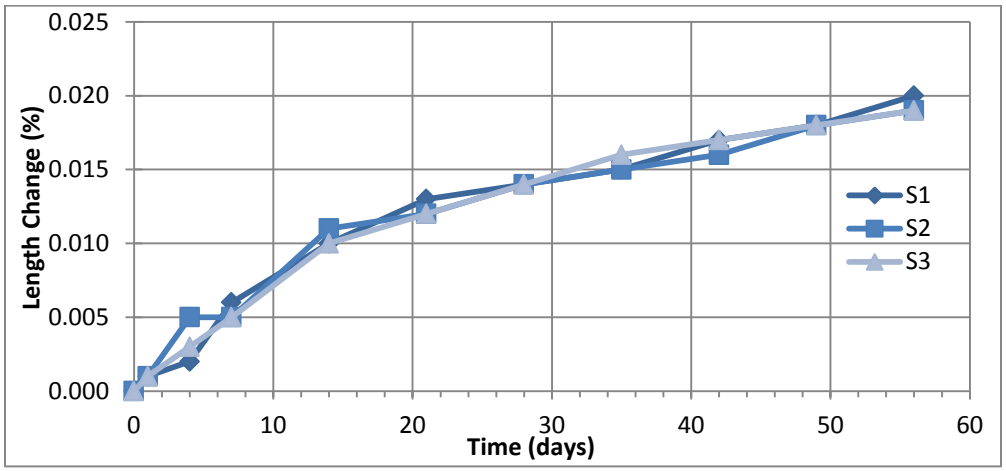

Figure A.23. Mix 1 autogenous shrinkage results

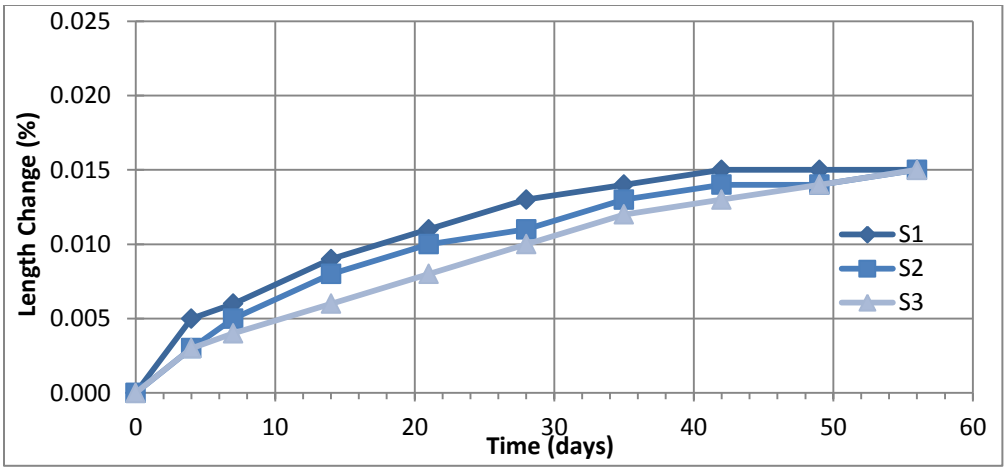

Figure A.24. Mix 2 autogenous shrinkage results

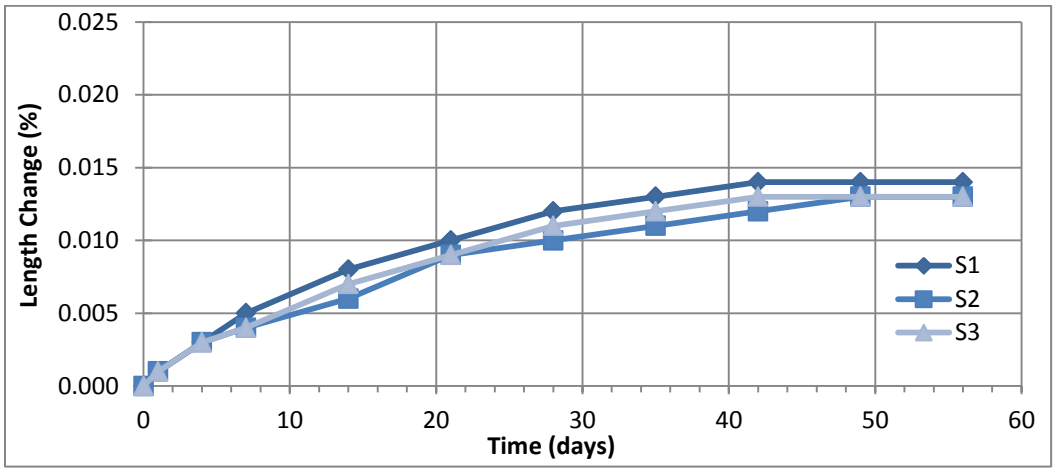

Figure A.25. Mix 3 autogenous shrinkage results

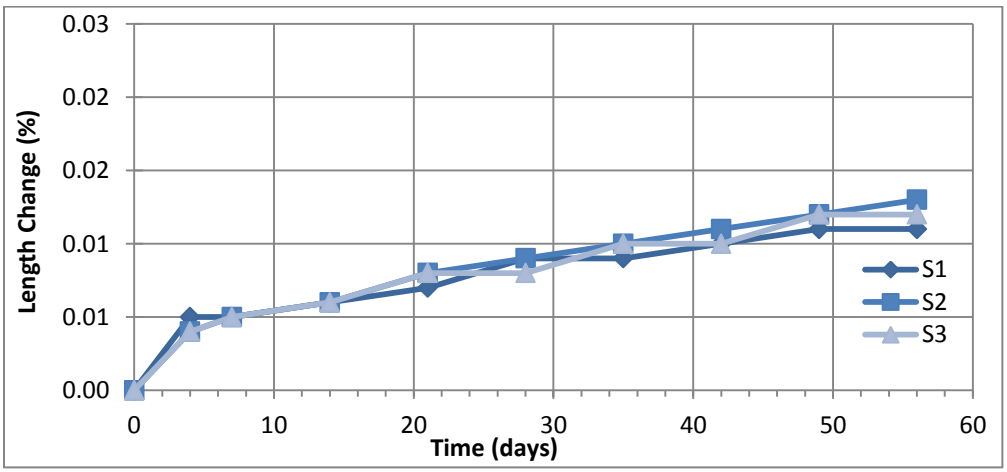

Figure A.26. Mix 4 autogenous shrinkage results

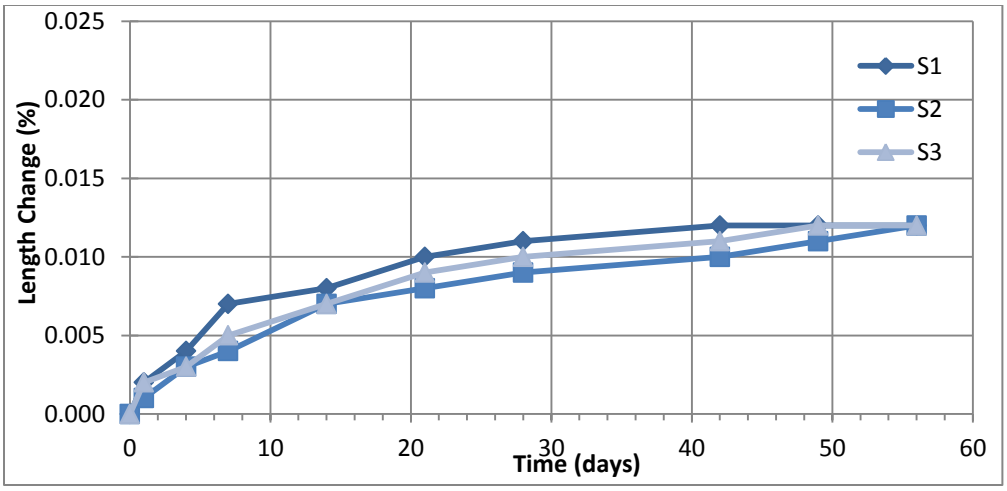

Figure A.27. Mix 5 autogenous shrinkage results

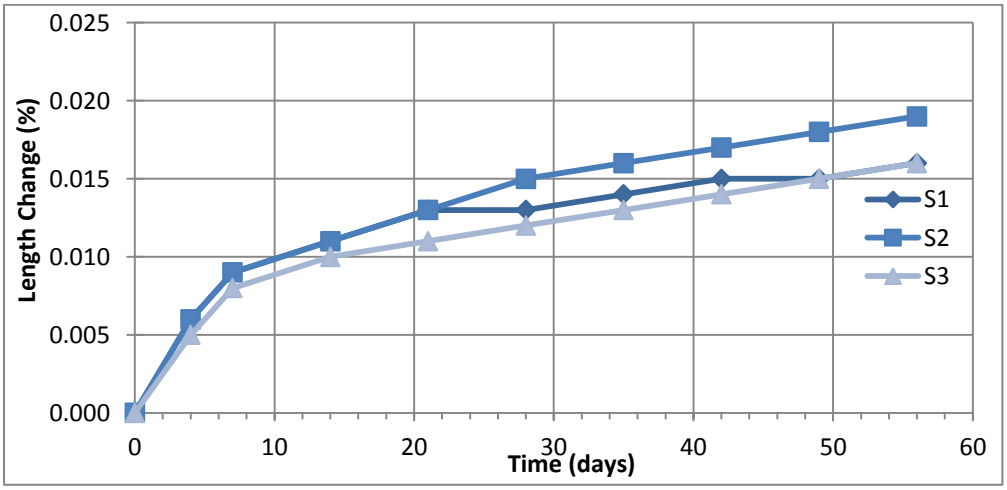

Figure A.28. Mix 6 autogenous shrinkage results

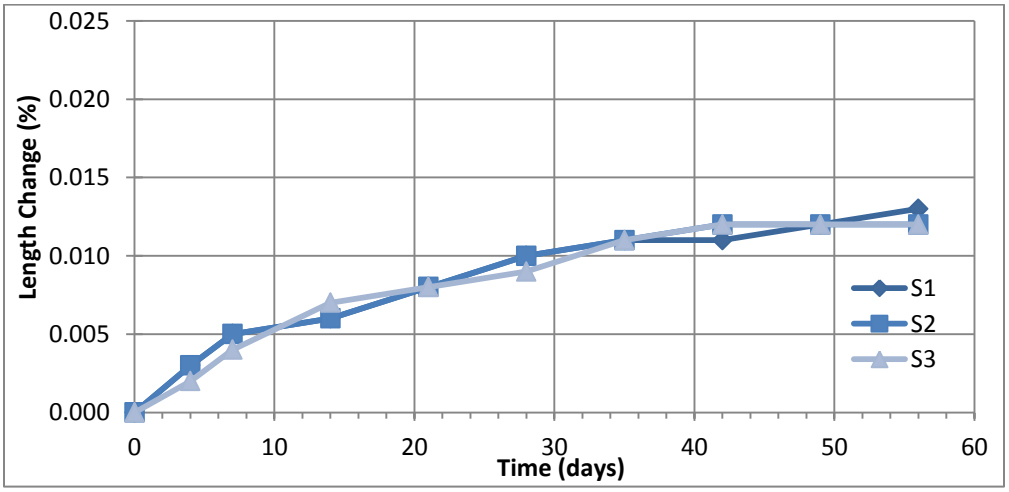

Figure A.29. Mix 7 autogenous shrinkage results

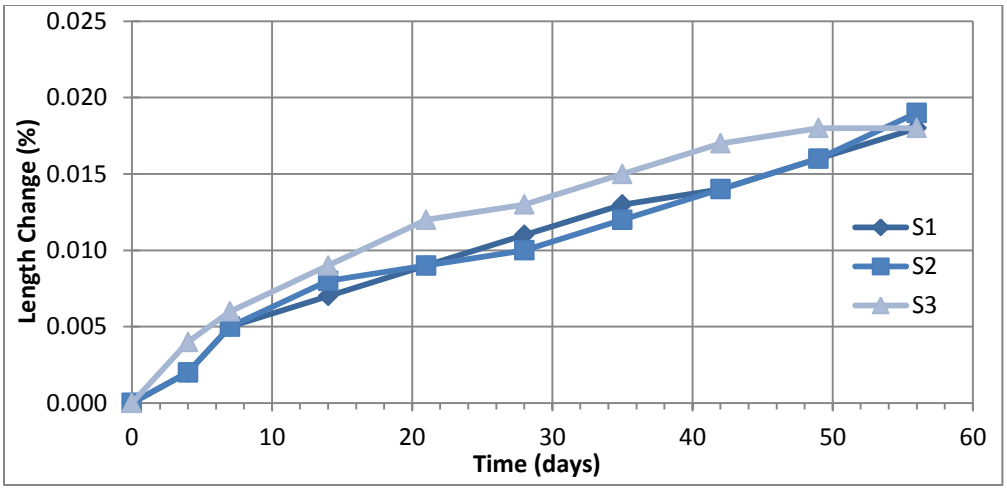

Figure A.30. Mix 8 autogenous shrinkage results

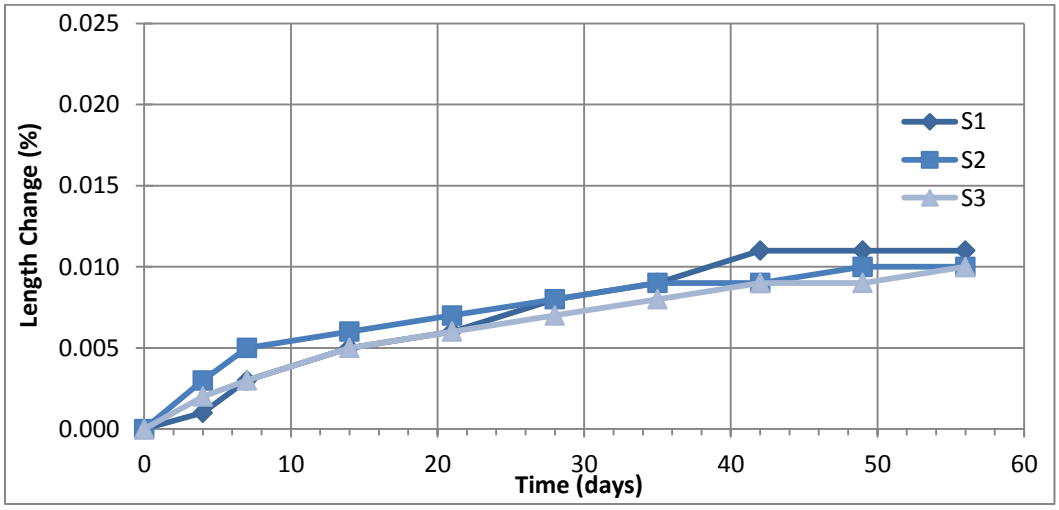

Figure A.31. Mix 9 autogenous shrinkage results

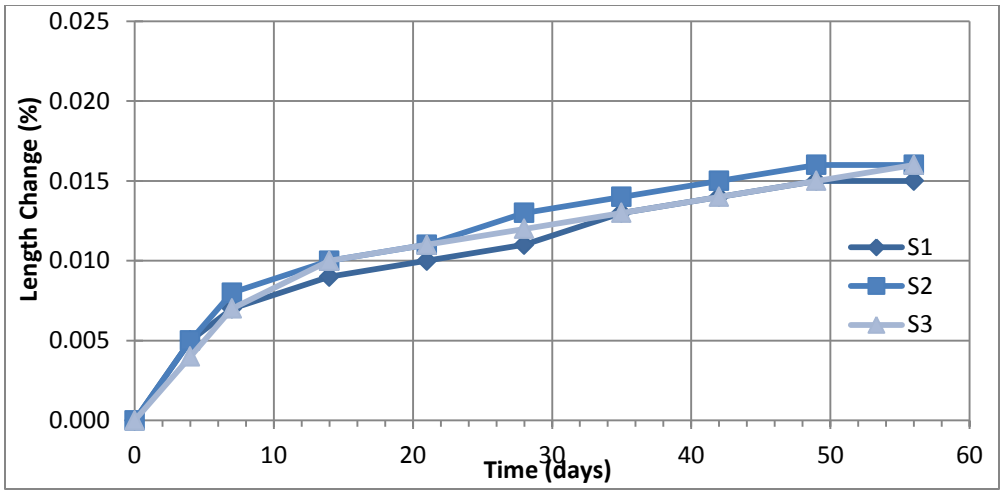

Figure A.32. Mix 10 autogenous shrinkage results

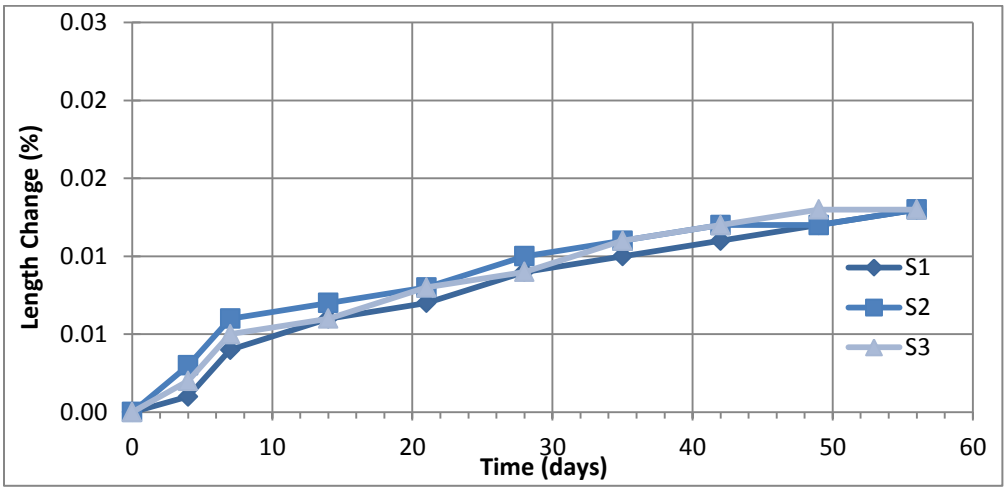

Figure A.33. Mix 11 autogenous shrinkage results

A.3 Free Shrinkage Test Results

A.3.1 Mortar

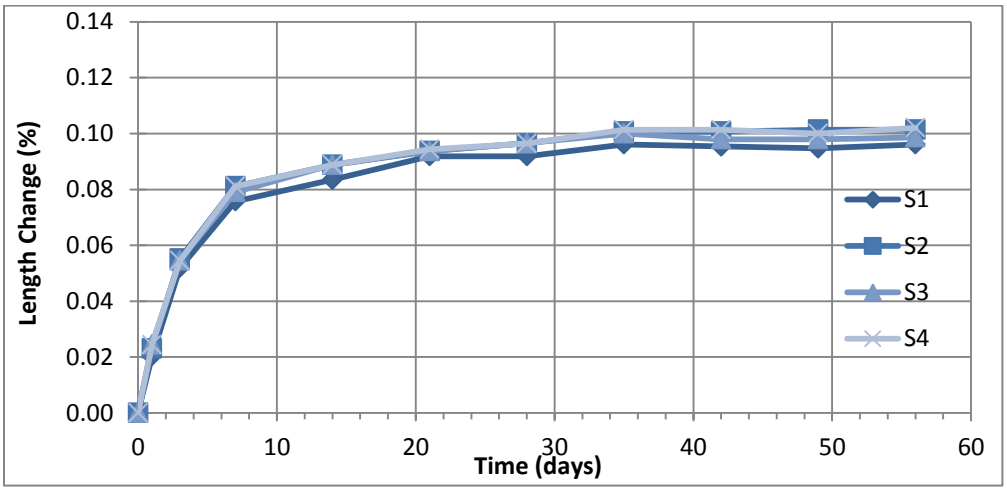

Figure A.34. Mix 1 free drying shrinkage results

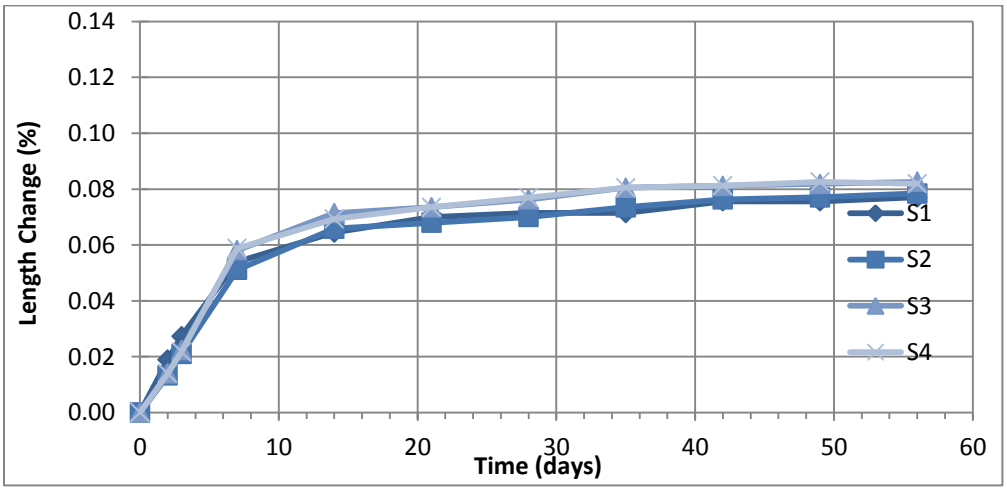

Figure A.35. Mix 2 free drying shrinkage results

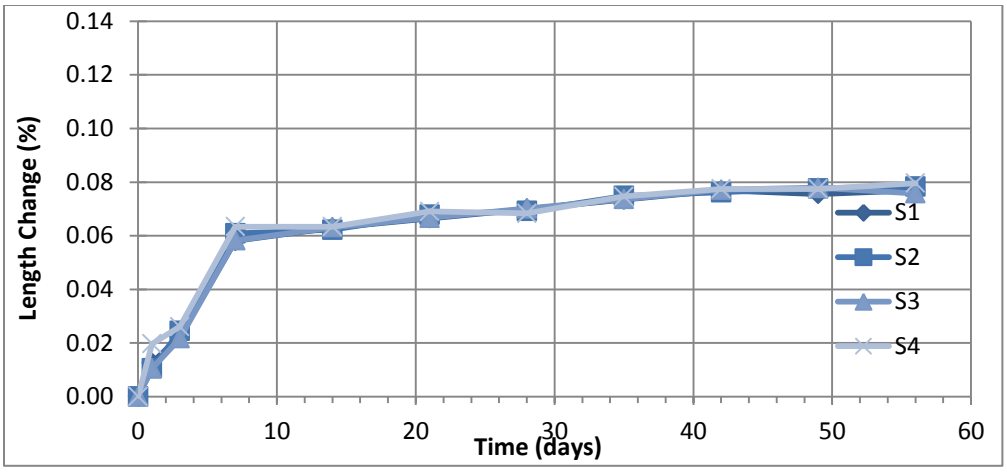

Figure A.36. Mix 3 free drying shrinkage results

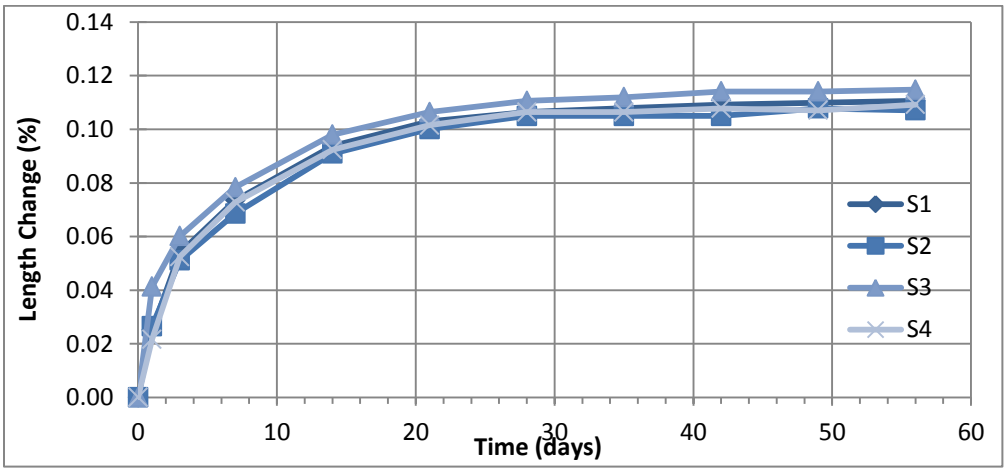

Figure A.37. Mix 4 free drying shrinkage results

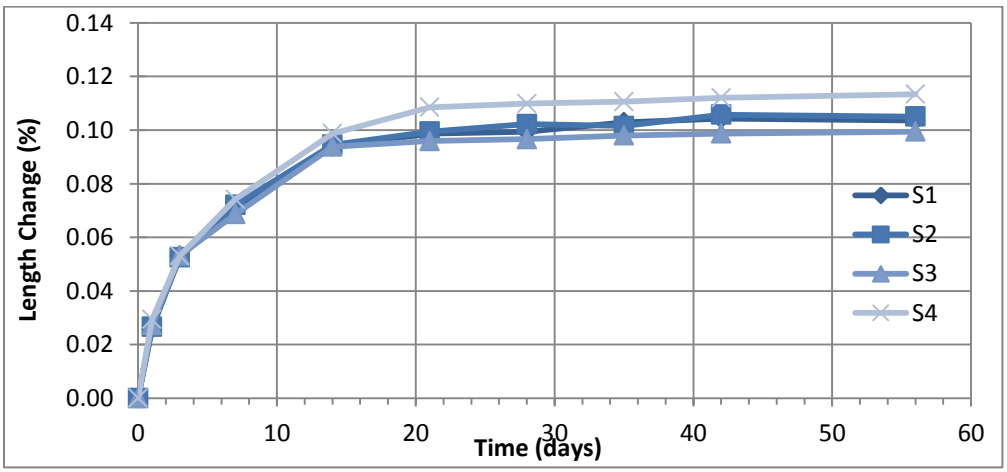

Figure A.38. Mix 5 free drying shrinkage results

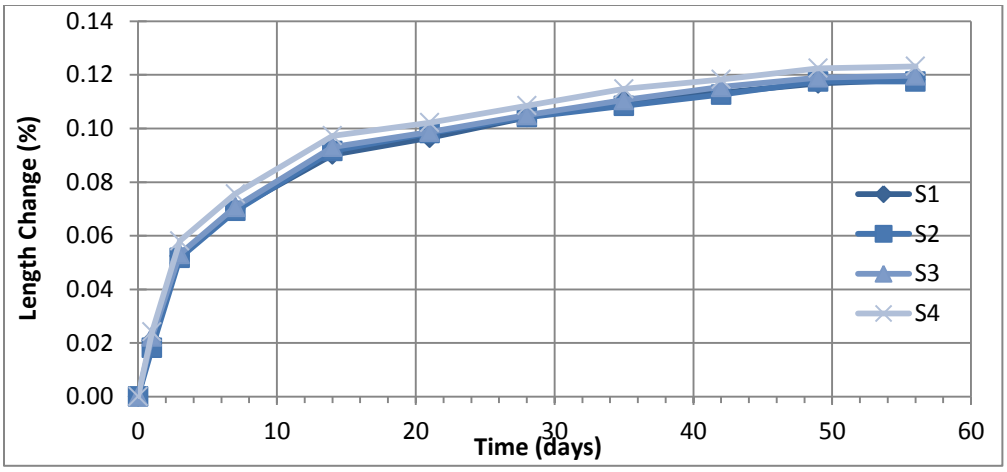

Figure A.39. Mix 6 free drying shrinkage results

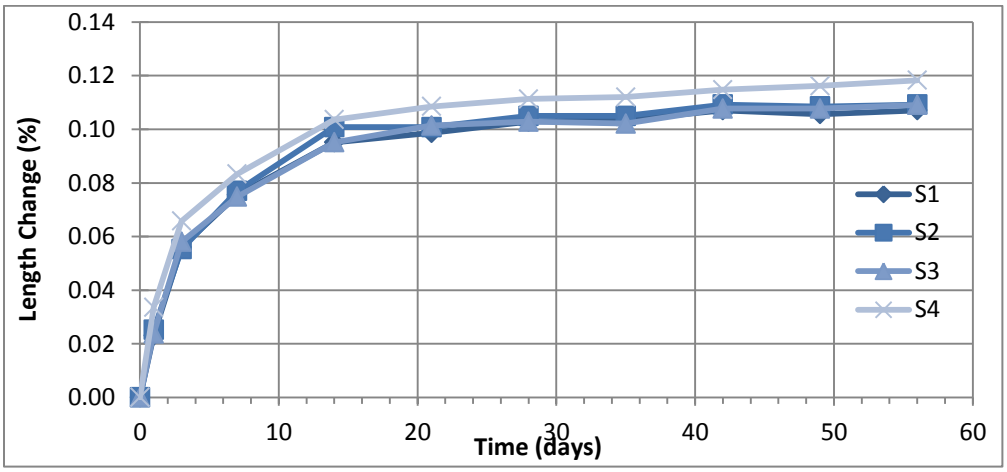

Figure A.40. Mix 7 free drying shrinkage results

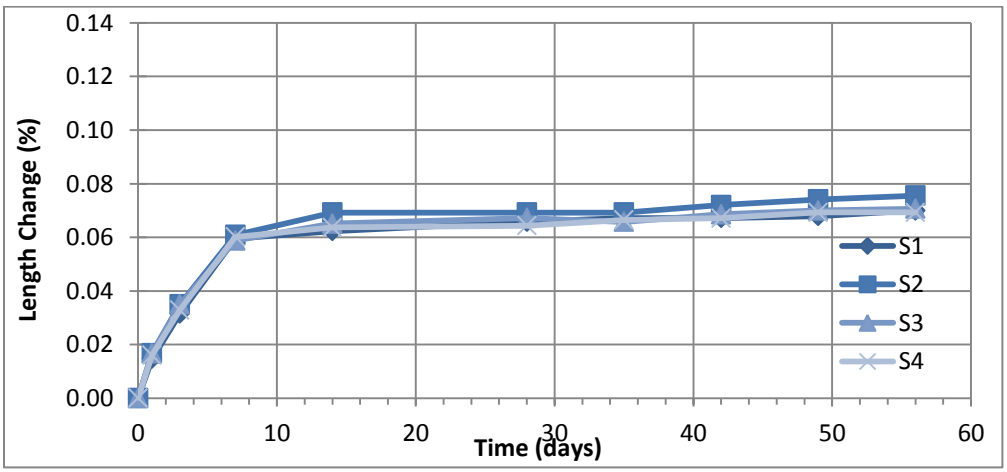

Figure A.41. Mix 8 free drying shrinkage results

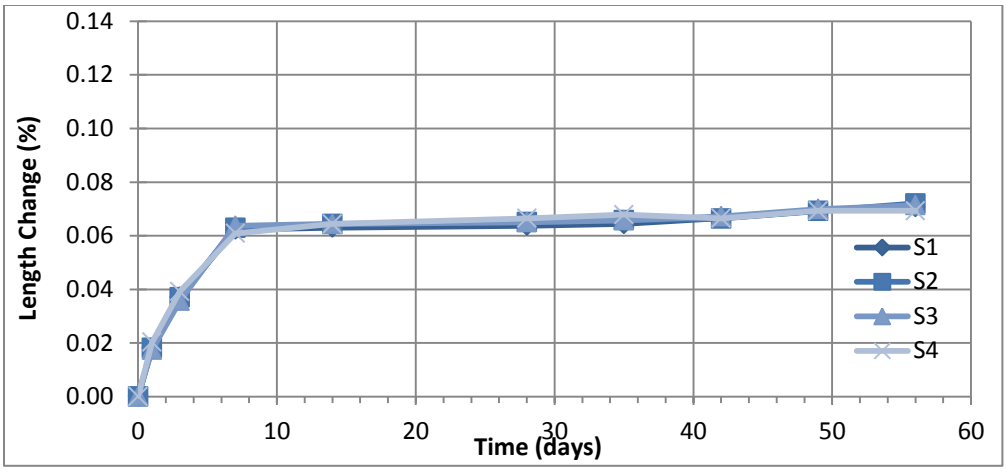

Figure A.42. Mix 9 free drying shrinkage results

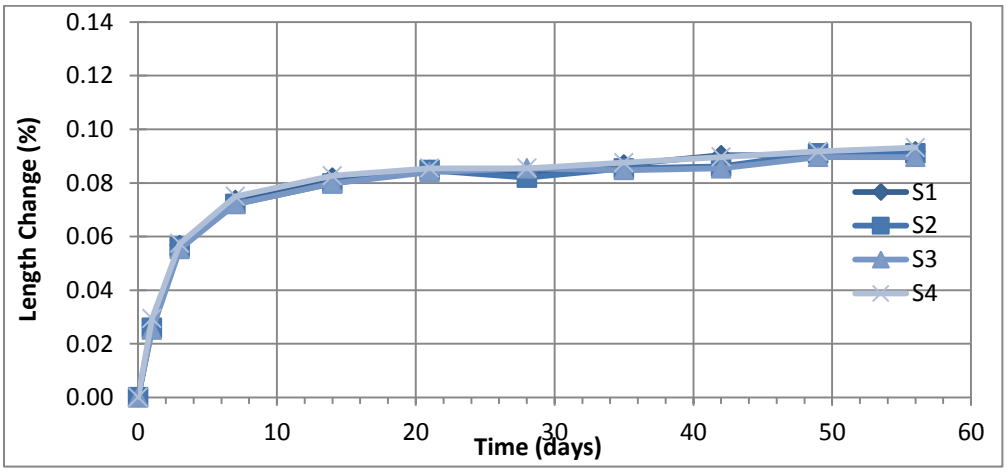

Figure A.43. Mix 10 free drying shrinkage results

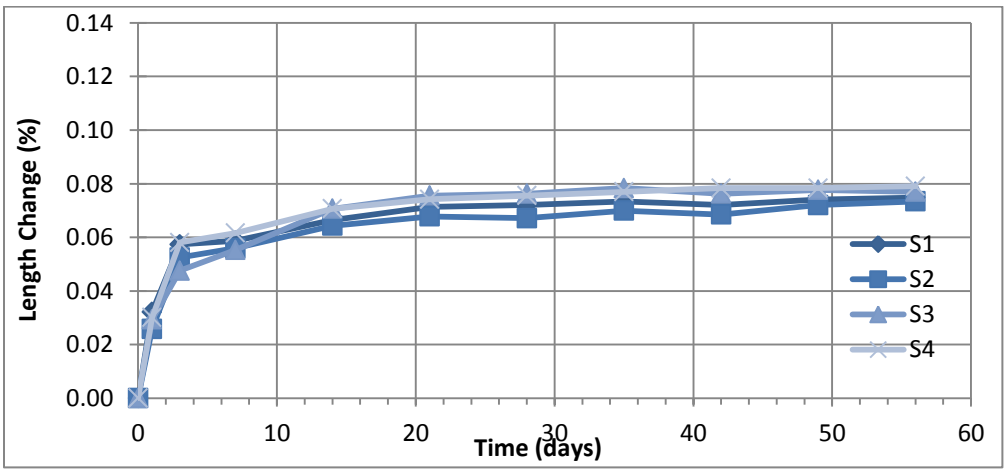

Figure A.44. Mix 11 free drying shrinkage results

A.3.2 Concrete

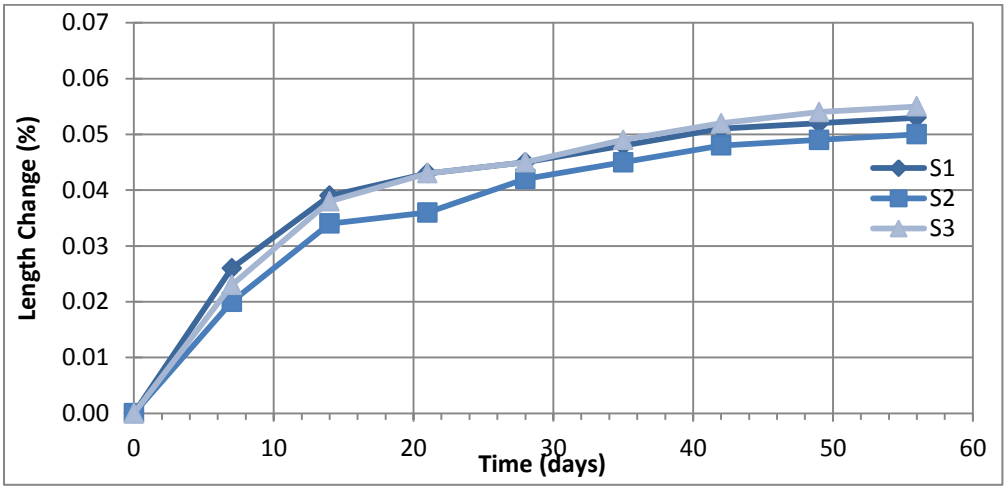

Figure A.45. Mix 1 free drying shrinkage results

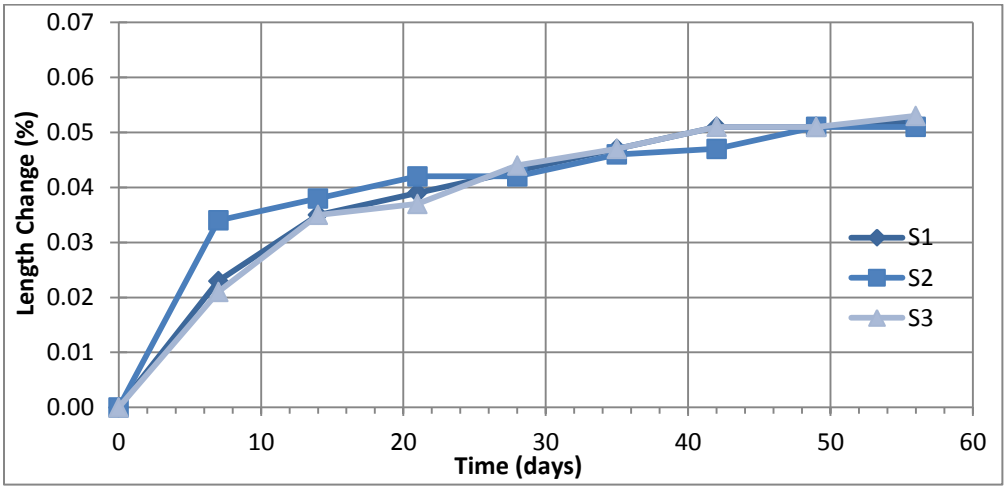

Figure A.46. Mix 2 free drying shrinkage results

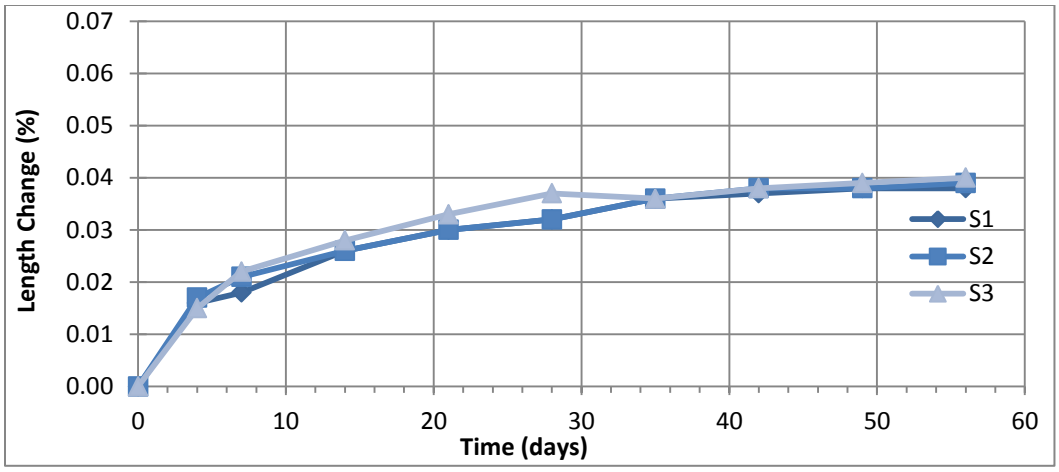

Figure A.47. Mix 3 free drying shrinkage results

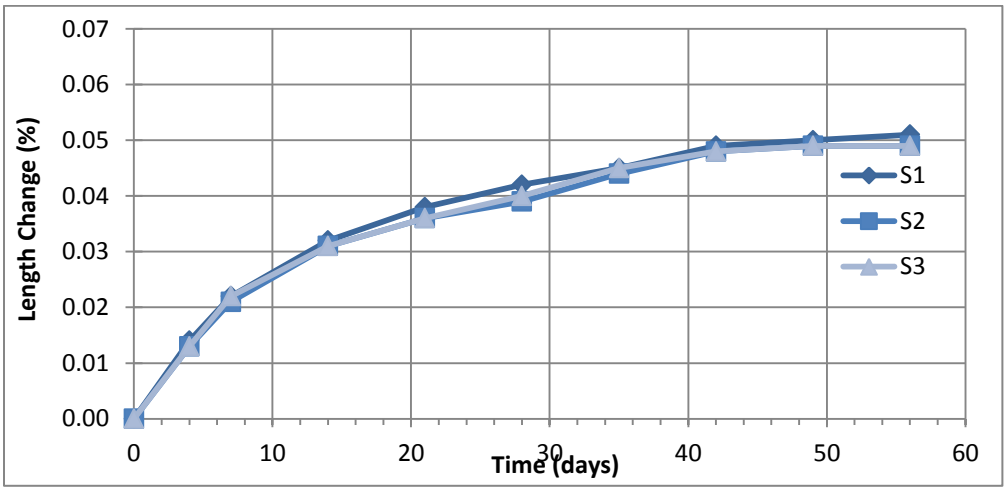

Figure A.48. Mix 4 free drying shrinkage results

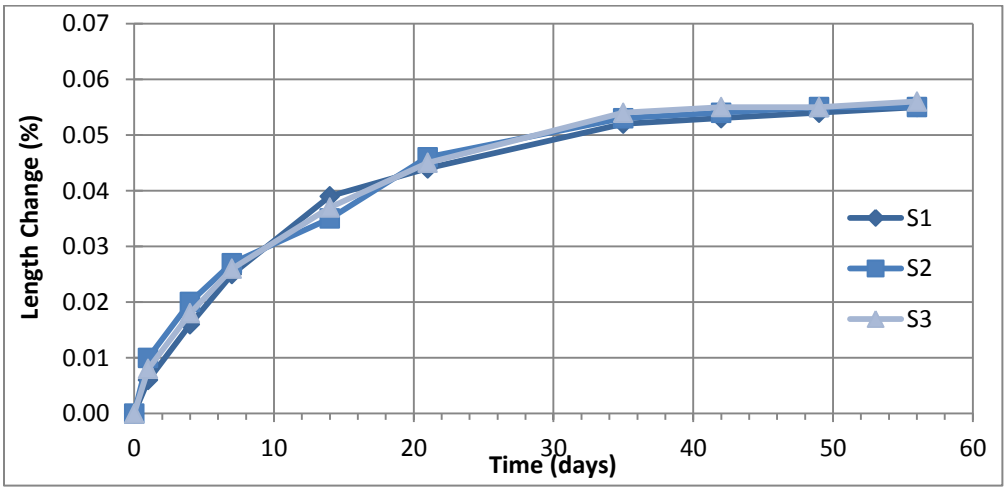

Figure A.49. Mix 5 free drying shrinkage results

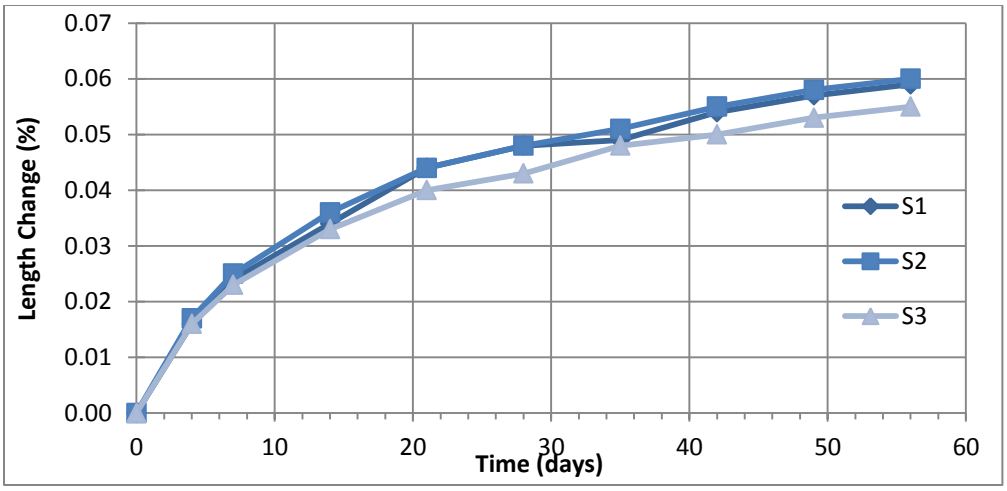

Figure A.50. Mix 6 free drying shrinkage results

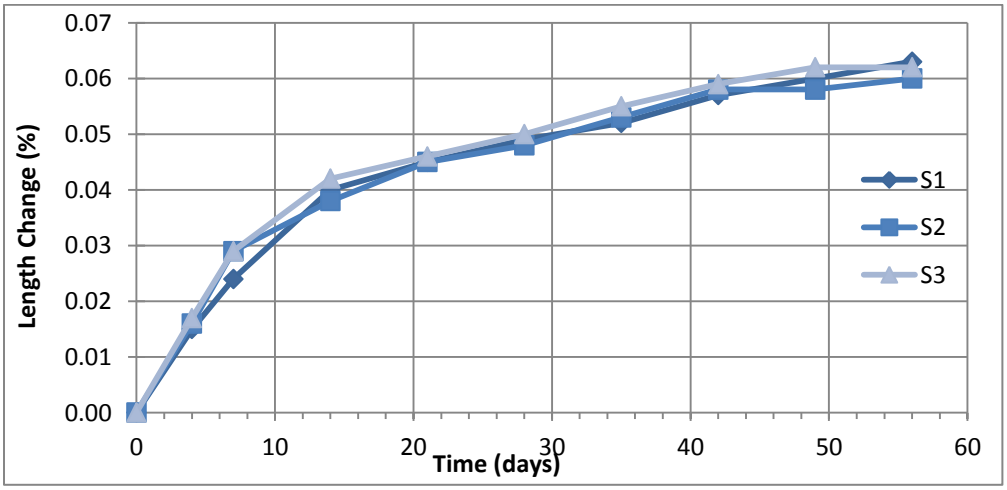

Figure A.51. Mix 7 free drying shrinkage results

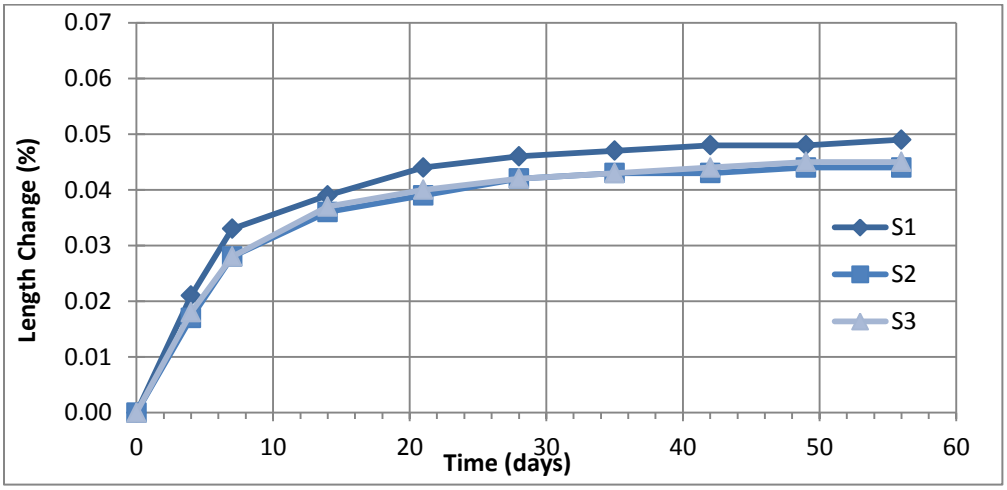

Figure A.52. Mix 8 free drying shrinkage results

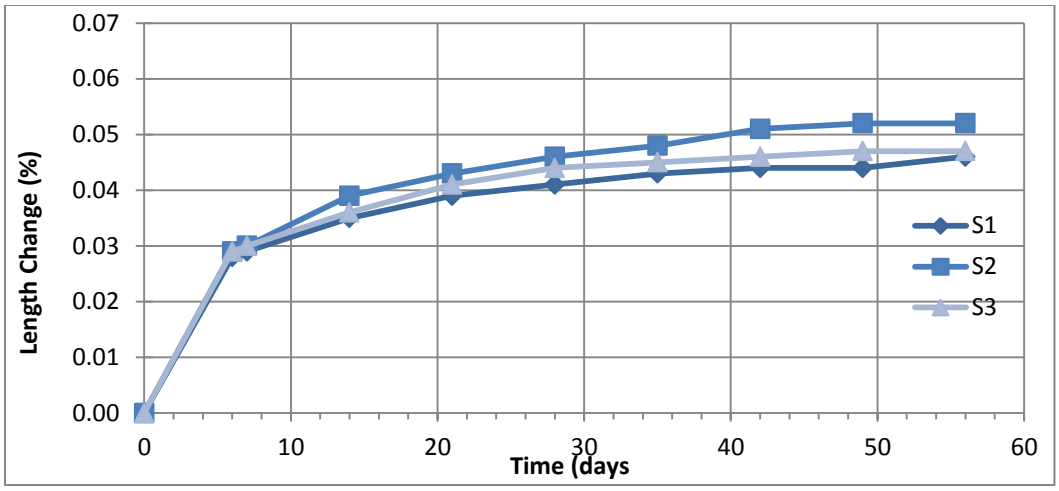

Figure A.53. Mix 9 free drying shrinkage results

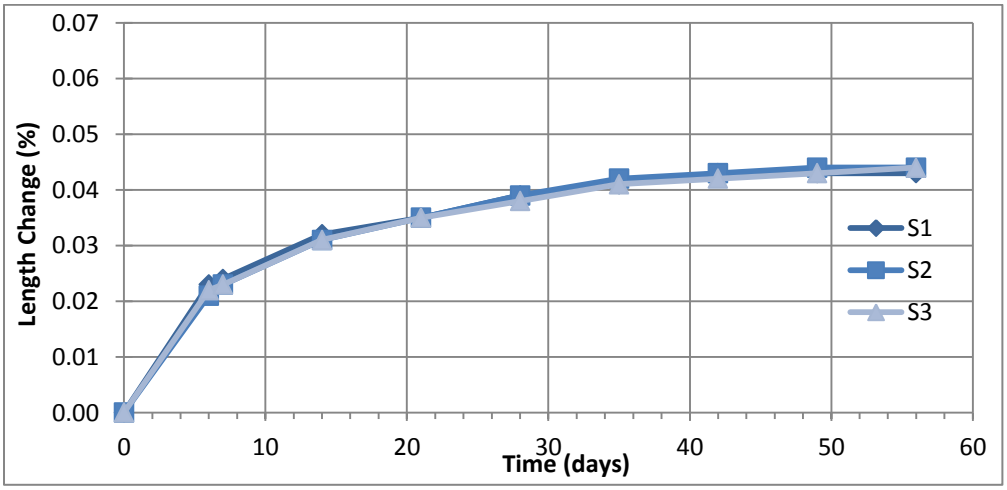

Figure A.54. Mix 10 free drying shrinkage results

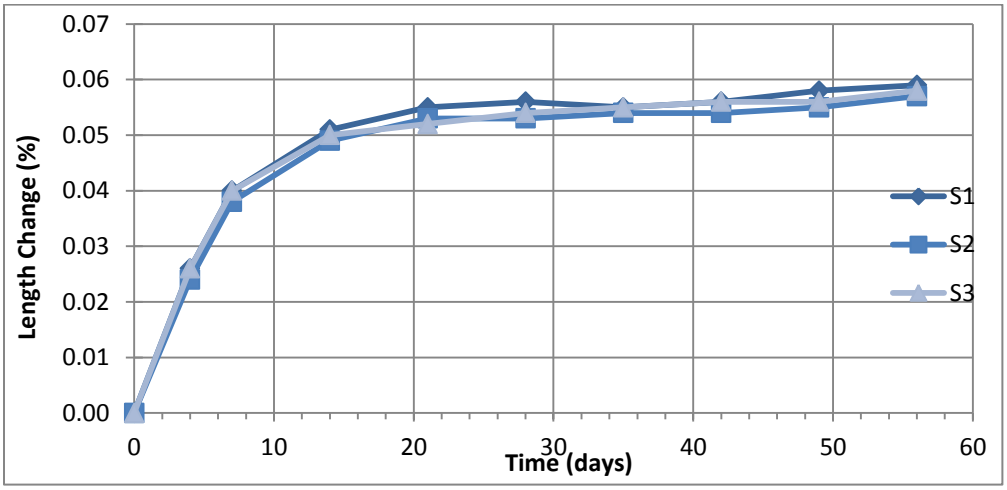

Figure A.55. Mix 11 free drying shrinkage results

A.4 Restrained Shrinkage Test Results

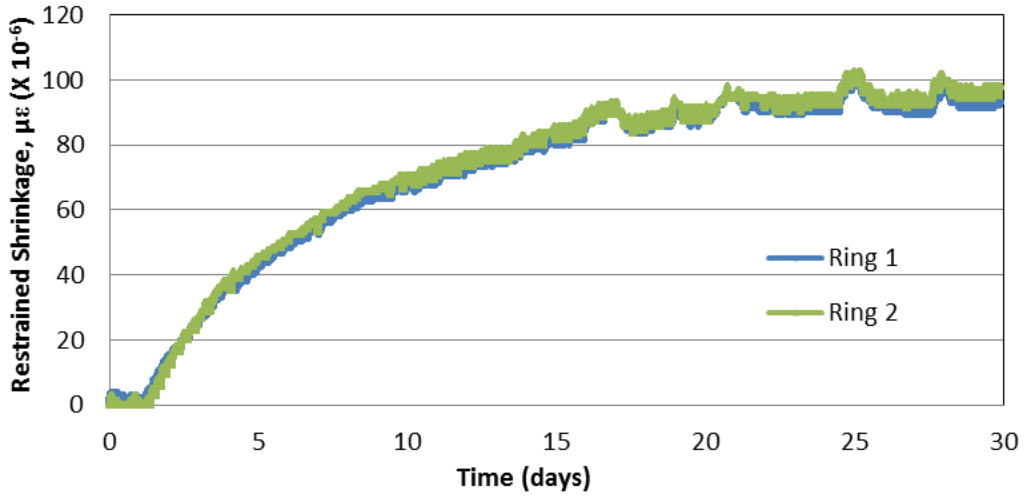

Figure A.56. Mix 1 restrained shrinkage results

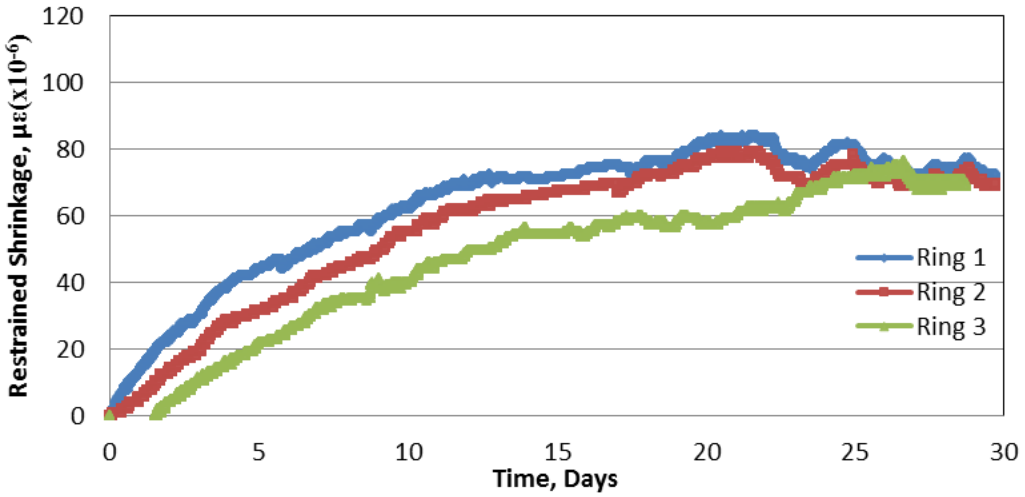

Figure A.57. Mix 2 restrained shrinkage results

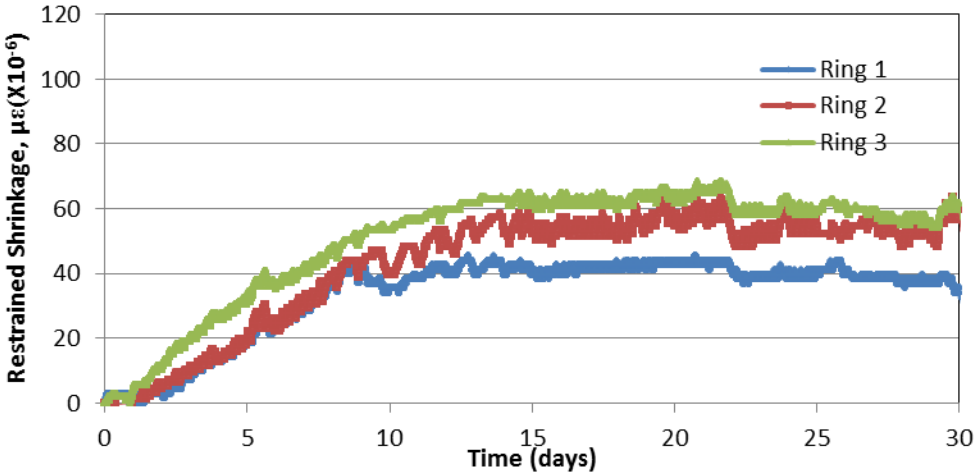

Figure A.58. Mix 3 restrained shrinkage results

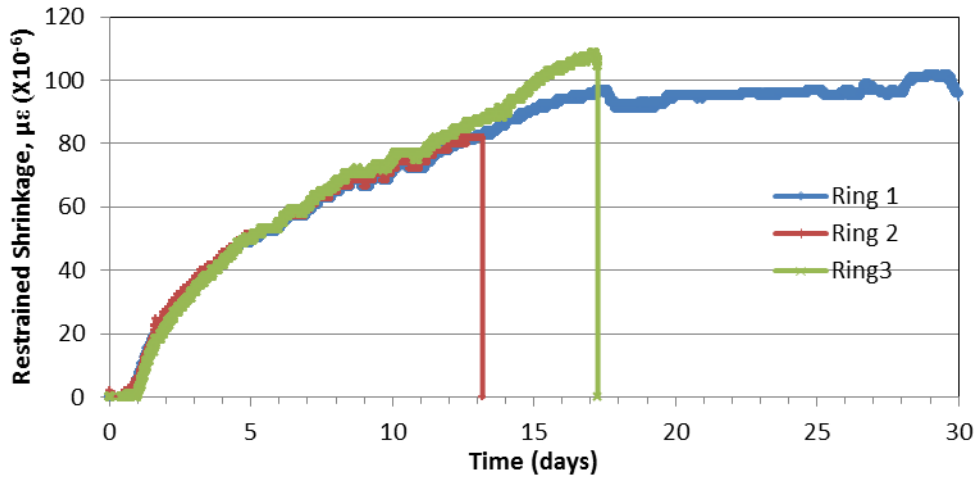

Figure A.59. Mix 4 restrained shrinkage result

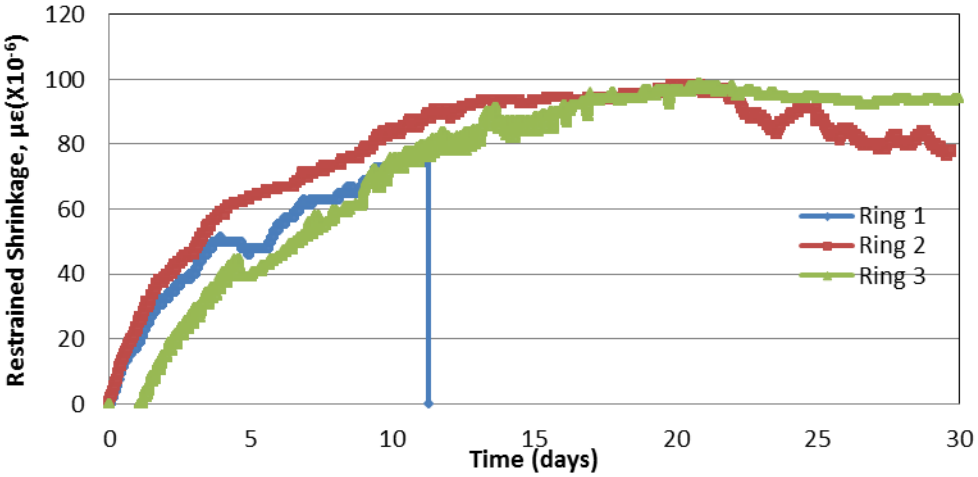

Figure A.60. Mix 5 restrained shrinkage results

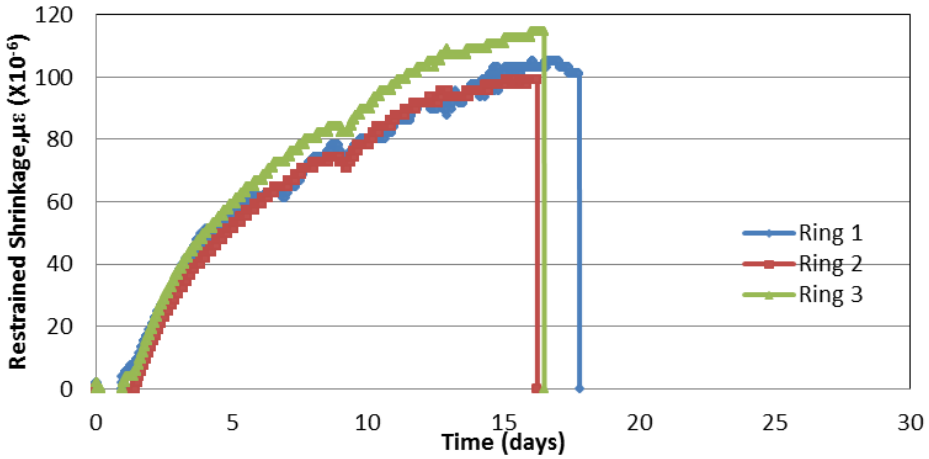

Figure A.61. Mix 6 restrained shrinkage results

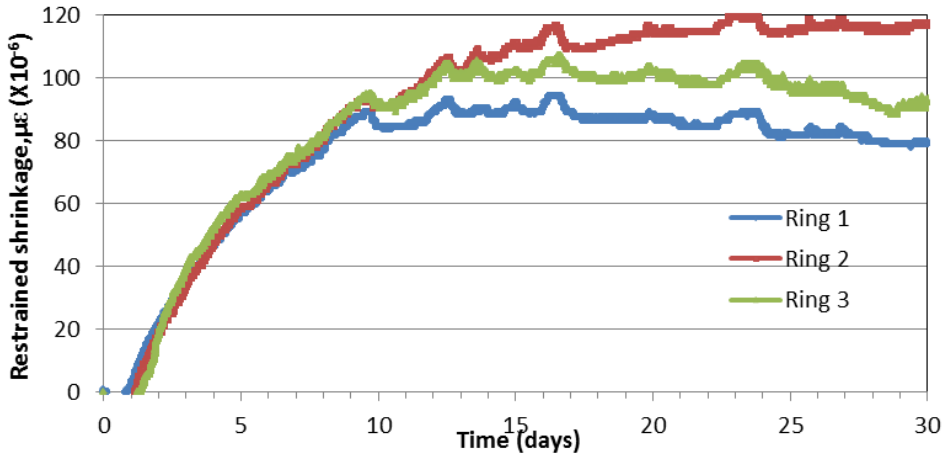

Figure A.62. Mix 7 restrained shrinkage results

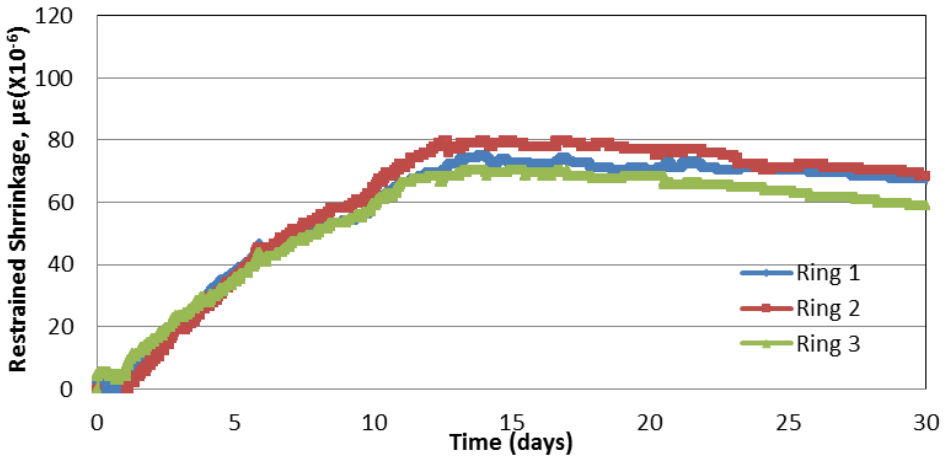

Figure A.63. Mix 8 restrained shrinkage results

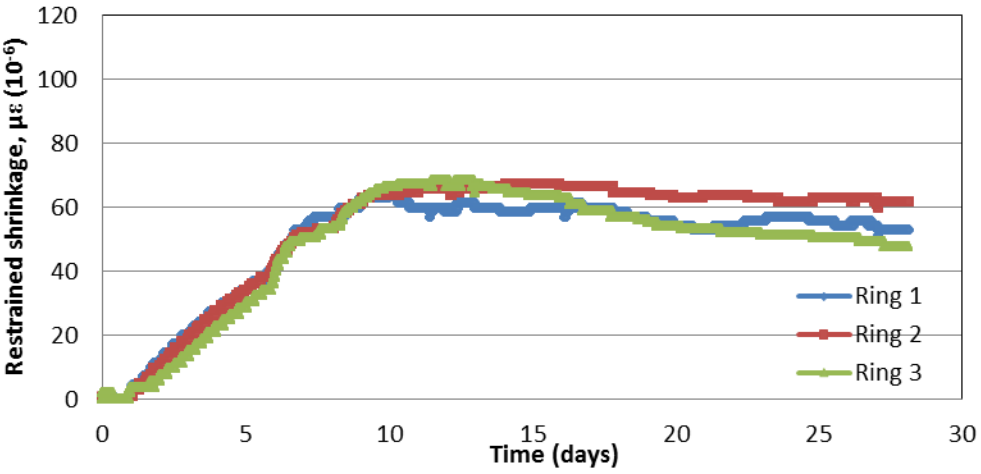

Figure A.64. Mix 9 restrained shrinkage results

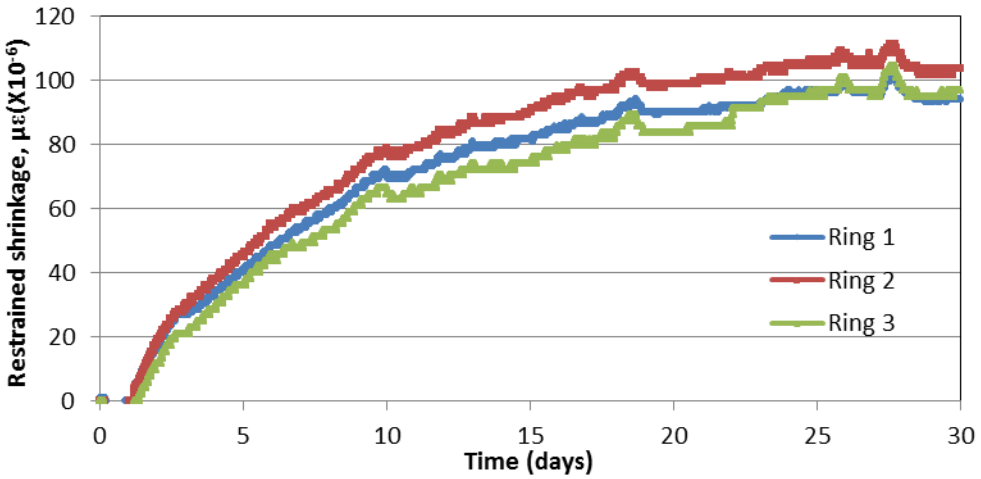

Figure A.65. Mix 10 restrained shrinkage results

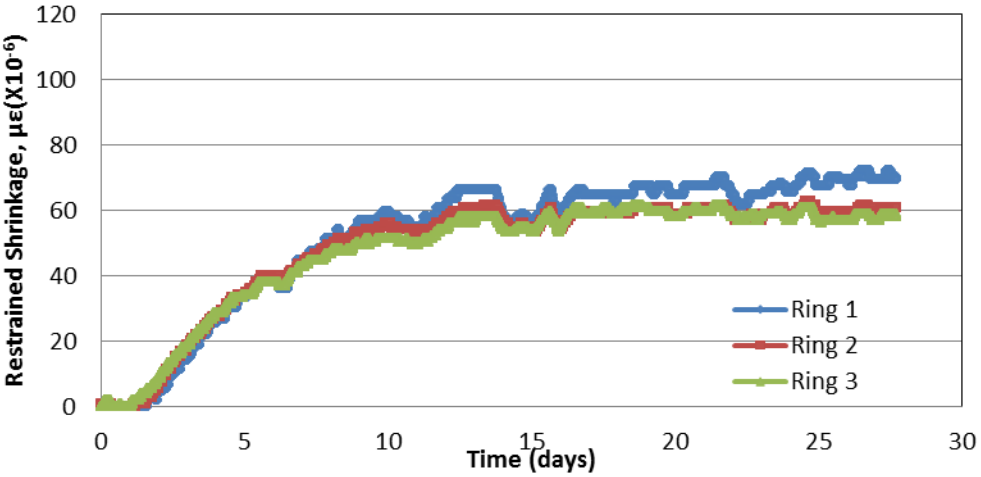

Figure A.66. Mix 11 restrained shrinkage results

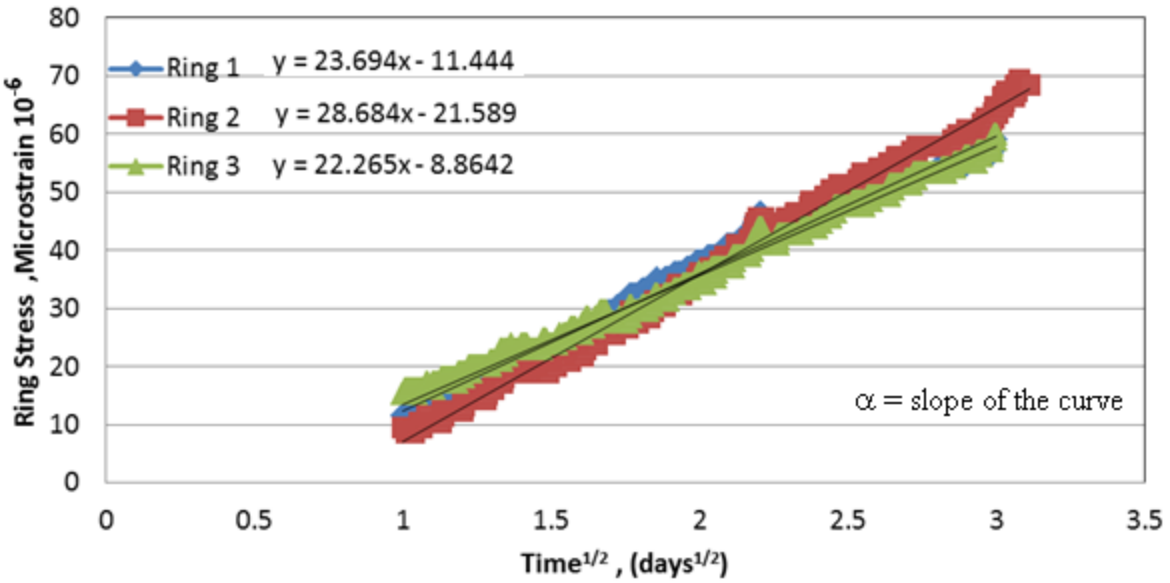

Figure A.67. Determination of strain rate (α) from restrained shrinkage test results (Mix 11)

A.5 Prediction Models for Creep

Creep is the increase in strain of a solid under a sustained stress with time. Creep strain includes two components: a basic creep and a drying creep. The basic creep, $C_{0,}$ is the creep occurring when there is no moisture exchange between the concrete and the ambient medium. Drying creep, $C_{d,}$ is the additional creep experienced when the concrete is allowed to dry while under sustained load. The sum of basic and drying creep is referred to as the total creep. The creep strain per unit of applied stress is defined as specific creep. The ratio between the creep strain (C) and the instantaneous or elastic strain due to the stress (q_1) is defined as creep coefficient (φ).

A.5.1 B3 Model

Among many models, the RILEM B3 model is considered in this study because of its simplicity and effectiveness (Bazant and Baweja 1995, 2000). The model is based on a systematic theoretical formulation of the basic physical phenomena involved, couples creep and shrinkage, and agrees better with the most test data that exist in the literature.

The B3 model is often applied for portland cement concrete with the following property range:

$$0.35 \leq w/c \leq 0.85,\ 2.5 \leq a/c \leq 13.5 \qquad \textbf{(A-1)}$$

$$2{,}500 \text{ psi} \leq f_c \leq 10{,}000 \text{ psi},\ 10 \text{ lb/ft}^3 \leq c \leq 45 \text{ lb/ft}^3 \qquad \textbf{(A-2)}$$

where: w is water content in lb/ft^3, c is cement content in lb/ft^3, a is total aggregate content in lb/ft^3, and f_c is the 28 day compressive strength of concrete in psi or MPa.

The model gives the compliance function for strain (creep and elastic strain) at time t due to a unit uniaxial constant stress applied at the age of t' as follows:

$$J(t,t') = q_1 + C_0(t,t') + C_d(t,t',t_0) \quad \textbf{(A-3)}$$

where: q_1 is the instantaneous or elastic strain due to the stress; $C_0(t,t')$ is basic creep (no moisture movement); and $C_d(t,t''t_0)$ is drying creep.

Creep coefficient $\varphi(t,t')$ calculated from the compliance function:

$$\varphi(t,t') = E(t')\, J(t,t') - 1 \quad \textbf{(A-4)}$$

where: $E(t')$ is the static modulus of elasticity at load age of t'.

The calculation of the basic creep derived from the time rate of basic creep. The derived equation for normal concrete is as follows.

$$C_0 = q_2\, Q(t,t') + q_3 \ln[1 + (t - t')^n] + q_4 \ln(t/t') \quad \textbf{(A-5)}$$

where: $Q(t, t')$ is a given in Table A.1, where n=0.1, q_2, q_3 and q_4 are empirical constitutive parameters. The parameters q_2, q_3 and q_4 represent aging viscoelastic compliance, non-aging viscoelastic compliance and flow compliance respectively.

$$q_1 = 0.6 \times 10^6/E_{28},\ E_{28} = 57000\sqrt{f_c}\ (\text{fc psi}) \quad \textbf{(A-6)}$$

$$q_2 = 451.1c^{0.5}f_c^{-0.9},\ q_3 = 0.29\ (w/c)^4 q_2,\ q_4 = 0.14(a/c)^{-0.7} \quad \textbf{(A-7)}$$

Table A.1. Values of function Q(t,t') for m = 0.5 and n = 0.1

	log t'								
log (t-t')	0.0	0.5	1.0	1.5	2.0	2.5	3.0	3.5	4.0
-2.0	0.4890	0.2750	0.1547	0.08677	0.04892	0.02751	0.01547	0.008699	0.004892
-1.5	0.5347	0.3009	0.1693	0.09519	0.05353	0.03010	0.01693	0.009519	0.005353
-1.0	0.5586	0.3284	0.1848	0.1040	0.05846	0.03288	0.01849	0.01040	0.005846
-0.5	0.6309	0.3571	0.2013	0.1133	0.06372	0.03583	0.02015	0.01133	0.006372
0.0	0.6754	0.3860	0.2185	0.1231	0.06929	0.03897	0.02192	0.01233	0.006931
0.5	0.7108	0.4125	0.2357	0.1334	0.07516	0.04229	0.02379	0.01338	0.007524
1.0	0.7352	0.4335	0.2514	0.1436	0.08123	0.04578	0.02576	0.01449	0.008149
1.5	0.7505	0.4480	0.2638	0.1529	0.08727	0.04397	0.02782	0.01566	0.008806
2.0	0.7597	0.4570	0.2724	0.1602	0.09276	0.05239	0.02994	0.01687	0.009494
2.5	0.7652	0.4624	0.2777	0.1652	0.09708	0.05616	0.03284	0.01812	0.01021
3.0	0.7684	0.4656	0.2808	0.1683	0.1000	0.05869	0.03393	0.01935	0.01094
3.5	0.7703	0.4675	0.2827	0.1702	0.1018	0.06041	0.03541	0.02045	0.01166
4.0	0.7714	0.4686	0.2838	0.1713	0.1029	0.06147	0.03641	0.02131	0.01230
4.5	0.7720	0.4692	0.2844	0.1719	0.1036	0.06210	0.03702	0.02190	0.01280
5.0	0.7724	0.4696	0.2848	0.1723	0.1038	0.06247	0.03739	0.02225	0.01314

Shrinkage:

$$\varepsilon_{s\infty} = -\alpha_1 \cdot \alpha_2 \cdot [26w^{2.1} f_c^{-0.28} + 270] \text{ (in } 10^{-6}) \quad \textbf{(A-8)}$$

$$k_t = 190.8 t_0^{-0.08} \cdot f_c^{-1/4} \text{ days/in}^2 \quad \textbf{(A-9)}$$

where: α_1 is 1.0 for Type I cement, 0.85 for Type II cement and 1.1 for Type III cement, α_2 is 0.75 for steam curing, 1.2 for sealed or normal curing in air with protection against drying 1.0 for curing in water or at 100% relative humidity.

$$q_5 = 7.57 \times 10^5 f_c^{-1} |\varepsilon_{sh\infty}|^{-0.6} \quad \textbf{(A-10)}$$

Humidity dependence:

$$k_h = (1 - h^3) \text{ for } h \leq 0.98$$

$$k_h = -0.2 \text{ for } h = 1, \text{ interpolate for } 0.98 \leq h \leq 1 \quad \textbf{(A-11)}$$

Size dependence:

$$\tau_{sh} = k_t (k_s D)^2, \; D = 2v/s \quad \textbf{(A-12)}$$

where: k_s = 1.00 for and infinite slab, 1.15 for an infinite cylinder, 1.25 for an infinite square prism, 1.30 for a sphere, and1.55 for a cube.

Sample Calculation

The input data used is for the sample calculation is from Mix 1 for the 28th day of drying at 50% relative humidity after 7 days of 100% relative humidity curing.

Relative humidity = 50%

Volume/surface ratio (Prismatic specimen) = 0.662

Cementitious material content = 24.7 lb/ft^3

Water content = 10.7 lb/ft^3

Total aggregate content = 104.3 lb/ft^3

Water/cementitious material ratio = 0.43

Aggregate/cement ratio = 4.22

Compressive strength at 28 days = 3790 psi

Relative humidity factor (h) = 0.50

Estimated elastic modulus (6) E_{28} = $57000*\sqrt{fc}$
= 3,509,090 psi

q_1 = $0.6*10^6/E_{28}$
= $0.6*10^6/3.5*10^6$
= 0.171

q_2 = $451.1c^{0.5}f_c^{-0.9}$
= $451.1*24.7^{0.5}*3790^{-0.9}$
= 1.348

q_3 = $0.29\ (w/c)^4q_2$
= $0.29\ *(0.433)^4*1.348$
= 0.01376

By interpolation from Table A.1, Q(t,t') = 0.3784

α_1 = 1 (Type 1 cement) α_2 = 1 (curing under 100% relative humidity)

$\varepsilon_{s\infty}$ = $-\alpha_1\cdot\alpha_2\cdot[26w^{2.1}f_c^{-0.28}+270]$
= $1*1*(26*10.7^{2.1}3790^{-0.28}+270)$
= 775.68 (in $*10^{-6}$) = $\varepsilon_{sh\infty}$

q_5 $= 7.57 \times 10^5 f_c^{-1} |\varepsilon_{sh\infty}|^{-0.6}$
$= 7.57*10^5 3790^{-1} |775.68|^{-0.6}$
$= \underline{10.74}$

k_s (shape factor) $= 1.25$ (infinite square prism)

k_t $= 190.8 t_0^{-0.08} \cdot f_c^{-1/4}$
$= 190.8*7^{-0.08}.3790^{-1/4}$
$= \underline{27.19}$ days/in^2

τ_{sh} $= k_t (k_s D)^2$
$= 27.19*(1*2*0.6617)^2$
$= \underline{74.41}$

S (t) $= \tanh [(t - t_o)/ \tau_{sh}]^{0.5}$
$= \underline{0.605}$

S (t') $= \tanh [(t' - t_o)/ \tau_{sh}]^{0.5}$
$= \underline{0}$

H (t) $= 1-(1-h)*S(t)$
$= \underline{0.697}$

H (t') $= 1-(1-h)*S(t')$
$= \underline{1}$

$C_o(t,t')$ $= q_2 * Q(t,t') + q_3 * \ln[1+(tt')^n] + q_4 \ln(t/t')$
$= \underline{0.546}$

$C_d(t,t',t_o)$ $= q_5 * [\exp\{-8H(t)\} - \exp\{-8H(t')\}]^{1/2}$

$C_d(t,t',t_o)$ $= 0.2415$

$J(t,t')$ $= q_1 + C_o(t,t') + C_d(t,t',t_o)$
$= \underline{0.958}$

$\emptyset(t,t')$ $= E(t') * J(t,t') - 1$
$= 3.50*0.958 - 1$
$= \underline{2.363}$

A.5.2 Modified NCHRP 496 Model

The NCHRP model has been modified for high strength concrete. These equations were developed because the existing LRDF provisions for estimation of creep did not provide a reliable estimate for high strength concrete.

$$\varphi(t,t_i) = 1.9\, k_{td}\, k_{vs}\, k_f\, k_{hc}\, t_i^{-0.118} \qquad \textbf{(A-13)}$$

Ambient Relative humidity correction factor k_{hc}:

$$k_{hc} = 1.56 - 0.008RH \quad \textbf{(A-14)}$$

Size Correction factor k_{vs}:

$$k_{vs} = 1.45 - 0.13\left(\frac{v}{s}\right) \quad \textbf{(A-15)}$$

Strength correction factor k_f:

$$k_f = \frac{5}{(1 + f'_{ci})}, \text{ where } f'_{ci} = 0.8f'_c \quad \textbf{(A-16)}$$

Time development factor k_{td}:

$$k_{td} = \frac{t}{(61 - 4f'_{ci} + t)}, \text{ where t is the time for loading} \quad \textbf{(A-17)}$$

Sample Calculation

The input data used is for the sample calculation is from Mix 1 for the 28th day of drying at 50% relative humidity after 7 days of 100% relative humidity curing.

k_{vs}	= 1.45 – 0.13(v/s) = 1.45 – 0.13*0.6617 = <u>1.364</u>
k_{hc}	= 1.56 – 0.008RH =1.56-0.008*50 = <u>1.16</u>
k_f	= 5/(1+f'$_{ci}$) = 5/(1 + 0.8*3.79) = <u>1.24</u>
For ultimate creep coefficient, k_{td}	= 1.00
$\varphi(t,t_i)$	= 1.9 $k_{td}\, k_{vs}\, k_f\, k_{hc}\, t_i^{-0.118}$ = <u>2.515</u>

Table A.2. Summary of calculated creep coefficient

Mix	Creep Coefficient (28 day)		
	B3 Model	NCHRP Model	Average
1	2.36	2.52	2.44
2	2.19	2.34	2.26
3	2.40	2.87	2.63
4	2.31	2.38	2.35
5	2.36	2.56	2.46
6	2.08	1.80	1.94
7	2.33	2.43	2.38
8	2.45	2.67	2.56
9	2.64	3.14	2.89
10	2.18	2.17	2.17
11	2.47	2.81	2.64

A.6 Test Data for Mechanical Tests

A.6.1 Compressive Strength

Table A.3. Results of compressive strength test

Compressive Strength (psi)												
Age (days)	Sample #	Mix 1	Mix 2	Mix 3	Mix 4	Mix 5	Mix 6	Mix 7	Mix 8	Mix 9	Mix 10	Mix 11
1	Sample 1	1273	1228	935	2418	1604	3529	1388	787	498	1401	396
	Sample 2	1328	1095	887	1959	1525	3542	1198	847	493	1358	441
3	Sample 1	1871	2570	1970	2699	2282	4150	2303	1341	952	2386	863
	Sample 2	1912	2516	2100	2757	2249	4157	2068	1387	877	2430	876
7	Sample 1	2445	3390	2564	3101	2497	4812	3043	1814	1528	3358	1808
	Sample 2	2559	3307	2608	3661	2643	4665	2866	1820	1393	3256	1884
14	Sample 1	3222	3984	2927	3684	3359	5177	3516	2549	1937	4172	2638
	Sample 2	3000	4008	3073	3690	3128	5305	3553	2536	2047	4055	2913
28	Sample 1	3864	4495	3521	4093	3654	5696	4130	3559	2856	4525	3159
	Sample 2	3716	4536	3388	4073	3684	6032	3800	3513	2733	4683	3365
56	Sample 1	3970	4698	3687	4502	4111	6988	4070	4845	3871	5038	4004
	Sample 2	4072	5151	3519	4508	3899	6488	4254	4551	4106	4932	3641

A.6.2 Elastic Modulus

Table A.4. Results of elastic modulus test

Elastic Modulus (X 10^6psi)												
Age (days)	**Sample #**	**Mix 1**	**Mix 2**	**Mix 3**	**Mix 4**	**Mix 5**	**Mix 6**	**Mix 7**	**Mix 8**	**Mix 9**	**Mix 10**	**Mix 11**
1	Sample 1	2.10	1.90	1.65	3.40	3.14	4.35	3.40	2.60	1.65	2.50	1.85
	Sample 2	3.20	2.00	1.80	3.70	2.92	4.45	3.50	2.45	1.50	2.60	1.85
3	Sample 1	1.90	3.40	2.50	3.85	3.05	4.35	3.30	3.35	1.95	3.45	2.60
	Sample 2	3.30	3.40	2.40	3.85	3.70	4.55	3.20	2.90	1.95	3.60	2.80
7	Sample 1	3.50	3.60	3.10	4.25	4.10	4.70	3.75	3.25	3.10	3.60	3.70
	Sample 2	4.10	3.80	3.10	4.50	4.10	4.50	3.70	3.20	3.50	3.20	3.55
14	Sample 1	3.95	3.75	3.40	4.40	4.20	4.70	4.00	3.50	3.35	3.60	3.70
	Sample 2	4.00	3.75	3.60	4.30	4.35	4.60	3.94	3.70	3.40	3.70	3.90
28	Sample 1	3.90	3.70	3.60	4.35	4.40	5.20	3.90	4.00	3.60	3.80	3.80
	Sample 2	3.95	4.00	3.80	4.30	4.90	5.05	4.00	4.05	3.45	3.90	3.90
56	Sample 1	4.30	3.90	3.90	4.60	4.80	5.55	3.85	4.25	3.80	3.85	3.90
	Sample 2	3.90	3.80	3.95	4.50	4.70	5.35	4.05	4.20	3.85	3.95	4.00

A.6.3 Splitting Tensile Strength

Table A.5. Results of splitting tensile strength test

Split Tensile Strength (psi)											
Age (days)	**Mix 1**	**Mix 2**	**Mix 3**	**Mix 4**	**Mix 5**	**Mix 6**	**Mix 7**	**Mix 8**	**Mix 9**	**Mix 10**	**Mix 11**
1	188	171	140	246	128	350	133	109	40	153	65
3	287	292	219	290	199	400	243	196	89	243	104
7	303	319	289	301	279	391	287	229	210	310	274
14	338	352	337	322	318	439	392	289	281	406	363
28	420	427	384	353	352	469	441	356	383	504	372
56	430	532	408	361	428	518	465	366	460	524	421